

Simen Havik

Escape from the Flatland: Synthesis of Tetrahydropyran Substituted Pyrrolopyrimidines as CSF-1R Inhibitors

Master's thesis in Chemical Engineering and Biotechnology

Supervisor: Bård Helge Hoff

Co-supervisor: Frithjof Bjørnstad

June 2021

Simen Havik

Escape from the Flatland: Synthesis of Tetrahydropyran Substituted Pyrrolopyrimidines as CSF-1R Inhibitors

Master's thesis in Chemical Engineering and Biotechnology
Supervisor: Bård Helge Hoff
Co-supervisor: Frithjof Bjørnstad
June 2021

Norwegian University of Science and Technology
Faculty of Natural Sciences
Department of Chemistry



Norwegian University of
Science and Technology

I hereby declare that this master's thesis is an independent work according to the exam regulations of the Norwegian University of Science and Technology.

Trondheim, June 12, 2021

Simen Havik

Simen Havik

Preface

The work in this master's thesis has been conducted at the Department of Chemistry at The Norwegian University of Science and Technology during the spring of 2021. The supervisors of this master's thesis have been Professor Bård Helge Hoff and PhD Candidate Frithjof Bjørnstad.

Firstly, I would like to thank Bård for very helpful guidance and always finding time to answer questions about lab work or writing. Secondly, I would like to thank Frithjof and PhD candidate Thomas Ihle Aarhus for all the guidance, fun conversations and "guttastemning" we've had in the lab this last year. Thank you to the rest of the Hoff/Sundby family for including me in the research group and for additional guidance from the weekly group meetings.

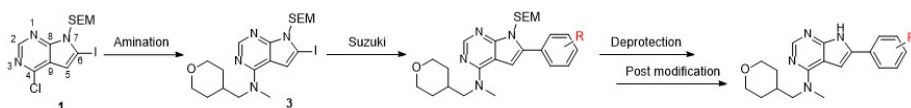
I would also like to thank Susana Villa Gonzalez for the help of running MS experiments and helping to confirm the structures of the synthesized compounds. A special note to Roger Aarvik for always supplying chemicals in the time of need and to Torun Margareta Melø for guidance at the NMR-lab.

I would like to thank my family for the support and motivation during my years studying at NTNU. A special thanks to all my friends for having lunch together every day for the last year during the COVID-19 pandemic, making the days much easier and fun.

Abstract

Overexpression of the colony-stimulating factor 1 receptor, CSF-1R has been implicated in many pathological conditions such as cancer development and bone disorders. CSF-1R has therefore been a target of great interest for the treatment of these disease states. The aim of this masters thesis was to synthesize new CSF-1R inhibitors based on the pyrrolopyrimidine scaffold, as well as evaluate their inhibition activity towards CSF-1R in enzymatic studies.

The pyrrolopyrimidines were prepared by a thermal amination at C-4 of 4-chloro-6-iodo-7-((2-(trimethylsilyl)ethoxy)methyl)-7*H*-pyrrolo[2,3-*d*]pyrimidine. This was followed by selective Suzuki cross-coupling reactions with various aryl boronic acids with functional groups in either *para* or *meta* position at the C-6 carbon resulting in high yields. The target inhibitors were synthesized by removal of the protective SEM-group on the pyrrole in addition to a couple of post modification reactions on selected compounds. The target inhibitors were isolated in varying yields and high purities.



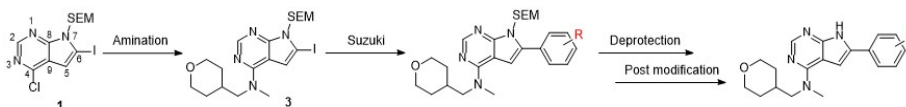
Deprotection of both a SEM-group and a Boc group to synthesize an aniline product turned out to be problematic and resulted in incomplete conversion and observation of several byproducts in the isolated product. An alternative synthesis route was carried out to synthesize the deprotected aniline product by reduction of a deprotected nitro compound, which resulted in high purity and yields.

During this masters thesis a total of 12 target molecules were tested for their CSF-1R inhibition activity. The compounds proved to be highly potent with low IC_{50} values in the range of 0.4-1.9 nM. The CSF-1R inhibitors were also tested for their inhibition activity against various kinases without showing any relevant off-target effect on six other tyrosine kinases.

Sammendrag

Overekspressjon av den kolonistimulerende faktor 1-reseptoren, CSF-1R har blitt implisert i mange sykdomsforløp som for eksempel kreftdannelse og beinlidelser. CSF-1R kinasen har derfor vært et viktig mål for behandling av disse sykdommene. Målet med denne masteroppgaven var å syntetisere nye CSF-1R-hemmere basert på strukturen til pyrrolopyrimidiner, samt å teste deres enzyamtiske aktivitet som hemmere mot CSF-1R.

Pyrrolopyrimidinene i denne oppgaven ble fremstilt ved en termisk amineringsreaksjon ved C-4 av forbindelsen 4-kloro-6-iodo-7-((2-(trimetylsilyl)etoksy)metyl)-7H-pyrrolo [2,3-d]pyrimidin. Dette ble etterfulgt av selektive Suzuki-krysskoblinger med ulike borsyrer med funksjonelle grupper i både *para*- og *meta*-stilling ved C-6 karbonet som resulterte i høye utbytter. Målinhibitorene ble syntetisert ved fjerning av den beskyttende SEM-gruppen på pyrrolen i tillegg til et par tilleggsreaksjoner på utvalgte forbindelser. Molekylene ble isolert med varierende utbytter og høy renhet.



Avbeskyttelse av både en SEM-gruppe og en Boc-gruppe for å syntetisere et anilinprodukt viste seg å være problematisk og resulterte i ufullstendig omsetning, der det ble observert flere biprodukter i det isolerte produktet. En alternativ syntesevei ble utført for å syntetisere det avbeskyttede anilinproduktet ved reduksjon av en avbeskyttet nitroforbindelse, noe som resulterte i høy renhet og bedre utbytte.

I løpet av denne masteroppgaven ble totalt 12 målmolekyler testet for deres aktivitet som CSF-1R-hemmere. De 12 målmolekylene viste seg å ha en meget høy aktivitet som hemmere mot CSF-1R-kinasen med lave IC_{50} verdier i området 0.4-1.9 nM. Målmolekylene ble også testet for deres aktivitet som hemmere mot andre ulike kinaser uten å vise noen relevant aktivitet overfor disse.

Contents

Preface	i
Abstract	iii
Sammendrag	vi
Symbols and Abbreviations	vi
Compound Numbering	viii
1 Introduction and Theory	1
1.1 Protein Tyrosine Kinase	2
1.2 Colony-stimulating factor 1 receptor	3
1.2.1 CSF-1R and disease states	6
1.3 Pyrrolopyrimidines	7
1.4 Previous work	9
1.5 Directed metalation	10
1.6 Nucleophilic aromatic substitution	11
1.6.1 Buckwald-Hartwig amination	14
1.7 Suzuki-Miyaura cross-coupling	14
1.7.1 Mechanism	14
1.7.2 Catalysts	17
1.7.3 Side reactions and products	18
1.7.4 Selectivity in cross-coupling	20
1.8 SEM-deprotection	21
2 Results and Discussion	24
2.1 Amination	25
2.2 Suzuki Cross-Coupling	26
2.2.1 Synthesis of Compounds 4-8	27

2.2.2	Synthesis of compound 9-13	28
2.2.3	Summary of the Suzuki Cross-Couplings	30
2.3	SEM-Deprotection	33
2.3.1	Synthesis of compound 20	35
2.4	Post modifications	37
2.4.1	Synthesis of compound 17 by hydrolysis	37
2.4.2	Synthesis of compound 20 by reduction	39
2.4.3	Synthesis of compound 25 by acylation	40
2.5	Structure Elucidation	42
2.5.1	Common spectroscopic trends	43
2.5.2	Compounds 6, 7, 16 and 18	46
2.5.3	Compound 8 and 19	50
2.5.4	Compound 9 and 20	51
2.5.5	Compound 10 and 21	53
2.5.6	Compound 11 and 22	55
2.5.7	Compound 12 and 23	57
2.5.8	Compound 13 and 24	59
2.5.9	Compound 15 and 17	60
2.5.10	Compound 25	62
2.5.11	IR-spectroscopy	64
2.6	Biological activity	65
2.6.1	<i>In vitro</i> enzymatic assays	65
2.6.2	IC ₅₀ comparison of two different series	67
2.6.3	Testing towards other kinases	68
3	Conclusion	71
4	Future Work	73
5	Experimental	75

5.1	General Information	75
5.2	Synthesis of Compound 3	78
5.3	Synthesis of Compound 4	79
5.4	Synthesis of Compound 5	80
5.5	Synthesis of Compound 6	81
5.6	Synthesis of Compound 7	82
5.7	Synthesis of Compound 8	83
5.8	Synthesis of Compound 9	84
5.8.1	2 times 500 mg scale	84
5.9	Synthesis of Compound 10	85
5.10	Synthesis of Compound 11	87
5.11	Synthesis of Compound 12	88
5.12	Synthesis of Compound 13	89
5.12.1	100 mg scale	89
5.12.2	500 mg scale	89
5.13	Synthesis of Compound 14	90
5.14	Synthesis of Compound 15	91
5.15	Synthesis of Compound 16	92
5.16	Synthesis of Compound 17	93
5.17	Synthesis of Compound 18	94
5.18	Synthesis of Compound 19	95
5.19	Synthesis of Compound 20	96
5.19.1	By SEM-deprotection	96
5.19.2	By Reduction	97
5.20	Synthesis of Compound 21	98
5.21	Synthesis of Compound 22	99
5.22	Synthesis of Compound 23	100
5.23	Synthesis of Compound 24	101
5.23.1	Scale 100 mg	101

5.23.2 Scale 470 mg	102
5.24 Synthesis of Compound 25	103
References	104
A Spectroscopic data for Compound 1	i
B Spectroscopic data for Compound 3	ii
C Spectroscopic data for Compound 4	viii
D Spectroscopic data for Compound 5	xv
E Spectroscopic data for Compound 6	xxii
F Spectroscopic data for Compound 7	xxx
G Spectroscopic data for Compound 8	xxxviii
H Spectroscopic data for Compound 9	xliv
I Spectroscopic data for Compound 10	lii
J Spectroscopic data for Compound 11	lix
K Spectroscopic data for Compound 12	lxvi
L Spectroscopic data for Compound 13	lxxiii
M Spectroscopic data for Compound 14	lxxx
N Spectroscopic data for Compound 15	lxxxvii
O Spectroscopic data for Compound 16	xciv
P Spectroscopic data for Compound 17	ci

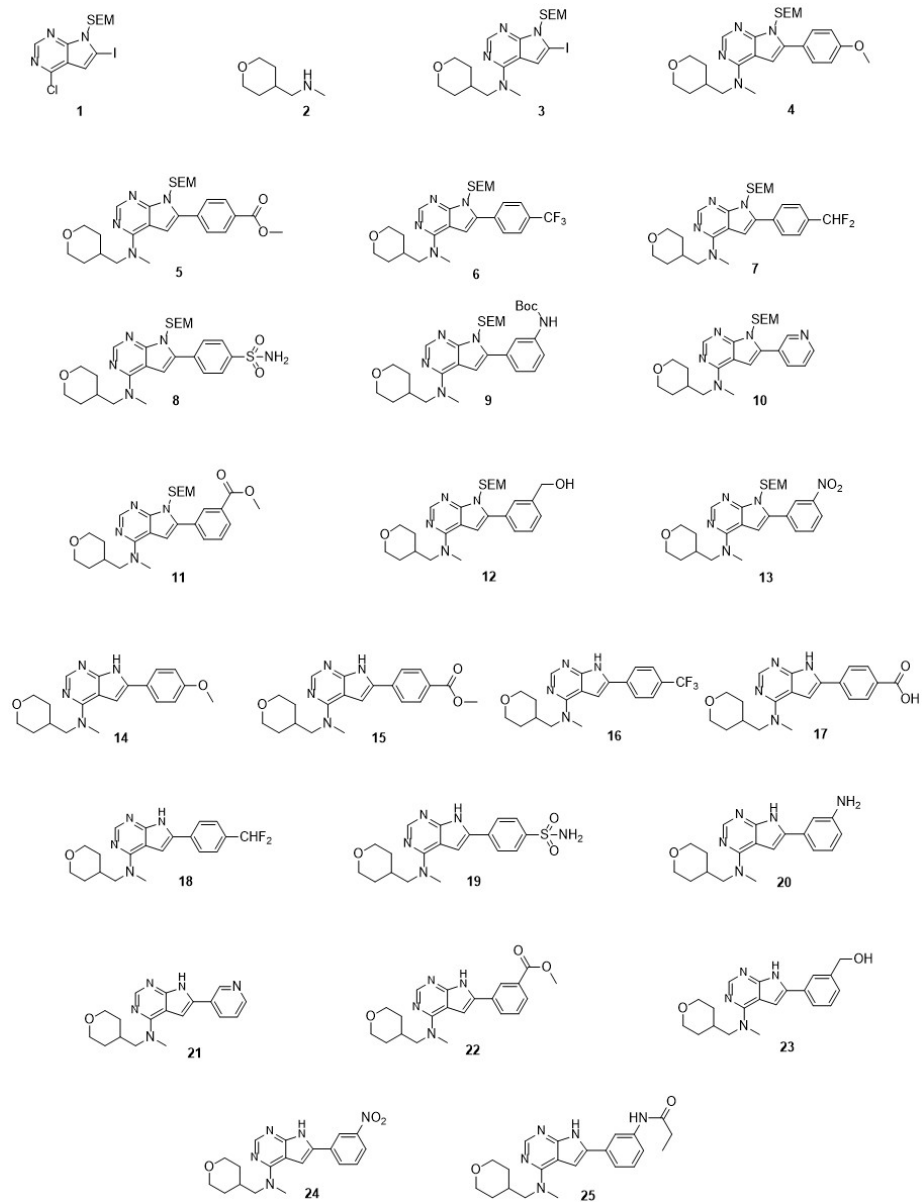
Q Spectroscopic data for Compound 18	cviii
R Spectroscopic data for Compound 19	cxv
S Spectroscopic data for Compound 20	cxxii
T Spectroscopic data for Compound 21	cxxix
U Spectroscopic data for Compound 22	cxviii
V Spectroscopic data for Compound 23	cxliii
W Spectroscopic data for Compound 24	cl
X Spectroscopic data for Compound 25	clvii

Symbols and Abbreviations

δ	Chemical shift [ppm]
$^{13}\text{C-NMR}$	Carbon nuclear magnetic resonance
$^1\text{H-NMR}$	Hydrogen nuclear magnetic resonance
ACN	Acetonitrile
Boc	<i>tert</i> -Butyloxycarbonyl
COSY	Correlation Spectroscopy
CSF-1	Colony Stimulating Factor 1
CSF-1R	Colony Stimulating Factor 1 Receptor
d	Doublet
DCM	Dichloromethane
DIPEA	<i>N,N</i> -Diisopropylethylamine
DNA	Deoxyribonucleic acid
eq.	Equivalents
FDA	Food and Drug Administration
h	Hours
HMBC	Heteronuclear Multiple Bond Correlation
HPLC	High Performance Liquid Chromatography
HRMS	High Resolution Mass Spectroscopy
HSQC	Heteronuclear Single Bond Correlation
IC ₅₀	Half maximum inhibitory concentration
IR	Infrared
<i>J</i>	Coupling Constant [Hz]
LDA	Lithium diisopropylamide
LPS	Lipopolysaccharide
m	Multiplet
m/z	Mass per charge ratio
Mp.	Melting Point

MS	Mass Spectroscopy
NMR	Nuclear Magnetic Resonance
NRTK	Non-receptor Protein Tyrosine Kinase
Pd(dppf)Cl ₂	[1,1-Bis(diphenylphosphino)ferrocene]dichloropalladium(II)
ppm	Parts per million
PTK	Protein Tyrosine Kinase
RNA	Ribonucleic acid
RTK	Receptor Protein Tyrosine Kinase
R _f	Retention Factor
s	Singlet
SEM	2-(Trimethylsilyl)ethoxymethyl
t	Triplet
<i>t_R</i>	Retention factor
TAM	Tumor-associated macrophages
TFA	Trifluoroacetic acid
THP	Tetrahydropyran
TLC	Thin Layer Chromatography

Compound Numbering



1 Introduction and Theory

Treatment therapies such as small molecule inhibitors and monoclonal antibodies have become an important field of research in the practice of oncology in recent years. Small molecule inhibitors can block intracellular signaling from tyrosine kinases such as colony-stimulating factor-1 CSF-1R, that can cause cell growth, proliferation and migration in cell tissues. Overexpression of signaling activity has been implicated in many pathological conditions such as cancer development and inflammation diseases. Inhibition of the signaling activity of tyrosine kinases can therefore be a possible treatment for these diseases.^{[1][2]}

The aim of this master thesis was to synthesize new CSF-1R inhibitors based on the pyrrolopyrimidine scaffold, as well as evaluate their inhibition activity towards the CSF-1R kinase in enzymatic studies. The general structure of the target molecules in this project is illustrated in Figure 1.1.

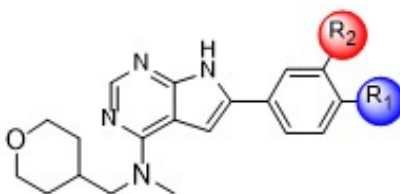


Figure 1.1: General structure of the target molecules in this masters thesis

Three derivatives based on this scaffold had been prepared prior to this thesis. These had shown remarkable high CSF-1R inhibitory activity. The effect of different substituent in *para* and *meta* position on the 6-aryl analogue was therefore further investigated in this thesis to get a better understanding of the structure-activity relationship (SAR).

1.1 Protein Tyrosine Kinase

Protein tyrosine kinases (PTK) are a family of enzymes that are characterized by their ability to catalyze the transfer of γ phosphate groups of ATP to hydroxyl groups of tyrosine residues on protein substrates.^{[3][4][5]} This process is called tyrosine phosphorylation and plays a key role in regulating multicellular processes in eukaryotic organisms such as proliferation, differentiation, metabolism, migration, and anti-apoptotic signaling of the cell. It is also an important mechanism for transmitting signals within a cell (signal transduction).^[6]

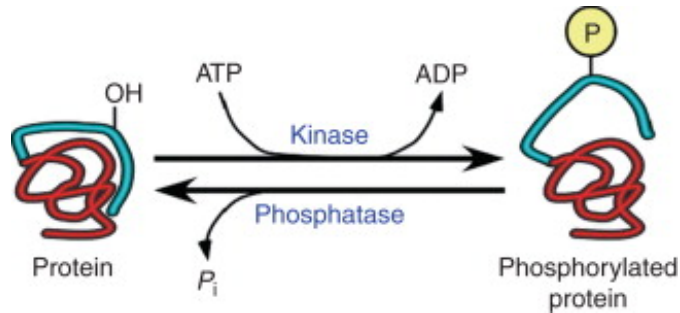


Figure 1.2: Protein phosphorylation catalyzing the transfer of phosphate to proteins by protein kinase^[7]

The two classes of PTKs which are present in cells are called receptor tyrosine kinases (RTK) and non-receptor tyrosine kinases (NRTK).^[3] There are a total of 90 unique tyrosine kinases present in the human genome, where 58 of them are of RTKs and 32 of them are NRTKs.^[8] The RTKs are transmembrane glycoproteins that possess an extracellular ligand-binding domain, an intracellular catalytic domain, and a transmembrane domain. The RTKs are activated when ligands are bound to their extracellular domain, which leads to dimerization and activation of the receptor's kinase activity. This triggers autophosphorylation of specific tyrosine residues in the kinase domain and creates phosphotyrosine

docking sites for proteins that transduce signals inside of the cell. The NRTks are cytoplasmic proteins that are important in the downstream signal transduction cascade within the cell. [4] [9] [10]

Regulation of the cellular activities in tyrosine kinases is of utmost importance for maintaining homeostasis. Over-expression and mutations of tyrosine kinases can cause abnormal and unregulated enzyme activities in the cells, which can result in diseases such as cancer. Tyrosine kinase inhibitors are therefore of clinical significance today for the development of therapeutic treatments of cancer and other disease states. [4] [6]

1.2 Colony-stimulating factor 1 receptor

Colony-stimulating factor receptor (CSF-1R) is a type III receptor tyrosine kinase, which is activated by the macrophage-colony-stimulating factor-1 (CSF-1), and primarily expressed on the surface of microglia, monocytes and macrophages. [2] [11] [12] Colony-stimulating factor-1 (CSF-1), a common type of cytokine, that regulates the survival, proliferation, differentiation, and function of cells of the mononuclear phagocytic lineage. IL-34 is another important cytokine that activates CSF-1R. [13] [14] [15]

The signal transduction pathways are activated by CSF-1 binding to its receptor on targeted cells. [14] The binding of CSF-1R to CSF-1 stabilizes dimerization of CSF-1R to activate the receptor through autophosphorylation of CSF-1R and phosphorylation of other downstream molecules. Triggering the phosphorylation can then initiate a series of membrane-proximal tyrosine phosphorylation cascades causing rapid stimulation of cytoskeletal remodeling, protein translation and increased gene expression. [16] Figure 1.3 shows the mechanism of signal transduction of CSF-1 expressed through CSF-1R causing the above processes.

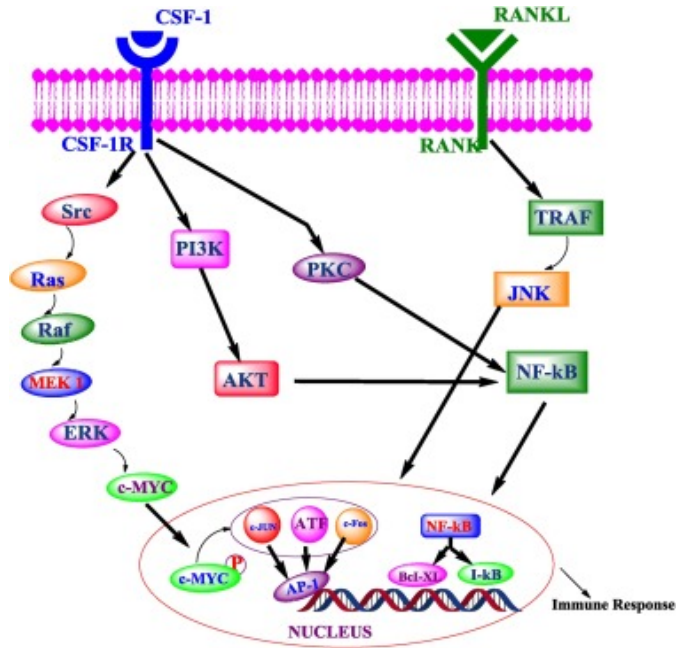


Figure 1.3: Signal transduction mechanism of CSF-1 when binding with CSF-1R. ^[11]

A number of disease states have overexpression of CSF-1 and/or CSF-1R. The growth of metastases of certain types of cancer, the promotion of osteoclast proliferation in bone osteolysis, and many inflammatory disorders are examples of some of these disease states. ^[17] It is indicated that microglial proliferation, neuronal damage, and disease progression are slowed down by inhibition of CSF-1R signaling. Inhibition of CSF-1R therefore represents a promising approach for the treatment of these diseases. ^[15]

Current research has shown that there are two possible methods for the inhibition of CSF-1R. The first method is based on the use of monoclonal antibodies that block the binding site of the receptor, to prevent the ligands CSF-1 and IL-34 from binding. As a result of this, CSF-1 is

prohibited from transmitting signals to among others tumor-associated macrophages (TAMs), a class of cells found in the body which are heavily associated with cancer-related inflammation. The second method is by the use of small molecules designed to block the tyrosine kinase activity of CSF-1R. The main difference between these two types of inhibitors is that the kinase inhibitors due to better accessibility are more likely to block autocrine signaling than the monoclonal antibodies.^{[18][19]} The signaling and blocking mechanism for the CSF-1R inhibitors are illustrated in Figure 1.4

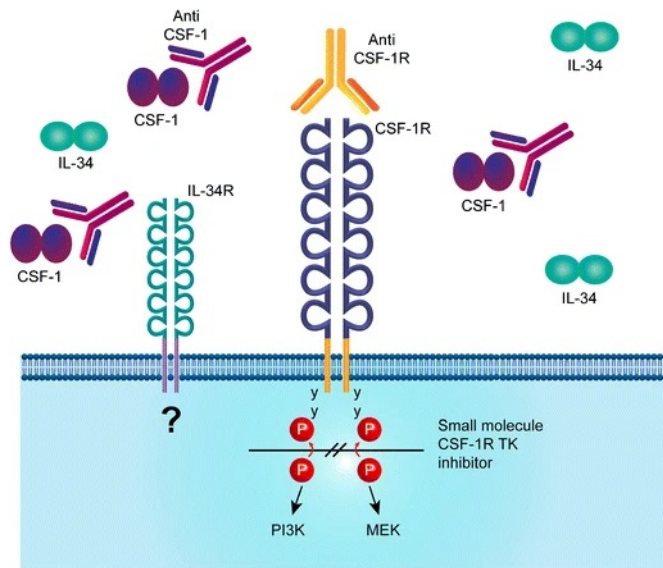


Figure 1.4: Signal inhibition mechanism of CSF-1R.^[19]

The small-molecule inhibitor PLX-3397, also called Turalio, is currently the most frequent used CSF-1R inhibitor in clinical studies towards various cancers.^[20] Inhibition of CSF-1R by PLX-3397 in mice has led to profound depletion of microglia in their central nervous system without reducing their cognitive function or giving them obvious behavioral ab-

normalities.^[2] PLX-3397 is today the only certified CSF-1R inhibitor approved by the FDA.^[21]

1.2.1 CSF-1R and disease states

The CSF-1R kinase is related to the initiation and development of several types of cancers, bone disorders, and inflammations due to mutation effects on the receptor function or by over-expression of its CSF-1 ligand.

The CSF-1R kinase is involved in regulating the function of tumor-associated macrophages, which are significant components of leukocytic infiltrate that promotes tumor progression. TAMs have been related to many cancer inflammations, due to their activation by CSF-1.^{[11][13]} CSF-1R inhibitors have become a target of study for the treatment of cancer-related disease states, and the development of new CSF-1R inhibitors is an ongoing process.^[22]

CSF-1 is also synthesized in a variety of cells, including among others bone cells.^[16] There are three different types of bone cells; osteoclasts (OCs), osteoblasts (OBs), and osteocytes (OSs). All of these cells have a unique function and are important for the remodeling and development of the skeleton and the bone marrow. The osteoblasts are responsible for forming new bones, while the osteoclasts, which originate from the monocyte/macrophage lineage, are responsible for the breakdown and resorption of old bones. The number and activity of osteoclasts decide the rate of bone resorption.^{[22][23]} Osteopetrosis and bone marrow failure are diseases that are caused by defective osteoclast activity, while osteoporosis is a disease caused by excess osteoclast activity.^[24] It is suggested in studies that osteoclasts develop in the presence of CSF-1.^{[25][26]} By suppressing the formation and activity of osteoclasts by blocking or depleting CSF-1R, the effect of pathological bone resorption

in bone diseases will be reduced.^[27]

In recent studies, several promising CSF-1R inhibitors for the treatment of bone diseases have come to light. The CSF-1R inhibitor PLX3397 has significantly reduced bone degradation caused by lipopolysaccharide (LPS), a polysaccharide that can cause bone loss due to stimulation of osteoclast formation. These findings suggest that a CSF-1R inhibitor could be examined further as a possible treatment for bone loss caused by LPS.^[28] Among other small molecule inhibitors, Ki20227 and GW2580 have been reported to inhibit bone destruction and joint connective tissue formation in human osteoclast cultures by blocking the activation of CSF-1R.^[27]^[29]^[30] Monoclonal antibodies such as AFS98 have also shown significant anti-inflammatory effects against bone and cartilage destruction by CSF-1R blocking.^[31] The structures of the small-molecule CSF-1R inhibitors are illustrated in Figure 1.5

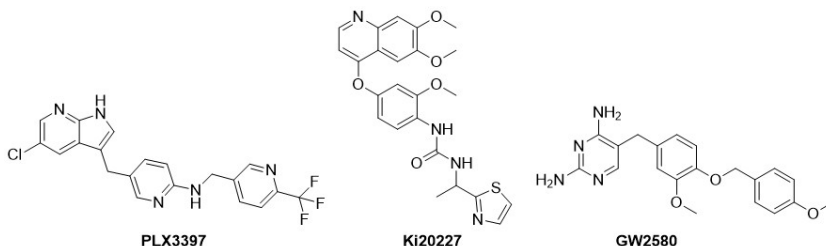


Figure 1.5: CSF-1R Kinase Inhibitors effective against bone diseases^[28] ^[29] ^[30]

1.3 Pyrrolopyrimidines

Pyrrolopyrimidines, also called 7-deazapurines, are bicyclic heterocyclic compounds consisting of a pyrimidine and pyrrole ring fused together. The six-membered pyrimidine ring contains two nitrogen atoms which withdraw electron density from the ring carbons making it resistant to electrophilic substitution. Thus, the electron deficiency at the carbons

makes the pyrimidine more available for nucleophilic attacks. Pyrimidine are especially activated for nucleophilic attacks in the 4-position, which is the most electron deficient part of the pyrimidine. The pyrrole ring contains one nitrogen atom and has a high reactivity in electrophilic substitution.^[32] In Figure 1.6 below the numbering systems used for pyrimidine, pyrrole, and pyrrolopyrimidine are illustrated.

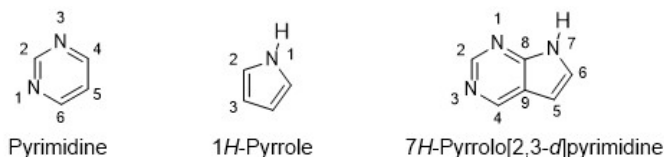
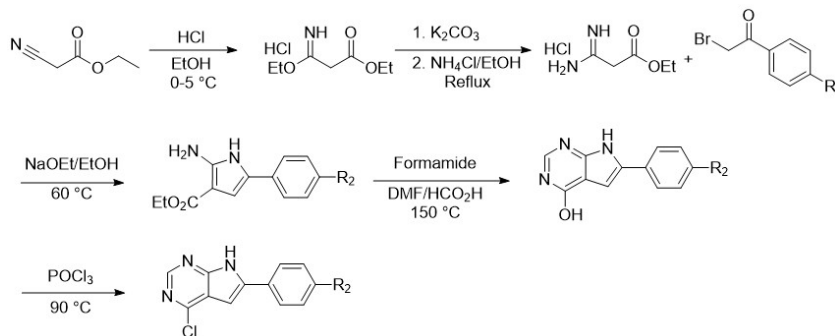


Figure 1.6: Structure and nomenclature for pyrimidines, pyrroles and pyrrolopyrimidines

Due to its structural similarities with purines, pyrrolopyrimidines can substitute purine nucleosides in DNA and RNA.^[33] The pyrrolopyrimidine scaffold has therefore been widely used as pharmacophores in medicinal research.^[34] Pyrrolopyrimidine derivatives are also known to exhibit antibiotic, anticancer, and anti-inflammatory activity^{[35][36]} as well as possessing inhibition properties of protein kinases.^[37]

Synthesis of pyrrolopyrimidines can be done with different routes. One method which has previously been employed in the research group^[38] is shown in Scheme 1.1.

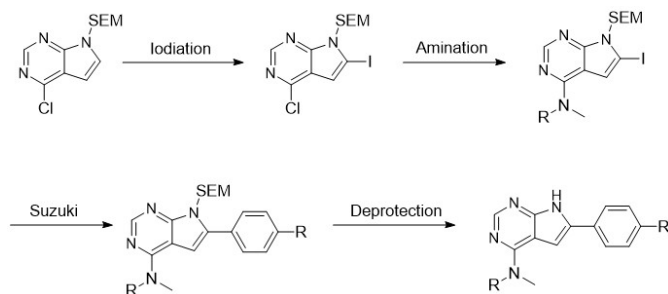


Scheme 1.1: Synthesis route toward 4-chloropyrrolopyrimidines.^[38]

An alternative way of making pyrrolopyrimidines are by a Ugi-Smiles/Sonogashira cascade followed by an efficient base-catalyzed intramolecular cyclization described by Kaïm *et al.*^[39]

1.4 Previous work

In earlier work within the research group, the development of new ways to inhibit colony-stimulating factor receptor (CSF-1R) as well as the epidermal growth factor receptor (EGFR) has been the main goal.^{[40][41]} The group has identified several potent CSF-1R and EGFR inhibitors based on the pyrrolopyrimidine scaffold as well as the furo^[42]- and thienopyrimidine scaffold^[43]. The synthetic routes planned for making the potential pyrrolopyrrolo[2,3-*d*]pyrimidine inhibitors have been well developed within the research group. The method is illustrated in Scheme 1.2 below.



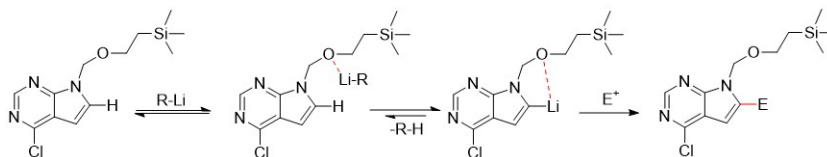
Scheme 1.2: Synthesis route for making potential pyrrolopyrimidine inhibitors

1.5 Directed metalation

Directed *ortho* metalation (DoM) is a reaction where aromatic rings or heterocyclic compounds can be deprotonated under strongly basic conditions on the *ortho*-position to a heteroatom-containing group. A strong alkyl lithium base is normally used, giving an *ortho*-lithium species.^[44] This species can be combined with different electrophiles, to provide new derivatives.^[45] There are several general features in a DoM reaction that must be present for the reaction to occur. A common DoM reaction is typically carried out under an inert atmosphere at $-78\text{ }^{\circ}\text{C}$ where an alkyl lithium reagent is added to the solution of the substrate, followed by the addition of the electrophile. In addition must the directed metalation group be resistant to nucleophilic attacks by the metalating reagent and contain at least one heteroatom to coordinate to the *ortho* metal atom in the intermediate structure.^[44]^[46]

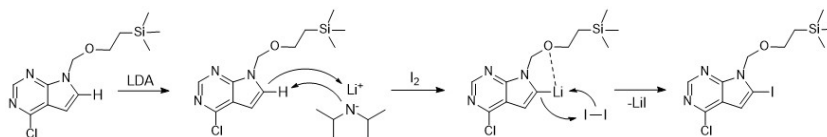
The SEM group acts as a directing group for pyrrole metalation as well as a protective group for the nitrogen on the pyrrole.^[47]^[48] Alternatively can *N*-sulfonyl groups be used as protecting groups^[49], which have been previously done by Zhao *et al.* to improve the reactivity at the C-6 carbon.^[50]^[41] The directed metalation reaction of pyrroles with a directing

SEM-group is illustrated in Scheme 1.3, and is used in the iodination of pyrrolopyrimidines.



Scheme 1.3: Directed *ortho* metalation for pyrrolopyrimidines with SEM as the directing metalation group (DMG).

The reaction is initiated with lithium diisopropylamide reacting with the pyrrolopyrimidine, introducing lithium to the C-6 position in the pyrrolopyrimidine. Iodine is then added to the lithiated C-6 position, giving an iodinated pyrrolopyrimidine product. A proposed mechanism for the direct metalation of the pyrrolopyrimidine is given in Scheme 1.4.

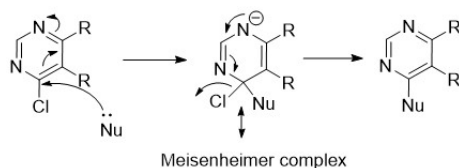


Scheme 1.4: Proposed mechanism for the directed *ortho* metalation

1.6 Nucleophilic aromatic substitution

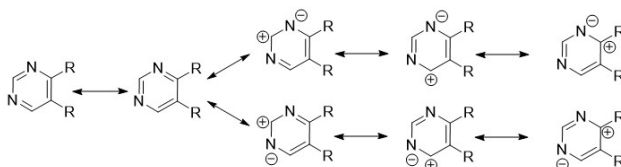
A nucleophilic aromatic substitution (S_NAr) is a reaction that occurs on an aromatic ring where a nucleophile replaces a leaving group on the aromatic ring. The nucleophilic substitution proceeds by a two-step mechanism; an addition step and an elimination step, where the leaving group usually is either *ortho* or *para* to one or more strong electron withdrawing groups.^{[51] [52]} In the first step of nucleophilic aromatic substitution a nucleophile adds to the aromatic ring, which leads to a negatively charged intermediate called a Meisenheimer complex.^{[53] [54]}

This addition is followed by the second step which consists of the elimination of the leaving group.^[52] The mechanism of a nucleophilic aromatic substitution for a general pyrimidine compound is illustrated in Scheme 1.5.^[52]



Scheme 1.5: Proposed mechanism of a nucleophilic aromatic substitution on a pyrimidine.

Several factors affect the rate of reaction in nucleophilic aromatic substitution. There are often used electron withdrawing groups (EWGs) on the aromatic substrate to make the ring more electron deficient, thus more susceptible for nucleophilic aromatic substitution.^{[55] [56]} The leaving group (X) also plays an important part in the rate of reaction. The high electronegativity of the halogen causes a decrease in the electron density at the site of the attack, resulting in a faster attack by the nucleophile. The order of the leaving group reactivity of halides is $X = F \gg Cl > Br > I$, with fluorine as the halogen with the most electron withdrawing properties.^{[55] [56]} The electronic effects are also used to stabilize the Meisenheimer intermediate through resonance by electron withdrawing groups in the positions *ortho* and *para* to the halogen atom. The mesomeric effect of the nitrogens in a pyrimidine ring leads the electron deficiency to carbons at C-2 and C-4 position, making them susceptible for a nucleophilic aromatic substitution.^{[54] [57]} The resonance stabilization of the Meisenheimer complex of pyrimidine compounds is illustrated in Scheme 1.6.



Scheme 1.6: Resonance structures of the Meisenheimer complex of pyrimidine. [32]

It has been the subject of debate on whether the rate-determining step in the mechanism of nucleophilic aromatic substitution is the formation step (step 1) or the decomposition of the intermediate complex (step 2). [55] [58] In aprotic solvents the rate-determining step is usually the loss of the leaving group, due to the high reactivity of nucleophiles in these solvents. [59] [60] The addition step is typically the rate-determining step in protic solvents, due to the stabilization of the negatively charged intermediates (Meisenheimer complexes) formed in this step. [59] [61] [62]

Nucleophilic aromatic substitution has in previous work by the research group been done by introducing amines to pyrrolopyrimidines under thermal conditions. [40] The rate determining step in this reaction is most likely the addition of the amine at the C-4 position. A pyrrolopyrimidine with a chloride atom in the C-4 position will be more susceptible to a nucleophilic aromatic substitution than with an iodine atom in the C-6 position of the pyrrole. The reason for this is that the chloride is a better leaving group than iodine, and because of the more electron deficient character of the pyrimidine ring than the electron rich pyrrole ring, thus making it more susceptible towards nucleophilic aromatic substitution. [32] [63]

1.6.1 Buchwald-Hartwig amination

An alternative method for forming C-N bonds is by a palladium-catalyzed Buchwald-Hartwig cross-coupling. The reaction usually proceeds in a reaction between aryl halides and amines with the presence of a palladium metal catalyst and a base. The base is typically present in stoichiometric amounts while the temperature is much lower compared to the nucleophilic aromatic substitution.^[64] Large bidentate phosphine ligands like diphenylphosphinobinaphthyl (BINAP) and diphenylphosphinoferrocene (DPPF) are typically complexed with the Pd⁽⁰⁾ catalyst, as they have proven to increase the rate and the yields of the cross-coupling reaction.^[65]^[66] Buchwald-Hartwig amination was not applied in this thesis because the thermal aminations proceeded well.

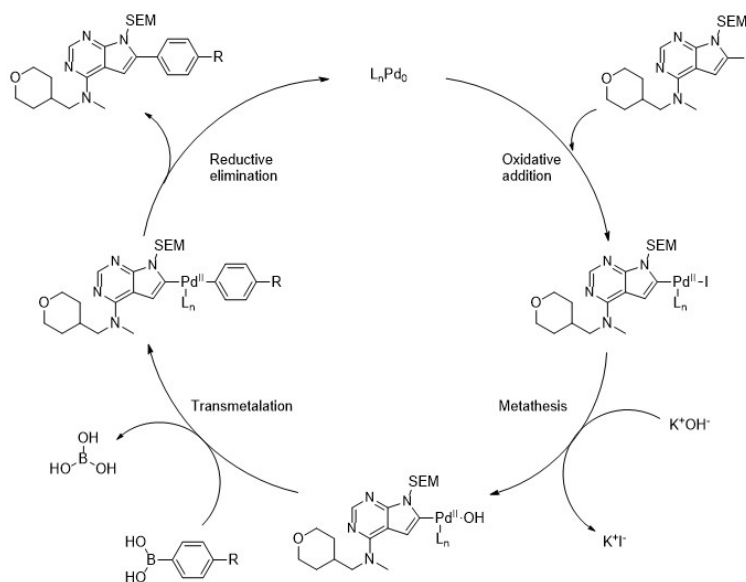
1.7 Suzuki-Miyaura cross-coupling

The Suzuki-Miyaura reaction is a metal-catalyzed cross-coupling reaction where new C-C bonds are formed.^[67]^[68] This cross-coupling reaction is one of the most widely applied reactions in modern organic synthesis.^[69] The Suzuki-Miyaura reaction was initially published in 1979^[70], and in 2010 Akira Suzuki was awarded the Nobel Prize in Chemistry, together with Richard F. Heck and Ei-ichi Negishi, for their work on palladium-catalyzed cross-couplings in organic synthesis.

1.7.1 Mechanism

The Suzuki cross-coupling reaction typically occurs in a palladium-catalyzed reaction between an organohalide/pseudohalide and a boronic compound (boronic acid or boronic ester) under basic conditions to give a coupled product.^[67] The mechanism can be viewed as a catalytic circle via three significant steps; oxidative addition, transmetalation, and reduc-

tive elimination.^[71] In the oxidative addition step an organopalladium species is formed by the addition of an aryl halide to the palladium complex. Pd⁰ is in this step oxidized to Pd^{II}.^{[72][73]} This is succeeded by the presence of a base that exchanges the halide on the organohalide compound with the anion of the base giving a more reactive intermediate.^{[69][74]} In the transmetalation step the aryl group from the boronic acid is transferred to the organopalladium species.^[68] Lastly, the reductive elimination provides the desired product and the active palladium catalyst is regenerated in the catalytic circle.^[74] The reaction mechanism of the Suzuki reaction is illustrated in Scheme 1.7

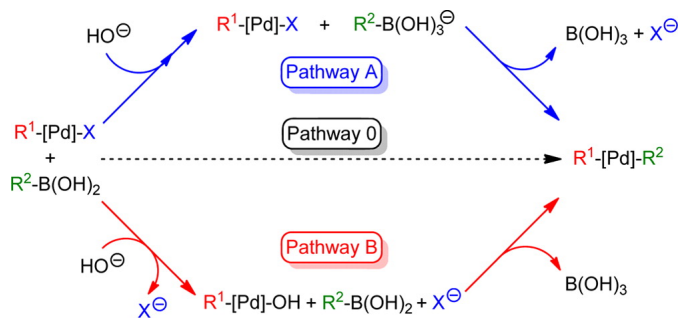


Scheme 1.7: Proposed mechanism for the Suzuki cross-coupling reaction of pyrrolopyrimidine **4-13**^[71]

The rate determining step in the Suzuki reaction is often considered to be the oxidative addition. Nevertheless, as it is reported by Smith *et al.* that the transmetalation step may be the rate-determining step when

using aryl iodine rather than aryl bromide.^[75] Aryl halides with adjacent electron withdrawing groups are more reactive to oxidative addition than those with donating groups, and will therefore increase the rate of the reaction.^[67] The ability of leaving groups is based on the strength of the carbon-halogen bonds and decreases in the order of $I > Br \gg Cl \gg F$.^[76]

Two alternative pathways have been proposed for the transmetalation step; the boronate pathway and the oxo-palladium pathway. The boronate pathway suggests that the base initially binds to the boronic acid forming the organoboronate species and then substitutes the leaving group in the coordination sphere of the palladium complex. The oxo-palladium pathway suggests a direct substitution between the base and the leaving group in the coordination sphere of the palladium complex.^[77] ^[68] ^[78] Scheme 1.8 illustrates the two pathways of the transmetalation step.



Scheme 1.8: The boronate (pathway A) and oxo-palladium pathway (pathway B) in the transmetalation step of the Suzuki reaction.^[78]

The electronic properties of the ligands on palladium play an important role in the final reductive elimination step of the catalytic cycle.^[79] Complexes with stronger electron donating ligands will react faster and enhance the rate in the reductive elimination step than with weak electron donating ligands. Electron poor complexes will therefore react faster

than electron rich complexes.^{[80] [81]} The presence of a base is also necessary for this step.^[71]

Another important issue is the "Bite angle" of the bidentate diphosphine ligands in Pd-complexes. Casey *et al.* defines the natural bite angle (β_n) as the preferred chelation angle only determined by the ligand backbone constraints.^[82] Wide bite angles and bulkiness of the ligands generally facilitate the reductive elimination in palladium catalysis, resulting in a more effective Suzuki cross coupling. A wide bite angle in metal complexes can have two different effects. Firstly, the effective steric bulk of the bidentate ligand increases, and secondly, can it favor or disfavor specified geometries in the transition metal complex.^[83]

1.7.2 Catalysts

The most commonly used catalysts in Suzuki cross-coupling today are palladium catalysts. The use of monodentate, bulky, and electron rich phosphine ligands, has greatly improved the selectivity and the efficiency of palladium catalyzed carbon-carbon reactions. The rate of both the oxidative addition step and the reductive elimination step gets enhanced by employing steric bulky and electron rich phosphine ligands. A possible reason for this is that the ligands have electron donating and bulky properties that are necessary for stabilizing the monoligated palladium complexes, which are critical intermediates in the catalytic circle.^{[84] [85]} The phosphine ligands also show other useful attributes like air stability and a high degree of thermal stability.^{[67] [86]} Some of the most common used palladium catalysts include Pd(PPh₃)₄, Pd(OAc)₂, Pd₂(dba)₃, Pd(dppf)Cl₂ and XPhos.^{[67] [87]} The electron rich ferrocene based palladium catalyst, Pd(dppf)Cl₂, has earlier been used in the research group affording full conversion after a short amount of time leading to good results.^[40] The structures of these common palladium catalysts are il-

illustrated in Figure 1.7

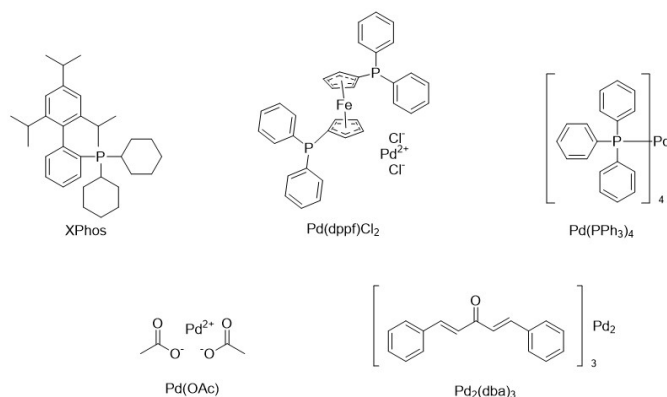
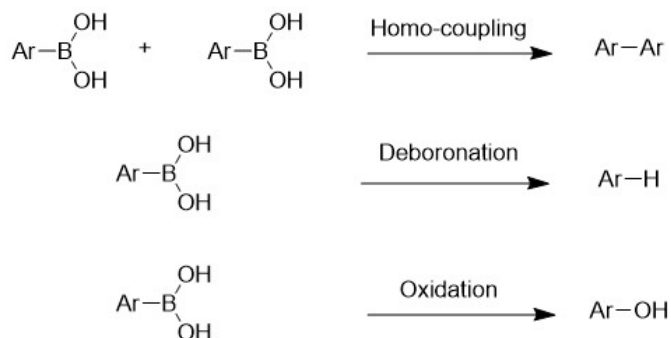


Figure 1.7: Structures for common palladium catalysts used in Suzuki cross-coupling

1.7.3 Side reactions and products

There can often occur side reactions and formation of byproducts in Suzuki cross-couplings. The most common types of side reactions affect the boronic reagent in the Suzuki reaction and include palladium catalyzed homocoupling, protodeboronation and oxidation.^{[69] [88]} Side reactions such as catalyst decomposition and dehalogenation of the organo halide are also common side reactions.^{[89] [90]} The side reactions of the boronic acids in the Suzuki cross-coupling reaction are illustrated in Scheme 1.9.



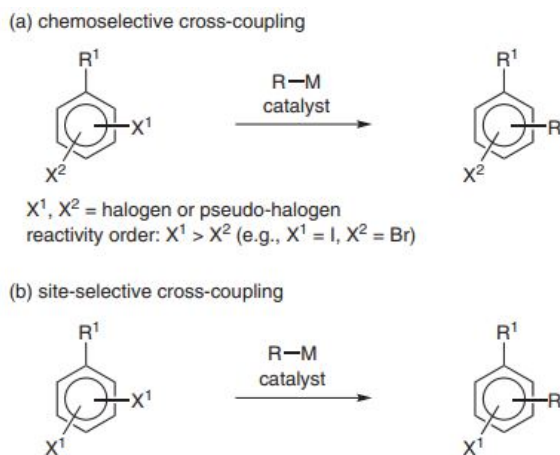
Scheme 1.9: Possible side reactions for boronic acids in Suzuki cross-coupling

Both the palladium catalyzed homocoupling and the oxidation are side reactions caused by undesired oxidative processes in the Suzuki cross coupling reaction. In the oxidation reaction hydroperoxides are generated in ethereal solvents via metal-catalyzed aerobic oxidation, which oxidates the boronic acid and produces a hydroxide product via hydrolysis. This side reaction can be prevented by adding a quenching reagent before the coupling, to eliminate the hydroperoxides in the solvent.^{[88][91]} The palladium catalyzed homo coupling reaction proceeds via a peroxy complex in the presence of dioxygen with palladium(0) to generate the byproduct of symmetrical biaryls. This homo-coupling reaction runs in competition with the desired Suzuki cross-coupling, due to a common palladium intermediate in the reaction process, and is therefore a common side reaction in Suzuki cross-coupling.^{[88][92]} The last side reaction of boronic acids in Suzuki cross-couplings is protodeboronation, which is a reaction where the boron from the organic fragment is exchanged for a proton.^{[88][93]}

1.7.4 Selectivity in cross-coupling

Selective coupling can be an important factor when developing a synthetic route to organic molecules. Selectivity can be achieved by using suitable starting materials, reagents, solvents, and reaction conditions.

The oxidative addition step is generally assumed to be the selectivity-determining step in cross coupling reactions.^[94] Selectivity between halo groups plays an important part in cross-coupling in the oxidative addition. Halo groups can be used to introduce a desired substituent to a specific position on the target molecule. This is called a chemoselective reaction. The reactivity order for the halo groups in chemoselective reactions are $I > Br > Cl > F$.^{[67][95]} The site of the reaction will usually happen where the weakest carbon-halogen bond is. A site-selective or regioselective cross-coupling happens if two similar halogens are present in the same molecule. The reaction is then usually favored at the more electron deficient position.^[95] Scheme 1.10 illustrates the difference of chemo- and regioselectivity in Suzuki cross-coupling.



Scheme 1.10: Chemo- and regioselectivity between halo groups in Suzuki cross-coupling^[95]

Regioselectivity in cross-coupling can also be influenced by steric and electronic effects, as well as directing groups at neighboring sites to the reactive position.^{[95][96]} It has also been proven by Strotman *et al* that it's possible to change the regioselectivity for some dihaloazoles, by changing the palladium catalyst allowing a Suzuki coupling at the less reactive carbon-halogen bond.^[97]

1.8 SEM-deprotection

The pyrrole group is a very reactive compound that is susceptible to electrophilic aromatic substitution due to the lone pair of electrons on its nitrogen atom and the consequent stabilisation of its intermediate structures.^[49] Due to the high reactivity of the pyrrole unit is it important to have control of the nucleophilicity of the electron rich pyrrolic core to avoid unwanted transformations. These unwanted reactions can inhibit desired nucleophilic reactions and can cause polymerization of the pyrrole. The reactivity of pyrroles is therefore often harnessed or controlled by the use of electron withdrawing protective or blocking groups to reduce the nucleophilicity of the pyrrole while also preventing unwanted substitution at specific positions.^{[49][98]}

There exist many available protection groups for the nitrogen atom in pyrrole rings. Sulfonyl groups are often used for pyrrole protection due to their strong electron withdrawing effect and their ability to decrease pyrrole reactivity. Sulfonyl groups such as benzenesulfonyl (Bs) and toluenesulfonyl (Ts) are some examples of common groups for pyrrole protection. Other common electron withdrawing groups for pyrrole protection include the *tert*-butoxycarbonyl (Boc) group, the triisopropylsilyl (TIPS) group and the 2-(trimethylsilyl)ethoxymethyl (SEM) group.^[49] The structure of these pyrrole protecting groups are given in Figure 1.8.

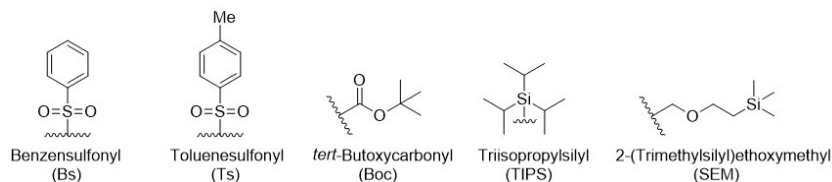
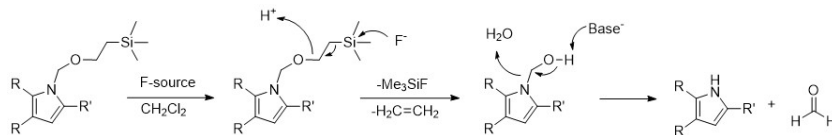


Figure 1.8: Structures of common pyrrole protecting groups.

Many protective groups are unsuitable for pyrrole protection due to harsh conditions for removal of the *N*-protecting group.^[99] The 2-(trimethylsilyl)ethoxymethyl (SEM) group is a stable *N*-protecting group for pyrroles that has proved to have high stability properties toward acidic, basic, reductive and oxidative conditions.^[48]^[49] It has been reported by Edwards *et al.* that the SEM-group also can be used as a directing group in direct metalation.^[47]

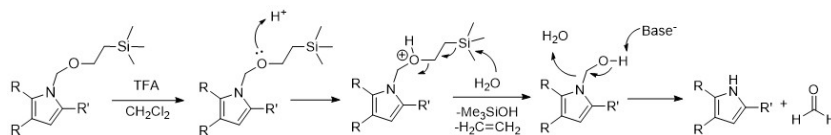
The removal of the protective SEM-group can be done by using fluoride sources such as, tetrabutyl ammonium fluoride (TBAF) in THF^[100]^[101] and lithium tetrafluoroborate (LiBF₄) in aqueous ammonia^[102]. A suggested mechanism for the SEM-protection reaction using fluoride sources is illustrated in Scheme 1.11.



Scheme 1.11: Proposed mechanism for the removal of the SEM-protection group on the pyrrole using a fluoride source.^[103]

The SEM-group can also be removed in acidic conditions with trifluoroacetic acid (TFA) in DCM followed by basic conditions.^[49] In previous work by the research group, SEM-deprotection reaction has been done in a two step reaction using the latter conditions.^[40] The first step intro-

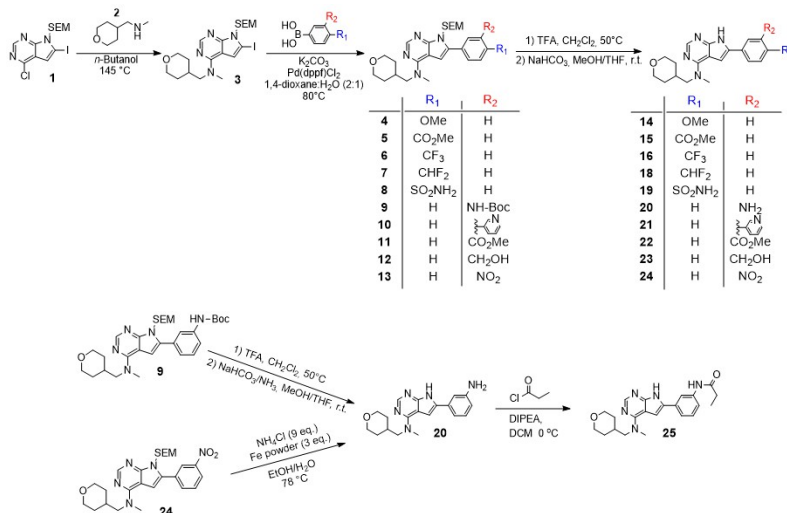
duces the pyrrolopyrimidine to TFA in DCM for removing the trimethylsilyl (SiMe_3) part of the SEM-group. The second step is done under basic conditions with saturated aqueous NaHCO_3 and THF, for removal of the remainder of the SEM-group, giving the desired product. A suggested mechanism for the SEM-protection reaction using acidic conditions is illustrated in Scheme 1.12.



Scheme 1.12: Proposed mechanism for the removal of the SEM-protection group on the pyrrole using an acidic conditions.

2 Results and Discussion

The aim of this master's thesis was to synthesize new CSF-1R inhibitors based on the pyrrolopyrimidine scaffold, as well as preparing pyrrolopyrimidine derivatives in enzymatic studies. The total synthesis route is shown in Scheme 2.1. The starting material of the synthesis, compound **1**, was previously prepared by direct metalation in the pre-master project^[104], thus the first step in the synthesis was a nucleophilic aromatic substitution with amine **2** at C-4 to obtain compound **3**. The second part of the synthesis was Suzuki cross-coupling reactions with different boronic acids at C-6 to obtain compound **4-13**. The final products **14-23** were obtained by removal of the SEM-protecting group on the pyrrole. Compound **17** was obtained by hydrolysis of the methyl ester **15** and compound **25** was prepared by acylation of the aniline **20**.



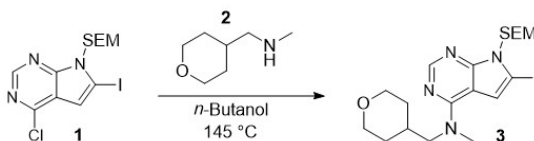
Scheme 2.1: Total synthesis route towards the target pyrrolopyrimidine compounds **14-25**.

There are a total of six subsections in this result and discussion chap-

ter. Section 2.1-2.4 covers the different synthetic steps performed in the synthesis route shown in Figure 2.1. The fifth subsection addresses the structural elucidation of the new pyrrolopyrimidines synthesized, while the final section presents the results of the CSF-1R inhibition activity .

2.1 Amination

Nucleophilic aromatic substitution was performed to introduce the amine **2** at the C-4 position on the pyrrolopyrimidine **1** to synthesize the key intermediate **3**. The reaction was carried out under an inert N₂-atmosphere at 145 °C, see Scheme 2.2. The thermal amination followed the procedure described by Kaspersen *et al.*^[41] Scheme 2.2 illustrates the thermal amination reaction.



Scheme 2.2: Nucleophilic aromatic substitution of compound **1** in position C-4.

The thermal amination reaction was performed at a 1.2 g scale to obtain the desired product **3**. Compound **1** was dissolved in *n*-butanol, before the secondary amine (1.5 eq.) **2** and DIPEA (1.5 eq.) were added to reaction mixture. DIPEA was used as a co-base to scavenge excess HCl produced in the reaction. Full conversion of the reaction was reached after 3.5 hours and the crude product was purified by silica-gel column chromatography using *n*-pentane/EtOAc (1/1) as the eluent system.

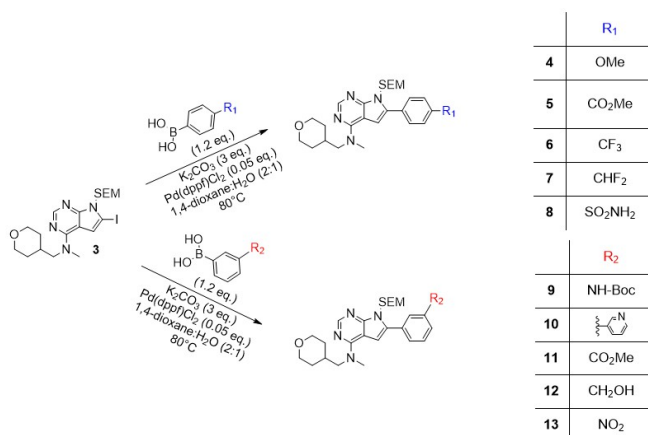
Compound **3** was isolated in a 78% yield as a transparent oil. This was the expected yield compared to earlier aminations done with the same amine **2** in the pre-master project.^[104] The previous experiments were done in a 500 mg scale, implicating that increasing the scale to 1.2 g

didn't affect the reaction in any significant way. The spectroscopic data of the pyrrolopyrimidine **3** are attached in Appendix B.

2.2 Suzuki Cross-Coupling

Suzuki cross-coupling between pyrrolopyrimidine **3** and various aryl boronic acids with functional groups in either *para* or *meta* position were performed to synthesize the 6-arylated derivatives **4-13**. The Suzuki cross-couplings followed the procedure described by Han *et al.*^[40]

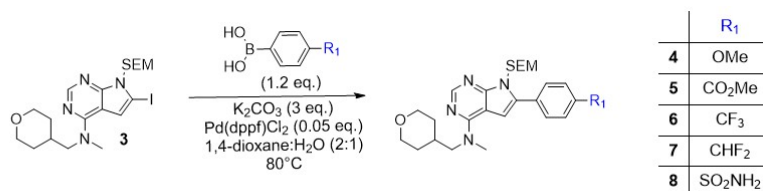
The Suzuki cross-couplings were carried out with the same reaction conditions used under the pre-master project.^[104] The pyrrolopyrimidine building block **3** was mixed with various aryl boronic acids (1.2 eq.), K₂CO₃ (3 eq.) as the base, Pd(dppf)Cl₂ (0.05 eq.) as the catalyst and degassed 1,4-dioxane/H₂O (2:1). The reactions were performed at 80 °C under an inert N₂-atmosphere. Scheme 2.3 illustrates the general reaction conditions for the Suzuki cross-coupling reactions between compound **3** and the various boronic acids.



Scheme 2.3: Synthesis of compounds **4-13** by Suzuki cross-coupling with the key intermediate **3**.

2.2.1 Synthesis of Compounds 4-8

Suzuki cross-couplings with five boronic acids with different functionalities in *para*-position were performed to synthesize compounds **4-8**, see Scheme 2.4. The reactions were conducted in three different scales; one in a 1000 g scale, one in a 400 mg scale and three in a 150 mg scale. The scale-up of the intermediate **4** was done due to the need of product in animal studies.



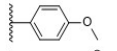
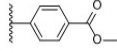
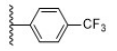
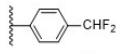
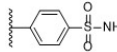
Scheme 2.4: Synthesis of compound **4-8** by Suzuki cross-coupling of compound **3**.

TLC and ¹H-NMR analysis confirmed that all five of the reactions reached full conversion within 10-30 minutes. All the reaction mixtures also changed from a transparent colour to a black-brown colour a few minutes after the initiation of the reactions. The reaction time between 4-methoxyphenylboronic acid and compound **3** was 30 minutes, which is slower than for the other substrates. A possible explanation could be that the solubility of the reactants was affected by the use of too little solvent in the reaction causing a slow mass transfer.

After work up, purification of the crude products was performed by silica-gel column chromatography using *n*-pentane/EtOAc (1/1) as the eluent system. The eluent system resulted in *R_f*-values between 0.29-0.38. The products were isolated as oils with various colours in high yields. The results from the Suzuki cross-coupling reactions with *para*-substituted

arylboronic acids are summarized in Table 2.1, in addition to scale and reaction time. The spectroscopic data of the compounds are attached in Appendix C-G.

Table 2.1: Results of the synthesis of the pyrrolopyrimidines **4-8**.

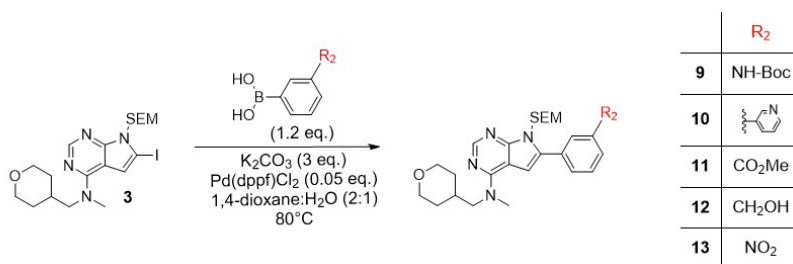
Comp.	Boronic acid	Scale [mg]	Conv. ^a [%]	Time [min]	State	Yield ^b [%]
4		1080	>99	30	Transparent oil	97
5		401	>99	11	Brown oil	78
6		150	>99	10	Transparent oil	94
7		150	>99	12	Transparent oil	99
8		150	>99	12	Brown oil	86

^a Conversion was measured by ¹H-NMR spectroscopy

^b Isolated yield after silica-gel column chromatography

2.2.2 Synthesis of compound **9-13**

Suzuki cross-couplings with boronic acids with different functionalities in *meta*-position were performed to synthesize compound **9-13**, see Scheme 2.5. The reactions were conducted in different scales within 100-500 mg.



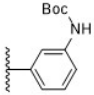
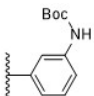
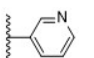
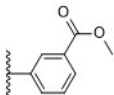
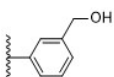
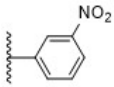
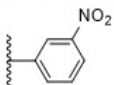
Scheme 2.5: Synthesis of compound **9-13** by Suzuki cross-coupling of compound **3**.

TLC and $^1\text{H-NMR}$ analysis confirmed that all of the reactions reached full conversion within 10-15 minutes. All the reaction mixtures also changed from a transparent colour to a black-brown colour a few minutes after initiation of the reactions.

After work up, purification of the crude products was performed by silica-gel column chromatography using *n*-pentane/EtOAc (1/1) as the eluent system. The products were isolated as oils with various colours and with high yields. Compounds **9** and **13** were prepared twice to provide enough material for later syntheses in the master project. The lower yield of 65% of the first reaction of compound **9** may have been due to crystallization on the silica-gel column.

The results from the Suzuki cross-coupling reactions with *meta*-substituted arylboronic acids are summarized in Table 2.2. The spectroscopic data of the compounds are attached in Appendix H-L.

Table 2.2: Results of the synthesis of the pyrrolopyrimidines **9-13**.

Comp.	Boronic acid	Scale [mg]	Conv. ^a [%]	Time [min]	State	Yield ^b [%]
9		501	>99	10	Transparent oil	65
9		501	>99	10	Transparent oil	77
10		266	>99	15	Transparent oil	82
11		202	>99	12	Transparent oil	89
12		150	>99	13	Red oil	85
13		101	>99	11	Yellow oil	98
13		501	>99	15	Yellow oil	94

^a) Conversion was measured by ¹H-NMR spectroscopy

^b) Isolated yield after silica-gel column chromatography

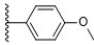
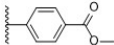
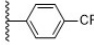
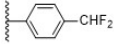
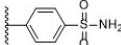
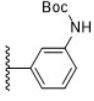
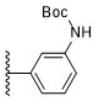
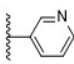
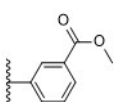
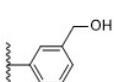
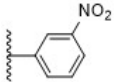
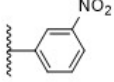
2.2.3 Summary of the Suzuki Cross-Couplings

All the Suzuki cross-couplings were performed between compound **3** and various aryl boronic acids with different functional groups in either *para* or *meta* position. The reaction conditions have been the same with respect to the equivalents of boronic acid, catalyst and base, with a constant reaction temperature of 80 °C. The solvents 1,4-dioxane and water have also been used with a ratio of 2:1. A total of 10 different

Suzuki cross-couplings have been performed to synthesize compound **4-13**. The results from the Suzuki cross coupling reactions are summarized in Table 2.3. The spectroscopic data of the cross-coupled compounds are attached in Appendix C-L.

Overall, the position or the electronic nature of the substituents, did not have a major impact on reaction rate, yield or purity. The lower rate in the case of compound **4** is most likely attributed to scale-up effects. This can be substantiated by that compound **4** was also prepared in the pre-master project in a considerably smaller scale with a reaction time similar to all the other compounds.^[104]

Table 2.3: Summary of the results obtained from the Suzuki cross-coupling reactions of the pyrrolopyrimidines **4-13**.

Comp.	Boronic acid	Scale [mg]	Conv. ^a [%]	Time [min]	State	Yield ^b [%]
4		1080	>99	30	Transparent oil	97
5		401	>99	11	Brown oil	78
6		150	>99	10	Transparent oil	94
7		150	>99	12	Transparent oil	99
8		150	>99	12	Brown oil	86
9		501	>99	10	Transparent oil	65
9		501	>99	10	Transparent oil	77
10		266	>99	15	Transparent oil	82
11		202	>99	12	Transparent oil	89
12		150	>99	13	Red oil	85
13		101	>99	11	Yellow oil	98
13		501	>99	15	Yellow oil	94

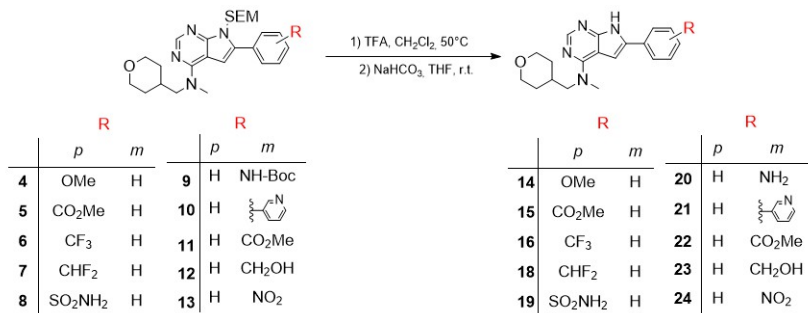
a) Conversion was measured by ¹H-NMR spectroscopy

b) Isolated yield after silica-gel column chromatography

2.3 SEM-Deprotection

The last synthesis step towards potential CSF-1R inhibitors was the removal of the SEM-protecting group which was performed in a two step process, see Figure 2.1. In the first step the pyrrolopyrimides were dissolved in trifluoroacetic acid (TFA) and CH_2Cl_2 , and stirred for 2.5-3.5 hours at 50 °C before they were concentrated in *vacuo*. The second step was performed at room temperature under basic conditions with saturated aqueous NaHCO_3 and THF.

Scheme 2.6 illustrates the general synthesis scheme of the target compounds **14-16** and **18-24** by the removal of the SEM-protecting group.



Scheme 2.6: Synthesis of the target inhibitors **14-16** and **18-24** by SEM-deprotection.

The conversion rate of the substrates was monitored by ¹H-NMR spectroscopy in both steps of the reaction to ensure full conversion. After work up, purification of the crude products was performed by silica-gel column chromatography, isolating the target compounds **14-16** and **18-24**. The purity of the target compounds was measured by HPLC with a desired high purity of over 95%. The results of the SEM-deprotection reactions are summarized in Table 2.4. The spectroscopic data of the isolated products are presented in Appendix M-W.

Table 2.4: Results of the SEM-deprotection performed to obtain target compound **14-16** and **18-24**

Compound	Scale [mg]	Reaction Time [h]		State	Yield [%]	Purity ^a [%]
		Step 1	Step 2			
14	1080	4	18	White solid	65	97
15	142	3.5	5	White solid	96	98
16	118	2.5	16	White solid	63	>99
18	103	2.5	16	White solid	80	97
19	121	2.5	16	White solid	95	96
20	264	3	18	White solid	58	95
21	180	3.5	18	White solid	70	99
22	150	2.5	16	White solid	64	>99
23	80	2.5	16	White solid	85	98
24	97	3	19	Yellow solid	65	98
24	471	2.5	17	Yellow solid	80	98

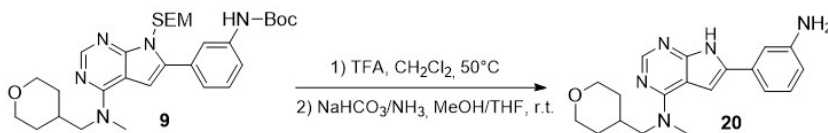
^a Purity was measured by HPLC

All the SEM-deprotection reactions were comparable in terms of reaction time for both steps. The reaction time in the first step varied between 2.5-3.5 hours, while the second step was usually stirred overnight due to mild reaction conditions. The difference in isolated yields varied greatly between the different substances with the yields ranging from 58-96%, even though the reactions conditions were similar for all the reactions. A possible reason for the products with modest yields may be due to a challenging work up because of the crystalline nature of the deprotected pyrrolopyrimidine compound and loss of product during silica gel column chromatography. The low yield of substance **20** is discussed in more detail in Section 2.3.1.

$^1\text{H-NMR}$ and $^{13}\text{C-NMR}$ analysis of the final products didn't show any unexpected peaks other than the product and solvent residues signals. The $^{19}\text{F-NMR}$ analysis of compound **16** however revealed the ^{19}F signal peak for trifluoroacetic acid (TFA) at -78.6 ppm, meaning that excess TFA had remained in the crude product after step two with basic conditions in the SEM-deprotection. Nevertheless, HPLC showed that the compound had a purity of over 99%. An article by Sloop *et. al.* reports that the range of ^{19}F chemical shifts for the TFA group generally differs from -85 to -67 ppm.^[105] No signs of excess TFA were found in the fluorine compound **18**.

2.3.1 Synthesis of compound **20**

The SEM-deprotection of compound **9** was performed two times to isolate the final product **20**. The synthesis of this aniline is looked closer in to because it is a precursor to the target amide **25**. This synthesis was performed with the reaction conditions in Scheme 2.7.



Scheme 2.7: Synthesis of the target compound **20** by SEM-deprotection.

The first step of the synthesis showed full conversion on both TLC and $^1\text{H-NMR}$ analysis for both reactions. The second step was performed with two different base systems. The first test reaction was performed with saturated aqueous NaHCO₃ and THF at room temperature and stirred overnight. Both $^1\text{H-NMR}$ analyses and TLC of the reaction showed incomplete conversion, so a different base system with 25 % aqueous NH₃-solution and MeOH was used instead in the second step of

the SEM-deprotection. This reaction was also performed at room temperature and stirred overnight. The reaction with NH_3/MeOH seemed to have full conversion as analysed by TLC and $^1\text{H-NMR}$. Due to an incomplete conversion to product in the reaction with the NaHCO_3 , only the product from the NH_3 reaction was worked-up and purified.

After work up, three rounds of purification by silica-gel column chromatography was needed to isolate compound **20** in a moderate yield of 58 % with a purity of 95%. $^1\text{H-NMR}$ analysis showed that some byproducts still were present in the isolated product, so HPLC analyses were therefore conducted after each purification to see the improvement of the purity. The results from the reactions are given in Table 2.5.

Table 2.5: Results from the synthesis of compound **20**

Entry	Base-system	Purity ^a 1 [%]	Purity ^a 2 [%]	Purity ^a 3 [%]	Yield [%]
1	NaHCO_3 , THF	-	-	-	-
2	NH_3 , MeOH	80	91	95	58

^a Purity was measured by HPLC

Mass spectroscopy and NMR characterization were conducted to try to identify the byproduct in the isolated product **20**. This indicated that the tetrahydropyran group (THP) had been cleaved off in the pyrrolopyrimidine compound, but the mass spectroscopy didn't propose any plausible molecular formulas that matched the observations from NMR-spectroscopy. The results indicated also that the byproduct was more unpolar than the main product. Figure 2.1 illustrates the chromatogram of the assumed byproduct compared to the isolated product **20**.

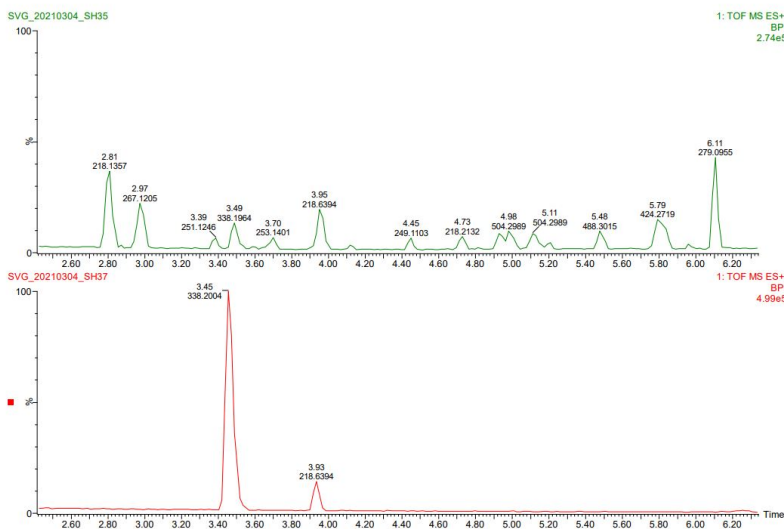


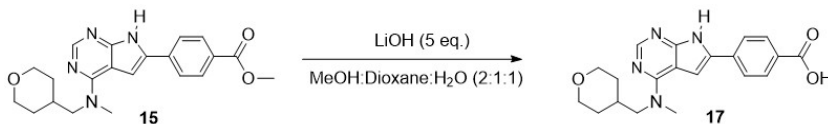
Figure 2.1: Chromatogram of the assumed byproduct and the isolated product **20**.

A common side product in SEM-deprotections is the formation of formaldehyde, see Section 1.8. It could be possible that the formaldehyde have reacted to the free benzylic amino group resulting in the unwanted byproduct. Due to the noticeable byproduct in the isolated product an alternative synthesis route was proposed to achieve a higher yield and purity of compound **20**, see Section 2.4.2.

2.4 Post modifications

2.4.1 Synthesis of compound **17** by hydrolysis

Hydrolysis of compound **15** was performed to replace the alkoxy group (OMe) of the ester with a hydroxy group to give the carboxylic acid **17**, see Scheme 2.8.



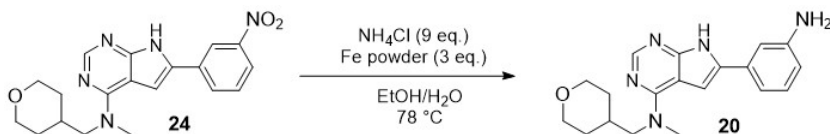
Scheme 2.8: Synthesis of the target compound **17** by hydrolysis.

The reaction was carried out at 50 °C by mixing the methyl ester **15** in a LiOH solution together with a 2:1:1 mixture of MeOH, 1,4-dioxane and water. The conversion of the substrate was monitored by TLC during the reaction, and the reaction was stopped after 24 hours with full conversion confirmed also by ¹H-NMR spectroscopy. The reaction mixture was then concentrated in *vacuo* before the residue was diluted with water. The pH of the diluted mixture was then adjusted to between 2.5-3.0 with HCl before the product **17** was isolated by cold filtration with a yield of 29%. The purity of the compound was measured by HPLC to 99%.

The cold filtration gave a very pure product but a major part was lost as it got stuck on the filtration paper. It was also believed that a sizable part of the product was lost in the diluted water mixture, due to the product's high solubility in the water. The filtrate was saved and used in extraction to try to recover more of the product. By extraction approximately 10% of the product was recovered but ¹H-NMR showed a very impure product. In conclusion the cold filtration was a better method than the extraction to obtain a pure hydrolysis product. Nevertheless, should there be investigated a better method to isolate the product in higher yields. The spectroscopic data of the isolated product **17** are presented in Appendix P.

2.4.2 Synthesis of compound **20** by reduction

Reduction of the nitro group in compound **24** was performed as an alternative way to synthesize the aniline compound **20**, see Scheme 2.9.



Scheme 2.9: Synthesis of the target compound **20** by reduction

Two reductions were performed; one test reaction at 37 mg and one larger scale reaction at 250 mg. The reactions were carried out by dissolving the nitro derivative **24**, NH₄Cl and iron powder in 7:3 degassed EtOH/H₂O under a N₂-atmosphere. The iron powder acted as the reducing agent in this reaction. Both reactions were stirred at 78 °C for 3 hours until full conversion was confirmed by ¹H-NMR spectroscopy. The change of the initial yellow colour in the reaction mixture, caused by the nitro group, to a more transparent colour was also a sign of full conversion. After work up, purification of the crude products was performed by silica-gel column chromatography isolating compound **20** in yields of 81 % and 63 % as white solids. The purity of the compounds was measured by HPLC with a desired high purity (>99%).

The reduction route for isolating compound **20** was a better method in comparison with the method described in Section 2.3.1 in regards to both yield and purity. The results of the reductions are given in Table 2.6. The spectroscopic data of the isolated product are presented in Appendix S.

Table 2.6: Results of the synthesis of compound **20** by reduction

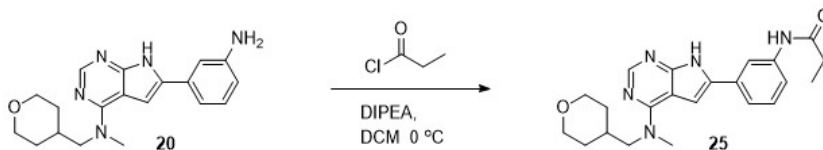
Experiment	Scale [mg]	Conversion ^a [%]	State	Yield [%]	Purity ^b [%]
1	37	>99	White solid	81	99
2	250	>99	White solid	63	99

^a Conversion was measured by ¹H-NMR spectroscopy

^b Purity was measured by HPLC

2.4.3 Synthesis of compound **25** by acylation

Acylation of the aniline compound **20** was performed to arrive at the amide **25**. The synthesis was carried out with the reaction conditions shown in Scheme 2.10.

**Scheme 2.10:** Synthesis of the target compound **25** by acylation.

The reaction was carried out in a 70 mg scale by dissolving the aniline **20** in DCM and DIPEA and then cooling down the mixture to 0 °C. Propionyl chloride was then added dropwise under a nitrogen atmosphere before the reaction mixture was stirred over night and quenched with NaHCO₃. ¹H-NMR showed full conversion of the substrate. After work up, purification of the crude product was performed by silica-gel column chromatography to isolate the target amide **25** in a yield of 69% and a purity of 98%. The spectroscopic data of the isolated product are presented in Appendix X.

The reaction between compound **20** and propionyl chloride was expected

to give a diacylated product at N-7 and N-25 when using 2.5 equivalents of the acyl chloride, but $^1\text{H-NMR}$ analysis and mass spectroscopy revealed that the acyl chloride had connected selectively to the N-25 atom in the product. A possible reason for this is that substituents on the pyrrole nitrogen are often very labile, and therefore easily cleaved of under harsh reaction conditions.

2.5 Structure Elucidation

To verify the identity of the new pyrrolopyrimidines synthesized, structure elucidation was performed. The NMR-spectroscopic methods ^1H -NMR, ^{13}C -NMR, ^{19}F -NMR, ^1H - ^1H COSY, ^1H - ^{13}C HSQC and ^1H - ^{13}C HMBC were used to assign the chemical shifts and confirm the structure of the compounds **6-13** and **16-25**. Compounds **1-5** and **14-15** were prepared and characterised in the pre-master project.^[104] The molecular formulas of the various compounds were determined by high-resolution mass spectroscopy (HRMS) and IR was used to confirm the presence of their functional groups. All the spectra can be found in Appendix A-W. Table 2.7 displays the signals of common solvents found in some of the ^1H - and ^{13}C spectra of the compounds.

Table 2.7: Signals of common solvents used in ^1H - and ^{13}C NMR.

	CDCl_3		$\text{DMSO-}d_6$	
	^1H	^{13}C	^1H	^{13}C
Solvent residue	7.26	77.16	2.50	39.52
H_2O	1.56	-	3.33	-
CH_2Cl_2	5.30	53.52	5.76	54.84
EtOAc	4.12, 2.05	21.04	1.99, 4.03	20.68

^1H -NMR spectroscopy was used to assign the proton shifts, the integrals, the multiplicity and the coupling constants for the protons in the synthesized compounds. ^1H - ^1H COSY spectroscopy was used to determine the correlation signals for the neighboring protons in the compounds. ^1H - ^{13}C HMBC, which shows the coupling between carbon and hydrogen atoms 2-4 carbon atoms away from the observed carbon, was then used to confirm the positions of the assigned protons.

The coupling between the carbon and its attached protons was determined by ^1H - ^{13}C HSQC. The quaternary carbons without protons were assigned with ^1H - ^{13}C HMBC. These ^1H - ^{13}C couplings are shown for compounds **4** and **14** in Figure 2.2. The ^1H - ^{13}C couplings of the other pyrrolopyrimidines connects in a similar matter due to their structural similarities.

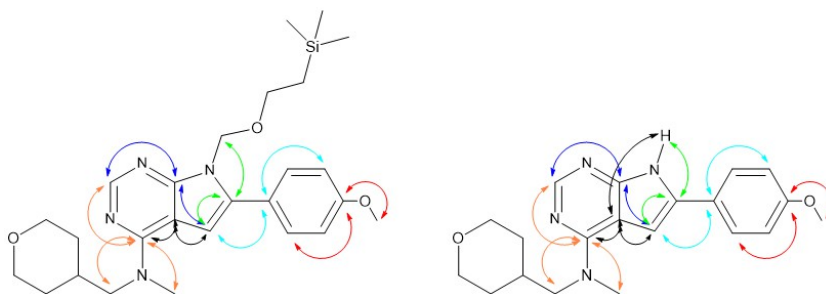


Figure 2.2: ^1H - ^{13}C HMBC connectivity used in the structural elucidation of the quaternary carbons in **4** and **14**

2.5.1 Common spectroscopic trends

The ^1H -NMR and ^{13}C -NMR shifts of the protected and deprotected compounds are very much alike, due to their structural similarities. There are generally only observed small variations in the chemical shifts. The aromatic ^1H and ^{13}C chemical shifts are influenced by the electron density in the ring and are generally found within 7-9 ppm for the ^1H -shifts and 110-135 ppm for the ^{13}C -shifts in the pyrrolopyrimidine compounds.

The ^1H -NMR and ^{13}C -NMR shift values of the tetrahydropyran (THP) group are normally around 3.82/3.23 ppm and 1.52/1.26 ppm, and 30.2 ppm and 66.7 ppm for the C-14 and C-15 atoms, respectively. Due to the complexity of some of the signals in the THP group, these are defined as multiplets. The ^1H -NMR signals of the THP unit are illustrated in Figure 2.3.

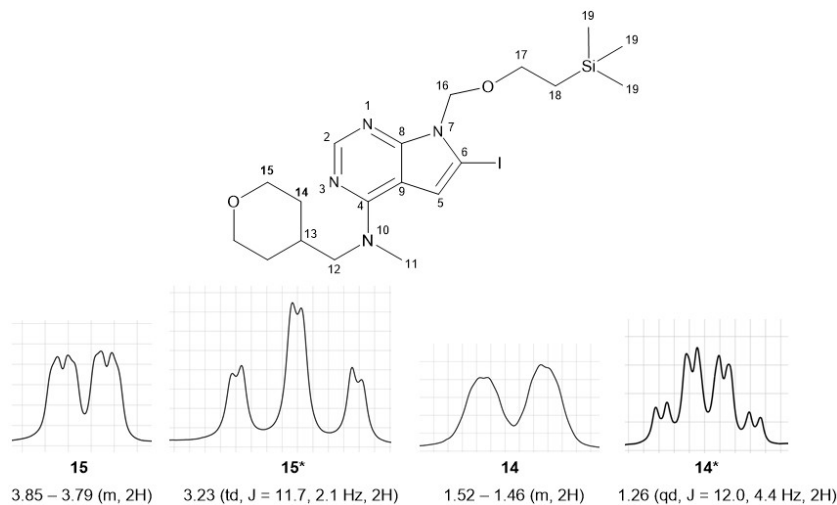


Figure 2.3: Common ¹H-NMR signals of the tetrahydropyran (THP) unit.

The signal at position 15 arises from the pair of equatorial protons adjacent to the oxygen atom. These should in theory give one large geminal split ($J \approx 12$ Hz) and two smaller vicinal connections (equatorial-axial + equatorial-equatorial).^[106] The fine splitting in the signal makes it hard to find straight peaks that are connected to calculate coupling constants, and it is therefore treated as a multiplet with a chemical shift around 3.85-3.79 ppm.

The signal at position 15* arises from the pair of axial protons adjacent to the oxygen atom. This signal should in theory give a ddd (doublet of doublet of doublet)^[106], but it seems that the geminal coupling constant is approximately equal to the vicinal (axial-axial) coupling constant ($J \approx 12$ Hz). This makes the signal appear like a td (triplet of doublets) with a chemical shift around 3.23 ppm.

The signal at position 14 arises from the pair of equatorial protons between the protons in position 15 and 13. This signal should in theory give a

dddd (doublet of doublet of doublet of doublet)^[106], but the fine splitting in the signal makes it hard to find straight peaks that are connected to calculate coupling constants, and it is therefore treated as a multiplet with a chemical shift around 1.52–1.46 ppm.

The axial pair of protons at position 14* acts the same way as the signal at position 15*. This signal should in theory give a dddd, but since the geminal coupling constant is approximately equal to the vicinal coupling constant, does the signal look like a qd (quartet of doublets).

The SEM-group in the protected pyrrolopyrimidines show distinct ¹H-NMR signals for the aliphatic protons in position 17 and 18, see Figure 2.4

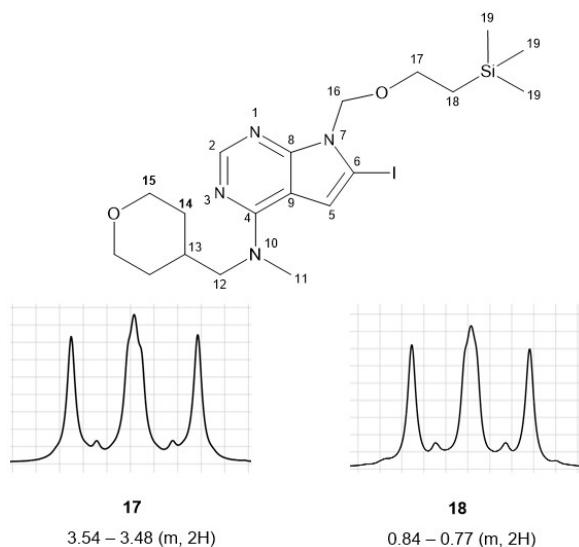


Figure 2.4: Common ¹H-NMR signals of the SEM group.

The ¹H-NMR signals at C-17 and C-18 should in theory both be triplets, but due to almost identical coupling constants and the high order splitting of the signals, both are therefore treated as multiplets with a chemi-

cal shift of 3.54–3.48 and 0.84–0.77 ppm, respectively. Both the ^1H -NMR signals for the protons in position C-16 and C-19 are observed as singlets at around 5.57 and -0.10 ppm, respectively.

The main differences of the protected and deprotected pyrrolopyrimidines are that the four signals from the aliphatic region of the SEM-group in compounds are gone in the deprotected compounds after removal of the SEM-group. The SEM-deprotection results in a new proton signal from the N-7 atom which is usually found around 12 ppm. The removal of the SEM protecting group also appears to cause a decrease of the chemical shift at the C-5 atom.

2.5.2 Compounds **6**, **7**, **16** and **18**

The ^1H -NMR and ^{13}C -NMR shifts for the difluoro- and trifluoro derivatives **6** and **7**, and **16** and **18** are presented in Table 2.8 and Table 2.9. The spectroscopic spectra for the compounds are given in Appendix E, F, O and Q

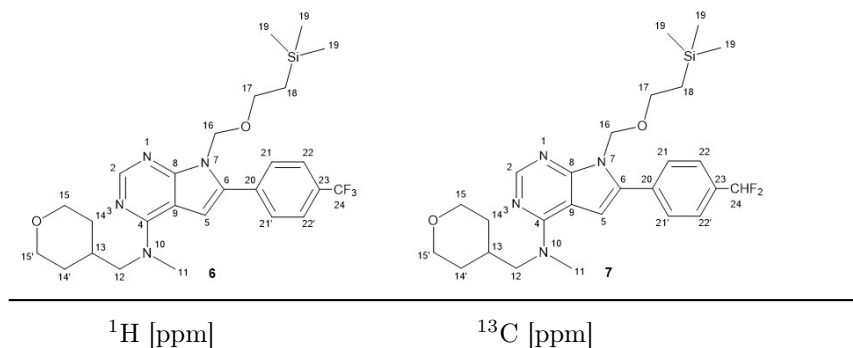
The aromatic carbons at position 22, 23 and 24 were observed as triplets in the ^{13}C -NMR spectra of compounds **7** and **18** and as quartets in the same positions for compounds **6** and **16**. These signals are triplets and quartets due to coupling with fluorine nuclei ("n+1" rule). The $^1\text{J}_{\text{CF}}$ coupling between carbon and fluorine in the CF_3 -group compound was 272.5 Hz and 271.4 Hz for compound **6** and **16**. The coupling constants in the *ipso* and *ortho* position for these compounds were both 31.6 Hz and 3.3 Hz respectively. These coupling constants corresponds well with earlier research done on C-F coupling done by Newmark *et al.*^[107] The $^1\text{J}_{\text{CF}}$ coupling constant for the CHF_2 -group was 235.9 Hz and 235.5 Hz for compound **7** and **18**. The coupling constants in the *ipso* and *ortho* position were 22.2 Hz and 5.9 Hz for compound **7** and 21.9 Hz and 6.0

Hz for compound **18**. These coupling constants corresponds well with common C-F shifts in CHF₂-groups.^[108]

The CHF₂-proton at position 24 for compounds **7** and **18** was also observed as a triplet in ¹H-NMR spectra due to hydrogen-fluorine coupling. The coupling constant for the CHF₂-proton was 56.1 Hz and 56.4 Hz for compounds **7** and **18** respectively.

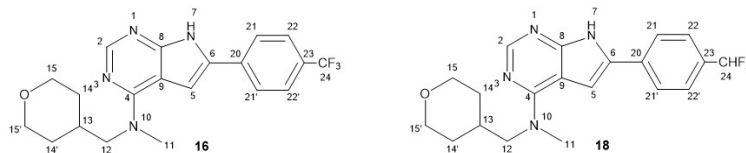
By comparing the CF₃-compounds with the CHF₂-compounds, large variations in ¹³C-shifts can be observed for the positions 23 and 24 in the compounds. The ¹³C chemical shift values have 8.5-8.6 higher ppm values in the CF₃-compounds than the CHF₂-analogues in the 24 position, but have 5.2-5.5 lower ppm values in the 23 position. The reason for the difference in the 24 position is that the CF₃-group is a more electron withdrawing group than the CHF₂ group, so it will decrease the electron density around the carbon nucleus and therefore resulting in a larger chemical shift values. Similar with the 23 position where the electron density is lower in the CHF₂ groups than the CF₃ group resulting in a larger chemical shift values in this position for the compounds **7** and **18**.^{[108] [109]}

Table 2.8: Assignment of ¹H- and ¹³C-NMR shifts for compounds **6** and **7**, obtained at 600 MHz and 150 MHz, respectively. All chemical shift values are given in ppm and the solvent used was DMSO-*d*₆.



Pos.	6	7	6	7
2	8.23	8.22	151.7	151.5
4	-	-	156.6	156.5
5	7.04	6.96	104.3	103.5
6	-	-	134.4	135.0
7	-	-	-	-
8	-	-	153.4	153.2
9	-	-	102.1	102.1
11	3.41	3.40	39.0	38.9
12	3.71	3.70	55.4	55.4
13	2.10-2.04	2.08-2.04	33.8	33.8
14/14'	1.52/1.28	1.52/1.28	30.2	30.2
15/15'	3.83/3.24	3.82/3.24	66.7	66.7
16	5.59	5.56	70.3	70.3
17	3.59	3.61	65.7	65.7
18	0.83	0.83	17.3	17.3
19	-0.10	-0.10	-1.5	-1.5
20	-	-	135.6	134.1
21	7.99	7.90	128.9	128.7
22	7.84	7.67	125.6	126.1
			(q, J = 3.3 Hz)	(t, J = 5.9 Hz)
23	-	-	128.1	133.3
			(q, J = 31.6 Hz)	(t, J = 22.2 Hz)
24	-	7.09	123.4	114.8
			(t, J = 56.1 Hz)	(q, J = 272.5 Hz)
				(t, J = 235.9 Hz)

Table 2.9: Assignment of ^1H - and ^{13}C -NMR shifts for compounds **16** and **18**, obtained at 600 MHz and 150 MHz, respectively. All chemical shift values are given in ppm and the solvent used was $\text{DMSO-}d_6$.



Pos.	^1H [ppm]		^{13}C [ppm]	
	16	18	16	18
2	8.14	8.13	151.7	151.5
4	-	-	156.6	156.5
5	7.28	7.21	101.3	100.4
6	-	-	131.2	131.8
7	12.31	12.23	-	-
8	-	-	153.2	153.1
9	-	-	103.3	103.3
11	3.41	3.41	38.9	38.9
12	3.70	3.70	55.3	55.3
13	2.10-2.04	2.08-2.04	33.9	33.9
14/14'	1.53/1.29	1.53/1.29	30.3	30.3
15/15'	3.83/3.24	3.83/3.24	66.7	66.7
16	-	-	-	-
17	-	-	-	-
18	-	-	-	-
19	-	-	-	-
20	-	-	135.5	134.0
21	8.09	8.01	125.0	124.8
22	7.76	7.61	125.7	126.2

(q, J = 3.3 Hz) (t, J = 6.0 Hz)

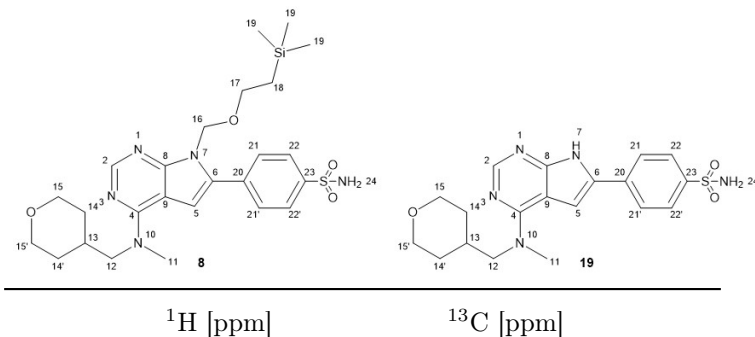
23	-	-	126.9	132.4
			(q, J =31.6 Hz)	(t, J =21.9 Hz)
24	-	7.04	123.4	114.9
		(t, J =56.4 Hz)	(q, J =271.4 Hz)	(t, J =235.5 Hz)

2.5.3 Compound **8** and **19**

The ^1H -NMR and ^{13}C -NMR shifts for sulfoamides **8** and **19** are presented in Table 2.10 and the spectroscopic spectra for the compounds are given in Appendix G and R

The ^1H -NMR and ^{13}C -NMR shifts of the two compounds are very much alike, due to their structural similarities. There are only observed small variations in the chemical shift values. The sulfonamide group in both the compounds have a very electron withdrawing character which removes electron density from the ring carbon in position 23, resulting in a higher chemical shift value than the rest of the ring carbons at 143.1 and 142.1 ppm for compounds **8** and **19**, respectively. The NH_2 group is observed at 7.43 and 7.35 ppm in the sulfoamides **8** and **19**, respectively.

Table 2.10: Assignment of ^1H - and ^{13}C -NMR shifts for compounds **8** and **19**, obtained at 600 MHz and 150 MHz, respectively. All chemical shift values are given in ppm and the solvent used was $\text{DMSO-}d_6$.



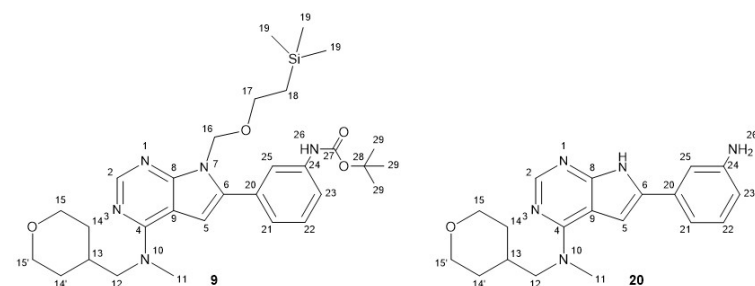
Pos.	8	19	8	19
2	8.22	8.14	151.7	151.7
4	-	-	156.6	156.6
5	7.02	7.26	104.1	101.2
6	-	-	134.5	131.4
7	-	12.27	-	-
8	-	-	153.4	153.2
9	-	-	102.1	103.4
11	3.41	3.42	39.0	39.0
12	3.71	3.71	55.4	55.3
13	2.08-2.04	2.08-2.04	33.9	33.9
14/14'	1.52/1.29	1.53-/1.29	30.2	30.3
15/15'	3.83/3.24	3.83/3.24	66.7	66.7
16	5.58	-	70.4	-
17	3.63	-	65.7	-
18	0.86	-	17.2	-
19	-0.08	-	-1.4	-
20	-	-	134.7	134.7
21	7.95	8.05	128.5	124.7
22	7.89	7.83	126.0	126.2
23	-	-	143.1	142.1
24	7.43	7.35	-	-

2.5.4 Compound **9** and **20**

The ^1H -NMR and ^{13}C -NMR shifts for compounds **9** and **20** are presented in Table 2.11 and the spectroscopic spectra for the compounds are given in Appendix H and S.

The Boc-protecting group in compound **9** is an electron withdrawing group that removes electron density from the amide proton at position 26 resulting it to have a high shift at 9.43 ppm. The 9 protons and the 3 carbons in position 29 of the Boc group is both observed as large singlets with a low chemical shift value at 1.48 ppm and 28.1 ppm in the ^1H - and ^{13}C -NMR spectra, respectively. The carbonyl carbon at position 27 in the Boc-group is observed with a high ^{13}C chemical shift value at 152.7 ppm. Removing the Boc-group results in a NH_2 group in position 26 in compound **20**, observed as a singlet in the ^1H -spectra. This is a very electron donating group that increases electron density in the aromatic ring resulting in a much lower chemical shift of 5.07 ppm in position 26. The increased electron density in the aromatic ring causes the chemical shift values of the neighboring carbons to the NH_2 -group in position 23 and 25 to decrease in compound **20** compared to compound **9**.

Table 2.11: Assignment of ^1H - and ^{13}C -NMR shifts for compounds **9** and **20**, obtained at 600 MHz and 150 MHz, respectively. All chemical shift values are given in ppm and the solvent used was $\text{DMSO-}d_6$.



Pos.	^1H [ppm]		^{13}C [ppm]	
	9	20	9	20
2	8.20	8.09	151.2	150.8
4	-	-	156.4	156.3
5	6.74	6.83	102.1	97.9

6	-	-	136.3	134.0
7	-	11.97	-	-
8	-	-	152.9	152.6
9	-	-	102.2	103.2
11	3.38	3.38	39.0	38.9
12	3.68	3.67	55.5	55.4
13	2.08-2.04	2.08-2.04	34.0	33.9
14/14'	1.53/1.29	1.55/1.27	30.3	30.3
15/15'	3.83/3.24	3.84/3.25	66.8	66.8
16	5.52	-	70.2	-
17	3.51	-	65.5	-
18	0.81	-	17.3	-
19	-0.11	-	-1.5	-
20	-	-	131.9	132.0
21	7.42	7.00	122.4	112.9
22	7.35	7.06	128.8	129.3
23	7.32	6.51	118.0	113.2
24	-	-	139.9	148.8
25	7.82	7.01	118.6	110.2
26	9.43	5.07	-	-
27	-	-	152.7	-
28	-	-	79.1	-
29	1.48	-	28.1	-

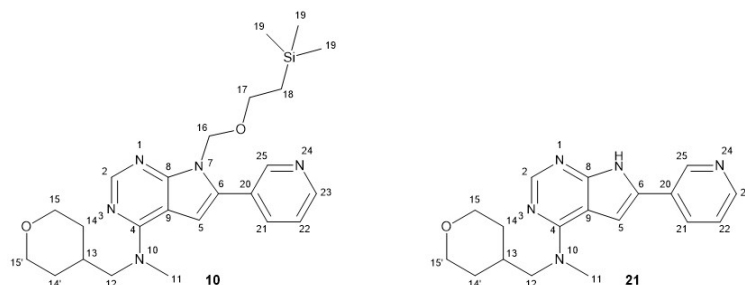
2.5.5 Compound 10 and 21

The ^1H -NMR and ^{13}C -NMR shifts for the 3-pyridyl derivatives **10** and **21** are presented in Table 2.12 and the spectroscopic spectra for the

compounds are given in Appendix I and T

One noticeable difference compared to other similar compounds are the high ^{13}C -shifts in position 23 and 25 between 146-149 ppm for both compound **10** and **21**. These high chemical shift values are due to the electronegative nitrogen atom in the pyridyl ring that removes electron density from the ring carbons next to the nitrogen.

Table 2.12: Assignment of ^1H - and ^{13}C -NMR shifts for compounds **10** and **21**, obtained at 600 MHz and 150 MHz, respectively. All chemical shift values are given in ppm and the solvent used was $\text{DMSO-}d_6$.



Pos.	^1H [ppm]		^{13}C [ppm]	
	10	21	10	21
2	8.22	8.13	151.5	151.5
4	-	-	156.5	156.5
5	7.02	7.24	103.7	100.3
6	-	-	132.7	129.8
7	-	12.27	-	-
8	-	-	153.2	153.1
9	-	-	102.1	103.2
11	3.41	3.41	38.9	38.9
12	3.70	3.70	55.4	55.3
13	2.10-2.04	2.10-2.04	33.9	33.9
14/14'	1.52/1.29	1.54/1.30	30.2	30.3

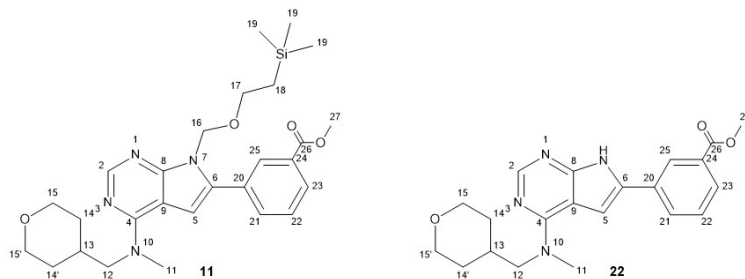
15/15'	3.83/3.24	3.83/3.24	66.7	66.8
16	5.57	-	70.2	-
17	3.59	-	65.7	-
18	0.83	-	17.3	-
19	-0.11	-	-1.5	-
20	-	-	127.7	127.6
21	8.16	8.24	135.5	131.6
22	7.52	7.44	123.6	123.7
23	8.60	8.46	148.8	147.9
24	-	-	-	-
25	8.94	9.11	149.0	146.0

2.5.6 Compound **11** and **22**

The ^1H -NMR and ^{13}C -NMR shifts for the *m*-methyl esters **11** and **22** are presented in Table 2.13 and the spectroscopic spectra for the compounds are given in Appendix J and T.

The ester present in both compounds **11** and **22** are electron withdrawing, causing a similar effect as described before. It is also noticeable that the C-26 carbon in both compounds have chemical ^{13}C -shifts of 165.9-166.2 ppm which is common shift values for carboxylic acid derivatives like esters. The protons in the methyl group at C-27 are also observed as large singlets at 3.88 and 3.90 ppm in the ^1H -NMR spectra.

Table 2.13: Assignment of ^1H - and ^{13}C -NMR shifts for compounds **11** and **22** obtained at 600 MHz and 150 MHz, respectively. All chemical shift values are given in ppm and the solvent used was DMSO- d_6 .



Pos.	^1H [ppm]		^{13}C [ppm]	
	11	22	11	22
2	8.22	8.12	151.5	151.4
4	-	-	156.5	156.6
5	6.96	7.18	103.3	100.0
6	-	-	132.1	131.8
7	-	12.29	-	-
8	-	-	153.0	153.1
9	-	-	102.1	103.3
11	3.41	3.41	39.0	38.9
12	3.70	3.70	55.4	55.3
13	2.10-2.03	2.10-2.01	33.9	33.9
14/14'	1.53/1.29	1.54/1.30	30.3	30.3
15/15'	3.83/3.24	3.84/3.25	66.7	66.8
16	5.52	-	70.3	-
17	3.59	-	65.5	-
18	0.86	-	17.3	-
19	-0.10	-	-1.4	-
20	-	-	134.9	132.2
21	8.02	8.15	133.2	129.3
22	7.64	7.57	129.2	129.3
23	7.99	7.85	128.6	127.7

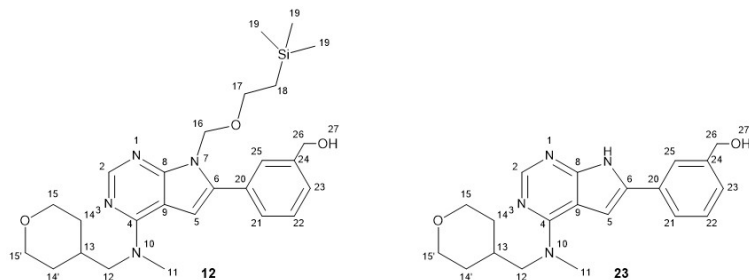
24	-	-	130.3	130.4
25	8.33	8.46	129.1	125.2
26	-	-	165.9	166.2
27	3.88	3.90	52.3	52.3

2.5.7 Compound **12** and **23**

The ^1H -NMR and ^{13}C -NMR shifts for the hydroxymethylene analogues **12** and **23** are presented in Table 2.14 and the spectroscopic spectra for the compounds are given in Appendix K and V.

Compared to compounds **11** and **22** in the previous section, the aromatic ring carbons and protons in compound **12** and **23** have lower chemical shifts. This is since the CH_2OH -group in compound **12** and **23** has a more electron donating character, than the electron-withdrawing carbonyl group in **11** and **22**. The alcohol protons at position 27 in the compounds **12** and **23** are observed as triplets with a chemical shift at 5.24 and 5.22 ppm in the ^1H -NMR spectra, while the CH_2 groups next to the hydroxy groups are observed as doublets with chemical ^1H shifts at 4.55 and 4.54 ppm, respectively.

Table 2.14: Assignment of ^1H - and ^{13}C -NMR shifts for compounds **12** and **23**, obtained at 600 MHz and 150 MHz, respectively. All chemical shift values are given in ppm and the solvent used was $\text{DMSO-}d_6$.



Pos.	^1H [ppm]		^{13}C [ppm]	
	12	23	12	23
2	8.20	8.10	151.2	151.1
4	-	-	156.4	156.4
5	6.82	7.04	102.3	98.8
6	-	-	136.3	133.1
7	-	12.10	-	-
8	-	-	152.9	152.8
9	-	-	102.1	103.3
11	3.39	3.41	38.9	38.9
12	3.69	3.69	55.4	55.4
13	2.08-2.04	2.08-2.04	33.9	33.9
14/14'	1.52/1.28	1.54/1.29	30.3	30.3
15/15'	3.83/3.24	3.83/3.24	66.7	66.7
16	5.52	-	70.3	-
17	3.58	-	65.6	-
18	0.83	-	17.3	-
19	-0.09	-	-1.4	-
20	-	-	131.2	131.3
21	7.61	7.74	126.9	123.1
22	7.44	7.37	128.4	128.6
23	7.37	7.24	126.1	125.5

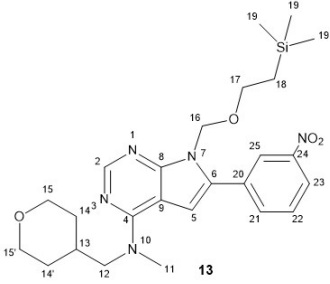
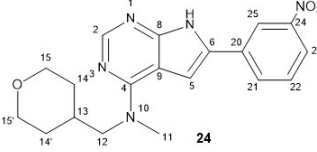
24	-	-	143.1	143.1
25	7.65	7.82	126.6	122.9
26	4.55	4.54	62.8	62.8
27	5.24	5.22	-	-

2.5.8 Compound 13 and 24

The ^1H -NMR and ^{13}C -NMR shifts for the nitro analogues **13** and **24** are presented in Table 2.15 and the spectroscopic spectra for the compounds are given in Appendix L and W.

The NO_2 -group is a very electron withdrawing group causing both the ^1H -NMR and ^{13}C -NMR shifts of compounds **13** and **24** to be high in the aromatic ring. Compared to compound **20** with the electron donating NH_2 -group, see Section 2.5.4, the ^1H -NMR and ^{13}C -NMR shifts of compound **24** are respectively 0.65-1.82 ppm and 1.0-17.6 ppm higher for the atoms in aromatic ring structure in position 21-25.

Table 2.15: Assignment of ^1H - and ^{13}C -NMR shifts for compounds **13** and **24**, obtained at 600 MHz and 150 MHz, respectively. All chemical shift values are given in ppm and the solvent used was $\text{DMSO}-d_6$.

				
	^1H [ppm]		^{13}C [ppm]	
Pos.	13	24	13	24

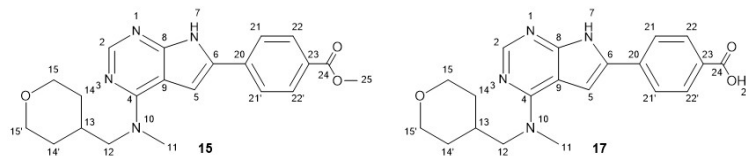
2	8.23	8.14	151.8	151.8
4	-	-	156.6	156.7
5	7.12	7.38	104.6	101.4
6	-	-	133.6	130.6
7	-	12.40	-	-
8	-	-	153.2	153.2
9	-	-	102.1	103.3
11	3.42	3.43	38.9	38.9
12	3.71	3.71	55.4	55.4
13	2.10-2.04	2.10-2.04	33.8	33.8
14/14'	1.52/1.29	1.53/1.29	30.2	30.3
15/15'	3.83/3.24	3.83/3.24	66.7	66.7
16	5.58	-	70.3	-
17	3.64	-	65.6	-
18	0.89	-	17.3	-
19	-0.08	-	-1.5	-
20	-	-	133.1	133.4
21	8.22	8.10	134.7	121.4
22	7.79	7.71	130.3	130.3
23	8.25	8.33	122.5	130.8
24	-	-	148.2	148.6
25	8.65	8.76	122.7	118.9

2.5.9 Compound 15 and 17

The ^1H -NMR and ^{13}C -NMR shifts for compounds **15** and **17** are presented in Table 2.16 and the spectroscopic spectra for the compounds are given in Appendix N and P.

There are only observed small variations in the chemical shifts. It is noticeable that the C-24 carbon in both compounds have chemical ^{13}C -shift values over 165 ppm which is common shift values for carboxylic acid derivatives and ester derivatives. The protons of the methyl group at C-25 in compound **15** are observed as a large singlet at 3.86 ppm in the ^1H -NMR spectra. The alcohol proton at C-25 in compound **17** is observed as a broad singlet with a chemical shift 12.89 ppm in the ^1H -NMR spectra. The proton in the hydroxy group gets a high chemical shift at 12.89 ppm due to the neighboring electron withdrawing ketone in compound **17**.

Table 2.16: Assignment of ^1H - and ^{13}C -NMR shifts for compounds **15** and **17**, obtained at 600 MHz and 150 MHz, respectively. All chemical shift values are given in ppm and the solvent used was $\text{DMSO-}d_6$.



Pos.	^1H [ppm]		^{13}C [ppm]	
	15	17	15	17
2	8.13	8.13	151.8	151.6
4	-	-	156.6	156.6
5	7.29	7.26	101.5	101.2
6	-	-	131.6	131.8
7	12.29	12.27	-	-
8	-	-	153.3	153.2
9	-	-	103.4	103.4
11	3.42	3.42	39.0	38.9
12	3.70	3.70	55.4	55.4
13	2.08-2.04	2.08-2.04	33.9	33.9

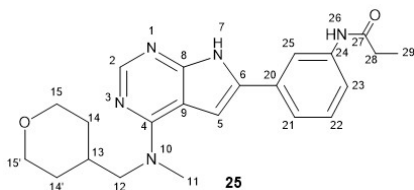
14/14'	1.54/1.29	1.53/1.30	30.3	30.3
15/15'	3.83/3.25	3.83/3.24	66.8	66.8
20	-	-	136.1	135.7
21	7.89	7.95	129.7	129.8
22	8.03	8.00	124.6	124.5
23	-	-	127.6	128.9
24	-	-	165.9	167.0
25	3.86	12.89	52.1	-

2.5.10 Compound 25

The ^1H -NMR and ^{13}C -NMR shifts for compound **25** are presented in Table 2.17 and the spectroscopic spectra for the compounds are given in Appendix X.

The amide proton at N-26 in compound **25** is observed as a singlet with a chemical shift of 9.90 ppm in the ^1H -NMR spectra. The electron withdrawing acyl group on compound **25** results in a much higher ^1H -shift on the N-25 atom compared to compound **20** with the electron donating NH_2 -group in the same position. The ^{13}C -shift in position 24 has a 9.1 lower ppm value in compound **25** than in compound **20**, due to a higher electron density around the C-24 carbon in compound **25**.

Table 2.17: Assignment of ^1H - and ^{13}C -NMR shifts for compound **25**, obtained at 600 MHz and 150 MHz, respectively. All chemical shift values are given in ppm and the solvent used was $\text{DMSO-}d_6$.



Name	^1H [ppm]	^{13}C [ppm]
Pos.	25	25
2	8.11	151.1
4	-	156.4
5	6.88	98.7
6	-	133.2
7	12.12	-
8	-	152.8
9	-	103.2
11	3.40	38.9
12	3.68	55.4
13	2.09-2.04	33.9
14/14'	1.55/1.29	30.3
15/15'	3.83/3.25	66.8
20	-	132.0
21	7.51	119.6
22	7.34	129.1
23	7.48	118.4
24	-	139.7
25	8.02	115.8
26	9.90	-
27	-	172.1
28	2.34	29.5
29	1.10	9.6

2.5.11 IR-spectroscopy

IR spectroscopy has been used to find the functional groups in all the new synthesized compounds. Due to the structural similarities of the synthesized compounds, the most important absorption peaks from the IR analysis are summarized in this chapter.^[110]

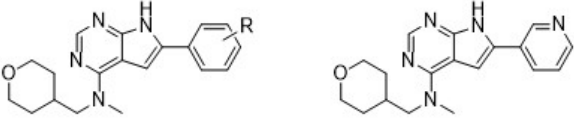
The medium absorption bands at 3000-2800 cm^{-1} represent C-H stretching of the aliphatic groups in all the compounds. The strong peak at 1570 cm^{-1} is observed in all spectra and correlates with the C=C vibrations contributed from aromatic ring mode. The C=C and C=N stretching from the aromatic rings are observed as weak to medium peaks between 1600-1300 cm^{-1} . The strong peaks at 1100-1050 cm^{-1} are caused by C-O stretching and represent the ether groups in the compounds. In-plane C-H bending in the aromatic compounds is found between 1300-1000 cm^{-1} . The absorption bands between 900-650 cm^{-1} are due to out-of-plane C-H stretching in the aromatic compounds.

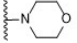
For the deprotected compounds, absorption bands between 3150-3050 cm^{-1} are observed due to N-H stretching. For the fluorine compounds **6**, **7**, **16** and **18**, C-F stretching is observed between 1400-1000 cm^{-1} . In compounds **5**, **11**, **15** and **22** a strong C=O stretch is observed between 1700-1750 cm^{-1} representing the ester group in their structures. In compound **9**, **20** and **25** a medium N-H stretch is observed between 3100-3300 cm^{-1} representing the amine/amide group in their structures.

2.6 Biological activity

2.6.1 *In vitro* enzymatic assays

The final pyrrolopyrimidines **14**, **15**, **16**, **17**, **20**, **21**, **22**, **23**, **24** and **25** were all tested by *in vitro* enzymatic assays, to determine their enzymatic inhibition towards CSF-1R. The assays were baselined towards the approved drugs PLX33997 and Erlotinib for comparison of enzymatic activity. The test concentration for the inhibition of CSF-1R was at 500 nM. The ATP concentration used in the experiments was equal to the Michael constant, K_M (approximately 10 μM). The IC_{50} value is defined as the concentration value needed of a drug to inhibit 50% of the targeted enzyme.^[111] The IC_{50} values are based on two or four titrations with 20 or 40 data points in each case. The results are shown in Table 2.18 alongside three compounds prepared by Thomas Ihle Aarhus.

Table 2.18: Percentage of CSF-1R inhibition and IC₅₀ values for the given pyrrolopyrimidines compared to the approved drug PLX3397.


Compound	R-group	CSF1R (%inhib.) ^{a)}	CSF1R IC ₅₀ (nM) ^{b)}	CSF1R IC ₅₀ (nM) Lanze ^{c)}
TIA05-028 ^{d)}	p-CH ₂ OH	101	0.5 ± 0.1	5
TIA05-032 ^{d)}	p-CH ₂ CH ₂ OH	100	<0.3	<0.3
TIA05-030 ^{d)}		104	<0.3	14
SH-01-18 ^{e)}	H	100	0.6 ± 0.0	6
SH-01-27 ^{e)}	F	97	0.8 ± 0.0	7
14	p-OMe	98	0.4 ± 0.1	<3
15	p-CO ₂ Me	99	1.5 ± 0.7	18
16	p-CF ₃	95	1.9 ± 0.2	29
17	p-CO ₂ H	99	0.4 ± 0.0	6
20	m-NH ₂	97	0.4 ± 0.0	4
21	^{f)}	96	1.4 ± 0.1	18
22	m-CO ₂ Me	96	2.2 ± 0.5	28
23	m-CH ₂ OH	97	0.6 ± 0.0	ND ^{g)}
24	m-NO ₂	98	2.7 ± 0.0	43
25	m-NHCOC ₂ H ₅	99	1.2 ± 0.1	13
PLX3397	-	100	5.4 ± 1.5	38

^{a)} Inhibition of CSF1R (%) at 500 nM test concentration. Average of two measurements Assay performed by ThermoFisher

^{b)} CSF1R IC₅₀-values based on two titration curves (20 data points) or more

^{c)} CSF1R IC₅₀-values by Lanze (Perkin Elmer) ATP is equal to Km= 2.5 mM.

^{d)} Compound prepared by PhD student Thomas Ihle Aarhus

^{e)} Compound prepared in the pre-master project. [104]

^{f)} See structure above Table 2.18.

^{g)} Not determined

The results from the enzymatic tests show that all of the pyrrolopyrimidine compounds show excellent inhibition activity towards CSF-1R, with inhibition from 95-100% and low IC₅₀-values in the range of 0.4-2.7 nM. All the compounds had IC₅₀-values lower (better) than the reference compound PLX3397. The data also indicate that having donating groups at the 6-aryl ring is somewhat positive. For instance has compound **20** with the electron donating group NH₂ a lower IC₅₀-value than compound **16** with the electron withdrawing CF₃-group. This effect of substitution pattern for the IC₅₀-values is also observed for the rest of the pyrrolopyrimidine compounds.

A study by Ritchie *et al.* shows that heteroaliphatic rings exerts beneficial effects in the case of solubility, lipophilicity, bioavailability and protein binding.^[112] The tetrahydropyran (THP) moiety of the pyrrolopyrimidine is therefore believed to play an important role for promoting activity, but also due to its solubilizing effect. Tetrahydropyrans are 6-membered oxygen-containing heterocycles with anti-inflammatory, analgesic and cytotoxic activity that can be used for the synthesis of biologically active compounds in medicinal chemistry.^{[113][114]} The IC₅₀-values for the pyrrolopyrimidine inhibitors containing THP are lower, compared to the already developed drug PLX3397. The tetrahydropyran moiety can therefore be of great interest in further research in the synthesis of pyrrolopyrimidine based CSF-1R inhibitors.

2.6.2 IC₅₀ comparison of two different series

The IC₅₀-values of the tetrahydropyran-based structures were compared to IC₅₀-values of the *m*-methylbenzyl series of compounds to investigate how the substitution pattern of the compounds affected the IC₅₀-values, see Figure 2.5. Comparing the IC₅₀-values of that of the *m*-methylbenzyl series of compounds, shows that the activity is less dependent of the sub-

stitution pattern in the case of the tetrahydropyran-based structures. The electron withdrawing groups are especially better tolerated in the current series of compounds. The figure also illustrates that the compounds with the THP group generally give lower IC_{50} -values than the series with the *m*-methylbenzyl group.

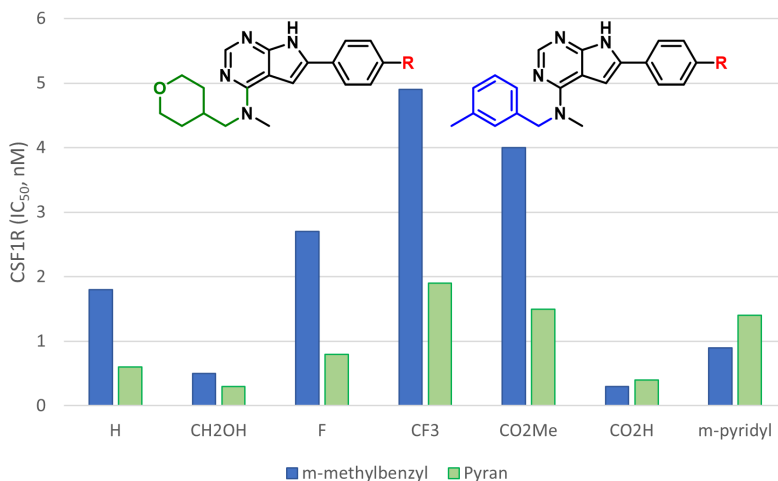
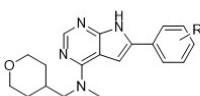


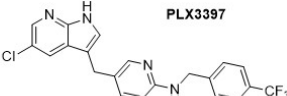
Figure 2.5: Comparison of the IC_{50} -values of the methylbenzyl and tetrahydropyran series of the pyrrolopyrimidine compounds. The data is not yet published.

2.6.3 Testing towards other kinases

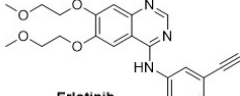
The selected inhibitors were also tested towards EGFR since this has been a major off-target for pyrrolopyrimidines. The test concentration towards EGFR was at 100 nM. Inhibition of various kinases (%) at 500 nM test concentration for selected pyrrolopyrimidine inhibitors was also tested. The results of these inhibition tests are presented in Table 2.19

Table 2.19: Percentage of inhibition of various kinases (%) at 500 nM test concentration values for the given pyrrolopyrimidines compared to the approved drugs PLX3397 and Erlotinib.

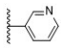




PLX3397



Erlotinib

Comp.	R-group	EGFR	ABL	ABL-	FLT3	FLT-	KIT	PDGFRB	
		a)	b)	H396P	b)	D835Y	b)	b)	
				b)					
				b)					
14	p-OMe	10	64	60	22	36	17	21	
15	p-CO ₂ Me	5	ND	ND	ND	ND	ND	ND	
				c)					
16	p-CF ₃	2	22	16	10	12	11	9	
17	p-CO ₂ H	10	37	31	20	24	14	27	
20	m-NH ₂	ND	54	58	35	42	19	24	
21		ND	37	34	11	14	8	11	
22	m-CO ₂ Me	ND	ND	ND	ND	ND	ND	ND	
23	m-CH ₂ OH	ND	43	39	26	29	15	16	
24	m-NO ₂	ND	ND	ND	ND	ND	ND	ND	
25	m-	ND	42	42	8	17	13	10	
NHCOC ₂ H ₅									
PLX3397	-	1	6	ND	56	ND	71	38	
Erlotinib	-	100	75	ND	ND	ND	17	<0	

a) Inhibition of EGFR (%) at 100 nM test concentration. Average of two measurements. Assay performed by ThermoFisher.

b) Inhibition of various kinases (%) at 500 nM test concentration. Average of two measurements

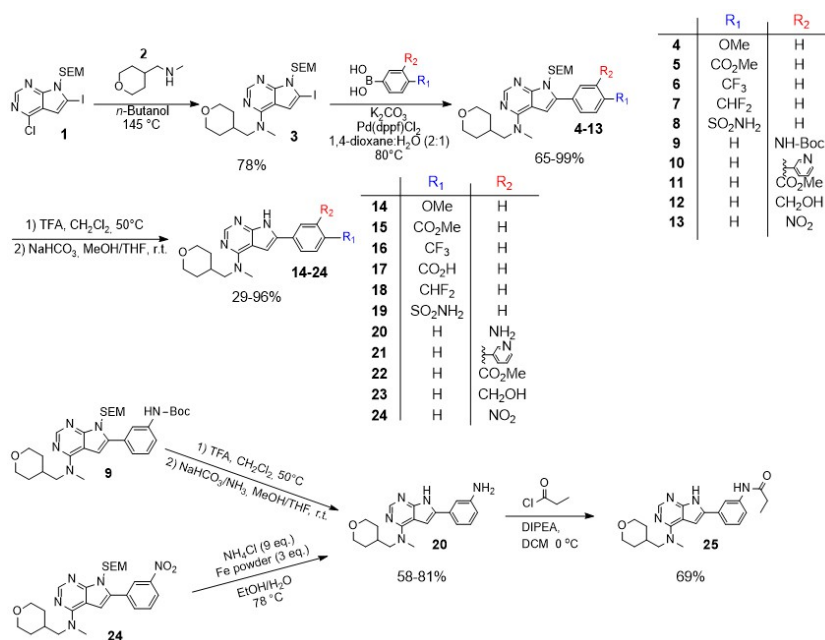
c) Not determined

The results from the enzymatic tests show that none of the inhibitors assayed had any relevant activity towards EGFR. This shows that substituting a benzene ring with a tetrahydropyran unit effectively removes EGFR activity. It is noticeable that compound **14**, **20**, **23** have moderate inhibition activity towards all the other kinases. An important element of these results is that FLT3, KIT and PDGFRB are in the same family as CSF-1R. The fact that these kinases are not inhibited to a large extent is seen as positive.

3 Conclusion

The aim of this master's thesis was to synthesize new CSF-1R inhibitors based on the pyrrolopyrimidine scaffold, as well as test their inhibition activity towards CSF-1R in enzymatic studies.

The pyrrolopyrimidines were prepared by a thermal amination reaction on the chloro-atom at C-4 of the compound 4-chloro-6-iodo-7-((2-(trimethylsilyl)ethoxy)methyl)-7*H*-pyrrolo[2,3-*d*]pyrimidine, followed by selective Suzuki cross-coupling reactions with various boronic acids at the C-6 carbon. The target compounds were synthesized by removal of the protective SEM-group on the pyrrole in addition to a couple of post-modification reactions on some selected deprotected compounds.



The nucleophilic aromatic substitution resulted in an isolated product

with a yield of 78%. The Suzuki cross-coupling reactions were conducted at C-6 to introduce various boronic acids with functional groups in either *para* or *meta* position, resulting in isolated products with varying yields between 65-99%.

The target molecules were synthesized by removal of the SEM group and by post modification reactions of the deprotected compounds, resulting in yields between 29-96% and desired high purities of over 95%. Deprotection of both a SEM-group and a Boc group to synthesize an aniline product turned out to be problematic and resulted in incomplete conversion and observation of several byproducts in the isolated product. An alternative synthesis route was carried out to synthesize the deprotected aniline product by reduction of a deprotected nitro compound, which resulted in high purity and yields.

During this master's thesis, a total of 12 target molecules were tested for their CSF-1R inhibition activity. The 12 target compounds proved to have a very high inhibition activity towards the CSF-1R kinase with low IC₅₀ values in the range of 0.4-1.9 nM. The target compounds were also tested for their inhibition activity against various kinases without showing any relevant activity towards the selected kinases.

4 Future Work

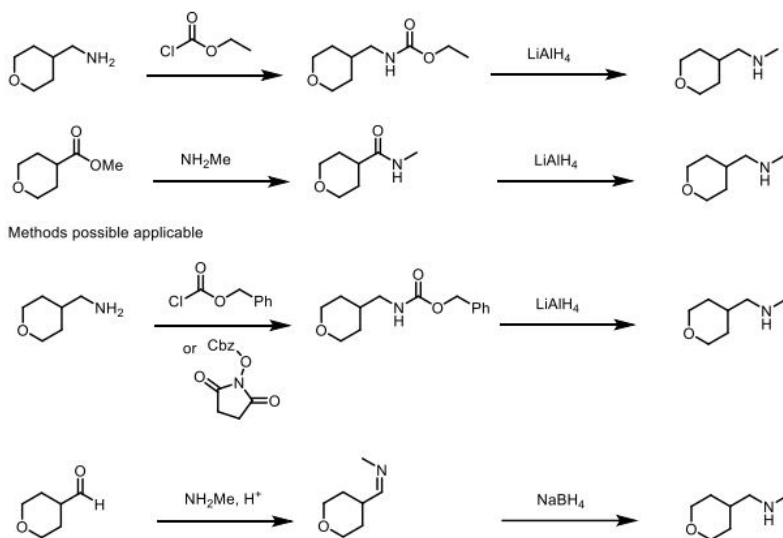
In this master's thesis a total of 18 new pyrrolopyrimidine compounds have been synthesized, of which 12 of them have been tested for their CSF-1R inhibition activity. These 12 target compounds have proved to have a very high inhibition activity and low IC₅₀ values towards the CSF-1R kinase, making them very promising as potential CSF-1R inhibitors. The target molecules **18** and **19** will be tested for their inhibition activity in the future, as they weren't finished synthesized when the other target compounds were sent for testing. *In vitro* ADME experiments and *in vivo* mice pharmacokinetic studies of the compounds have just been started.

Other future work will among others involve making new pyrrolopyrimidine derivatives for enzymatic testing. Hydrolysis of the methyl ester pyrrolopyrimidine **22** will be carried out to synthesize the corresponding carboxylic acid. Compound **24** will also be used in an acylation reaction with acryloyl chloride to synthesize a similar compound to the product **25**. Molecular modelling has indicated that the acrylamide could be an irreversible inhibitor of CSF-1R.

Further, it would have been interesting to synthesize inhibitors with different functional groups in the *ortho*-position at the coupled 6-aryl-group and compare the synthesis results and the biological effects with the already synthesized compounds.

The methyl-(tetrahydropyran-4-ylmethyl)-amine containing the THP group, is a secondary amine which is a very expensive compound. Self preparation of this amine may therefore be a possible solution for a more cost efficient way to synthesize the target pyrrolopyrimidines in the future. Some possible routes for the preparation of the THP amine are pre-

sented in Scheme 4.1 and include preparation of carbamates and amides followed by reduction and reductive amination.



Scheme 4.1: Proposed synthesis routes for the synthesis of the secondary amine containing the THP group.

In a further extension of this work, substitution of the THF group is a possible and exciting option. Work towards replacing the 6-aryl group by saturated ring structures are also on-going.

5 Experimental

5.1 General Information

All the reagents and solvents that have been used for the experiments are commercially available and have been purchased from Sigma-Aldrich. The materials were of analytical quality and were used without further purification. An oil bath was used to regulate the temperature if the reactions were conducted above room temperature. A magnetic stirrer coated with a teflon layer was used in all reactions. Distilled water was used. Dry solvents were acquired from a Braun MB SPS-800 Solvent Purification System when needed and were stored over molecular sieves (4 Å).

Separation Techniques

Thin layer chromatography (TLC; silica-gel on aluminum plates, F254, Merck) was used to monitor the reactions and for optimizing eluent systems in purification by column chromatography. UV-light (wavelength 254 nm and 365 nm) was used for the visualization of the TLC-plates.

Column chromatography was performed using silica-gel (40-63 mesh, 60 Å) as a stationary phase the eluent systems used are specified for each purification on the column.

Chromatographic Analyses

HPLC analyses were performed on an Agilent 1100-series instrument with a G1379A degasser, G1313A ALS autosampler and Agilent G1315D diode array detector. The chromatograms were recorded at 254 nm, using Agilent ChemStation as processing software. A Poroshell C18 column (100 x 4.6 mm) with pore size of 2.7 μm and a flow volume of 1

mL/min (linear gradient from H₂O + 0.1% TFA/ACN 90/10 to 0/100 over 5 minutes was used.

Spectroscopic Analyses

The infrared absorption (IR) spectra were recorded with a FTIR Thermo Nicolet Nexus FT-IR Spectrometer using a Smart Endurance reflection cell. The frequencies reported are in the range of 4000-400 cm⁻¹, where the strength of the absorption band are given as strong (s), medium (m) or weak (w).

¹H-NMR and ¹³C-NMR spectra were recorded on a ultrashielded Bruker Avance III HD NMR instrument equipped with a 5-mm SmartProbe z-gradient probe and SampleCase. ¹H-NMR spectra were recorded at 400 MHz or 600 MHz, while ¹³C-NMR spectra were recorded at 150 MHz. Deuterated DMSO, DMSO-*d*₆ or deuterated chloroform, CDCl₃ were used as solvents. ¹⁹F-NMR spectra were recorded at 565 MHz using hexafluorobenzene, C₆F₆ in DMSO-*d*₆, with a chemical shift at -164.9 ppm as a reference standard. The chemical shifts δ of protons are reported in parts per million (ppm) and their coupling constants (*J*) are reported in hertz (Hz). The chemical shifts are calibrated to the reference tetramethylsilane (TMS) in CDCl₃ (0.00 ppm in ¹H-NMR and ¹³C-NMR), or the solvent peak in DMSO-*d*₆ (2.50 ppm in ¹H-NMR and 39.52 ppm in ¹³C-NMR). Water is present in both CDCl₃ and DMSO-*d*₆ in the ¹H-NMR spectra at 1.56 ppm and 3.33 ppm. The multiplicity of the proton signals are reported as: s (singlet), d (doublet), t (triplet), dd (doublet of doublet), td (triplet of doublets), qd (quartet of doublets) and m (multiplet).

Accurate mass determination in positive or negative mode was performed on a "Synapt G2-S" Q-TOF instrument from Water TM. Samples were

ionized by the use of ASAP probe (APCI) or ESI probe. No chromatographic separation was used previous to the mass analysis. Calculated exact mass and spectra processing was done by Waters TM Software Masslynx V4.1 SCN871.

Melting point

Melting points were determined by a Stuart automatic melting point SMP40 instrument.

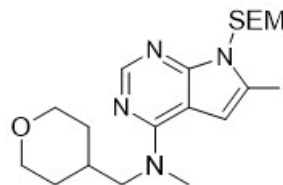
In vitro CSF-1R inhibitory potency

The compounds were supplied in a 10 mM DMSO solution, and enzymatic CSF1R inhibition potency was determined by Invitrogen (ThermoFisher) using their Z'-LYTE® assay technology.^[115] In short, the assay is based on fluorescence resonance energy transfer (FRET). In the primary reaction, the kinase transfers the gamma-phosphate of ATP to a single tyrosine residue in a synthetic FRET-peptide. In the secondary reaction, a site-specific protease recognizes and cleaves non-phosphorylated FRET-peptides. Thus, phosphorylation of FRET-peptides suppresses cleavage by the development reagent. Cleavage disrupts FRET between the donor (i.e., coumarin) and acceptor (i.e., fluorescein) fluorophores on the FRET-peptide, whereas uncleaved, phosphorylated FRET-peptides maintain FRET. A ratiometric method, which calculates the ratio (the emission ratio) of donor emission to acceptor emission after excitation of the donor fluorophore at 400 nm, is used to quantitate inhibition. All compounds were first tested for their inhibitory activity at 500 nM in duplicates. The potency observed at 500 nM was used to set starting point of the IC₅₀ titration curve, in which 1000 nM was used. The IC₅₀-values reported are based on the average of at least 2 titration curves (minimum 20 data points), and were calculated from activity data with

a four parameter logistic model using SigmaPlot (Windows Version 12.0 from Systat Software, Inc.) Unless stated otherwise the ATP concentration used was equal to K_m (ca 10 mM). The average standard deviation for single point measurements were <4%.

5.2 Synthesis of 6-iodo-*N*-methyl-*N*-((tetrahydro-2*H*-pyran-4-yl)methyl)-7-((2-(trimethylsilyl)ethoxy)methyl)-7*H*-pyrrolo[2,3-*d*]pyrimidin-4-amine (**3**)

Compound **1** (1.21 g, 2.95 mmol) was dissolved in *n*-BuOH (12 mL) and methyl-(tetrahydro-pyran-4-ylmethyl)-amine (576 mg, 4.46 mmol) and DIPEA (575 mg, 4.45 mmol) were added under an N_2 -atmosphere. The reaction mixture was heated to 145 °C and stirred for 3.5



hours, before it was cooled down to room temperature. Water (15 mL) was added to the residue and extracted with EtOAc (3 x 20 mL). The combined organic phases were washed with brine (20 mL), dried over Na_2SO_4 , filtered and concentrated in *vacuo*. The crude product was purified by silica-gel column chromatography (*n*-pentane/EtOAc, 1/1). The product **3** (1.14 g, 2.27 mmol), was isolated with a yield of 78% as a transparent oil.

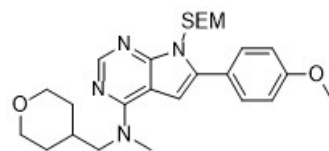
Spectroscopic data for compound **3** (Appendix B):

1H -NMR (600 MHz, $DMSO-d_6$) δ : 8.09 (s, 1H), 7.00 (s, 1H), 5.48 (s, 2H), 3.85–3.79 (m, 2H), 3.64 (d, $J = 7.4$ Hz, 2H), 3.54–3.48 (m, 2H), 3.32 (s, 3H) 3.23 (td, $J = 11.7, 2.1$ Hz, 2H), 2.08–2.04 (m, 1H), 1.52–1.46 (m, 2H), 1.26 (qd, $J = 12.0, 4.4$ Hz, 2H), 0.84–0.77 (m, 2H), -0.09 (s, 9H). ^{13}C -NMR (150 MHz, $DMSO-d_6$) δ : 155.3, 152.7, 151.1, 112.4, 104.2, 79.9, 72.7, 66.7 (2C), 65.5, 55.3, 38.8, 33.8, 30.2 (2C), 17.1, -1.4 (3C). IR

(neat, cm^{-1}) v : 2947 (m), 2916 (m), 2849 (m), 2836 (m), 1562 (s), 1547 (w), 1510 (w), 1416 (s), 1375 (m), 1367 (w), 1301 (m), 1285 (m), 1272 (m), 1240 (m), 1087 (s), 1033 (m), 904 (m), 831 (s), 774 (m), 749 (m)

5.3 Synthesis of 6-(4-methoxyphenyl)-*N*-methyl-*N*-((tetrahydro-2*H*-pyran-4-yl)methyl)-7-((2-(trimethylsilyl)ethoxy)methyl)-7*H*-pyrrolo[2,3-*d*]pyrimidin-4-amine (4)

Compound **3** (1.16 g, 2.31 mmol), (4-methoxyphenyl)boronic acid (419 mg, 2.76 mmol), K_2CO_3 (952 mg, 6.93 mmol) and $Pd(dppf)Cl_2$ (84.2 mg, 1.15 mmol) were dissolved in degassed 1,4-dioxane/ H_2O (2:1, 30 mL) under an N_2 -atmosphere and stirred at 80 °C for 30 minutes. The reaction was concentrated in *vacuo*, added water (40 mL) and extracted with CH_2Cl_2 (3 x 40 mL). The combined organic phases were washed with brine (40 mL), dried over Na_2SO_4 , filtered and concentrated in *vacuo*. The crude product was purified by silica-gel column chromatography (*n*-pentane/EtOAc, 1/1, $R_f=0.34$). The product **4** (1.08 g, 2.2 mmol), was isolated with a yield of 97% as a transparent oil.



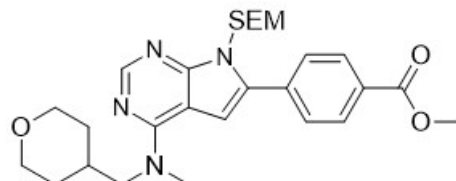
Spectroscopic data for compound **4** (Appendix C):

1H -NMR (600 MHz, $DMSO-d_6$) δ : 8.18 (s, 1H), 7.67 (d, $J = 8.8$ Hz, 2H), 7.05 (d, $J = 8.8$ Hz, 2H), 6.74 (s, 1H), 5.50 (s, 2H), 3.87–3.81 (m, 2H), 3.81 (s, 3H), 3.68 (d, $J = 7.4$ Hz, 2H), 3.63–3.57 (m, 2H), 3.38 (s, 3H), 3.24 (td, $J = 11.7, 2.1$ Hz, 2H), 2.08–2.04 (m, 1H), 1.55–1.49 (m, 2H), 1.28 (qd, $J = 12.1, 4.4$ Hz, 2H), 0.87–0.80 (m, 2H), -0.09 (s, 9H). ^{13}C -NMR (150 MHz, $DMSO-d_6$) δ : 159.2, 156.3, 152.7, 150.9, 136.1, 129.9 (2C), 123.8, 114.2 (2C), 102.1, 101.4, 70.2, 66.7 (2C), 65.6, 55.4, 55.2, 38.9, 33.9, 30.3 (2C), 17.4, -1.4 (3C). IR (neat, cm^{-1}) v : 2949

(m), 2916 (w), 2837 (m), 1567 (s), 1547 (w), 1498 (s), 1415 (m), 1306 (m), 1289 (w), 1246 (s), 1177 (m), 1071 (m), 1034 (m), 832 (s), 763 (m). HRMS (ASAP+, m/z): detected 483.2797, calculated for C₂₆H₃₉N₄O₃Si [M+H]⁺ 483.2791

5.4 Synthesis of methyl 4-(4-(methyl((tetrahydro-2*H*-pyran-4-yl) methyl)amino)-7-((2-(trimethylsilyl)ethoxy) methyl)-7*H*-pyrrolo[2,3-*d*]pyrimidin-6-yl)benzoate (**5**)

Compound **3** (401 mg, 0.797 mmol), 4-methoxycarbonylphenylboronic acid (171 mg, 0.952 mmol), K₂CO₃ (329 mg, 2.38 mmol) and Pd(dppf)Cl₂ (19.8 mg, 0.027 mmol) were dissolved in degassed 1,4-dioxane/H₂O (2:1, 12 mL) under an N₂-atmosphere and stirred at 60 °C for



11 minutes. The reaction was concentrated in *vacuo*, added water (20 mL) and extracted with CH₂Cl₂ (3 x 20 mL). The combined organic phases were washed with brine (30 mL), dried over Na₂SO₄, filtered and concentrated in *vacuo*. The crude product was purified by silica-gel column chromatography (*n*-pentane/EtOAc, 1/1, R_f=0.36). The product **5** (0.316 mg, 0.618 mmol), was isolated with a yield of 78% as a brown oil, HPLC purity 93%, t_R = 10.8 min.

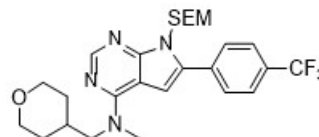
Spectroscopic data for compound **5** (Appendix D):

¹H-NMR (600 MHz, DMSO-*d*₆) δ: 8.22 (s, 1H), 8.04 (d, J = 8.5 Hz, 2H), 7.93 (d, J = 8.5 Hz, 2H), 7.04 (s, 1H), 5.58 (s, 2H), 3.88 (s, 3H), 3.86–3.80 (m, 2H), 3.71 (d, J = 7.4 Hz, 2H), 3.65–3.59 (m, 2H), 3.41 (s, 3H), 3.24 (td, J = 11.7, 2.1 Hz, 2H), 2.05 (dp, J = 11.3, 3.7 Hz, 1H), 1.55–1.49 (m, 2H), 1.29 (q, J = 12.5, 4.6 Hz, 2H), 0.87–0.80 (m, 2H),

-0.10 (s, 9H). ^{13}C -NMR (150 MHz, DMSO- d_6) δ : 165.9, 156.6, 153.5, 151.7, 136.2, 134.8, 129.5 (2C), 128.4 (2C), 104.2, 102.2, 70.4, 66.8 (2C), 65.8, 55.5, 52.3, 38.9, 33.8 30.3 (2C), 17.3, -1.4 (3C). IR (neat, cm^{-1}) ν : 2948 (m), 2931 (m), 2858 (w), 1721 (s), 1569 (s), 1545 (m), 1425 (m), 1313 (m), 1303 (m), 1276 (s), 1247 (m), 1183 (m), 1101 (w), 1090 (w), 1060 (s), 860 (w), 844 (w), 832 (s), 754 (s). HRMS (ASAP+, m/z): detected 511.2739, calculated for $\text{C}_{27}\text{H}_{39}\text{N}_4\text{O}_4\text{Si}$ $[\text{M}+\text{H}]^+$ 511.2741

5.5 Synthesis of *N*-methyl-*N*-((tetrahydro-2*H*-pyran-4-yl)methyl)-6-(4-(trifluoromethyl)phenyl)-7-((2-(trimethylsilyl)ethoxy) methyl)-7*H*-pyrrolo[2,3-*d*]pyrimidin-4-amine (**6**)

Compound **3** (150 mg, 0.299 mmol), 4-(trifluoromethyl)phenyl boronic acid (68.0 mg, 0.358 mmol), K_2CO_3 (124 mg, 0.896 mmol) and $\text{Pd}(\text{dppf})\text{Cl}_2$ (10.9 mg, 0.015 mmol) were dissolved in degassed 1,4-dioxane/ H_2O (2:1, 6 mL)



under an N_2 -atmosphere and stirred at 80 °C for 10 minutes. The reaction was concentrated in *vacuo*, added water (20 mL) and extracted with CH_2Cl_2 (3 x 20 mL). The combined organic phases were washed with brine (30 mL), dried over Na_2SO_4 , filtered and concentrated in *vacuo*. The crude product was purified by silica-gel column chromatography (*n*-pentane/ EtOAc , 1/1, $R_f=0.29$). The product **6** (123 mg, 0.279 mmol), was isolated with a yield of 94% as a transparent oil.

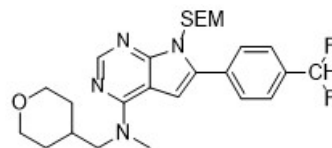
Spectroscopic data for compound **6** (Appendix E):

^1H -NMR (600 MHz, DMSO- d_6) δ : 8.23 (s, 1H), 7.99 (d, $J = 8.1$ Hz, 2H), 7.84 (d, $J = 8.2$ Hz, 2H), 7.04 (s, 1H), 5.59 (s, 2H), 3.86–3.80 (m, 2H), 3.71 (d, $J = 7.4$ Hz, 2H), 3.63–3.57 (m, 2H), 3.41 (s, 3H), 3.24 (td, $J =$

11.7, 2.1 Hz, 2H), 2.10 – 2.03 (m, 1H), 1.56–1.50 (m, 2H), 1.29 (qd, J = 12.3, 4.7 Hz, 2H), 0.86–0.79 (m, 2H), -0.11 (s, 9H). ^{13}C -NMR (150 MHz, DMSO- d_6) δ : 156.6, 153.4, 151.7, 135.7, 134.4, 128.9, 128.1 (q, J = 31.6 Hz, 1C), 125.6 (q, J = 3.3 Hz, 2C), 125.2, 123.4 (q, J = 272.5 Hz, 1C), 104.3, 102.1, 70.3, 66.7 (2C), 65.7, 55.4, 39.0, 33.9, 30.2 (2C), 17.3, -1.5 (3C). ^{19}F -NMR (565 MHz, DMSO- d_6 , C_6F_6) δ : -63.3 (3F). IR (neat, cm^{-1}) ν : 3404 (m), 3209 (w), 3094 (m), 2959 (w), 2932 (m), 2915 (m), 2843 (m), 2742 (w), 1668 (s), 1567 (s), 1550 (w), 1416 (m), 1323 (s), 1195 (m), 1156 (m), 1140 (s), 1115 (m), 1105 (s), 1093 (w), 1073 (m), 1060 (w), 1014 (m), 842 (m), 798 (m), 724 (m). HRMS (ASAP+, m/z): detected 521.2559 calculated for $\text{C}_{26}\text{H}_{36}\text{N}_4\text{O}_2\text{F}_3\text{Si}$ $[\text{M}+\text{H}]^+$ 521.2560.

5.6 Synthesis of 6-(4-(difluoromethyl)phenyl)-*N*-methyl-*N*-((tetrahydro-2*H*-pyran-4-yl)methyl)-7-((2-(trimethylsilyl)ethoxy)methyl)-7*H*-pyrrolo[2,3-*d*]pyrimidin-4-amine (7)

Compound **3** (150 mg, 0.299 mmol), 4-difluoromethyl-phenylboronic acid (61.6 mg, 0.358 mmol), K_2CO_3 (124 mg, 0.896 mmol) and $\text{Pd}(\text{dppf})\text{Cl}_2$ (10.9 mg, 0.015 mmol) were dissolved in degassed 1,4-dioxane/ H_2O (2:1, 6 mL)



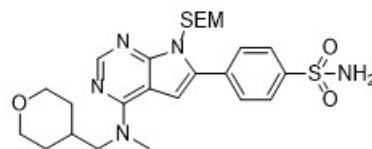
under an N_2 -atmosphere and stirred at 80 °C for 12 minutes. The reaction was concentrated in *vacuo*, added water (20 mL) and extracted with CH_2Cl_2 (3 x 20 mL). The combined organic phases were washed with brine (30 mL), dried over Na_2SO_4 , filtered and concentrated in *vacuo*. The crude product was purified by silica-gel column chromatography (*n*-pentane/ EtOAc , 1/1, $R_f=0.36$). The product **7** (149 mg, 0.296 mmol), was isolated with a yield of 99% as a transparent oil.

Spectroscopic data for compound **7** (Appendix F):

$^1\text{H-NMR}$ (600 MHz, $\text{DMSO-}d_6$) δ : 8.22 (s, 1H), 7.90 (d, $J = 8.4$ Hz, 2H), 7.68 (d, $J = 8.4$ Hz, 2H), 7.09 (t, $J_f = 56.1$ Hz, 1H), 6.96 (s, 1H), 5.56 (s, 2H), 3.86–3.80 (m, 2H), 3.70 (d, $J = 7.4$ Hz, 2H), 3.64–3.58 (m, 2H), 3.40 (s, 3H), 3.24 (td, $J = 11.7, 2.1$ Hz, 2H), 2.10–2.03 (m, 1H), 1.55–1.49 (m, 2H), 1.29 (qd, $J = 12.7, 4.5$ Hz, 2H), 0.86–0.79 (m, 2H), -0.10 (s, 9H). $^{13}\text{C-NMR}$ (150 MHz, $\text{DMSO-}d_6$) δ : 156.5, 153.2, 151.5, 135.0, 134.1, 133.3 (t, $J = 22.2$ Hz, 1C), 128.7, 126.1 (t, $J = 5.9$ Hz, 2C), 114.8 (t, $J = 235.9$ Hz, 1C), 103.5, 102.1, 70.3, 66.7 (2C), 65.7, 55.4, 38.9, 33.9, 30.3 (2C), 17.3, -1.5 (3C). $^{19}\text{F-NMR}$ (565 MHz, $\text{DMSO-}d_6$, C_6F_6) δ : -111.9 (2F). IR (neat, cm^{-1}) ν : 2952 (m), 2930 (m), 2844 (m), 1736 (s) 1568 (s), 1551 (s), 1416 (s), 1370 (s) 1308 (s), 1245 (s), 1070 (s), 1026 (m), 833 (s), 772 (m). HRMS (ASAP+, m/z): detected 503.2652 calculated for $\text{C}_{26}\text{H}_{37}\text{N}_4\text{O}_2\text{SiF}_2$ $[\text{M}+\text{H}]^+$ 503.2654.

5.7 Synthesis of 4-(4-(methyl((tetrahydro-2*H*-pyran-4-yl)methyl)amino)-7-((2-(trimethylsilyl)ethoxy)methyl)-7*H*-pyrrolo[2,3-*d*]pyrimidin-6-yl)benzenesulfonamide (8)

Compound **3** (150 mg, 0.299 mmol), (4-aminosulfonylphenyl) boronic acid (72.1 mg, 0.358 mmol), K_2CO_3 (124 mg, 0.896 mmol) and $\text{Pd}(\text{dppf})\text{Cl}_2$ (10.9 mg, 0.015 mmol) were dissolved in degassed 1,4-dioxane/ H_2O (2:1, 6 mL)



under an N_2 -atmosphere and stirred at 80 °C for 12 minutes. The reaction was concentrated in *vacuo*, added water (20 mL) and extracted with CH_2Cl_2 (3 x 20 mL). The combined organic phases were washed with brine (30 mL), dried over Na_2SO_4 , filtered and concentrated in *vacuo*.

The crude product was purified by silica-gel column chromatography (*n*-pentane/EtOAc, 1/1, $R_f=0.29$). The product **8** (137 mg, 0.257 mmol), was isolated with a yield of 86% as a transparent oil.

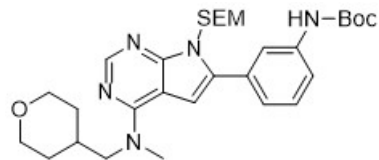
Spectroscopic data for compound **8** (Appendix G):

$^1\text{H-NMR}$ (600 MHz, $\text{DMSO-}d_6$) δ : 8.23 (s, 1H), 7.96 (d, $J = 8.5$ Hz, 2H), 7.90 (d, $J = 8.6$ Hz, 2H), 7.43 (s, 2H), 7.02 (s, 1H), 5.58 (s, 2H), 3.86–3.80 (m, 2H), 3.71 (d, $J = 7.4$ Hz, 2H), 3.66–3.60 (m, 2H), 3.41 (s, 3H), 3.24 (td, $J = 11.7, 2.1$ Hz, 2H), 2.11–2.01 (m, 1H), 1.55–1.49 (m, 2H), 1.29 (qd, $J = 16.4, 8.3$ Hz, 2H), 0.89–0.82 (m, 2H), -0.08 (s, 9H). $^{13}\text{C-NMR}$ (150 MHz, $\text{DMSO-}d_6$) δ : 156.6, 153.4, 151.7, 143.1, 134.7, 134.6, 128.5 (2C), 126.0 (2C), 104.1, 102.1, 70.4, 66.7 (2C), 65.7, 55.4, 39.0, *z* 33.9, 30.2 (2C), 17.3, -1.4 (3C). IR (neat, cm^{-1}) ν : 3213 (m), 2952 (m), 2930 (s), 2916 (s), 2850 (m), 1738 (m) 1571 (s), 1552 (s), 1336 (s), 1320 (s), 1161 (s), 1145 (s), 1078 (s), 968 (m), 836 (s), 811 (s) 797 (s), 779 (s), 751 (s), 609 (m), 546 (m). HRMS (ASAP+, m/z): detected 532.2411 calculated for $\text{C}_{25}\text{H}_{38}\text{N}_5\text{O}_4\text{SiS}$ $[\text{M}+\text{H}]^+$ 532.2414.

5.8 Synthesis of *tert*-butyl (3-(4-(methyl((tetrahydro-2*H*-pyran-4-yl)methyl)amino)-7-((2-(trimethylsilyl)ethoxy)methyl)-7*H*-pyrrolo[2,3-*d*]pyrimidin-6-yl)phenyl)carbamate (**9**)

5.8.1 2 times 500 mg scale

Compound **3** (501 mg, 0.995 mmol), 3-(*N*-Boc-amino)phenylboronic acid (283 mg, 1.19 mmol), K_2CO_3 (413 mg, 2.99 mmol) and $\text{Pd}(\text{dppf})\text{Cl}_2$ (36.4 mg, 0.049 mmol) were dissolved in degassed 1,4-dioxane/ H_2O (2:1, 15 mL) under an N_2 -atmosphere and stirred at 80 °C for 10 min-



utes. The reaction was concentrated in *vacuo*, added water (20 mL) and extracted with CH₂Cl₂ (3 x 20 mL). The combined organic phases were washed with brine (30 mL), dried over Na₂SO₄, filtered and concentrated in *vacuo*. The crude product was purified by silica-gel column chromatography (*n*-pentane/EtOAc, 1/1, R_f=0.21). The product **9** (362 mg, 0.637 mmol), was isolated with a yield of 65% as a transparent oil.

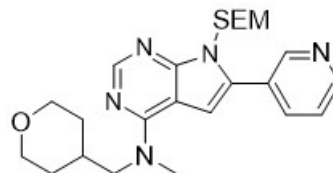
The reaction was run a second time isolating product **9** (437 mg, 0.769 mmol), with a yield of 77% as a transparent oil.

Spectroscopic data for compound **9** (Appendix H):

¹H-NMR (600 MHz, DMSO-*d*₆) δ: 9.43 (s, 1H), 8.20 (s, 1H), 7.82 (s, 1H), 7.43 (d, J = 7.5 Hz, 1H), 7.35 (t, J = 7.7 Hz, 1H), 7.32 (d, J = 7.6 Hz, 1H), 6.74 (s, 1H), 5.52 (s, 2H), 3.86–3.80 (m, 2H), 3.69 (d, J = 7.4 Hz, 2H), 3.54–3.48 (m, 2H), 3.38 (s, 2H), 3.25 (td, J = 11.7, 2.0 Hz, 2H), 2.10–2.03 (m, 1H), 1.57–1.51 (m, 2H), 1.48 (s, 9H), 1.29 (qd, J = 12.6, 4.5 Hz, 2H), 0.84–0.77 (m, 2H), -0.11 (s, 9H). ¹³C-NMR (150 MHz, DMSO-*d*₆) δ: 156.4, 152.9, 152.7, 151.2, 139.9, 136.4, 131.9, 128.9, 122.4, 118.6, 118.0, 102.2, 102.0, 79.1, 70.2, 66.8 (2C), 65.5, 55.5, 39.0, 34.0, 30.3 (2C), 28.1, 17.3, -1.5 (3C). IR (neat, *cm*⁻¹) *v*: 3289 (m), 2950 (s), 2930 (s), 2845 (m), 1724 (s), 1568 (s), 1529 (w), 1415 (w), 1365 (w), 1305 (w), 1234 (m), 1156 (s), 1070 (m), 1037 (w), 855 (w), 833 (m), 761 (m), 698 (w) 457 (w). HRMS (ASAP+, *m/z*): detected 568.3321 calculated for C₃₀H₄₆N₅O₄Si [M+H]⁺ 568.3319.

5.9 Synthesis of *N*-methyl-6-(pyridin-3-yl)-*N*-((tetrahydro-2*H*-pyran-4-yl)methyl)-7-((2-(trimethylsilyl)ethoxy)methyl)-7*H*-pyrrolo[2,3-*d*]pyrimidin-4-amine (10)

Compound **3** (266 mg, 0.529 mmol), 3-pyridinylboronic acid (78.1 mg, 0.635 mmol), K_2CO_3 (219 mg, 1.59 mmol) and $Pd(dppf)Cl_2$ (19.4 mg, 0.026 mmol) were dissolved in degassed 1,4-dioxane/ H_2O (2:1, 12 mL) under an



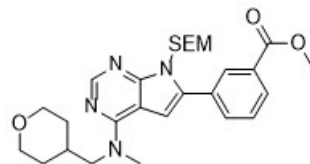
N_2 -atmosphere and stirred at 80 °C for 15 minutes. The reaction was concentrated in *vacuo*, added water (20 mL) and extracted with CH_2Cl_2 (3 x 20 mL). The combined organic phases were washed with brine (30 mL), dried over Na_2SO_4 , filtered and concentrated in *vacuo*. The crude product was purified by silica-gel column chromatography (*n*-pentane/ $EtOAc$, 1/1, $R_f=0.14$). The product **10** (187 mg, 0.412 mmol), was isolated with a yield of 82% as a transparent oil.

Spectroscopic data for compound **10** (Appendix I):

1H -NMR (600 MHz, $DMSO-d_6$) δ : 8.94 (dd, $J = 2.4, 0.9$ Hz, 1H), 8.60 (dd, $J = 4.8, 1.6$ Hz, 1H), 8.22 (s, 1H), 8.18 – 8.13 (m, 1H), 7.52 (ddd, $J = 8.0, 4.8, 0.9$ Hz, 1H), 7.02 (s, 1H), 5.57 (s, 2H), 3.86–3.80 (m, 2H), 3.71 (d, $J = 7.4$ Hz, 2H), 3.62–3.56 (m, 2H), 3.41 (s, 3H), 3.24 (td, $J = 11.7, 2.1$ Hz, 2H), 2.11 – 2.03 (m, 1H), 1.55–1.49 (m, 2H), 1.29 (q, $J = 12.3, 4.4$ Hz, 2H), 0.86–0.79 (m, 2H), -0.11 (s, 9H). ^{13}C -NMR (150 MHz, $DMSO-d_6$) δ : 156.5, 153.2, 151.5, 149.0, 148.8, 135.5, 132.7, 127.8, 123.6, 103.7, 102.1, 70.2, 66.7 (2C), 65.7, 55.4, 38.9, 33.9, 30.2 (2C), 17.3, -1.4 (3C). IR (neat, cm^{-1}) ν : 2949 (m), 2924 (m), 2842 (m), 1736 (w) 1567 (s), 1414 (m) 1307 (m), 1246 (m), 1071 (m), 833 (m), 769 (m), 753 (w), 711 (w), 693 (w). HRMS (ASAP+, m/z): detected 454.2639 calculated for $C_{24}H_{36}N_5O_2Si$ $[M+H]^+$ 454.2638.

5.10 Synthesis of methyl 3-(4-(methyl((tetrahydro-2H-pyran-4-yl)methyl)amino)-7-((2-(trimethylsilyl)ethoxy)methyl)-7H-pyrrolo[2,3-d]pyrimidin-6-yl)benzoate (11)

Compound **3** (202 mg, 0.398 mmol), 3-methoxycarbonyl phenyl boronic acid (86.0 mg, 0.478 mmol), K₂CO₃ (165 mg, 1.19 mmol) and Pd(dppf)Cl₂ (14.6 mg, 0.019 mmol) were dissolved in degassed 1,4-dioxane/H₂O (2:1, 6 mL) under an N₂-atmosphere and stirred at 80 °C for



12 minutes. The reaction was concentrated in *vacuo*, added water (20 mL) and extracted with CH₂Cl₂ (3 x 20 mL). The combined organic phases were washed with brine (30 mL), dried over Na₂SO₄, filtered and concentrated in *vacuo*. The crude product was purified by silica-gel column chromatography (*n*-pentane/EtOAc, 1/1, R_f=0.21). The product **11** (182 mg, 0.356 mmol), was isolated with a yield of 89% as a transparent oil.

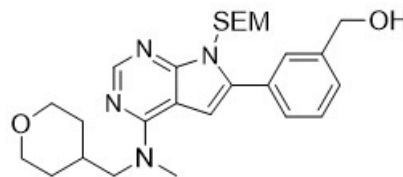
Spectroscopic data for compound **11** (Appendix J):

¹H-NMR (600 MHz, DMSO-*d*₆) δ: 8.33 (td, J = 1.8, 0.5 Hz, 1H), 8.22 (s, 1H), 8.02 (ddd, J = 7.8, 1.9, 1.2 Hz, 1H), 7.99 (ddd, J = 7.8, 1.7, 1.1 Hz, 1H), 7.64 (t, J = 8.0 Hz, 1H), 6.96 (s, 1H), 5.52 (s, 2H), 3.88 (s, 3H), 3.86–3.80 (m, 2H), 3.70 (d, J = 7.4 Hz, 2H), 3.62–3.56 (m, 2H), 3.41 (s, 3H), 3.24 (td, J = 11.7, 2.1 Hz, 2H), 2.03–2.10 (m, 1H), 1.56–1.50 (m, 2H), 1.29 (qd, J = 12.3, 4.6 Hz, 2H), 0.89–0.82 (m, 2H), -0.10 (s, 9H).
¹³C-NMR (150 MHz, DMSO-*d*₆) δ: 165.9, 156.5, 153.0, 151.5, 134.9, 133.2, 132.1, 130.3, 129.2, 129.1, 128.6, 103.3, 102.1, 70.3, 66.7 (2C), 65.5, 55.4, 52.3, 39.0, 33.9, 30.3 (2C), 17.3, -1.4 (3C). IR (neat, cm⁻¹) *v*: 2949 (m), 2930 (m), 2841 (m), 1723 (s), 1567 (s), 1550 (w), 1415 (w),

1310 (m), 1268 (m), 1243 (m) 1214 (w), 1072 (m), 1033 (w), 833 (s), 776 (w), 750 (s), 693 (m). HRMS (ASAP+, m/z): detected 511.2740 calculated for C₂₇H₃₉N₄O₄Si [M+H]⁺ 511.2741.

5.11 Synthesis of (3-(4-(methyl((tetrahydro-2*H*-pyran-4-yl)methyl)amino)-7-((2-(trimethylsilyl)ethoxy)methyl)-7*H*-pyrrolo[2,3-*d*]pyrimidin-6-yl)phenyl)methanol(**12**)

Compound **3** (150 mg, 0.299 mmol), 3-(hydroxymethyl)phenylboronic acid (54.4 mg, 0.358 mmol), K₂CO₃ (124 mg, 0.896 mmol) and Pd(dppf)Cl₂ (10.9 mg, 0.015 mmol) were dissolved in degassed 1,4-dioxane/H₂O (2:1, 6 mL) under an N₂-atmosphere and stirred at 80 °C for



13 minutes. The reaction was concentrated in *vacuo*, added water (20 mL) and extracted with CH₂Cl₂ (3 x 20 mL). The combined organic phases were washed with brine (30 mL), dried over Na₂SO₄, filtered and concentrated in *vacuo*. The crude product was purified by silica-gel column chromatography (*n*-pentane/EtOAc, 1/1, R_f=0.26). The product **12** (123 mg, 0.255 mmol), was isolated with a yield of 85% as a red, transparent oil.

Spectroscopic data for compound **12** (Appendix K):

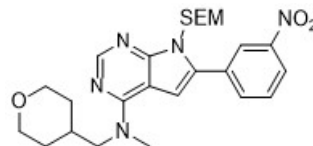
¹H-NMR (600 MHz, DMSO-*d*₆) δ: 8.20 (s, 1H), 7.65 (s, 1H), 7.62 (d, J = 7.7 Hz, 1H), 7.44 (t, J = 7.6 Hz, 1H), 7.38 (d, J = 7.9 Hz, 1H), 6.82 (s, 1H), 5.52 (s, 2H), 5.25 (t, J = 5.7 Hz, 1H), 4.56 (d, J = 5.7 Hz, 2H), 3.86–3.80 (m, 2H), 3.70 (d, J = 7.4 Hz, 2H), 3.62–3.56 (m, 2H), 3.40 (s, 3H), 3.24 (td, J = 11.7, 2.1 Hz, 2H), 2.12 – 2.02 (m, 1H), 1.55–1.49 (m, 2H), 1.29 (qd, J = 12.2, 4.5 Hz, 2H), 0.87–0.80 (m, 2H), -0.09 (s, 9H). ¹³C-NMR (150 MHz, DMSO-*d*₆) δ: 156.4, 152.9, 151.2,

143.1, 136.3, 131.3, 128.4, 126.9, 126.6, 126.1, 102.2, 102.1, 70.3, 66.7 (2C), 65.6, 62.8, 55.4, 38.9, 33.9, 30.3 (2C), 17.3, -1.4 (3C). IR (neat, cm^{-1}) ν : 3398 (w), 3280 (w), 2949 (m), 2919 (m), 2844 (m), 1737 (m), 1568 (s), 1549 (w), 1415 (m), 1306 (m), 1246 (m), 1071 (m), 1036 (m), 833 (m), 762 (m), 702 (w). HRMS (ASAP+, m/z): detected 483.2789 calculated for $C_{26}H_{39}N_4O_3Si$ $[M+H]^+$ 483.2791.

5.12 Synthesis of *N*-methyl-6-(3-nitrophenyl)-*N*-((tetrahydro-2*H*-pyran-4-yl)methyl)-7-((2-(trimethylsilyl)ethoxy)methyl)-7*H*-pyrrolo[2,3-*d*]pyrimidin-4-amine (**13**)

5.12.1 100 mg scale

Compound **3** (101 mg, 0.199 mmol), 3-nitrophenylboronic acid (40.0 mg, 0.238 mmol), K_2CO_3 (82.5 mg, 0.597 mmol) and $Pd(dppf)Cl_2$ (7.28 mg, 0.0099 mmol) were dissolved in degassed 1,4-dioxane/ H_2O (2:1, 4.5 mL) under an



N_2 -atmosphere and stirred at 80 °C for 11 minutes. The reaction was concentrated in *vacuo*, added water (20 mL) and extracted with CH_2Cl_2 (3 x 20 mL). The combined organic phases were washed with brine (30 mL), dried over Na_2SO_4 , filtered and concentrated in *vacuo*. The crude product was purified by silica-gel column chromatography (*n*-pentane/ $EtOAc$, 1/1, $R_f=0.28$). The product **13** (97.2 mg, 0.195 mmol), was isolated with a yield of 98% as a yellow oil.

5.12.2 500 mg scale

Compound **3** (500 mg, 1.01 mmol), 3-nitrophenylboronic acid (202 mg, 1.21 mmol), K_2CO_3 (419 mg, 3.03 mmol) and $Pd(dppf)Cl_2$ (36.9 mg, 0.0505 mmol) were dissolved in degassed 1,4-dioxane/ H_2O (2:1, 15 mL)

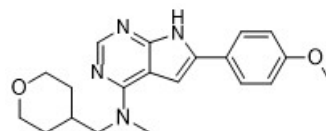
under an N₂-atmosphere and stirred at 80 °C for 15 minutes. The reaction was concentrated in *vacuo*, added water (20 mL) and extracted with CH₂Cl₂ (3 x 20 mL). The combined organic phases were washed with brine (30 mL), dried over Na₂SO₄, filtered and concentrated in *vacuo*. The crude product was purified by silica-gel column chromatography (*n*-pentane/EtOAc, 1/1, R_f=0.22). The product **13** (470.8 mg, 0.946 mmol), was isolated with a yield of 94% as a yellow oil.

Spectroscopic data for compound **13** (Appendix L):

¹H-NMR (600 MHz, DMSO-*d*₆) δ: 8.65 (t, J = 2.0 Hz, 1H), 8.25 (ddd, J = 8.2, 2.3, 1.0 Hz, 1H), 8.23 (s, 1H), 8.22 (ddd, J = 7.8, 1.9, 1.2 Hz, 1H), 7.13 (s, 1H), 5.58 (s, 2H), 3.86–3.80 (m, 2H), 3.72 (d, J = 7.4 Hz, 2H), 3.67–3.61 (m, 2H), 3.42 (s, 3H), 3.24 (td, J = 11.7, 2.1 Hz, 2H), 2.11 – 2.03 (m, 1H), 1.56–1.50 (m, 2H), 1.29 (qd, J = 12.1, 4.5 Hz, 2H), 0.92–0.85 (m, 2H), -0.08 (s, 9H). ¹³C-NMR (150 MHz, DMSO-*d*₆) δ: 156.6, 153.2, 151.8, 148.2, 134.7, 133.6, 133.1, 130.3, 122.7, 122.5, 104.6, 102.1, 70.3, 66.7 (2C), 65.6, 55.4, 38.9, 33.9, 30.2, 17.3, -1.5 (3C). IR (neat, cm⁻¹) *v*: 3054 (w), 2987 (w), 2306 (w), 1572 (w), 1421 (w), 1264 (s), 895 (w), 730 (s) 703 (s). HRMS (ASAP+, m/z): detected 498.2535, calculated for C₂₅H₃₆N₅O₄Si [M+H]⁺ 498.2537

5.13 Synthesis of 6-(4-methoxyphenyl)-*N*-methyl-*N*-((tetrahydro-2*H*-pyran-4-yl)methyl)-7*H*-pyrrolo[2,3-*d*]pyrimidin-4-amine (**14**)

Compound **4** (1.08 g, 2.24 mmol) was stirred in TFA (7 mL) and CH₂Cl₂ (25 mL) at 50 °C for 3 hours. The reaction mixture was concentrated in *vacuo* and then stirred in THF (20 mL) and NaHCO₃ (20 mL) for 18 hours at room temper-



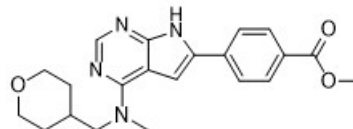
ature. The reaction mixture was concentrated in *vacuo* before it was stirred with CH₂Cl₂/MeOH (4:1, 50 mL) and filtered through celite. The reaction mixture was concentrated in *vacuo*. The crude product was purified by silica-gel column chromatography (CH₂Cl₂/MeOH, 9/1, R_f=0.37). The product **14** (501 mg, 1.4 mmol), was isolated with a yield of 65% as a white powder. Mp. 220-224 °C. Purity 97%, t_R = 5.8 min.

Spectroscopic data for compound **14** (Appendix M):

¹H-NMR (600 MHz, DMSO-*d*₆) δ: 12.02 (s, 1H), 8.09 (s, 1H), 7.81 (d, J = 8.8 Hz, 2H), 6.99 (d, J = 8.9 Hz, 2H), 6.93 (s, 1H), 3.86–3.80 (m, 2H), 3.79 (s, 3H), 3.68 (d, J = 7.4 Hz, 2H), 3.39 (s, 3H), 3.24 (td, J = 11.7, 2.1 Hz, 2H), 2.08-2.04 (m, 1H), 1.57–1.51 (m, 2H), 1.29 (qd, J = 11.7, 4.5 Hz, 2H). ¹³C-NMR (150 MHz, DMSO-*d*₆) δ: 158.6, 156.2, 152.6, 150.6, 133.1, 126.9 (2C), 124.2, 114.2 (2C), 103.1, 97.4, 66.7 (2C), 55.3, 55.2, 38.9, 33.9, 30.3 (2C). IR (neat, cm⁻¹) *v*: 3084 (w), 2947 (m), 2918 (m), 2833 (m), 2737 (w), 1565 (s), 1498 (s), 1439 (m), 1414 (m), 1319 (m), 1287 (m), 1250 (s), 1177 (m), 1096 (m), 1026 (m), 834 (s), 756 (w). HRMS (ASAP+, m/z): detected 353.1978, calculated for C₂₀H₂₅N₄O₂ [M+H]⁺ 353.1978

5.14 Synthesis of methyl 4-(4-(methyl((tetrahydro-2H-pyran-4-yl)methyl)amino)-7H-pyrrolo[2,3-*d*]pyrimidin-6-yl)benzoate (**15**)

Compound **5** (142 mg, 0.277 mmol) was stirred in TFA (1.5 mL) and CH₂Cl₂ (6 mL) at 50 °C for 3.5 hours. The reaction mixture was concentrated in *vacuo* and then stirred in THF (7.5 mL) and NaHCO₃ (7.5 mL) for 5 hours at room temperature. The reaction mixture was concentrated in *vacuo* before it



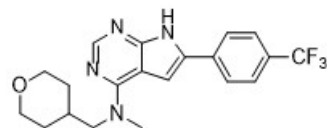
was stirred with CH₂Cl₂/MeOH (4:1, 50 mL) and filtered through celite. The reaction mixture was concentrated in *vacuo*. The crude product was purified by silica-gel column chromatography (CH₂Cl₂/MeOH, 9/1, R_f=0.32). The product **15** (101 mg, 0.265 mmol), was isolated with a yield of 96% as a white powder. Mp. >238 °C (decomposed). Purity 98%, t_R = 6.8 min.

Spectroscopic data for compound **15** (Appendix N):

¹H-NMR (600 MHz, DMSO-*d*₆) δ: 12.29 (s, 1H), 8.13 (s, 1H), 8.03 (d, J = 8.6 Hz, 2H), 7.98 (d, J = 8.6 Hz, 2H), 7.29 (s, 1H), 3.86 (s, 3H), 3.86–3.80 (m, 2H), 3.70 (d, J = 7.4 Hz, 2H), 3.42 (s, 3H), 3.25 (td, J = 11.7, 2.1 Hz, 2H), 2.08–2.04 (m, 1H), 1.57–1.51 (m, 2H), 1.30 (qd, J = 12.2, 4.4 Hz, 2H). ¹³C-NMR (150 MHz, DMSO-*d*₆) δ: 165.9, 156.6, 153.2, 151.7, 136.0, 131.5, 129.6 (2C), 127.6, 124.5 (2C), 103.4, 101.5, 66.8 (2C), 55.3, 52.1, 39.0, 33.9, 30.3 (2C). IR (neat, cm⁻¹) ν: 3124 (w), 2949 (m), 2917 (m), 2838 (m), 1707 (s), 1668 (m), 1571 (s), 1547 (w), 1432 (w), 1416 (w), 1276 (m), 1194 (m), 1141 (m), 1105, 1095 (m), 1080 (m), 848 (w), 799 (m), 760 (m), 725 (w), 519 (w). HRMS (ASAP+, m/z): detected 381.1927, calculated for C₂₁H₂₅N₄O₃ [M+H]⁺ 381.1927.

5.15 Synthesis of *N*-methyl-*N*-((tetrahydro-2*H*-pyran-4-yl)methyl)-6-(4-(trifluoromethyl)phenyl)-7*H*-pyrrolo[2,3-*d*]pyrimidin-4-amine (**16**)

Compound **6** (118 mg, 0.227 mmol) was stirred in TFA (1.2 mL) and CH₂Cl₂ (4.8 mL) at 50 °C for 2.5 hours. The reaction mixture was concentrated in *vacuo* and then stirred in THF (6 mL) and NaHCO₃ (6 mL) for 16 hours at room temperature. The reaction mixture was concentrated in *vacuo* before it was



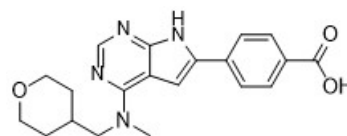
stirred with $\text{CH}_2\text{Cl}_2/\text{MeOH}$ (4:1, 50 mL) and filtered through celite. The reaction mixture was concentrated in *vacuo*. The crude product was purified by silica-gel column chromatography ($\text{CH}_2\text{Cl}_2/\text{MeOH}$, 9/1, $R_f=0.43$). The product **16** (55.7 mg, 0.143 mmol), was isolated with a yield of 63% as a white powder. Mp. 261.0-266.2 °C. Purity >99%, $t_R = 7.1$ min.

Spectroscopic data for compound **16** (Appendix O):

$^1\text{H-NMR}$ (600 MHz, $\text{DMSO-}d_6$) δ : 12.31 (s, 1H), 8.14 (s, 1H), 8.10 (d, $J = 8.1$ Hz, 2H), 7.77 (d, $J = 8.2$ Hz, 2H), 7.29 (s, 1H), 3.86–3.80 (m, 2H), 3.71 (d, $J = 7.4$ Hz, 2H), 3.42 (s, 3H), 3.25 (td, $J = 11.7, 2.1$ Hz, 2H), 2.12 – 2.02 (m, 1H), 1.57–1.51 (m, 2H), 1.31 (td, $J = 12.4, 4.4$ Hz, 2H). $^{13}\text{C-NMR}$ (150 MHz, $\text{DMSO-}d_6$) δ : 156.6, 153.2, 151.8, 135.5, 131.2, 126.9 (q, $J = 31.6$ Hz), 125.7 (q, $J = 3.3$ Hz, 2C) 125.2, 125.0, 123.4 (q, $J = 271.4$ Hz), 103.3, 101.3, 66.7 (2C), 55.3, 39.0, 33.9, 30.3 (2C). $^{19}\text{F-NMR}$ (565 MHz, $\text{DMSO-}d_6$, C_6F_6) δ : -63.1 (3F), -75.8. IR (neat, cm^{-1}) ν : 3404 (m), 3209 (w), 3094 (m), 2959 (w), 2932 (m), 2915 (m), 2843 (m), 2742 (w), 1668 (s), 1567 (s), 1550 (w), 1416 (m), 1323 (s), 1195 (m), 1156 (m), 1140 (s), 1115 (m), 1105 (s), 1093 (w), 1073 (m), 1060 (w), 1014 (m), 842 (m), 798 (m), 724 (m). HRMS (ASAP+, m/z): detected 391.1750, calculated for $\text{C}_{20}\text{H}_{22}\text{N}_4\text{OF}_3$ $[\text{M}+\text{H}]^+$ 391.1746

5.16 Synthesis of 4-(4-(methyl((tetrahydro-2H-pyran-4-yl)methyl)amino)-7H-pyrrolo[2,3-d]pyrimidin-6-yl)benzoic acid (17)

Compound **15** (95.0 mg, 0.249 mmol, 1 eq.) was added LiOH solution (29.9 mg, 1.25 mmol, 5 eq.), MeOH (4 mL), H_2O (2 mL) and dioxane (2 mL). The solution was stirred for 64 hours at room temperature. The reaction



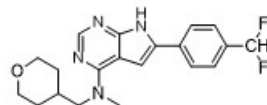
mixture was concentrated in *vacuo* before the residue was diluted in water (10 mL). The reaction mixture was then acidified to pH 3 with HCl (2M, 1 mL). The solid formed **17** was purified by cold filtration and was isolated with a yield of 29% as a white powder. Mp. >239 °C (decomposed). Purity 99%, $t_R = 5.4$ min.

Spectroscopic data for compound **17** (Appendix N):

$^1\text{H-NMR}$ (600 MHz, DMSO- d_6) δ : 12.89 (s, 1H), 12.27 (s, 1H), 8.13 (s, 1H), 8.01 (d, $J = 8.5$ Hz, 2H), 7.95 (d, $J = 8.5$ Hz, 2H), 7.26 (s, 1H), 3.86–3.80 (m, 2H), 3.70 (d, $J = 7.4$ Hz, 2H), 3.42 (s, 3H), 3.25 (td, $J = 11.7, 2.1$ Hz, 2H), 2.11 – 2.02 (m, 1H), 1.57–1.51 (m, 2H), 1.30 (qd, $J = 12.1, 4.4$ Hz, 2H). $^{13}\text{C-NMR}$ (150 MHz, DMSO- d_6) δ : 167.0, 156.6, 153.2, 151.6, 135.7, 131.8, 129.8 (2C), 128.9, 124.5 (2C), 103.4, 101.2, 66.8 (2C), 55.4, 38.9, 33.9, 30.3 (2C). IR (neat, cm^{-1}) ν : 3485 (m), 3368 (m), 3219 (s), 2941 (m), 2598 (w), 2477 (w), 1672 (m), 1579 (s), 1557 (w), 1542 (w), 1518 (w), 1373 (w), 1275 (s), 1250 (s), 1222 (m), 1182 (m), 1079 (s), 983 (m), 797 (w), 759 (s), 730 (m), 693 (w), 676 (w), 467 (w). HRMS (ASAP+, m/z): detected 367.1771, calculated for $\text{C}_{20}\text{H}_{23}\text{N}_4\text{O}_3$ $[\text{M}+\text{H}]^+$ 367.1770.

5.17 Synthesis of 6-(4-(difluoromethyl)phenyl)-*N*-methyl-*N*-((tetrahydro-2*H*-pyran-4-yl)methyl)-7*H*-pyrrolo[2,3-*d*]pyrimidin-4-amine (**18**)

Compound **7** (103 mg, 0.205 mmol) was stirred in TFA (1.2 mL) and CH_2Cl_2 (4.8 mL) at 50 °C for 2.5 hours. The reaction mixture was concentrated in *vacuo* and then stirred in THF (6 mL) and NaHCO_3 (6 mL) for 16 hours at room temperature. The reaction mixture was concentrated in *vacuo* before it was stirred with



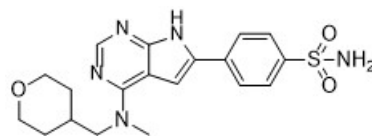
CH₂Cl₂/MeOH (4:1, 50 mL) and filtered through celite. The reaction mixture was concentrated in *vacuo*. The crude product was purified by silica-gel column chromatography (CH₂Cl₂/MeOH, 9/1, R_f=0.53). The product **18** (60.7 mg, 0.163 mmol), was isolated with a yield of 80% as a yellow solid. Mp. >235 °C (decomposed). Purity 97%, t_R = 7.1 min.

Spectroscopic data for compound **18** (Appendix Q):

¹H-NMR (600 MHz, DMSO-*d*₆) δ: 12.23 (s, 1H), 8.13 (s, 1H), 8.02 (d, J = 8.1 Hz, 2H), 7.61 (d, J = 7.9 Hz, 2H), 7.21 (s, 1H), 7.04 (t, J_F = 56.4 Hz, 1H), 3.86–3.80 (m, 2H), 3.70 (d, J = 7.4 Hz, 2H), 3.41 (s, 3H), 3.25 (td, J = 11.7, 2.1 Hz, 2H), 2.10–2.03 (m, 1H), 1.57–1.51 (m, 2H), 1.30 (qd, J = 12.3, 4.5 Hz, 2H). ¹³C-NMR (150 MHz, DMSO-*d*₆) δ: 156.6, 153.1, 151.5, 134.1, 132.5 (t, J = 21.9 Hz), 131.8, 126.2 (t, J = 6.0 Hz, 2C), 124.9, 114.9 (t, J = 235.5 Hz, 2C), 103.3, 100.4, 66.(2C), 55.3, 39.0, 33.9, 30.3 (2C). ¹⁹F-NMR (565 MHz, DMSO-*d*₆, C₆F₆) δ : -111.5 (2F). IR (neat, cm⁻¹) *v*: 3080 (m), 2952 (m), 2922 (m), 2848 (m), 1732 (s), 1565 (s), 1547 (s), 1510 (m), 1414 (m), 1365 (m), 1322 (m), 1302 (m), 1279 (m), 1264 (m), 1234 (m), 1223 (m), 1140 (m), 1065 (s), 1014 (s), 983 (m), 920 (m), 873 (w), 844 (w), 810 (w), 795 (w), 766 (w), 742 (w). HRMS (ASAP+, m/z): detected 373.1841, calculated for C₂₀H₂₃N₄OF₂ [M+H]⁺ 373.1840

5.18 Synthesis of 4-(4-(methyl((tetrahydro-2*H*-pyran-4-yl)methyl)amino)-7*H*-pyrrolo[2,3-*d*]pyrimidin-6-yl)benzenesulfonamide (**19**)

Compound **8** (121 mg, 0.227 mmol) was stirred in TFA (1.2 mL) and CH₂Cl₂ (4.8 mL) at 50 °C for 2.5 hours. The reaction mixture was concentrated in *vacuo* and then stirred in THF (6 mL)



and NaHCO_3 (6 mL) for 16 hours at room temperature. The reaction mixture was concentrated in *vacuo* before it was stirred with $\text{CH}_2\text{Cl}_2/\text{MeOH}$ (4:1, 50 mL) and filtered through celite. The reaction mixture was concentrated in *vacuo*. The crude product was purified by silica-gel column chromatography ($\text{CH}_2\text{Cl}_2/\text{MeOH}$, 9/1, $R_f=0.26$). The product **19** (86.6 mg, 0.216 mmol), was isolated with a yield of 95% as a white solid. Mp. >235 °C (decomposed). Purity 96%, $t_R = 4.9$ min.

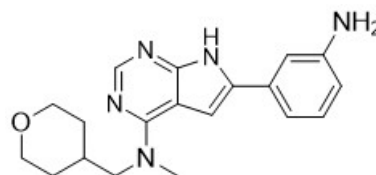
Spectroscopic data for compound **19** (Appendix R):

$^1\text{H-NMR}$ (600 MHz, $\text{DMSO}-d_6$) δ : 12.27 (s, 1H), 8.14 (s, 1H), 8.06 (d, $J = 8.6$ Hz, 2H), 7.83 (d, $J = 8.6$ Hz, 2H), 7.35 (s, 2H), 7.27 (s, 1H), 3.86–3.80 (m, 2H), 3.70 (d, $J = 7.4$ Hz, 2H), 3.42 (s, 3H), 3.25 (td, $J = 11.7, 2.1$ Hz, 2H), 2.12 – 2.02 (m, 1H), 1.57–1.51 (m, 2H), 1.30 (qd, $J = 12.4, 4.4$ Hz, 2H). $^{13}\text{C-NMR}$ (150 MHz, $\text{DMSO}-d_6$) δ : 156.6, 153.2, 151.7, 142.1, 134.7, 131.4, 126.2 (2C), 124.7 (2C), 103.4, 101.2, 66.8 (2C), 55.3, 39.0, 33.9, 30.2 (2C). IR (neat, cm^{-1}) ν : 3309 (m), 3211 (m), 3100 (m), 2920 (m), 2849 (m), 1694 (w), 1571 (s), 1543 (m), 1340 (m), 1325 (m), 1161 (s), 1087 (m), 767 (m), 703 (m), 541 (w). HRMS (ASAP+, m/z): detected 402.1602, calculated for $\text{C}_{19}\text{H}_{24}\text{N}_5\text{O}_3\text{S}$ $[\text{M}+\text{H}]^+$ 402.1600

5.19 Synthesis of 6-(3-aminophenyl)-*N*-methyl-*N*-((tetrahydro-2*H*-pyran-4-yl)methyl)-7*H*-pyrrolo[2,3-*d*]pyrimidin-4-amine (**20**)

5.19.1 By SEM-deprotection

Compound **9** (264 mg, 0.465 mmol) was stirred in TFA (2 mL) and CH_2Cl_2 (10 mL) at 50 °C for 3 hours. The reaction mixture was concentrated in *vacuo* and then stirred in THF (12 mL) and



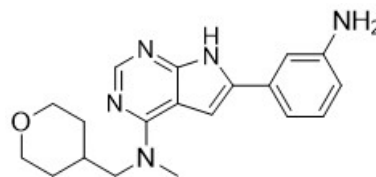
NaHCO₃ (12 mL) over night at room temperature. The reaction mixture was concentrated in *vacuo* before it was stirred with CH₂Cl₂/MeOH (4:1, 50 mL) and filtered through celite. The reaction mixture was concentrated in *vacuo*. The crude product was purified over three rounds by silica-gel column chromatography (CH₂Cl₂/MeOH, 9/1, R_f=0.28). The product **20** (90.5 mg, 0.268 mmol), was isolated with a yield of 58% as a white powder. Mp. 196.2-201.3 °C. Purity 95%, t_R = 4.1 min.

Spectroscopic data for compound **20** (Appendix S):

¹H-NMR (600 MHz, DMSO-*d*₆) δ: 11.97 (s, 1H), 8.09 (s, 1H), 7.06 (t, J = 8.0 Hz, 1H), 7.02–6.97 (m, 2H), 6.83 (s, 1H), 6.56–6.45 (m, 1H), 5.08 (s, 2H), 3.87–3.81 (m, 2H), 3.67 (d, J = 7.3 Hz, 2H), 3.38 (s, 3H), 3.25 (td, J = 11.7, 2.1 Hz, 2H), 2.13–1.98 (m, 1H), 1.57–1.51 (m, 2H), 1.29 (qd, J = 11.7, 4.5 Hz, 2H). ¹³C-NMR (150 MHz, DMSO-*d*₆) δ: 156.3, 152.6, 150.8, 148.8, 134.0, 132.0, 129.3, 113.4, 112.9, 110.2, 103.2, 97.9, 66.7 (2C), 55.4, 38.9, 33.9, 30.3 (2C). IR (neat, cm⁻¹) *v*: 3301 (m), 3172 (m), 2948 (m), 2928 (m), 2909 (m), 2835 (m), 1566 (s), 1509 (w), 1418 (w), 1405 (w), 1346 (w), 1320 (w), 1299 (w), 1234 (w), 1081 (m), 850 (m), 792 (m), 782 (m), 757 (m), 693 (w). HRMS (ASAP+, m/z): detected 338.1998, calculated for C₁₉H₂₄N₅O [M+H]⁺ 338.1981.

5.19.2 By Reduction

Compound **24** (37.3 mg, 0.101 mmol), NH₄Cl (48.9 mg, 0.914 mmol) and iron powder (17.0 mg, 0.305 mmol) were dissolved in degassed EtOH (2.1 ml) and water (0.9 ml) under an N₂-atmosphere. The reaction mixture was stirred at 78 °C for 3 hours. The reaction mixture was filtrated through celite and extracted with CH₂Cl₂ (50 ml) and water (2

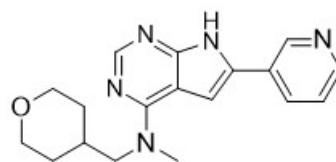


x 50 ml). The organic phase was washed with brine (30 ml), dried over Na₂SO₄, filtrated and concentrated in *vacuo*. The product was isolated as a white solid in a 81% yield (27.9 mg, 0.0827 mmol).

Compound **24** (250 mg, 0.680 mmol), NH₄Cl (328 mg, 6.12 mmol) and iron powder (114 mg, 2.04 mmol) were dissolved in degassed EtOH (14 ml) and water (6 ml) under an N₂-atmosphere. The reaction mixture was stirred at 78 °C for 3 hours. The reaction mixture was filtrated through celite and extracted with CH₂Cl₂ (50 ml) and water (2 x 50 ml). The organic phase was washed with brine (30 ml), dried over Na₂SO₄, filtrated and concentrated in *vacuo*. Product **20** was isolated as a white solid in a 56% yield (128 mg, 0.378 mmol). Mp. 196.2-201.3 °C. Purity 99%, *t*_R = 4.1 min.

5.20 Synthesis of *N*-methyl-6-(pyridin-3-yl)-*N*-((tetrahydro-2*H*-pyran-4-yl)methyl)-7*H*-pyrrolo[2,3-*d*]pyrimidin-4-amine (**21**)

Compound **10** (180 mg, 0.397 mmol) was stirred in TFA (1.5 mL) and CH₂Cl₂ (6 mL) at 50 °C for 3.5 hours. The reaction mixture was concentrated in *vacuo* and then stirred in THF (7.5 mL) and NaHCO₃ (7.5 mL) over night at room temperature. The reaction mixture was concentrated in *vacuo* before it was stirred with CH₂Cl₂/MeOH (4:1, 50 mL) and filtered through celite. The reaction mixture was concentrated in *vacuo*. The crude product was purified by silica-gel column chromatography (CH₂Cl₂/MeOH, 9/1, R_f=0.52). The product **21** (89.3 mg, 0.276 mmol), was isolated with a yield of 70% as a white powder. Mp. 233.1-235.2 °C. Purity 99%, *t*_R = 3.5 min.

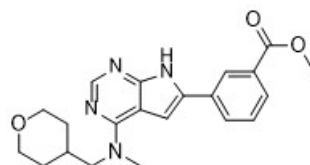


Spectroscopic data for compound **21** (Appendix T):

$^1\text{H-NMR}$ (600 MHz, $\text{DMSO-}d_6$) δ : 12.27 (s, 1H), 9.13-9.11 (m, 1H), 8.47 (dd, $J = 4.7, 1.6$ Hz, 1H), 8.27 – 8.18 (m, 1H), 8.13 (s, 1H), 7.44 (ddd, $J = 8.0, 4.8, 0.9$ Hz, 1H), 7.24 (s, 1H), 3.86–3.80 (m, 2H), 3.70 (d, $J = 7.4$ Hz, 2H), 3.41 (s, 3H), 3.25 (td, $J = 11.7, 2.1$ Hz, 2H), 2.10 – 2.03 (m, 1H), 1.57–1.51 (m, 2H), 1.30 (qd, $J = 12.3, 4.5$ Hz, 2H). $^{13}\text{C-NMR}$ (150 MHz, $\text{DMSO-}d_6$) δ : 156.5, 153.1, 151.5, 147.9, 146.0, 131.6, 129.8, 127.6, 123.7, 103.2, 100.3, 66.8 (2C), 55.3, 39.0, 33.9, 30.3 (2C). IR (neat, cm^{-1}) ν : 3095 (m), 2946 (m), 2912 (m), 2745 (m), 1564 (s), 1538 (w), 1512 (m), 1424 (m), 1410 (m), 1331 (m), 1317 (m), 1298 (w), 1092 (w), 844 (m), 759 (m). HRMS (ASAP+, m/z): detected 324.1825, calculated for $\text{C}_{18}\text{H}_{22}\text{N}_5\text{O}$ $[\text{M}+\text{H}]^+$ 324.1824

5.21 Synthesis methyl 3-(4-(methyl((tetrahydro-2H-pyran-4-yl)methyl)amino)-7H-pyrrolo[2,3-d]pyrimidin-6-yl)benzoate (**22**)

Compound **11** (150 mg, 0.285 mmol) was stirred in TFA (1.2 mL) and CH_2Cl_2 (4.8 mL) at 50 °C for 2.5 hours. The reaction mixture was concentrated in *vacuo* and then stirred in THF (6 mL) and NaHCO_3 (6 mL) for 16 hours at room temperature. The reaction mixture was concentrated in *vacuo* before it was stirred with $\text{CH}_2\text{Cl}_2/\text{MeOH}$ (4:1, 50 mL) and filtered through celite. The reaction mixture was concentrated in *vacuo*. The crude product was purified by silica-gel column chromatography ($\text{CH}_2\text{Cl}_2/\text{MeOH}$, 9/1, $R_f=0.43$). The product **22** (69.3 mg, 0.182 mmol), was isolated with a yield of 64% as a white powder. Mp. 206.2-210.9 °C. Purity >99%, $t_R = 4.2$ min.



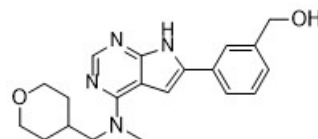
Spectroscopic data for compound **22** (Appendix U):

$^1\text{H-NMR}$ (600 MHz, $\text{DMSO-}d_6$) δ : 12.29 (s, 1H), 8.48 – 8.44 (m, 1H), 8.16-8.13 (m, 1H), 8.12 (s, 1H), 7.87-7.84 (m, 1H), 7.57 (t, $J = 7.8$ Hz, 1H), 7.18 (s, 1H), 3.90 (s, 3H), 3.87–3.81 (m, 2H), 3.70 (d, $J = 7.4$ Hz, 2H), 3.42 (s, 3H), 3.25 (td, $J = 11.7, 2.1$ Hz, 2H), 2.10-2.01 (m, 1H), 1.57–1.51 (m, 2H), 1.30 (qd, $J = 12.1, 4.5$ Hz, 2H). $^{13}\text{C-NMR}$ (150 MHz, $\text{DMSO-}d_6$) δ : 166.2, 156.6, 153.1, 151.4, 132.2, 131.8, 130.4, 129.3, 127.7, 125.2, 103.3, 100.0, 66.8 (2C), 55.3, 52.3, 38.9, 33.9, 30.3 (2C). IR (neat, cm^{-1}) ν : 3086 (m), 2924 (m), 2840 (m), 2722 (w), 1710 (s), 1571 (s), 1536 (w), 1512 (m), 1432 (w), 1413 (w), 1344 (w), 1329 (m), 1289 (m), 1256 (s), 1114 (w), 1091 (w), 1081 (m), 968 (m), 846 (m), 789 (m), 747 (s). HRMS (ASAP+, m/z): detected 381.1924, calculated for $\text{C}_{21}\text{H}_{25}\text{N}_4\text{O}_3$ $[\text{M}+\text{H}]^+$ 381.1927

5.22 Synthesis of (3-(4-(methyl((tetrahydro-2*H*-pyran-4-yl)methyl)amino)-7*H*-pyrrolo[2,3-*d*]pyrimidin-6-yl)phenyl)methanol (**23**)

Compound **12** (80.0 mg, 0.169 mmol) was stirred in TFA (1.2 mL) and CH_2Cl_2 (4.8 mL) at 50 °C for 2.5 hours. The reaction mixture was concentrated in *vacuo* and then stirred in THF (6 mL) and NaHCO_3 (6 mL) for 16 hours at room temperature.

The reaction mixture was concentrated in *vacuo* before it was stirred with $\text{CH}_2\text{Cl}_2/\text{MeOH}$ (4:1, 50 mL) and filtered through celite. The reaction mixture was concentrated in *vacuo*. The crude product was purified by silica-gel column chromatography ($\text{CH}_2\text{Cl}_2/\text{MeOH}$, 9/1, $R_f=0.18$). The product **23** (50.8 mg, 0.144 mmol), was isolated with a yield of 85% as a white powder. Mp. >229 °C (decomposed). Purity



98%, $t_R = 5.2$ min.

Spectroscopic data for compound **23** (Appendix V):

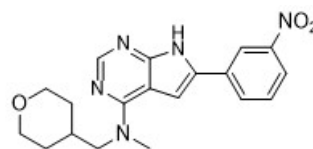
$^1\text{H-NMR}$ (600 MHz, $\text{DMSO-}d_6$) δ : 12.10 (s, 1H), 8.10 (s, 1H), 7.82 (ap s, 1H), 7.75-7.73 (m, 1H), 7.38 (t, $J = 7.7$ Hz, 1H), 7.25 (d, $J = 6.8$ Hz, 1H), 7.05 (ap s, 1H), 5.23 (t, $J = 5.7$ Hz, 1H), 4.54 (d, $J = 5.7$ Hz, 2H), 3.87-3.81 (m, 2H), 3.69 (d, $J = 7.4$ Hz, 2H), 3.41 (s, 3H), 3.25 (td, $J = 11.7, 2.1$ Hz, 2H), 2.12 - 2.01 (m, 1H), 1.57-1.51 (m, 2H), 1.27 (dd, $J = 12.5, 4.0$ Hz, 2H). $^{13}\text{C-NMR}$ (150 MHz, $\text{DMSO-}d_6$) δ : 156.4, 152.8, 151.1, 143.1, 133.1, 131.3, 128.6, 125.5, 123.1, 122.9, 103.3, 98.8, 66.7 (2C), 62.9, 55.3, 38.9, 33.9, 30.3 (2C). IR (neat, cm^{-1}) ν : 3426 (m), 3184 (m), 3103 (m), 2913 (m), 2843 (m), 2737 (m), 1733 (w), 1568 (s), 1539 (m), 1514 (m), 1437 (m), 1410 (m), 1318 (m), 1301 (m), 790 (w), 758 (m). HRMS (ASAP+, m/z): detected 353.1980, calculated for $\text{C}_{20}\text{H}_{25}\text{N}_4\text{O}_2$ $[\text{M}+\text{H}]^+$ 353.1978.

5.23 Synthesis of *N*-methyl-6-(3-nitrophenyl)-*N*-((tetrahydro-2*H*-pyran-4-yl)methyl)-7*H*-pyrrolo[2,3-*d*]pyrimidin-4-amine (**24**)

5.23.1 Scale 100 mg

Compound **13** (97.0 mg, 0.195 mmol) was stirred in TFA (1.2 mL) and CH_2Cl_2 (4.8 mL) at 50 °C for 3 hours. The reaction mixture was concentrated in *vacuo* and then stirred in THF (6 mL) and NaHCO_3 (6 mL) over night at room temperature.

The reaction mixture was concentrated in *vacuo* before it was stirred with $\text{CH}_2\text{Cl}_2/\text{MeOH}$ (4:1, 50 mL) and filtered through celite. The reaction mixture was concentrated in *vacuo*. The crude product was purified by silica-gel column chromatography ($\text{CH}_2\text{Cl}_2/\text{MeOH}$, 9/1,



$R_f=0.59$). The product **24** (46.8 mg, 0.0877 mmol), was isolated with a yield of 65% as a yellow powder. Mp. >248 °C (decomposed). Purity 98%, $t_R = 6.3$ min.

5.23.2 Scale 470 mg

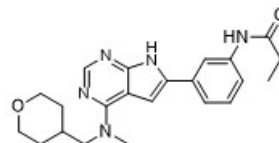
Compound **13** (471 mg, 0.946 mmol) was stirred in TFA (3.0 mL) and CH_2Cl_2 (15 mL) at 50 °C for 2.5 hours. The reaction mixture was concentrated in *vacuo* and then stirred in THF (18 mL) and NaHCO_3 (18 mL) over night at room temperature. The reaction mixture was concentrated in *vacuo* before it was stirred with $\text{CH}_2\text{Cl}_2/\text{MeOH}$ (4:1, 50 mL) and filtered through celite. The reaction mixture was concentrated in *vacuo*. The crude product was purified by silica-gel column chromatography ($\text{CH}_2\text{Cl}_2/\text{MeOH}$, 9/1, $R_f=0.27$). The product **24** (278 mg, 0.757 mmol), was isolated with a yield of 80% as a yellow powder, purity 98%, $t_R = 6.3$ min. Mp. >248 °C (decomposed).

Spectroscopic data for compound **24** (Appendix W):

$^1\text{H-NMR}$ (600 MHz, $\text{DMSO}-d_6$) δ : 12.40 (s, 1H), 8.77 (t, $J = 2.0$ Hz, 1H), 8.35-8.32 (m, 1H), 8.14 (s, 1H), 8.10 (ddd, $J = 8.2, 2.3, 0.9$ Hz, 1H), 7.71 (t, $J = 8.0$ Hz, 1H), 7.38 (s, 1H), 3.86-3.80 (m, 2H), 3.71 (d, $J = 7.4$ Hz, 2H), 3.43 (s, 3H), 3.25 (td, $J = 11.7, 2.1$ Hz, 2H), 2.12-2.02 (m, 1H), 1.57-1.51 (m, 2H), 1.30 (qd, $J = 12.1, 4.6$ Hz, 2H). $^{13}\text{C-NMR}$ (150 MHz, $\text{DMSO}-d_6$) δ : 156.7, 153.2, 151.8, 148.6, 133.4, 130.8, 130.6, 130.3, 121.4, 118.9, 103.3, 101.4, 66.8 (2C), 55.3, 38.9, 33.8, 30.3 (2C). IR (neat, cm^{-1}) ν : 3209 (m), 3134 (m), 2927 (m), 2835 (m), 1597 (w), 1577 (m), 1564 (s), 1546 (m), 1524 (m), 1510 (s), 1402 (m), 1345 (m), 1329 (w), 1318 (w), 1285 (m), 1140 (m), 1093 (m), 1069 (m), 920 (m), 849 (m), 779 (s), 737 (s), 690 (m). HRMS (ASAP+, m/z): detected 368.1725, calculated for $\text{C}_{19}\text{H}_{22}\text{N}_5\text{O}_3$ $[\text{M}+\text{H}]^+$ 368.1723

5.24 Synthesis of *N*-(3-(4-(methyl((tetrahydro-2*H*-pyran-4-yl)methyl)amino)-7*H*-pyrrolo[2,3-*d*]pyrimidin-6-yl)phenyl)propionamide (**25**)

Compound **20** (70 mg, 0.207 mmol) was dissolved in CH₂Cl₂ (3 mL), and DIPEA (0.072 mL, 0.415 mmol) and cooled to 0 °C. Propionyl chloride (0.036 mL, 0.415 mmol) was added dropwise under nitrogen atmosphere. The reaction



mixture was stirred for 2 hours before the reaction was quenched with saturated NaHCO₃ (10 mL) and extracted with EtOAc (3×30 mL). The combined organic phases were dried over Na₂SO₄ and concentrated in *vacuo*. (CH₂Cl₂/MeOH, 9/1, R_f=0.25). The product **25** (64.6 mg, 0.144 mmol), was isolated with a yield of 69% as a white powder. Mp. 199.7–205.1 °C. Purity 98%, t_R = 5.8 min.

Spectroscopic data for compound **25** (Appendix X):

¹H-NMR (600 MHz, DMSO-*d*₆) δ: 12.13 (s, 1H), 9.90 (s, 1H), 8.11 (s, 1H), 8.03 (s, 1H), 7.51 (d, J = 7.8 Hz, 1H), 7.48 (d, J = 8.5 Hz, 1H), 7.34 (t, J = 7.9 Hz, 1H), 6.88 (s, 1H), 3.87–3.81 (m, 2H), 3.68 (d, J = 7.4 Hz, 2H), 3.40 (s, 3H), 3.25 (td, J = 11.7, 2.1 Hz, 2H), 2.34 (q, J = 7.5 Hz, 2H), 2.11 – 2.02 (m, 1H), 1.58–1.52 (m, 2H), 1.29 (qd, J = 12.1, 4.5 Hz, 2H), 1.10 (t, J = 7.5 Hz, 3H). ¹³C-NMR (150 MHz, DMSO-*d*₆) δ: 172.1, 156.4, 152.9, 151.1, 139.7, 133.2, 132.0, 129.1, 119.6, 118.4, 115.8, 103.2, 98.7, 66.8 (2C), 55.4, 38.9, 34.0, 30.3 (2C), 29.5, 9.6. IR (neat, cm⁻¹) *v*: 3213 (m), 3053 (m), 2953 (s), 2931 (s), 2851 (s), 1734 (m), 1571 (s), 1264 (s), 1077 (s), 836 (s), 731 (s), 703 (s). HRMS (ASAP+, *m/z*): detected 394.2239, calculated for C₂₂H₂₈N₅O₂ [M+H]⁺ 394.2243.

References

- [1] David E Gerber. Targeted therapies: a new generation of cancer treatments. *American family physician*, 77(3):311–319, feb 2008.
- [2] Michael A. Cannarile, Martin Weisser, Wolfgang Jacob, Anna Maria Jegg, Carola H. Ries, and Dominik Rüttinger. Colony-stimulating factor 1 receptor (CSF1R) inhibitors in cancer therapy. *Journal for ImmunoTherapy of Cancer*, 5(1):1–13, 2017. doi: 10.1186/s40425-017-0257-y.
- [3] Stevan R Hubbard and Jeffrey H Till. Protein Tyrosine Kinase Structure and Function. *Annual Review of Biochemistry*, 69(1): 373–398, 2000. doi: 10.1146/annurev.biochem.69.1.373. URL <https://doi.org/10.1146/annurev.biochem.69.1.373>.
- [4] Fleur Broekman, Elisa Giovannetti, and Godefridus J Peters. Tyrosine kinase inhibitors: Multi-targeted or single-targeted? *World Journal of Clinical Oncology*, 2(2):80–3, 2011. doi: 10.5306/wjco.v2.i2.80.
- [5] Joseph Schlessinger. Cell Signaling by Receptor Tyrosine Kinases. *Cell*, 103(2):211–225, oct 2000. doi: 10.1016/S0092-8674(00)00114-8. URL [https://doi.org/10.1016/S0092-8674\(00\)00114-8](https://doi.org/10.1016/S0092-8674(00)00114-8).
- [6] Tony Hunter. The Croonian Lecture 1997. The phosphorylation of proteins on tyrosine: Its role in cell growth and disease. *Philosophical Transactions of the Royal Society B: Biological Sciences*, 353(1368):583–605, 1998. doi: 10.1098/rstb.1998.0228.
- [7] T J Weber. 2.24 - Protein Kinases. In Charlene A McQueen, editor, *Comprehensive Toxicology (Second Edition)*, pages 473–493. Elsevier, Oxford, second edition edition, 2010. ISBN 978-0-08-046884-

6. doi: <https://doi.org/10.1016/B978-0-08-046884-6.00225-6>.
URL <https://www.sciencedirect.com/science/article/pii/B9780080468846002256>.
- [8] D. R. Robinson, Y. M. Wu, and S. F. Lin. The protein tyrosine kinase family of the human genome. *Oncogene*, 19(49):5548–5557, 2000. doi: 10.1038/sj.onc.1203957.
- [9] Manash K. Paul and Anup K. Mukhopadhyay. Tyrosine kinase – Role and significance in Cancer. *International Journal of Medical Sciences*, 1(283):101–115, 2012. doi: 10.7150/ijms.1.101.
- [10] Stevan R Hubbard, Moosa Mohammadi, and Joseph Schlessinger. Autoregulatory Mechanisms in Protein-tyrosine Kinases*. *Journal of Biological Chemistry*, 273(20):11987–11990, 1998. doi: <https://doi.org/10.1074/jbc.273.20.11987>.
URL <https://www.sciencedirect.com/science/article/pii/S0021925819842175>.
- [11] Archana Kumari, Om Silakari, and Rajesh K Singh. Recent advances in colony stimulating factor-1 receptor/c-FMS as an emerging target for various therapeutic implications. *Biomedicine & pharmacotherapy = Biomedecine & pharmacotherapie*, 103:662–679, 2018. doi: 10.1016/j.biopha.2018.04.046.
- [12] Fiona J. Pixley and E. Richard Stanley. *Cytokines and cytokine receptors regulating cell survival, proliferation, and differentiation in hematopoiesis*, volume 3. Elsevier Inc., second edition edition, 2010. doi: 10.1016/B978-0-12-374145-5.00319-3.
- [13] Violeta Chitu and E. Richard Stanley. Colony-stimulating factor-1 in immunity and inflammation. *Current Opinion in Immunology*, 18(1):39–48, 2006. doi: 10.1016/j.coi.2005.11.006.

- [14] E. Richard Stanley, Karen L. Berg, Douglas B. Einstein, Pierre S.W. Lee, Fiona J. Pixley, Yun Wang, and Yee Guide Yeung. Biology and action of colony-stimulating factor-1. *Molecular Reproduction and Development*, 46(1):4–10, 1997. doi: 10.1002/(SICI)1098-2795(199701)46:1<4::AID-MRD2>3.0.CO;2-V.
- [15] Diego Gómez-Nicola, Nina L. Fransen, Stefano Suzzi, and V. Hugh Perry. Regulation of microglial proliferation during chronic neurodegeneration. *Journal of Neuroscience*, 33(6):2481–2493, 2013. doi: 10.1523/JNEUROSCI.4440-12.2013.
- [16] Fiona J. Pixley and E. Richard Stanley. CSF-1 regulation of the wandering macrophage: Complexity in action. *Trends in Cell Biology*, 14(11):628–638, 2004. doi: 10.1016/j.tcb.2004.09.016.
- [17] Mohammed I El-Gamal, Hanan S Anbar, Kyung Ho Yoo, and Chang-Hyun Oh. FMS Kinase Inhibitors: Current Status and Future Prospects. *Medicinal Research Reviews*, 33(3):599–636, 2013. doi: <https://doi.org/10.1002/med.21258>.
- [18] David A Hume and Kelli P A MacDonald. Therapeutic applications of macrophage colony-stimulating factor-1 (CSF-1) and antagonists of CSF-1 receptor (CSF-1R) signaling. *Blood*, 119(8): 1810–1820, 2012. doi: 10.1182/blood-2011-09-379214.
- [19] Florent Peyraud, Sophie Cousin, and Antoine Italiano. CSF-1R Inhibitor Development: Current Clinical Status. *Current Oncology Reports*, 19(11):70, 2017. doi: 10.1007/s11912-017-0634-1. URL <https://doi.org/10.1007/s11912-017-0634-1>.
- [20] Troy L Merry, Anna E S Brooks, Stewart W Masson, Shannon E Adams, Jagdish K Jaiswal, Stephen M F Jamieson, and Peter R Shepherd. The CSF1 receptor inhibitor pexidartinib (PLX3397)

- reduces tissue macrophage levels without affecting glucose homeostasis in mice. *International Journal of Obesity*, 44(1):245–253, 2020. doi: 10.1038/s41366-019-0355-7.
- [21] FDA approves pexidartinib for tenosynovial giant cell tumor, 2019. URL <https://www.fda.gov/drugs/resources-information-approved-drugs/fda-approves-pexidartinib-tenosynovial-giant-cell-tumor>.
- [22] Mohammed I El-Gamal, Shahad K Al-Ameen, Dania M Al-Koumi, Mawadda G Hamad, Nouran A Jalal, and Chang-Hyun Oh. Recent Advances of Colony-Stimulating Factor-1 Receptor (CSF-1R) Kinase and Its Inhibitors. *Journal of Medicinal Chemistry*, 61(13):5450–5466, 2018. doi: 10.1021/acs.jmedchem.7b00873. URL <https://doi.org/10.1021/acs.jmedchem.7b00873>.
- [23] Roy Yuen-chi Lau and Xia Guo. A Review on Current Osteoporosis Research: With Special Focus on Disuse Bone Loss. *Journal of Osteoporosis*, 2011:293808, 2011. doi: 10.4061/2011/293808. URL <https://doi.org/10.4061/2011/293808>.
- [24] Christian E Jacome-Galarza, Gulce I Percin, James T Muller, Elvira Mass, Tomi Lazarov, Jiri Eitler, Martina Rauner, Vijay K Yadav, Lucile Crozet, Mathieu Bohm, Pierre-Louis Loyher, Gerard Karsenty, Claudia Waskow, and Frederic Geissmann. Developmental origin, functional maintenance and genetic rescue of osteoclasts. *Nature*, 568(7753):541–545, 2019. doi: 10.1038/s41586-019-1105-7. URL <https://doi.org/10.1038/s41586-019-1105-7>.
- [25] D L Lacey, E Timms, H.-L Tan, M J Kelley, C R Dunstan, T Burgess, R Elliott, A Colombero, G Elliott, S Scully, H Hsu, J Sullivan, N Hawkins, E Davy, C Capparelli, A Eli, Y.-X Qian,

- S Kaufman, I Sarosi, V Shalhoub, G Senaldi, J Guo, J Delaney, and W J Boyle. Osteoprotegerin Ligand Is a Cytokine that Regulates Osteoclast Differentiation and Activation. *Cell*, 93(2):165–176, 1998. doi: [https://doi.org/10.1016/S0092-8674\(00\)81569-X](https://doi.org/10.1016/S0092-8674(00)81569-X). URL <https://www.sciencedirect.com/science/article/pii/S009286740081569X>.
- [26] V Shalhoub, G Elliott, L Chiu, R Manoukian, M Kelley, N Hawkins, E Davy, G Shimamoto, J Beck, S A Kaufman, G Van, S Scully, M Qi, M Grisanti, C Dunstan, W J Boyle, and D L Lacey. Characterization of osteoclast precursors in human blood. *British Journal of Haematology*, 111(2):501–512, 2000. doi: <https://doi.org/10.1111/j.1365-2141.2000.02379.x>.
- [27] Se Hwan Mun, Peter Sang Uk Park, and Kyung-Hyun Park-Min. The M-CSF receptor in osteoclasts and beyond. *Experimental & Molecular Medicine*, 52(8):1239–1254, 2020. doi: [10.1038/s12276-020-0484-z](https://doi.org/10.1038/s12276-020-0484-z). URL <https://doi.org/10.1038/s12276-020-0484-z>.
- [28] Xin-fang Wang, Ya-juan Wang, Tong-ying Li, Jiang-xue Guo, Fang Lv, Cheng-li Li, and Xing-tao Ge. Colony-stimulating factor 1 receptor inhibition prevents against lipopolysaccharide -induced osteoporosis by inhibiting osteoclast formation. *Biomedicine & Pharmacotherapy*, 115:108916, 2019. doi: <https://doi.org/10.1016/j.biopha.2019.108916>. URL <https://www.sciencedirect.com/science/article/pii/S0753332219305153>.
- [29] Hiroaki Ohno, Yasunori Uemura, Hideko Murooka, Hiromi Takanashi, Takemi Tokieda, Yumiko Ohzeki, Kazuo Kubo, and Isao Serizawa. The orally-active and selective c-Fms tyrosine kinase inhibitor Ki20227 inhibits disease progression in a collagen-

- induced arthritis mouse model. *European journal of immunology*, 38(1):283–291, jan 2008. doi: 10.1002/eji.200737199.
- [30] James G Conway, Heather Pink, Mandy L Bergquist, Bajin Han, Scott Depee, Sarva Tadepalli, Peiyuan Lin, R Christian Crumrine, Jane Binz, Richard L Clark, Jeffrey L Selph, Stephen A Stimpson, Jeff T Hutchins, Stanley D Chamberlain, and Thomas A Brodie. Effects of the cFMS Kinase Inhibitor 5-(3-Methoxy-4-((4-methoxybenzyl)oxy)benzyl)pyrimidine-2,4-diamine (GW2580) in Normal and Arthritic Rats. *Journal of Pharmacology and Experimental Therapeutics*, 326(1):41–50, 2008. ISSN 0022-3565. doi: 10.1124/jpet.107.129429. URL <https://jpet.aspetjournals.org/content/326/1/41>.
- [31] Myew-Ling Toh, Jean-Yves Bonnefoy, Nathalie Accart, Sandrine Cochin, Sandy Pohle, Hélène Haegel, Micael De Meyer, Christophe Zemmour, Xavier Preville, Christine Guillen, Christine Thiouellet, Philippe Ancian, Anja Lux, Bettina Sehnert, Falk Nimmerjahn, Reinhard E Voll, and Georg Schett. Bone- and Cartilage-Protective Effects of a Monoclonal Antibody Against Colony-Stimulating Factor 1 Receptor in Experimental Arthritis. *Arthritis and Rheumatology*, 66(11):2989–3000, 2014. doi: <https://doi.org/10.1002/art.38624>. URL <https://onlinelibrary.wiley.com/doi/abs/10.1002/art.38624>.
- [32] J.A. Joule and K. Mills. *Heterocyclic chemistry: 5th ed.*, chapter 13-16, pages 249 – 320. Wiley, Chichester, U.K., 2010.
- [33] Pavla Perlíková and Michal Hocek. Pyrrolo[2,3-d]pyrimidine (7-deazapurine) as a privileged scaffold in design of antitumor and antiviral nucleosides. *Medicinal Research Reviews*, 37(6):1429–1460, 2017. doi: <https://doi.org/10.1002/med.21465>.

- [34] Weihe Zhang, Jing Liu, Michael A. Stashko, and Xiaodong Wang. Efficient solution-phase synthesis of 4,5,7-trisubstituted pyrrolo[3,2- d]pyrimidines. *ACS Combinatorial Science*, 15(1): 10–19, 2013. doi: 10.1021/co300106f.
- [35] M. L. Quijano, M. Noguera, M. Melguizo, G. Alvarez De Cienfuegos, M. Melgarejo, and A. Sanchez. Aminopyrimidines and derivatives. 271-synthesis, anticancer and antimicrobiological activities of 7-glycopyranosyl- pyrimidines2. *Nucleosides and Nucleotides*, 8 (8):1519–1528, 1989. doi: 10.1080/07328318908048859.
- [36] Laurens M. De Coen, Thomas S.A. Heugebaert, Daniel García, and Christian V. Stevens. Synthetic Entries to and Biological Activity of Pyrrolopyrimidines. *Chemical Reviews*, 116(1):80–139, 2016. doi: 10.1021/acs.chemrev.5b00483.
- [37] Reid M McCarty and Vahe Bandarian. Biosynthesis of pyrrolopyrimidines. *Bioorganic Chemistry*, 43:15–25, 2012. doi: <https://doi.org/10.1016/j.bioorg.2012.01.001>.
- [38] Svein Jacob Kaspersen, Christopher Sørum, Veronica Willassen, Erik Fuglseth, Eli Kjøbli, Geir Bjørkøy, Eirik Sundby, and Bård Helge Hoff. Synthesis and in vitro EGFR (ErbB1) tyrosine kinase inhibitory activity of 4-N-substituted 6-aryl-7H-pyrrolo[2,3-d]pyrimidine-4-amines. *European Journal of Medicinal Chemistry*, 46(12):6002–6014, 2011. doi: <https://doi.org/10.1016/j.ejmech.2011.10.012>.
- [39] Laurent El Kaïm, Laurence Grimaud, and Simon Wagschal. Toward Pyrrolo[2,3-d]pyrimidine Scaffolds. *The Journal of Organic Chemistry*, 75(15):5343–5346, 2010. doi: 10.1021/jo100759b.
- [40] Jin Han, Silje Henriksen, Kristin G. Nørsett, Eirik Sundby, and

- Bård Helge Hoff. Balancing potency, metabolic stability and permeability in pyrrolopyrimidine-based EGFR inhibitors. *European Journal of Medicinal Chemistry*, 124:583–607, 2016. doi: 10.1016/j.ejmech.2016.08.068.
- [41] Svein Jacob Kaspersen, Jin Han, Kristin G. Nørsett, Line Rydså, Eli Kjøbli, Steffen Bugge, Geir Bjørkøy, Eirik Sundby, and Bård Helge Hoff. Identification of new 4-N-substituted 6-aryl-7H-pyrrolo[2,3-d]pyrimidine-4- amines as highly potent EGFR-TK inhibitors with Src-family activity. *European Journal of Pharmaceutical Sciences*, 59(1):69–82, 2014. doi: 10.1016/j.ejps.2014.04.011.
- [42] Jin Han, Svein Jacob Kaspersen, Sondre Nervik, Kristin G Nørsett, Eirik Sundby, and Bård Helge Hoff. Chiral 6-aryl-furo[2,3-d]pyrimidin-4-amines as EGFR inhibitors. *European Journal of Medicinal Chemistry*, 119:278–299, 2016. doi: <https://doi.org/10.1016/j.ejmech.2016.04.054>. URL <https://www.sciencedirect.com/science/article/pii/S0223523416303476>.
- [43] Steffen Bugge, Svein Jacob Kaspersen, Synne Larsen, Unni Nonstad, Geir Bjørkøy, Eirik Sundby, and Bård Helge Hoff. Structure–activity study leading to identification of a highly active thienopyrimidine based EGFR inhibitor. *European Journal of Medicinal Chemistry*, 75:354–374, 2014. doi: <https://doi.org/10.1016/j.ejmech.2014.01.042>. URL <https://www.sciencedirect.com/science/article/pii/S0223523414000889>.
- [44] Victor Snieckus. Directed Ortho Metalation. Tertiary Amide and O-Carbamate Directors in Synthetic Strategies for Polysubstituted Aromatics. *Chemical Reviews*, 90(6):879–933, 1990. doi: 10.1021/cr00104a001.

- [45] Manfred Schlosser. The 2×3 Toolbox of Organometallic Methods for Regiochemically Exhaustive Functionalization. *Angewandte Chemie International Edition*, 44(3):376–393, 2005. doi: 10.1002/anie.200300645.
- [46] L Kurti and B Czako. *Strategic Applications of Named Reactions in Organic Synthesis*. Elsevier Science, 2005.
- [47] Martin P. Edwards, Annette M. Doherty, Steven V. Ley, and Helen M. Organ. Preparation of 2-substituted pyrroles and indoles by regioselective alkylation and deprotection of 1-(2-trimethylsilylethoxymethyl)pyrrole and 1-(2-trimethylsilylethoxymethyl) indole. *Tetrahedron*, 42(13): 3723–3729, 1986. doi: 10.1016/S0040-4020(01)87342-7.
- [48] Joseph M Muchowski and Dennis R Solas. Protecting groups for the pyrrole and indole nitrogen atom. The [2-(trimethylsilyl)ethoxy]methyl moiety. Lithiation of 1-[[2-(trimethylsilyl)ethoxy]methyl]pyrrole. *The Journal of Organic Chemistry*, 49(1):203–205, 1984. doi: 10.1021/jo00175a053.
- [49] Benoit Jolicoeur, Erin E Chapman, Alison Thompson, and William D Lubell. Pyrrole protection. *Tetrahedron*, 62(50):11531–11563, 2006. doi: <https://doi.org/10.1016/j.tet.2006.08.071>.
- [50] Xinge Zhao, Wei Huang, Yazhou Wang, Minhang Xin, Qiu Jin, Jianfeng Cai, Feng Tang, Yong Zhao, and Hua Xiang. Discovery of novel Bruton’s tyrosine kinase (BTK) inhibitors bearing a pyrrolo[2,3-d]pyrimidine scaffold. *Bioorganic & Medicinal Chemistry*, 23(4):891–901, 2015. doi: <https://doi.org/10.1016/j.bmc.2014.10.043>.
- [51] Joseph F. Bunnett and Roland E. Zahler. Aromatic nucleophilic

- substitution reactions. *Chemical Reviews*, 49(2):273–412, 1951. doi: 10.1021/cr60153a002.
- [52] Henk C. Van Der Plas. The SN(ANRORC) Mechanism: A New Mechanism for Nucleophilic Substitution. *Accounts of Chemical Research*, 11(12):462–468, 1978. doi: 10.1021/ar50132a005.
- [53] Jakob Meisenheimer. Ueber reactionen aromatischer nitrokörper. *Justus Liebigs Annalen der Chemie*, 323(2):205–246, 1902. doi: <https://doi.org/10.1002/jlac.19023230205>.
- [54] Constanze N. Neumann, Jacob M. Hooker, and Tobias Ritter. Concerted nucleophilic aromatic substitution with 19F- and 18F-. *Nature*, 534(7607):369–373, 2016. doi: 10.1038/nature17667.
- [55] J. F. Bunnett. Mechanism and reactivity in aromatic nucleophilic substitution reactions. *Q. Rev. Chem. Soc.*, 12(1):1–16, 1958. doi: 10.1039/QR9581200001.
- [56] Steven W Goldstein, Ashley Bill, Jyothi Dhuguru, and Ola Ghoneim. Nucleophilic Aromatic Substitution—Addition and Identification of an Amine. *Journal of Chemical Education*, 94(9):1388–1390, 2017. doi: 10.1021/acs.jchemed.6b00680. URL <https://doi.org/10.1021/acs.jchemed.6b00680>.
- [57] Francois Terrier. Rate and equilibrium studies in Jackson-Meisenheimer complexes. *Chemical Reviews*, 82(2):77–152, 1982. doi: 10.1021/cr00048a001. URL <https://doi.org/10.1021/cr00048a001>.
- [58] Mar Gómez Gallego and Miguel A Sierra. *Level 3 - Case 33 The Rate-Determining Step in the SNAr Reaction*, pages 217–223. Springer Berlin Heidelberg, Berlin, Heidelberg, 2004. ISBN

- 978-3-642-18788-9. doi: 10.1007/978-3-642-18788-9_33. URL https://doi.org/10.1007/978-3-642-18788-9_33.
- [59] E V Anslyn, D A Dougherty, E V Dougherty, and University Science Books. *Modern Physical Organic Chemistry*. University Science Books, 2006. p. 611-612.
- [60] Pengju Ji, John H Atherton, and Michael I Page. The Kinetics and Mechanisms of Aromatic Nucleophilic Substitution Reactions in Liquid Ammonia. *The Journal of Organic Chemistry*, 76(9): 3286–3295, 2011. doi: 10.1021/jo200170z. URL <https://doi.org/10.1021/jo200170z>.
- [61] Giuseppe Bartoli and Paolo Edgardo Todesco. Nucleophilic substitution. Linear free energy relations between reactivity and physical properties of leaving groups and substrates. *Accounts of Chemical Research*, 10(4):125–132, 1977. doi: 10.1021/ar50112a004.
- [62] J. F. Bunnett, Edgar W. Garbisch, and Kenneth M. Pruitt. The “Element Effect” as a Criterion of Mechanism in Activated Aromatic Nucleophilic Substitution Reactions. *Journal of the American Chemical Society*, 79(2):385–391, 1957. doi: 10.1021/ja01559a040.
- [63] Mieczysław Mąkosza. Nucleophilic substitution of hydrogen in electron-deficient arenes, a general process of great practical value. *Chemical Society Reviews*, 39(8):2855–2868, 2010. doi: 10.1039/b822559c.
- [64] John F Hartwig. Transition Metal Catalyzed Synthesis of Arylamines and Aryl Ethers from Aryl Halides and Triflates: Scope and Mechanism. *Angewandte Chemie (International*

- ed. in English*), 37(15):2046–2067, 1998. doi: 10.1002/(SICI)1521-3773(19980817)37:15<2046::AID-ANIE2046>3.0.CO;2-L.
- [65] Michael S Driver and John F Hartwig. A Second-Generation Catalyst for Aryl Halide Amination: Mixed Secondary Amines from Aryl Halides and Primary Amines Catalyzed by (DPPF)PdCl₂. *Journal of the American Chemical Society*, 118(30):7217–7218, 1996. doi: 10.1021/ja960937t.
- [66] John P Wolfe, Seble Wagaw, and Stephen L Buchwald. An Improved Catalyst System for Aromatic CarbonNitrogen Bond Formation: The Possible Involvement of Bis(Phosphine) Palladium Complexes as Key Intermediates. *Journal of the American Chemical Society*, 118(30):7215–7216, 1996. doi: 10.1021/ja9608306.
- [67] Norio Miyaura and Akira Suzuki. Palladium-Catalyzed Cross-Coupling Reactions of Organoboron Compounds. *Chemical Reviews*, 95(7):2457–2483, 1995. doi: 10.1021/cr00039a007.
- [68] Manuel A. Ortuno, Agustí Lledós, Feliu Maseras, and Gregori Ujaque. The transmetalation process in Suzuki-Miyaura reactions: Calculations indicate lower barrier via boronate intermediate. *ChemCatChem*, 6(11):3132–3138, 2014. doi: 10.1002/cctc.201402326.
- [69] Alastair J.J. Lennox and Guy C. Lloyd-Jones. Selection of boron reagents for Suzuki-Miyaura coupling. *Chemical Society Reviews*, 43(1):412–443, 2014. doi: 10.1039/c3cs60197h.
- [70] Norio Miyaura, Kinji Yamada, and Akira Suzuki. Our Continuous Discovered. *Tetrahedron Letters*, 20(36):3437–3440, 1979.
- [71] Christian Amatore, Anny Jutand, and Gaëtan Le Duc. Kinetic Data for the Transmetalation/Reductive Elimination in

- Palladium-Catalyzed Suzuki–Miyaura Reactions: Unexpected Triple Role of Hydroxide Ions Used as Base. *Chemistry – A European Journal*, 17(8):2492–2503, 2011. doi: <https://doi.org/10.1002/chem.201001911>.
- [72] Christian Amatore and Fernando Pfluger. Mechanism of oxidative addition of palladium(0) with aromatic iodides in toluene, monitored at ultramicroelectrodes. *Organometallics*, 9(8):2276–2282, 1990. doi: 10.1021/om00158a026.
- [73] Marcial Moreno-Mañas, Montserrat Pérez, and Roser Pleixats. Palladium-catalyzed suzuki-type self-coupling of arylboronic acids. a mechanistic study. *The Journal of Organic Chemistry*, 61(7): 2346–2351, 1996. doi: 10.1021/jo9514329.
- [74] Sambasivarao Kotha, Kakali Lahiri, and Kashinath Dhurke. Recent applications of the suzuki—miyaura cross-coupling reaction in organic synthesis. *Tetrahedron*, 58:9633–9695, 2002. doi: 10.1016/S0040-4020(02)01188-2.
- [75] George B Smith, George C Dezeny, David L Hughes, Anthony O King, and Thomas R Verhoeven. Mechanistic studies of the suzuki cross-coupling reaction. *The Journal of Organic Chemistry*, 59(26): 8151–8156, 1994. doi: 10.1021/jo00105a036.
- [76] Jennifer M Schomaker and Thomas J Delia. Arylation of Halogenated Pyrimidines via a Suzuki Coupling Reaction. *The Journal of Organic Chemistry*, 66(21):7125–7128, 2001. doi: 10.1021/jo010573+.
- [77] Alastair J J Lennox and Guy C Lloyd-Jones. Transmetalation in the Suzuki–Miyaura Coupling: The Fork in the Trail. *Angewandte*

- Chemie International Edition*, 52(29):7362–7370, 2013. doi: <https://doi.org/10.1002/anie.201301737>.
- [78] Max García-Melchor, Ataulpa A C Braga, Agustí Lledós, Gregori Ujaque, and Feliu Maseras. Computational Perspective on Pd-Catalyzed C–C Cross-Coupling Reaction Mechanisms. *Accounts of Chemical Research*, 46(11):2626–2634, 2013. doi: 10.1021/ar400080r.
- [79] John F Hartwig. Electronic Effects on Reductive Elimination To Form Carbon-Carbon and Carbon-Heteroatom Bonds from Palladium(II) Complexes. *Inorganic Chemistry*, 46(6):1936–1947, 2007. doi: 10.1021/ic061926w.
- [80] John J Low and William A Goddard. Theoretical studies of oxidative addition and reductive elimination. 3. Carbon-hydrogen and carbon-carbon reductive coupling from palladium and platinum bis(phosphine) complexes. *Journal of the American Chemical Society*, 108(20):6115–6128, 1986. doi: 10.1021/ja00280a003.
- [81] Kazuyuki Tatsumi, Roald Hoffmann, Akio Yamamoto, and John K Stille. Reductive Elimination of d8-Organotransition Metal Complexes. *Bulletin of the Chemical Society of Japan*, 54(6):1857–1867, 1981. doi: 10.1246/bcsj.54.1857.
- [82] Charles P Casey and Gregory T Whiteker. The Natural Bite Angle of Chelating Diphosphines. *Israel Journal of Chemistry*, 30(4):299–304, 1990. doi: <https://doi.org/10.1002/ijch.199000031>.
- [83] Mandy-Nicole Birkholz (née Gensow), Zoraida Freixa, and Piet W N M van Leeuwen. Bite angle effects of diphosphines in C–C and C–X bond forming cross coupling reactions. *Chem. Soc. Rev.*, 38(4):1099–1118, 2009. doi: 10.1039/B806211K.

- [84] Ruben Martin and Stephen L Buchwald. Palladium-Catalyzed SuzukiMiyaura Cross-Coupling Reactions Employing Dialkylbiaryl Phosphine Ligands. *Accounts of Chemical Research*, 41(11):1461–1473, 2008. doi: 10.1021/ar800036s.
- [85] Robin B Bedford and Samantha L Welch. Palladacyclic phosphinite complexes as extremely high activity catalysts in the Suzuki reaction. *Chem. Commun.*, 1:129–130, 2001. doi: 10.1039/B008470K.
- [86] John P Wolfe, Robert A Singer, Bryant H Yang, and Stephen L Buchwald. Highly Active Palladium Catalysts for Suzuki Coupling Reactions. *Journal of the American Chemical Society*, 121(41):9550–9561, 1999. doi: 10.1021/ja992130h.
- [87] Jan H. Kirchhoff, Chaoyang Dai, and Gregory C. Fu. A method for palladium-catalyzed cross-couplings of simple alkyl chlorides: Suzuki reactions catalyzed by [pd2(dba)3]/pcy3. *Angewandte Chemie International Edition*, 41(11):1945–1947, 2002. doi: [https://doi.org/10.1002/1521-3773\(20020603\)41:11<1945::AID-ANIE1945>3.0.CO;2-7](https://doi.org/10.1002/1521-3773(20020603)41:11<1945::AID-ANIE1945>3.0.CO;2-7).
- [88] Alastair J J Lennox and Guy C Lloyd-Jones. The Slow-Release Strategy in Suzuki–Miyaura Coupling. *Israel Journal of Chemistry*, 50(5-6):664–674, 2010. doi: <https://doi.org/10.1002/ijch.201000074>. URL <https://onlinelibrary.wiley.com/doi/abs/10.1002/ijch.201000074>.
- [89] Christopher J Mathews, Paul J Smith, and Thomas Welton. Palladium catalysed Suzuki cross-coupling reactions in ambient temperature ionic liquids. *Chem. Commun.*, 14:1249–1250, 2000. doi: 10.1039/B002755N. URL <http://dx.doi.org/10.1039/B002755N>.

- [90] Lukáš Jedinák, Renáta Zátopková, Hana Zemánková, Alena Šustková, and Petr Cankař. The Suzuki–Miyaura Cross-Coupling Reaction of Halogenated Aminopyrazoles: Method Development, Scope, and Mechanism of Dehalogenation Side Reaction. *The Journal of Organic Chemistry*, 82(1):157–169, 2017. doi: 10.1021/acs.joc.6b02306.
- [91] Henry G Kuivila and Albert G Armour. Electrophilic Displacement Reactions. IX. Effects of Substituents on Rates of Reactions between Hydrogen Peroxide and Benzenboronic Acid. *Journal of the American Chemical Society*, 79(21):5659–5662, 1957. doi: 10.1021/ja01578a020. URL <https://doi.org/10.1021/ja01578a020>.
- [92] Carlo Adamo, Christian Amatore, Ilaria Ciofini, Anny Jutand, and Hakim Lakmini. Mechanism of the Palladium-Catalyzed Homocoupling of Arylboronic Acids: Key Involvement of a Palladium Peroxo Complex. *Journal of the American Chemical Society*, 128(21):6829–6836, 2006. doi: 10.1021/ja0569959. URL <https://doi.org/10.1021/ja0569959>.
- [93] Henry G Kuivila, Joseph F Reuwer, and John A Mangravite. Electrophilic Displacement Reactions. XVI. Metal Ion Catalysis in the Protodeboronation of Areneboronic Acids. *Journal of the American Chemical Society*, 86(13):2666–2670, 1964. doi: 10.1021/ja01067a031. URL <https://doi.org/10.1021/ja01067a031>.
- [94] Claude Y Legault, Yeimy Garcia, Craig A Merlic, and K N Houk. Origin of Regioselectivity in Palladium-Catalyzed Cross-Coupling Reactions of Polyhalogenated Heterocycles. *Journal of the American Chemical Society*, 129(42):12664–12665, 2007. doi: 10.1021/ja075785o.

- [95] Jia Rui Wang and Kei Manabe. Transition-metal-catalyzed site-selective cross-coupling of di- and polyhalogenated compounds. *Synthesis*, 9:1405–1427, 2009. doi: 10.1055/s-0029-1216632.
- [96] Ian J S Fairlamb. Regioselective (site-selective) functionalisation of unsaturated halogenated nitrogen, oxygen and sulfur heterocycles by Pd-catalysed cross-couplings and direct arylation processes. *Chem. Soc. Rev.*, 36(7):1036–1045, 2007. doi: 10.1039/B611177G.
- [97] Neil A Strotman, Harry R Chobanian, Jiafang He, Yan Guo, Peter G Dormer, Christina M Jones, and Janelle E Steves. Catalyst-Controlled Regioselective Suzuki Couplings at Both Positions of Dihaloimidazoles, Dihalooxazoles, and Dihalothiazoles. *The Journal of Organic Chemistry*, 75(5):1733–1739, 2010. doi: 10.1021/jo100148x.
- [98] Alison Thompson, R Jonathan Butler, Meaghan N Grundy, Andrea B E Laltoo, Katherine N Robertson, and T Stanley Cameron. Sulfur-Based Protecting Groups for Pyrroles and the Facile Deprotection of 2-(2,4-Dinitrobenzene)sulfinyl and Sulfonyl Pyrroles. *The Journal of Organic Chemistry*, 70(9):3753–3756, 2005. doi: 10.1021/jo050077b.
- [99] Carlos Gonzalez, Robert Greenhouse, Ramon Tallabs, and Joseph M Muchowski. Protecting groups for the pyrrole nitrogen atom. The 2-chloroethyl, 2-phenylsulfonylethyl, and related moieties. *Canadian Journal of Chemistry*, 61(8):1697–1702, 1983. doi: 10.1139/v83-290.
- [100] Keli Cui, Meng Gao, Hongyi Zhao, Dongfeng Zhang, Hong Yan, and Haihong Huang. An Efficient Synthesis of Aryl-Substituted Pyrroles by the Suzuki–Miyaura Coupling Reaction of SEM-

- Protected Pyrroles. *Molecules*, 24(8), 2019. doi: 10.3390/molecules24081594.
- [101] Guanglin Luo, Ling Chen, and Gene Dubowchik. Regioselective Protection at N-2 and Derivatization at C-3 of Indazoles. *The Journal of Organic Chemistry*, 71(14):5392–5395, 2006. doi: 10.1021/jo060607j.
- [102] Qiyan Lin, David Meloni, Yongchun Pan, Michael Xia, James Rodgers, Stacey Shepard, Mei Li, Laurine Galya, Brian Metcalf, Tai-Yuen Yue, Pingli Liu, and Jiacheng Zhou. Enantioselective Synthesis of Janus Kinase Inhibitor INCB018424 via an Organocatalytic Aza-Michael Reaction. *Organic Letters*, 11(9):1999–2002, 2009. doi: 10.1021/ol900350k.
- [103] Toshiyuki Kan, Masaru Hashimoto, Mitsutoshi Yanagiya, and Haruhisa Shirahama. Effective deprotection of 2-(trimethylsilylethoxy)methylated alcohols (SEM ethers). Synthesis of thyriferyl-23 acetate. *Tetrahedron Letters*, 29(42):5417–5418, 1988. doi: [https://doi.org/10.1016/S0040-4039\(00\)82883-X](https://doi.org/10.1016/S0040-4039(00)82883-X).
- [104] Simen Havik. Synthesis of pyrrolopyrimidine based csf-1r inhibitors containing tetrahydropyran. Pre-master project, NTNU, 2020.
- [105] Joseph Sloop. 19-Fluorine nuclear magnetic resonance chemical shift variability in trifluoroacetyl species. *Reports in Organic Chemistry*, 2013:1–12, 2013. doi: 10.2147/ROC.538495.
- [106] James Nowick. Multiplet Guide and Workbook. University of California-Irvine. URL <https://www.chem.uci.edu/~jsnowick/groupweb/files/MultipletGuideV4.pdf>. p. 1-24.
- [107] Richard A Newmark and James R Hill. Carbon-13-fluorine-

- 19 coupling constants in benzotrifluorides. *Organic Magnetic Resonance*, 9(10):589–592, 1977. doi: <https://doi.org/10.1002/mrc.1270091008>. URL <https://onlinelibrary.wiley.com/doi/abs/10.1002/mrc.1270091008>.
- [108] *The CF₂ Group*, chapter 4, pages 133–186. John Wiley and Sons, Ltd, 2016. ISBN 9781118831106. doi: <https://doi.org/10.1002/9781118831106.ch4>.
- [109] *The Trifluoromethyl Group*, chapter 5, pages 187–235. John Wiley and Sons, Ltd, 2016. ISBN 9781118831106. doi: <https://doi.org/10.1002/9781118831106.ch5>.
- [110] Robert. M Silverstein, Francis X. Webster, and David J. Kiemle. *Spectrometric Identification of Organic Compounds*. Wiley, 7th edition, 2005.
- [111] Yesmine Ben Henda, Anis Labidi, Ingrid Arnaudin, Nicolas Bridiau, Régis Delatouche, Thierry Maugard, Jean-Marie Piot, Frédéric Sannier, Valérie Thiéry, and Stéphanie Bordenave-Juchereau. Measuring Angiotensin-I Converting Enzyme Inhibitory Activity by Micro Plate Assays: Comparison Using Marine Cryptides and Tentative Threshold Determinations with Captopril and Losartan. *Journal of Agricultural and Food Chemistry*, 61(45):10685–10690, 2013. doi: 10.1021/jf403004e.
- [112] Timothy J Ritchie, Simon J F Macdonald, Robert J Young, and Stephen D Pickett. The impact of aromatic ring count on compound developability: further insights by examining carbo- and hetero-aromatic and -aliphatic ring types. *Drug Discovery Today*, 16(3):164–171, 2011. doi: <https://doi.org/10.1016/j.drudis.2010.11.014>.

- [113] Martina Stekrova, Päivi Mäki-Arvela, Narendra Kumar, Erfan Behravesht, Atte Aho, Quentin Balme, Konstantin P Volcho, Nariman F Salakhutdinov, and Dmitry Yu. Murzin. Prins cyclization: Synthesis of compounds with tetrahydropyran moiety over heterogeneous catalysts. *Journal of Molecular Catalysis A: Chemical*, 410:260–270, 2015. doi: <https://doi.org/10.1016/j.molcata.2015.09.021>.
- [114] Nadiah Mad Nasir, Kristaps Ermanis, and Paul A Clarke. Strategies for the construction of tetrahydropyran rings in the synthesis of natural products. *Org. Biomol. Chem.*, 12(21):3323–3335, 2014. doi: 10.1039/C4OB00423J. URL <http://dx.doi.org/10.1039/C4OB00423J>.
- [115] B.A. Pollok, B.D. Hamman, S.M. Rodems, and L.R. Makings. *Optical probes and assays*. WO 2000066766 A1, 5-5-2000.

A Spectroscopic data for Compound 1

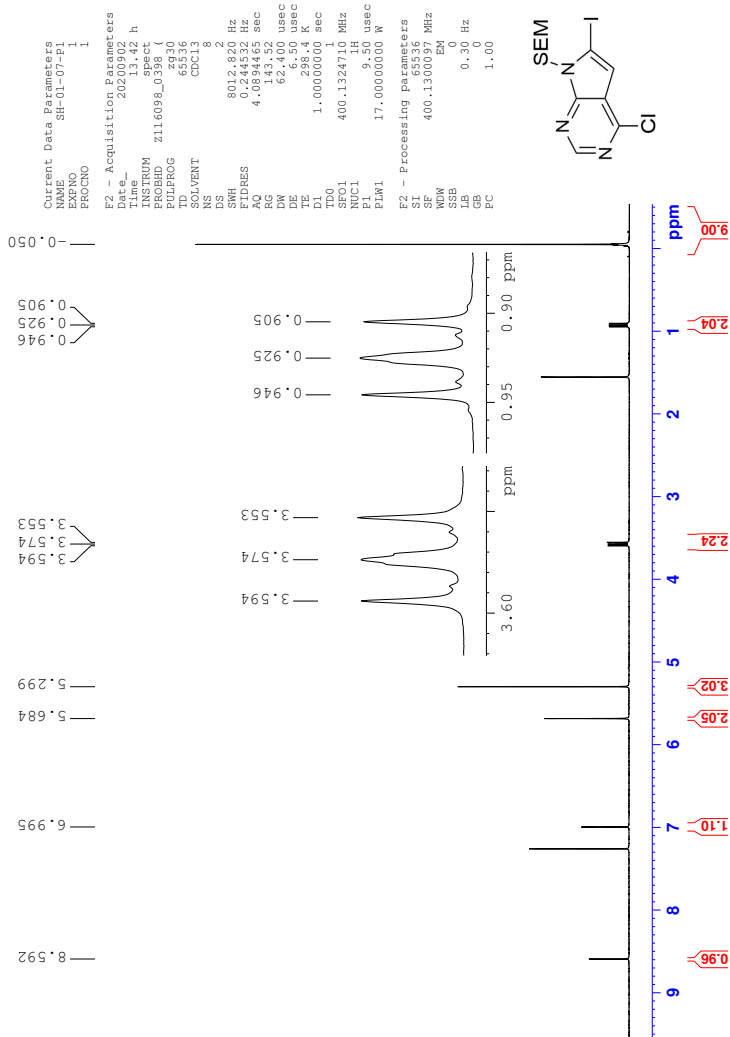


Figure A.1: ^1H NMR spectrum of compound 1

B Spectroscopic data for Compound 3

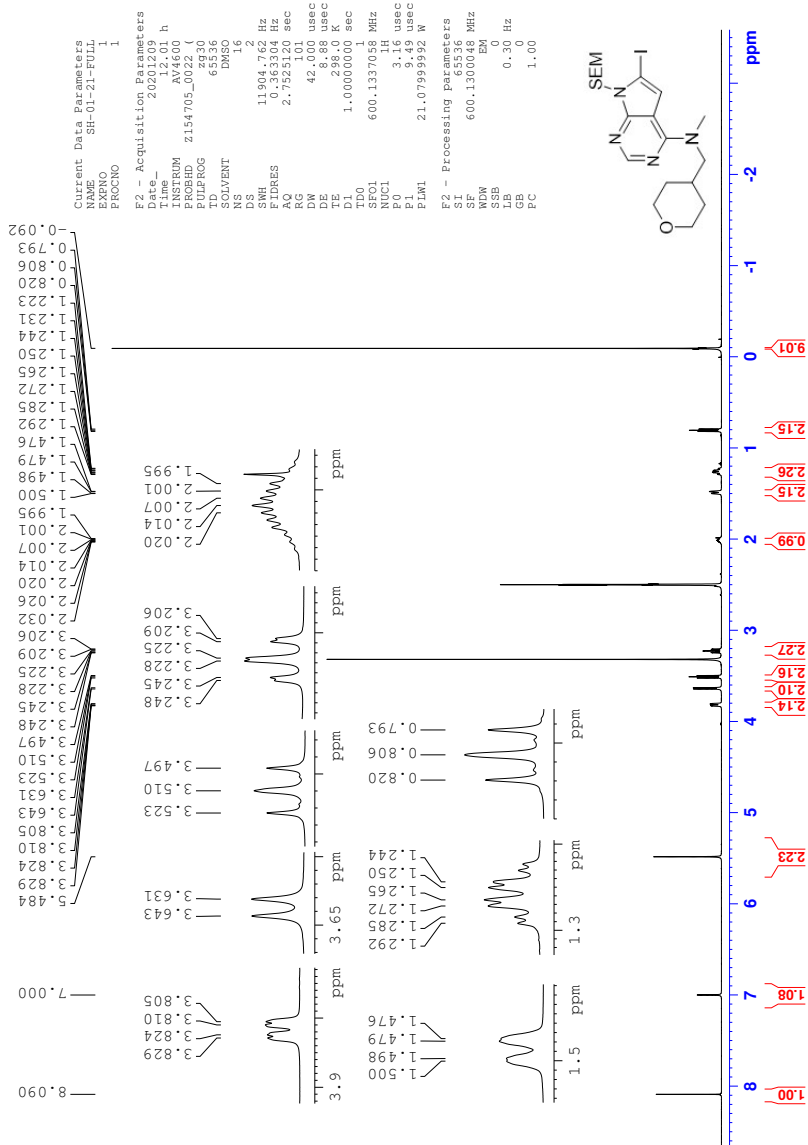


Figure B.1: ^1H NMR spectrum of compound 3

Current Data Parameters
 NAME SH-01-21-FULL
 EXPNO 2
 PROCNO 1
 F2 - Acquisition Parameters
 Date_ 20201209
 Time 11:46:00 h
 INSTRUM AV460
 PROBHD Z154705_0022 (1
 PULPROG zgpg30
 TD 65836
 SOLVENT NS
 NS 1024
 DS 4
 SWH 35714.285 Hz
 FIDRES 0.16769 Hz
 AQ 0.3175140 sec
 RG 101
 DN 14,000 usec
 DE 29.50 usec
 TE 298.2 K
 D1 2.00000000 sec
 D11 0.03000000 sec
 ADO 150.9178981 MHz
 NU01 13C
 P0 4.00 usec
 PL 86.612,00 usec
 SFO1 600.1324005 MHz
 SFO2 600.1324005 MHz
 NUC2 1H
 CDEPRG12 waltz65
 PCPD2 21.07985000 usec
 PLW1 0.38744000 W
 PLW2 0.38744000 W
 PLW3 0.19487999 W
 F2 - Processing Parameters
 SF 150.9028812 MHz
 EQ EM
 NDM 0
 LSS 0
 GB 0
 PC 1.40

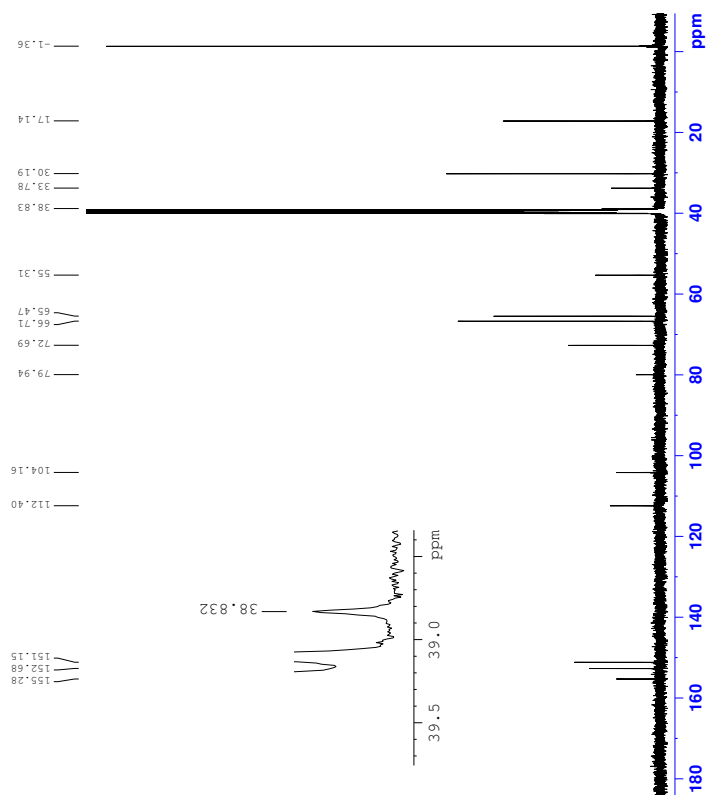


Figure B.2: ^{13}C NMR spectrum of compound 3

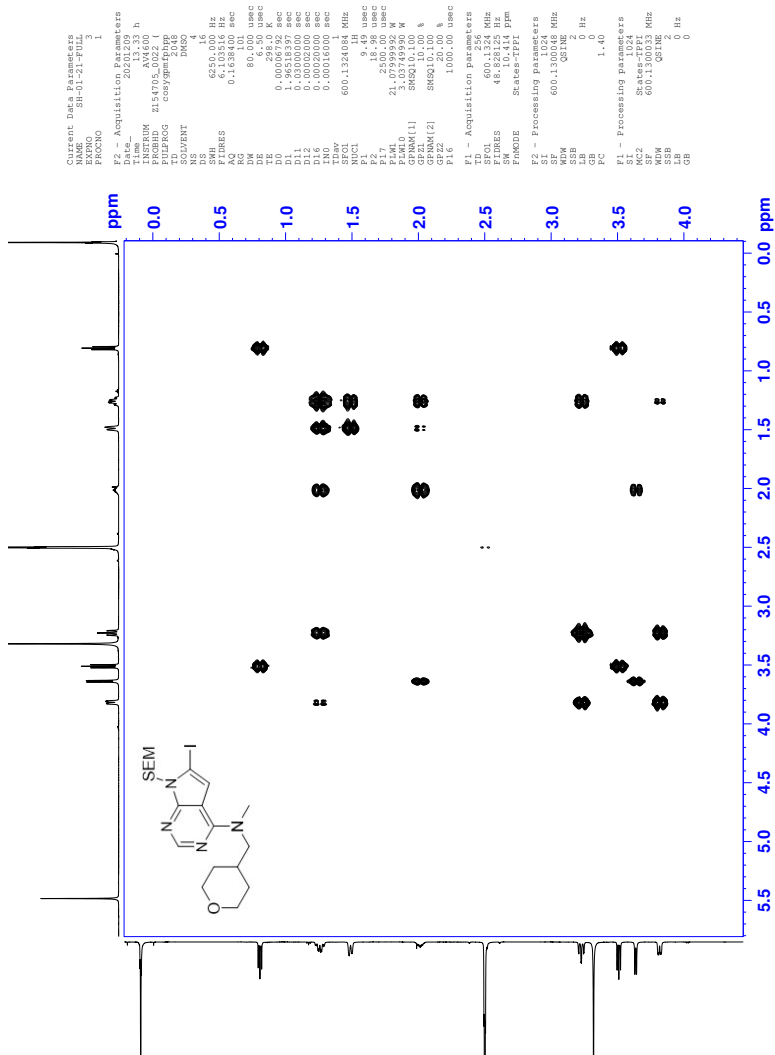
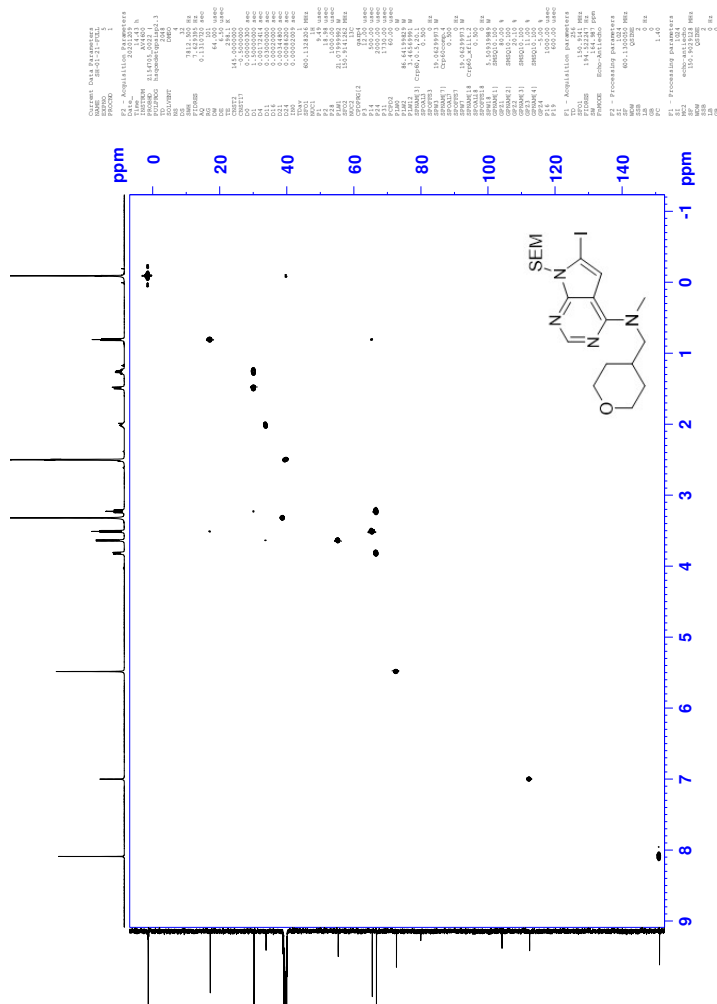
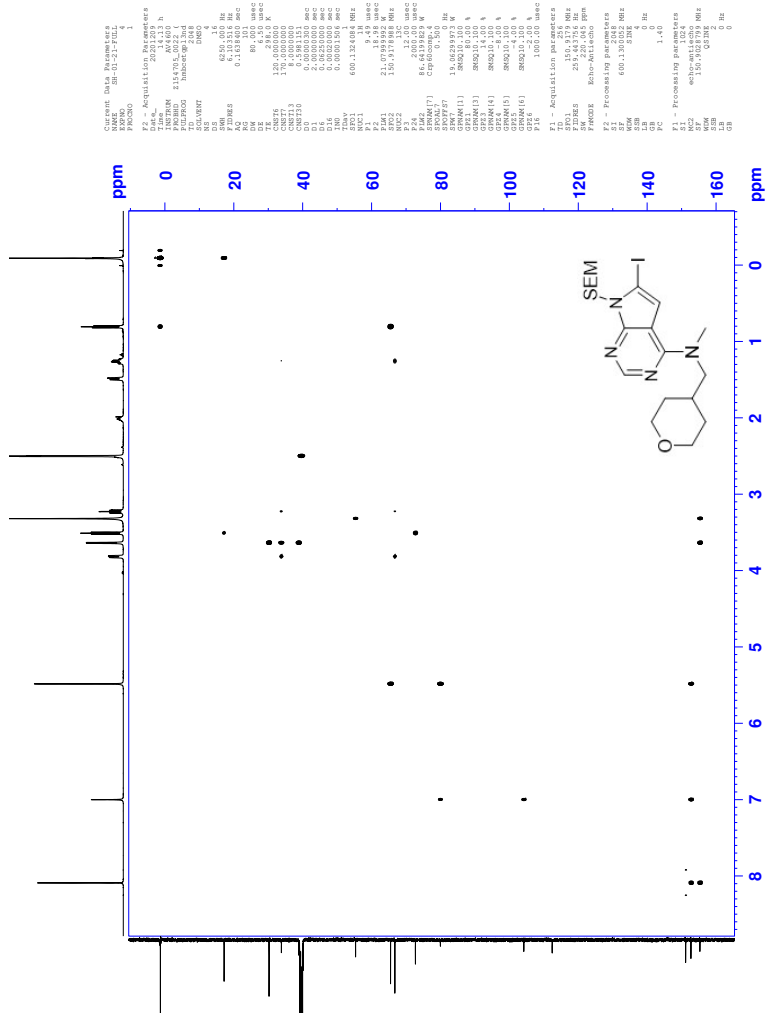


Figure B.3: COSY spectrum of compound 3



NAME: TKJ4520_02
DATE_: 2023-11-14
PROCNO: 1
INSTRUM: spect
PROBHD: 5 mm QNP 1H/13
PULPROG: zgpg30
TD: 65536
SFO: 400.146
AQ: 0.055625000
RG: 3276.8
SD: 0.00000000
WDW: EM
SS: 0
LB: 0.3
GB: 0
PC: 163.5
EC: 1.12
F2 - Acquisition parameters
F1 - Processing parameters
SFO: 400.146000 MHz
P1: 12.00
PC: 163.50
PR: 0.00000000
RG: 3276.80
WDW: EM
SS: 0.00000000
LB: 0.30000000
GB: 0.00000000
PC: 163.50000000
EC: 1.12000000
F2 - Acquisition parameters
F1 - Processing parameters
SFO: 400.146000 MHz
P1: 12.00
PC: 163.50
PR: 0.00000000
RG: 3276.80
WDW: EM
SS: 0.00000000
LB: 0.30000000
GB: 0.00000000
PC: 163.50000000
EC: 1.12000000

Figure B.4: HSQC spectrum of compound 3



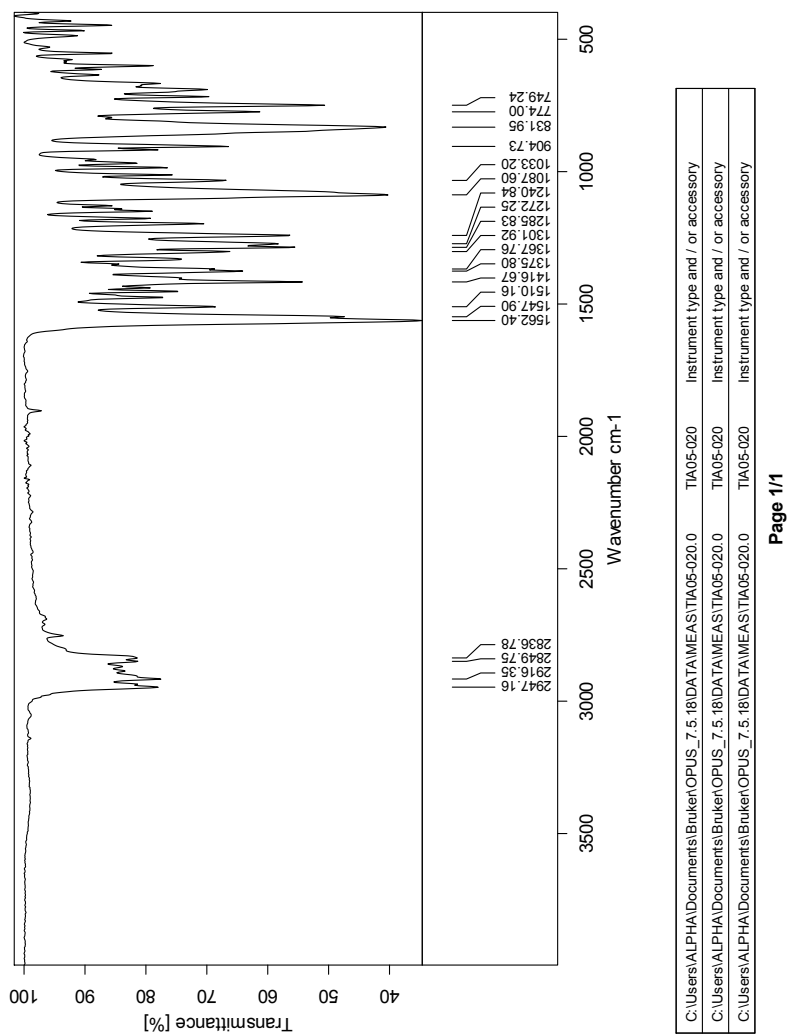
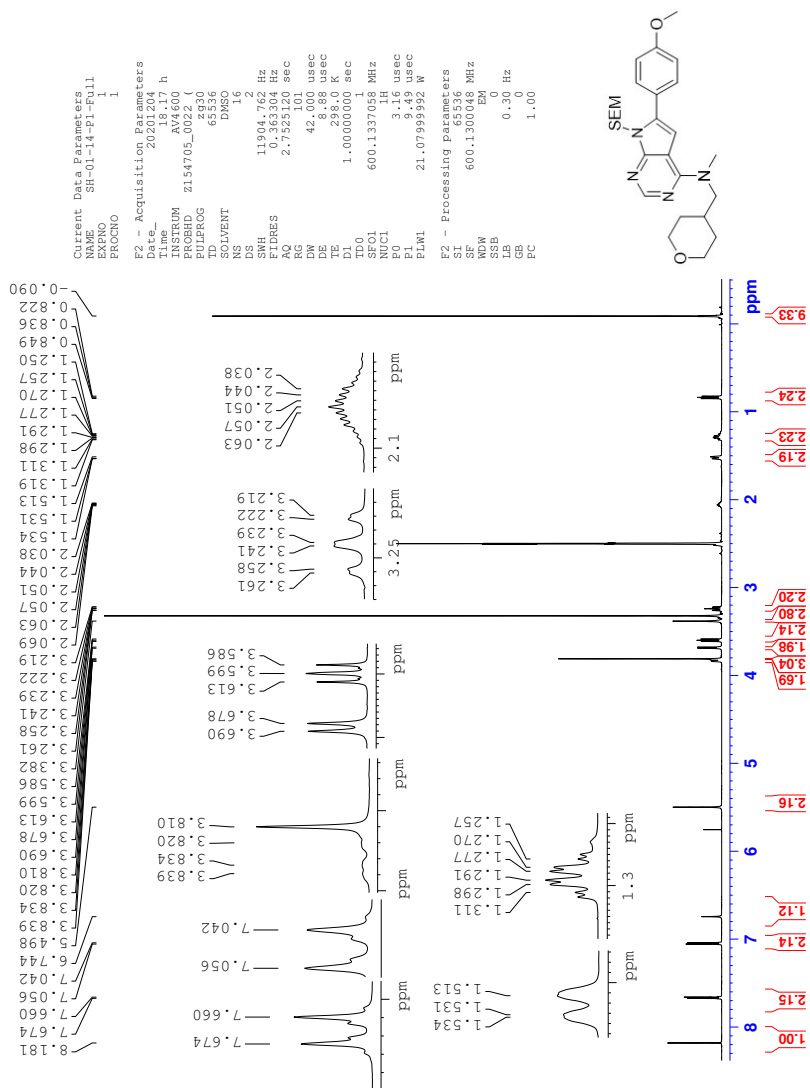


Figure B.6: IR spectrum of compound 3

C Spectroscopic data for Compound 4

Figure C.1: ^1H NMR spectrum of compound 4

```

Current Data Parameters
NAME      SH-01-14-Pl-Full
PROCNO    1
F2 - Acquisition Parameters
Date_     2017/07/07
Time      13:10 h
INSTRUM   AV4600
PROBHD    E154705_0022 (
PULPROG   zgpg30
SOLVENT    DMSO
NS         1024
DS         4
SS         35714.284 Hz
ETDRES    1.089913 Hz
AQ         0.9175040 sec
RG         101
DE         14.650 usec
TE         298.0 K
D1         2.0000000 sec
D11        0.03000000 sec
SFO1       150.9178988 MHz
NUC1       13C
P0         4.00 usec
PC         60.00 usec
PLM1       86.6419829 MHz
SFO2        600.1324005 MHz
NUC2        1H
CPDPRG2   waltz16
NUC3        13C
PLM2        21.079999992 W
PLM3        0.38744000 W
PLM13       0.19487999 W
F2 - Processing parameters
SI         32768
SF         150.9028812 MHz
WDW        EM
SSB        0
LB         1.00 Hz
GB         0
PC         1.40

```

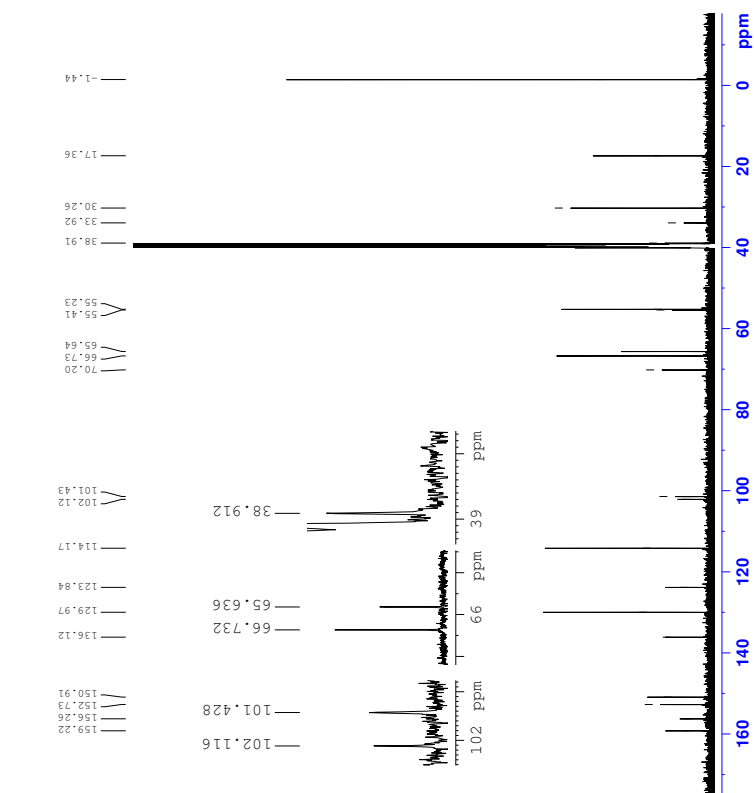
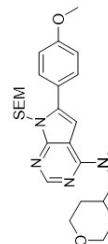


Figure C.2: ^{13}C NMR spectrum of compound 4

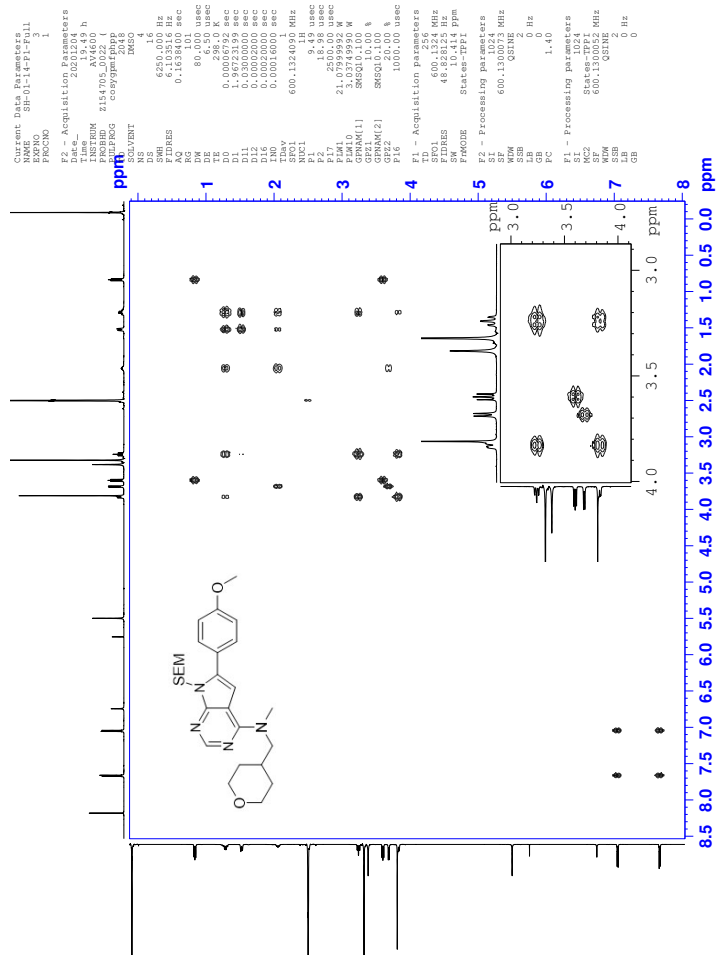


Figure C.3: COSY spectrum of compound 4

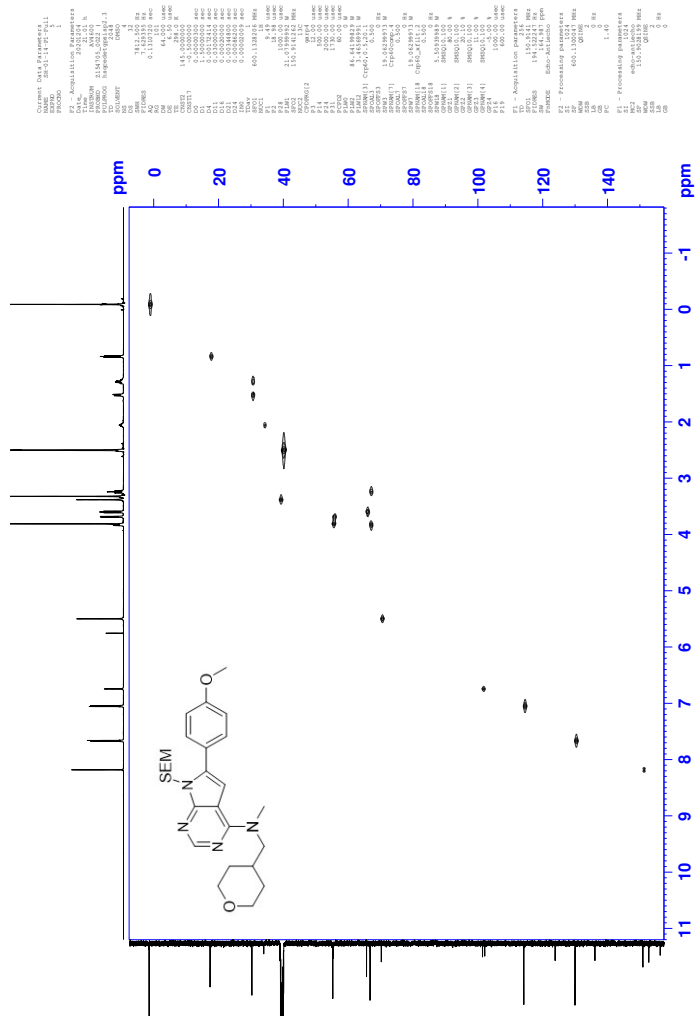


Figure C.4: HSQC spectrum of compound 4

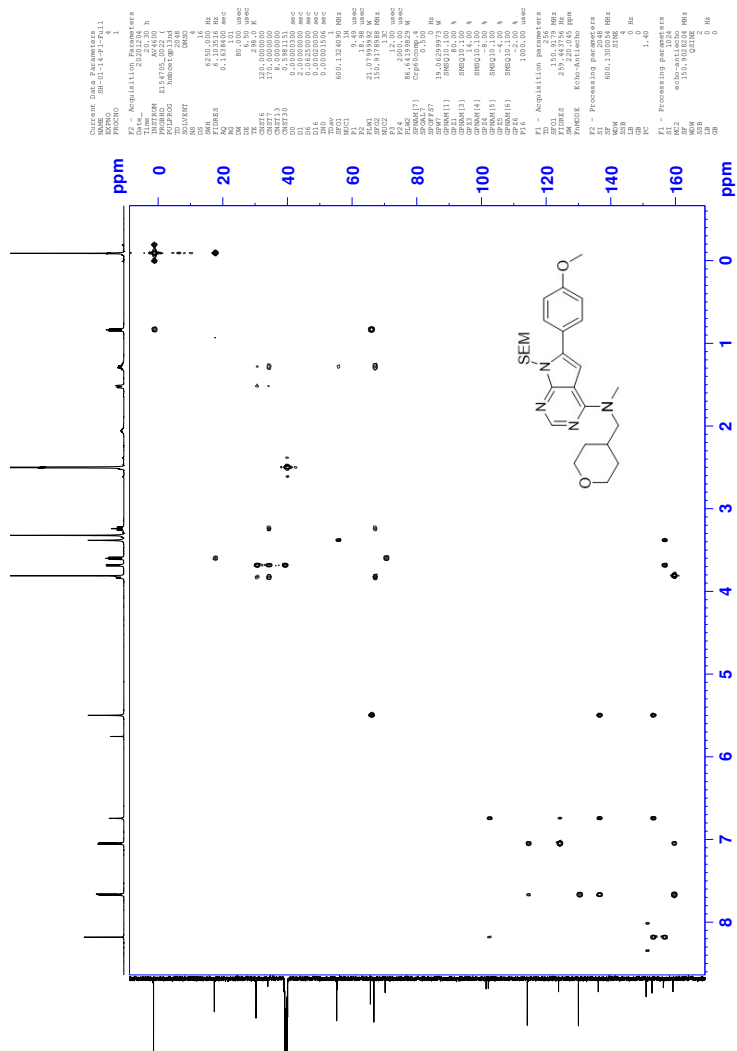


Figure C.5: HMBC spectrum of compound 4

Elemental Composition Report

Page 1

Single Mass Analysis

Tolerance = 2.0 PPM / DBE: min = -50.0, max = 100.0

Element prediction: Off

Number of isotope peaks used for i-FIT = 6

Monoisotopic Mass, Even Electron Ions

4147 formula(e) evaluated with 4 results within limits (all results (up to 1000) for each mass)

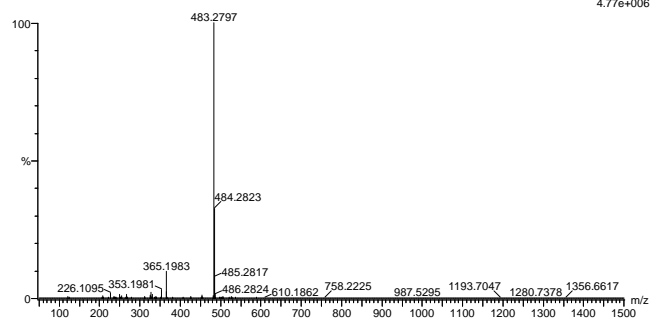
Elements Used:

C: 0-100 H: 0-100 N: 0-8 O: 0-8 Na: 0-1 Si: 0-2

2020 377.68 (0.552) AM2 (Ar,35000.0,0.00,0.00); Cm (55.58)

1: TOF MS ES+

4.77e+006



Mass	Calc. Mass	mDa	PPM	DBE	i-FIT	Norm	Conf (%)	Formula
483.2797	483.2791	0.6	1.2	10.5	1900.7	0.000	100.00	C26 H39 N4 O3
	483.2799	-0.2	-0.4	2.5	1915.5	14.738	0.00	Si C20 H44 N4 O4 Na
	483.2800	-0.3	-0.6	19.5	1917.1	16.381	0.00	Si2 C35 H35 N2
	483.2795	0.2	0.4	3.5	1917.8	17.029	0.00	C21 H40 N4 O7 Na

Figure C.6: MS spectrum of compound 4

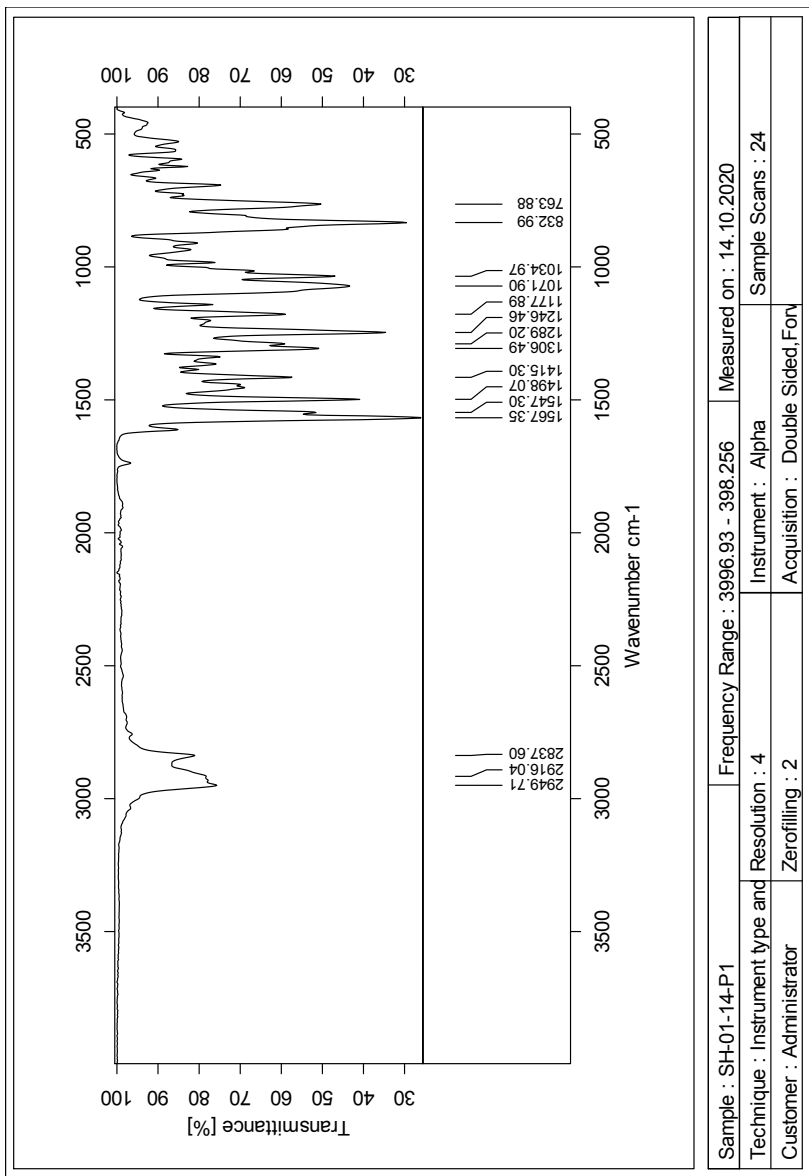
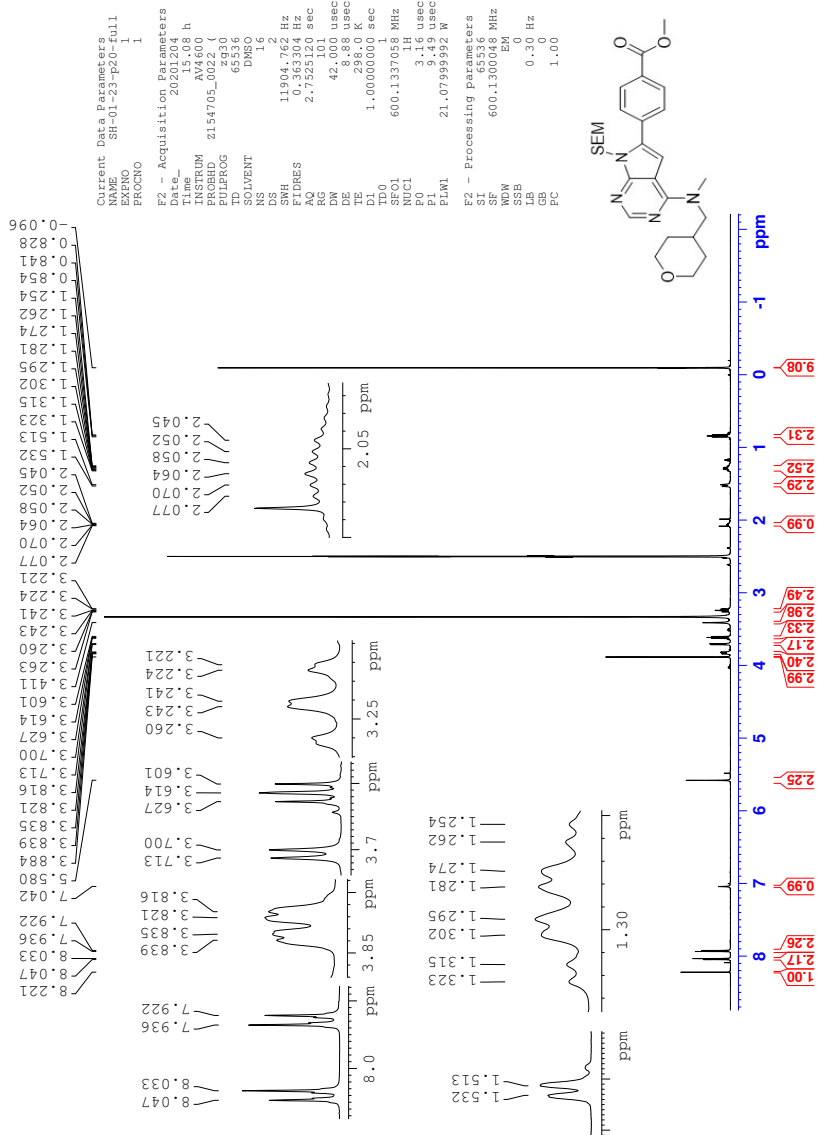


Figure C.7: IR spectrum of compound 4

D Spectroscopic data for Compound 5

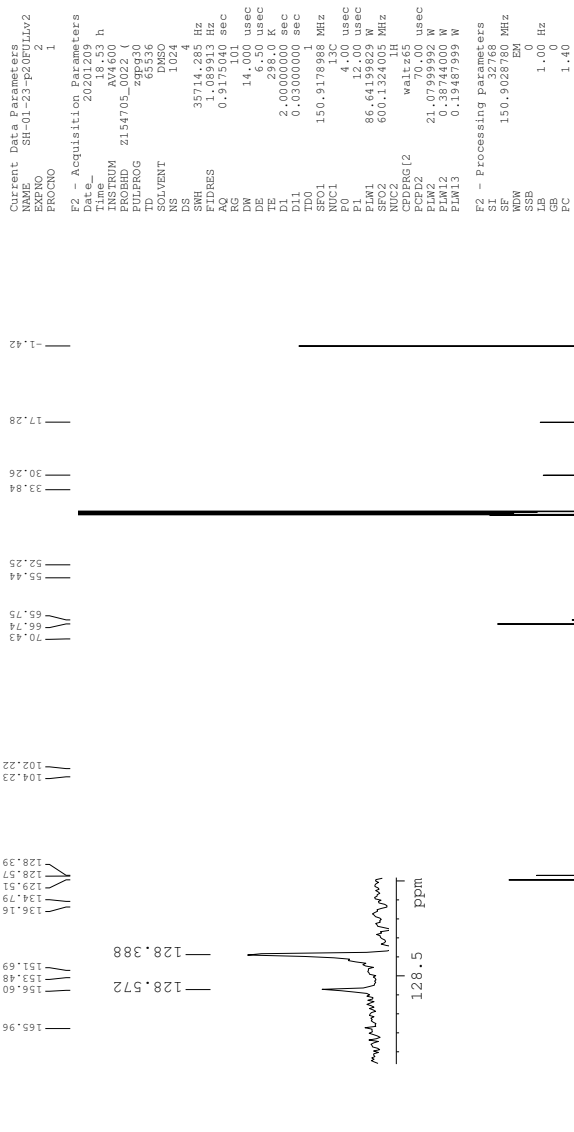


Figure D.2: ^{13}C NMR spectrum of compound 5

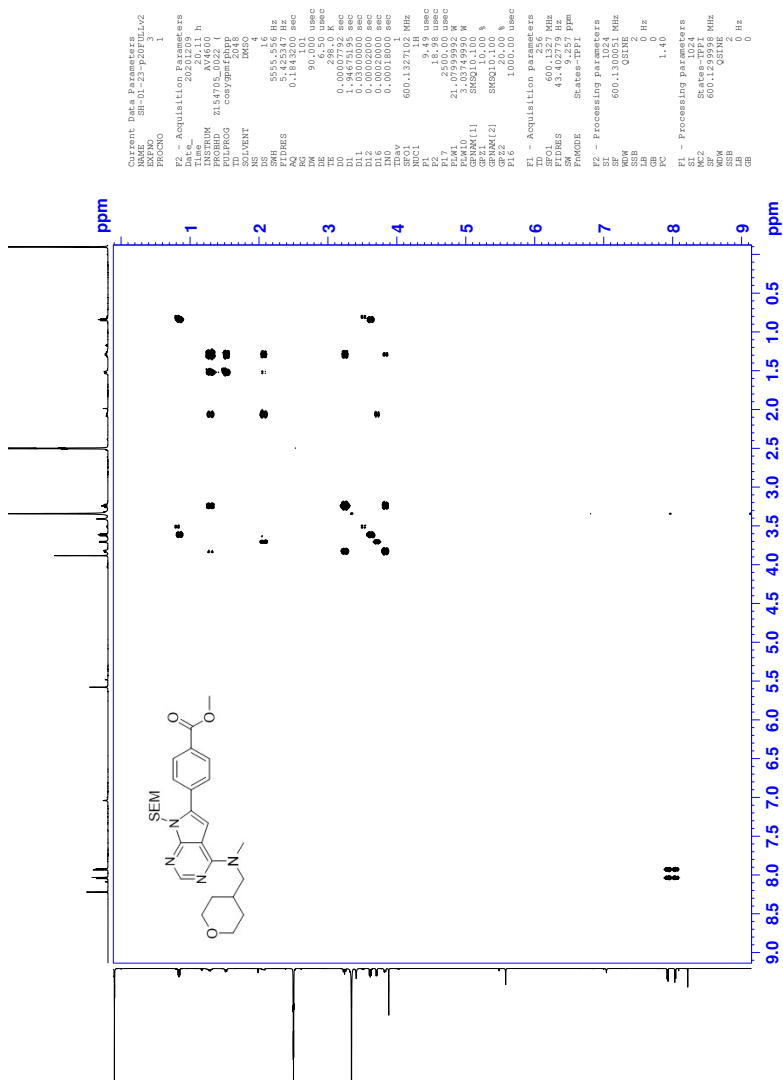


Figure D.3: COSY spectrum of compound 5

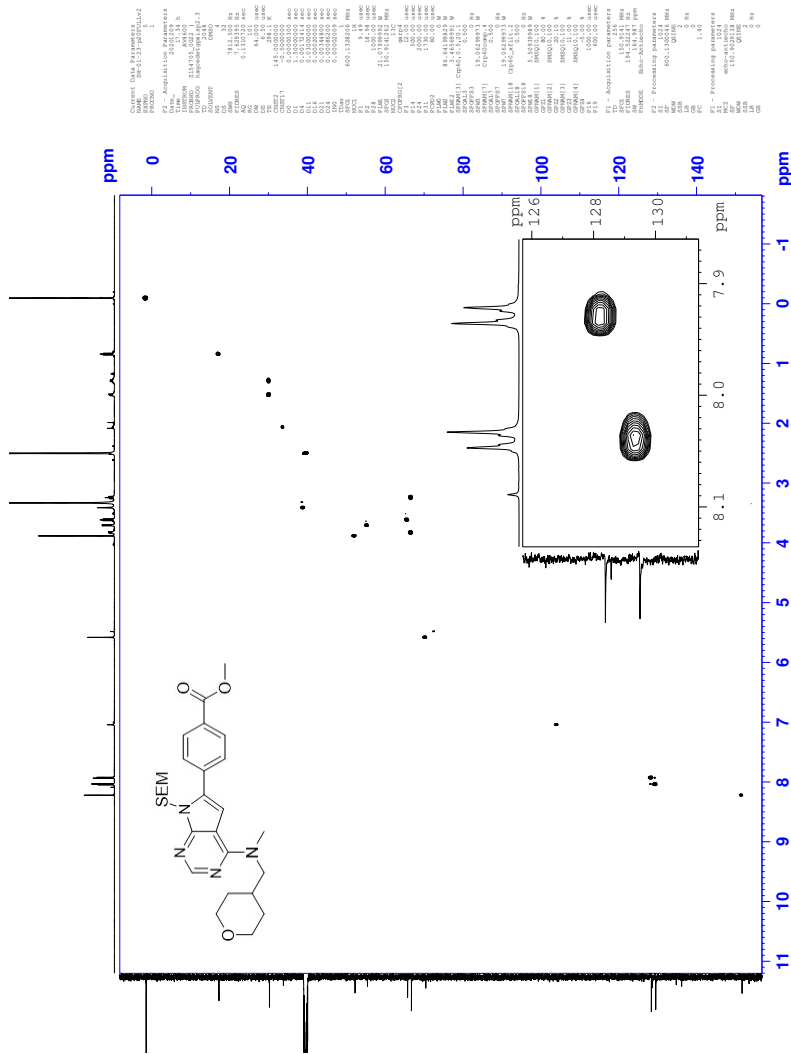


Figure D.4: HSQC spectrum of compound 5

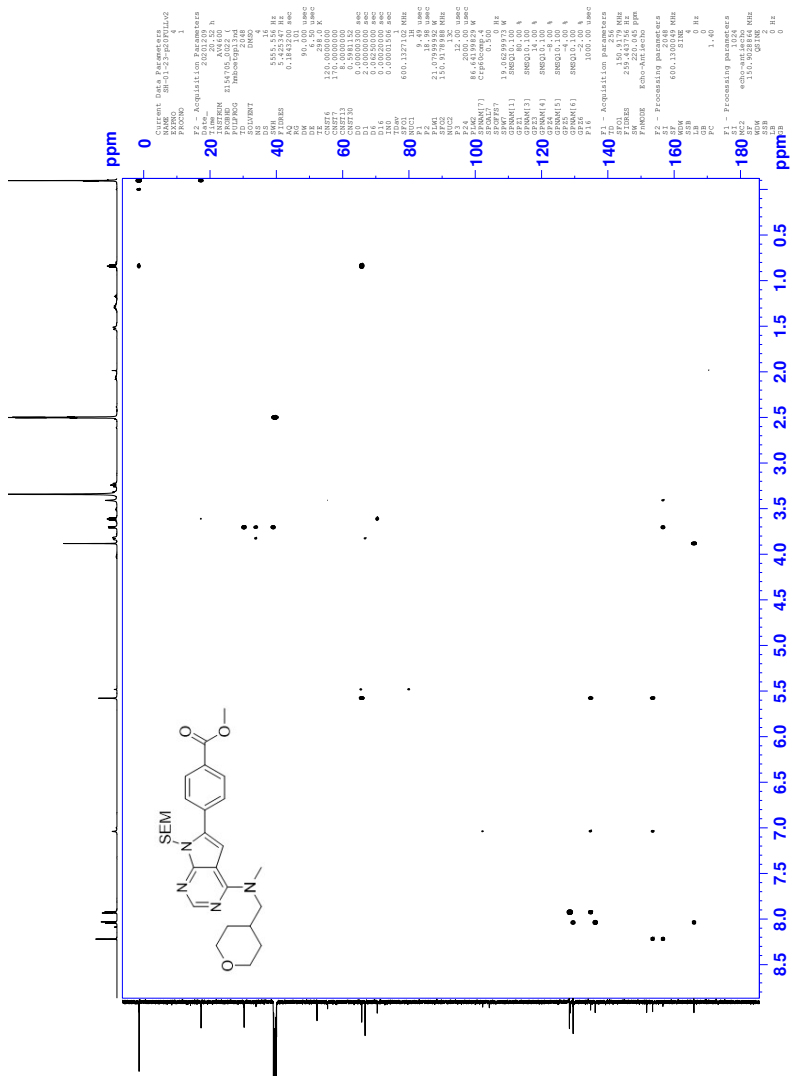


Figure D.5: HMBC spectrum of compound 5

Elemental Composition Report

Page 1

Single Mass Analysis

Tolerance = 2.0 PPM / DBE: min = -50.0, max = 100.0

Element prediction: Off

Number of isotope peaks used for i-FIT = 6

Monoisotopic Mass, Even Electron Ions

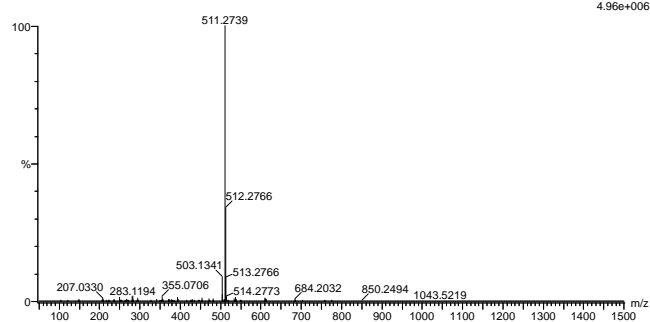
3107 formula(e) evaluated with 4 results within limits (all results (up to 1000) for each mass)

Elements Used:

C: 0-100 H: 0-100 N: 0-10 O: 0-10 Si: 0-2

2020 443.83 (0.787) AM2 (Ar,35000.0,0.00,0.00); Cm (83.88)

1: TOF MS ES+



Mass	Calc. Mass	mDa	PPM	DBE	i-FIT	Norm	Conf (%)	Formula
511.2739	511.2741	-0.2	-0.4	11.5	1929.3	0.000	100.00	C27 H39 N4 O4 S1
	511.2741	-0.2	-0.4	8.5	1941.2	11.861	0.00	C20 H35 N10 O6
	511.2745	-0.6	-1.2	7.5	1945.1	15.716	0.00	C19 H39 N10 O3 S12
	511.2732	0.7	1.4	2.5	1944.9	15.509	0.00	C18 H43 N6 O7 S12

Figure D.6: MS spectrum of compound 5

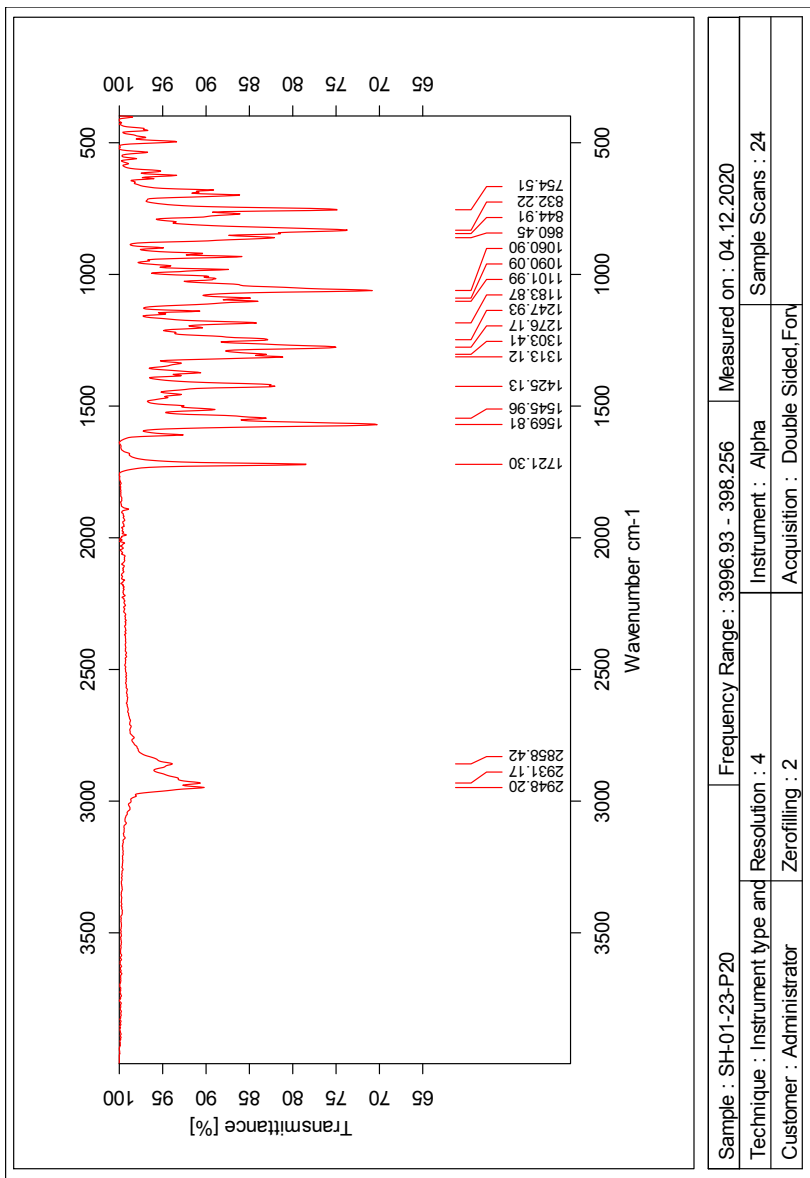
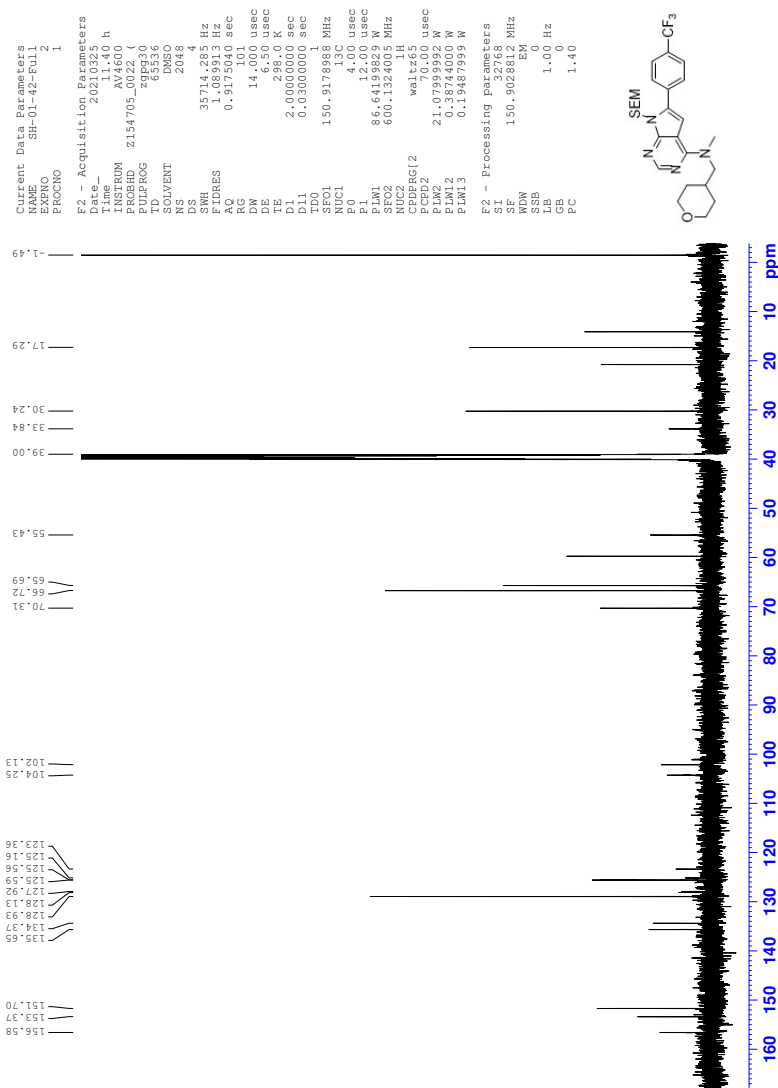


Figure D.7: IR spectrum of compound 5

Figure E.2: ^{13}C NMR spectrum of compound 6

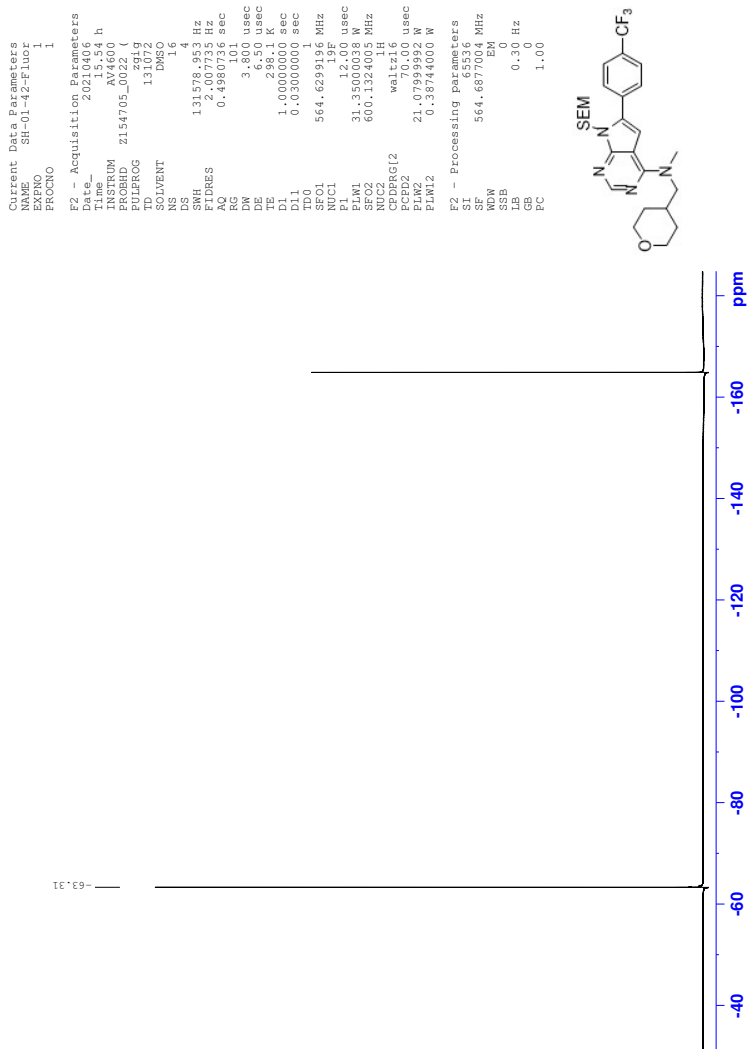


Figure E.3: ^{19}F NMR spectrum of compound 6

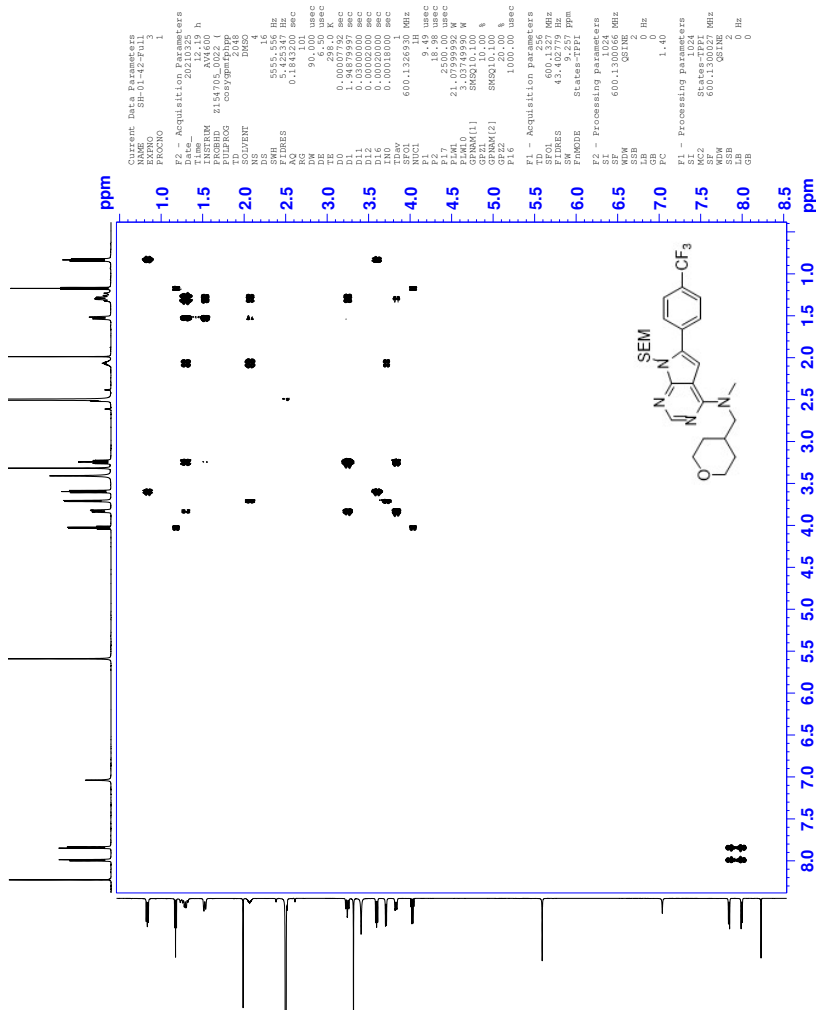


Figure E.4: COSY spectrum of compound 6

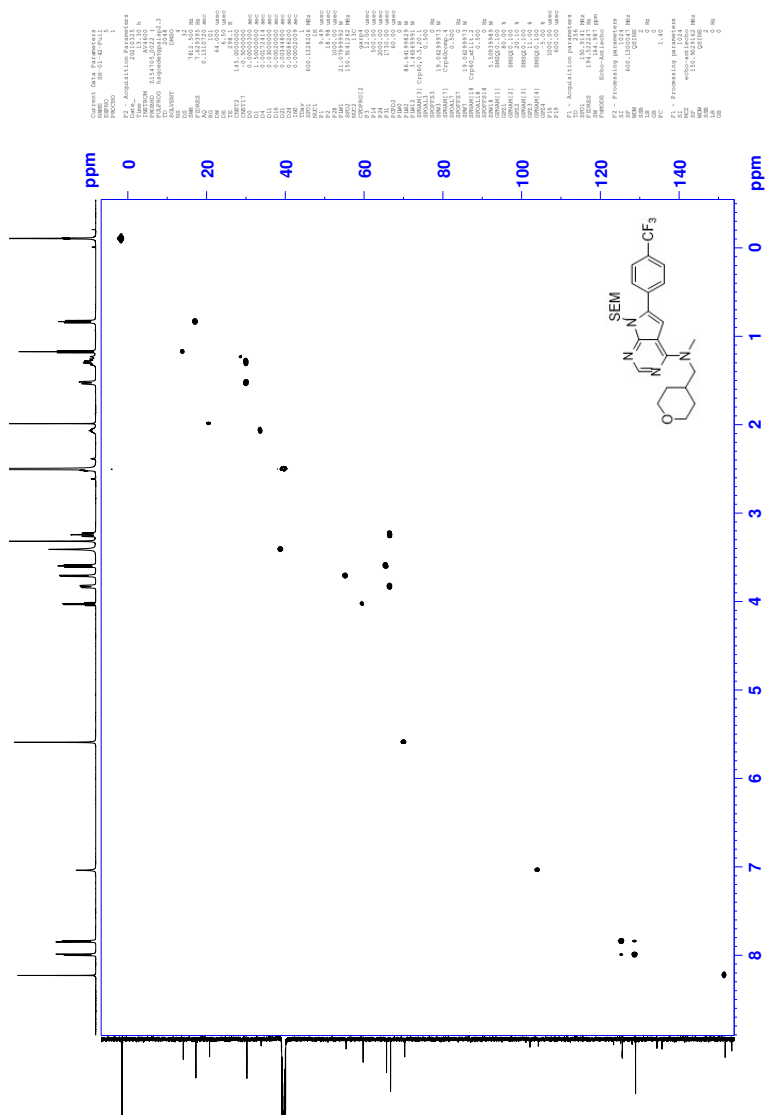


Figure E.5: HSQC spectrum of compound 6

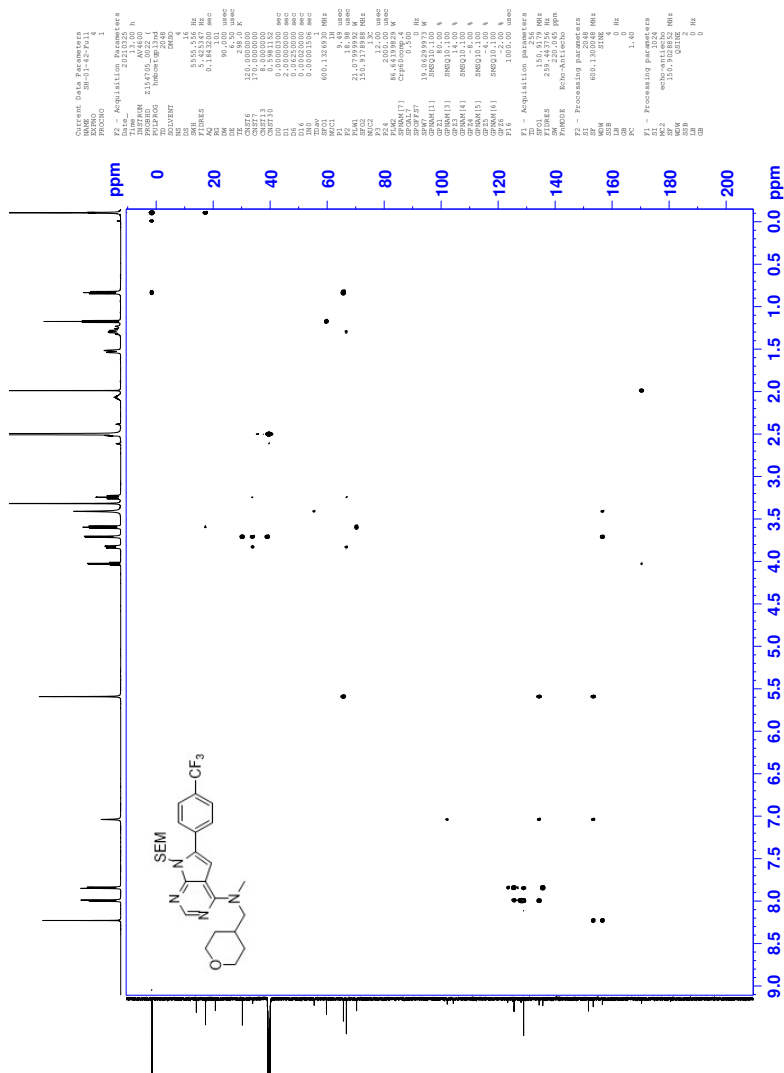


Figure E.6: HMBC spectrum of compound 6

Elemental Composition Report

Page 1

Single Mass Analysis

Tolerance = 2.0 PPM / DBE: min = -10.0, max = 50.0

Element prediction: Off

Number of isotope peaks used for i-FIT = 6

Monoisotopic Mass, Even Electron Ions

8814 formula(e) evaluated with 18 results within limits (all results (up to 1000) for each mass)

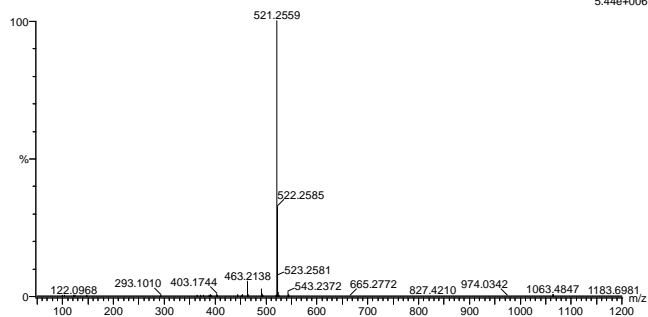
Elements Used:

C: 0-100 H: 0-100 N: 0-4 O: 0-8 F: 0-4 Na: 0-1 Si: 0-2

2021-159.95 (1.063) AM2 (Ar:35000.0,0.00,0.00); Cm (90:95)

1: TOF MS ES+

5.44e+006



Mass	Calc. Mass	mDa	PPM	DBE	i-FIT	Norm	Conf (%)	Formula
521.2559	521.2560	-0.1	-0.2	10.5	1719.3	0.906	40.42	C26 H36 N4 O2 F3 S1
	521.2558	0.1	0.2	1.5	1719.1	0.793	45.25	C22 H41 O7 F4 S1
	521.2560	-0.1	-0.2	10.5	1720.7	2.367	9.38	C26 H38 N4 O4 Na S1
	521.2557	0.2	0.4	17.5	1727.5	9.143	0.01	C31 H37 N4 Si2
	521.2556	0.3	0.6	6.5	1727.3	8.916	0.01	C23 H40 N4 O2 F2 Na Si2
	521.2556	0.3	0.6	12.5	1728.0	9.623	0.01	C30 H34 N2 F4 Na
	521.2555	0.4	0.8	8.5	1726.4	8.038	0.03	C27 H42 O5 F S12
	521.2563	-0.4	-0.8	3.5	1730.2	11.850	0.00	C21 H37 N4 O6 F3 Na
	521.2564	-0.5	-1.0	14.5	1723.3	4.963	0.70	C29 H34 N4 O4 F
	521.2554	0.5	1.0	-2.5	1726.3	7.995	0.03	C19 H45 O7 F3 Na Si2
	521.2553	0.6	1.2	18.5	1724.5	6.159	0.21	C32 H33 N4 O3
	521.2565	-0.6	-1.2	-6.5	1725.8	7.445	0.06	C16 H46 O8 F4 Na S12
	521.2566	-0.7	-1.3	4.5	1725.6	7.254	0.07	C24 H43 O6 F2 S12
	521.2551	0.8	1.5	9.5	1721.6	3.286	3.74	C28 H38 O8 F
	521.2551	0.8	1.5	7.5	1727.8	9.434	0.01	C24 H36 N4 O5 F2

Figure E.7: MS spectrum of compound 6

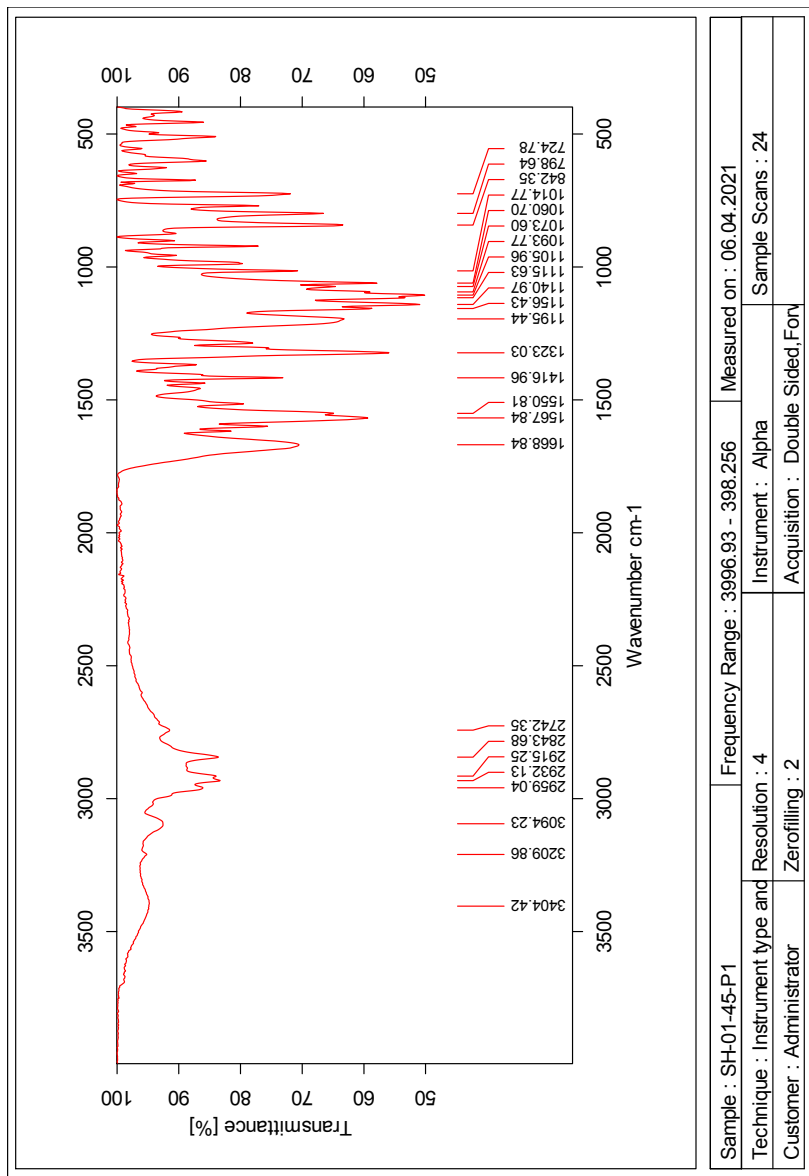


Figure E.8: IR spectrum of compound 6

F Spectroscopic data for Compound 7

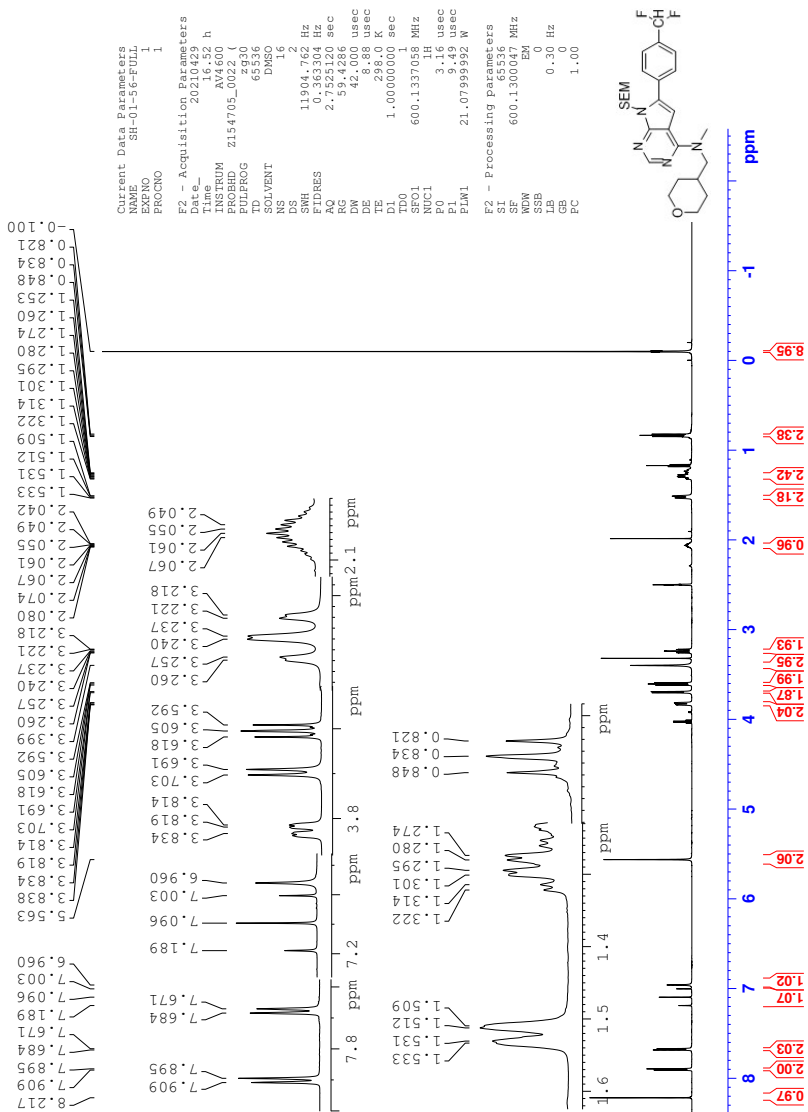


Figure F.1: ^1H NMR spectrum of compound 7

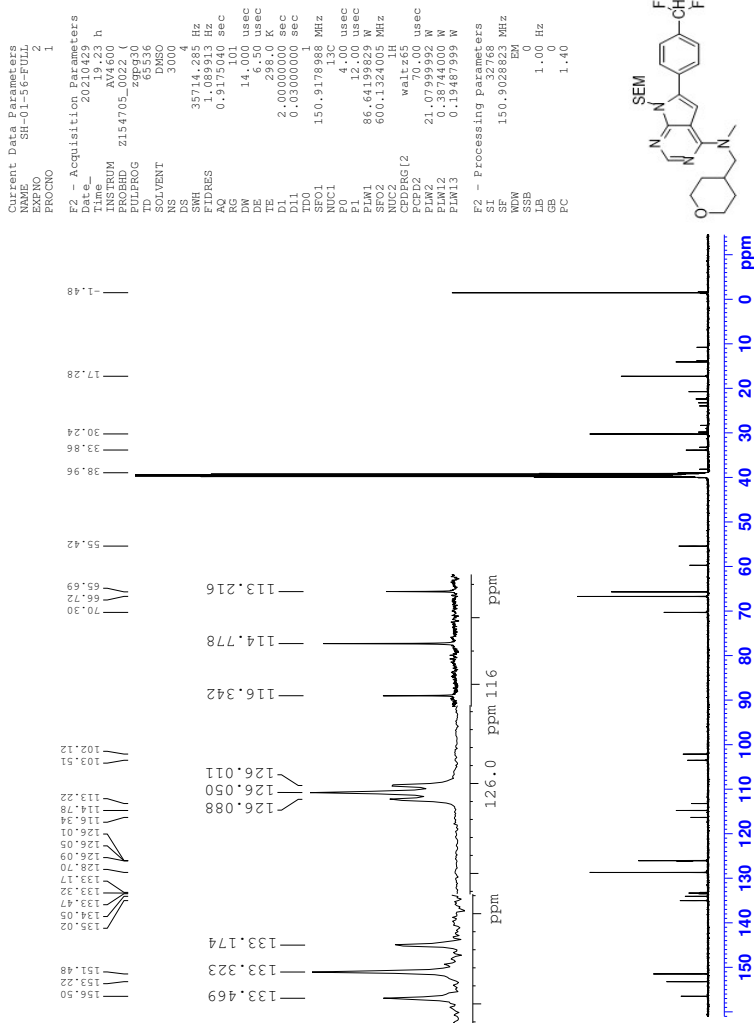
Figure F.2: ^{13}C NMR spectrum of compound 7



Figure F.3: ^{19}F NMR spectrum of compound 7

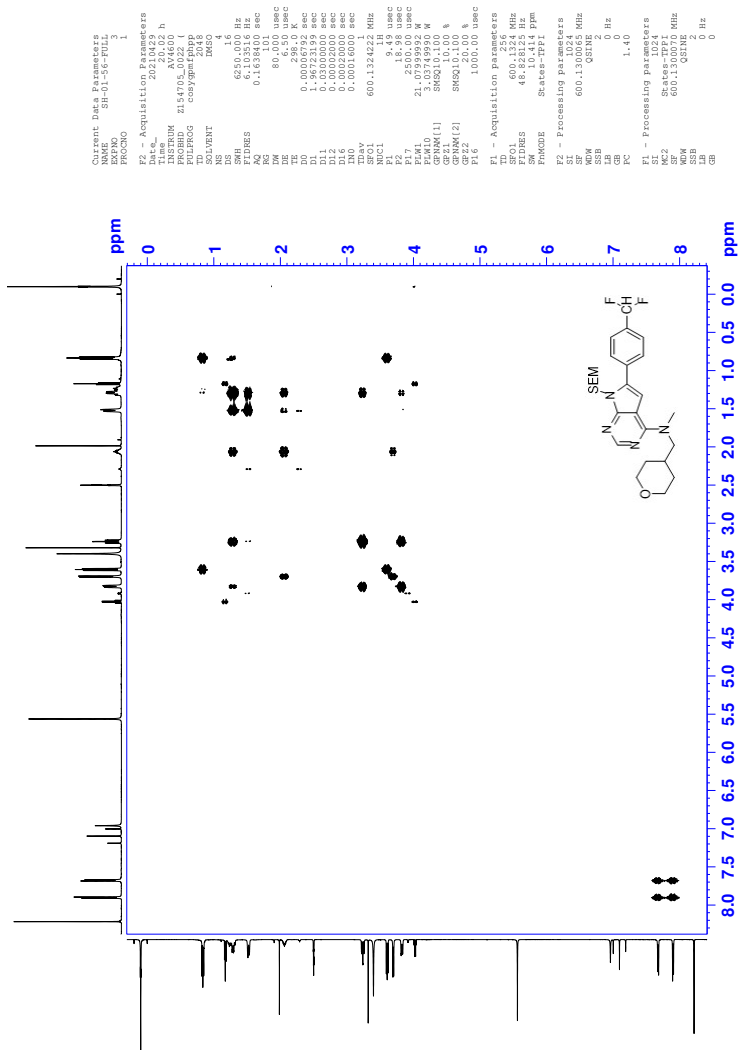


Figure F.4: COSY spectrum of compound 7

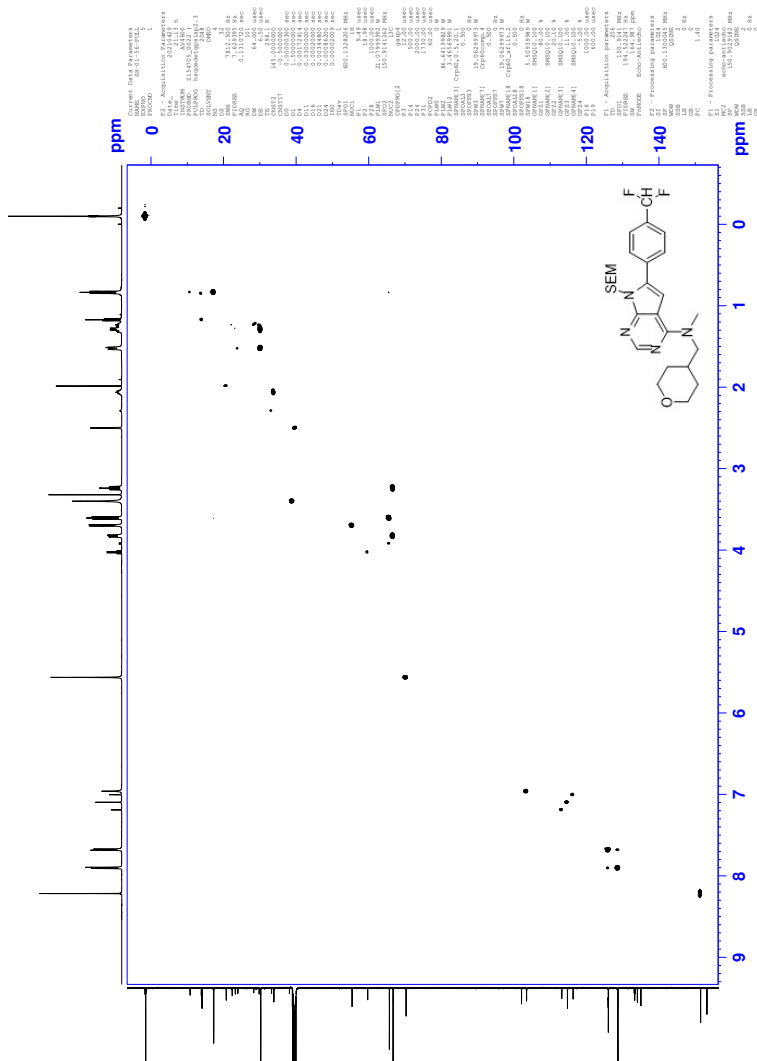


Figure F.5: HSQC spectrum of compound 7

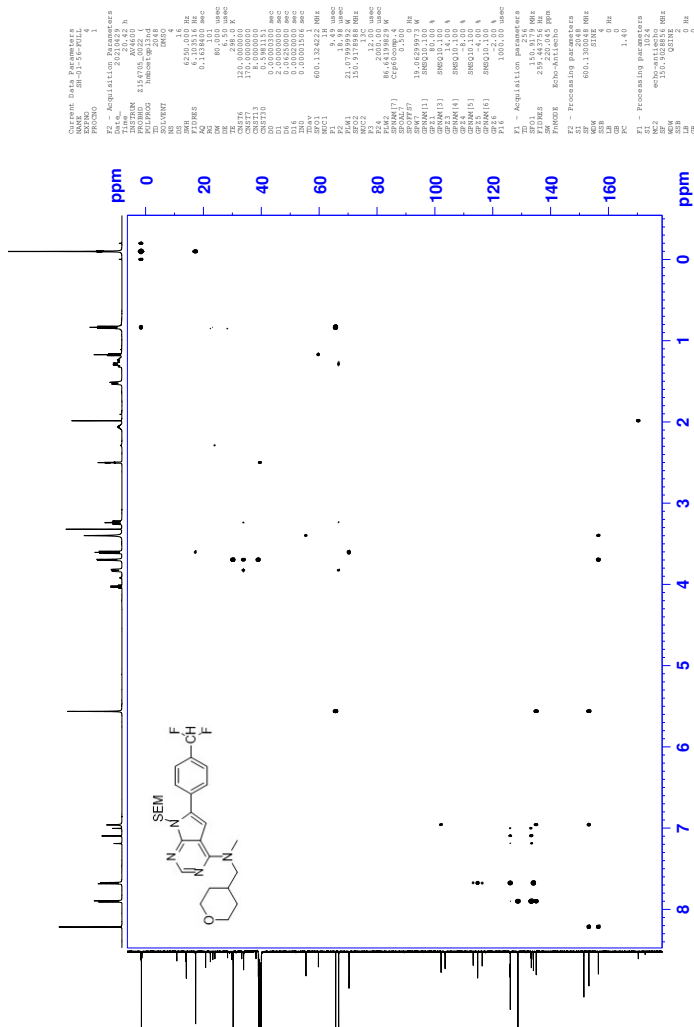


Figure F.6: HMBC spectrum of compound 7

Elemental Composition Report

Page 1

Single Mass Analysis

Tolerance = 2.0 PPM / DBE: min = -10.0, max = 50.0

Element prediction: Off

Number of isotope peaks used for i-FIT = 6

Monoisotopic Mass, Even Electron Ions

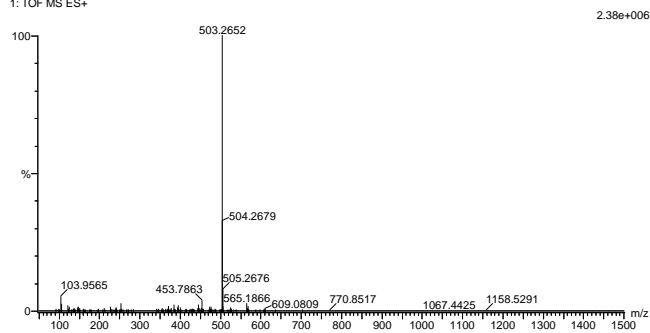
5803 formula(e) evaluated with 10 results within limits (all results (up to 1000) for each mass)

Elements Used:

C: 0-100 H: 0-100 N: 0-5 O: 0-12 Si: 0-2 F: 0-3

2021-300 166 (1.562) AM2 (Ar,35000.0,0.00,0.00); Cm (165:169)

1: TOF MS ES+



Minimum: -10.0

Maximum: 5.0 2.0 50.0

Mass	Calc. Mass	mDa	PPM	DBE	i-FIT	Norm	Conf (%)	Formula
503.2652	503.2652	0.0	0.0	1.5	1861.7	0.633	53.10	C22 H42 O7 Si F3
503.2654	-0.2	-0.4	10.5	1862.2	1.078	34.02		C26 H37 N4 O2 Si F2
503.2645	0.7	1.4	9.5	1863.6	2.478	8.39		C28 H39 O8
503.2658	-0.6	-1.2	14.5	1864.8	3.677	2.53		C29 H35 N4 O4
503.2642	1.0	2.0	14.5	1865.5	4.418	1.21		C29 H36 N4 O Si F
503.2648	0.4	0.8	-3.5	1866.5	5.339	0.48		C16 H44 N2 O12 Si F
503.2656	-0.4	-0.8	5.5	1867.4	6.316	0.18		C25 H40 O9 F
503.2660	-0.8	-1.6	4.5	1869.0	7.867	0.04		C24 H44 O6 Si2 F
503.2643	0.9	1.8	-7.5	1869.1	7.979	0.03		C13 H46 N2 O10 Si2 F3
503.2649	0.3	0.6	8.5	1869.8	8.731	0.02		C27 H43 O5 Si2

Figure F.7: MS spectrum of compound 7

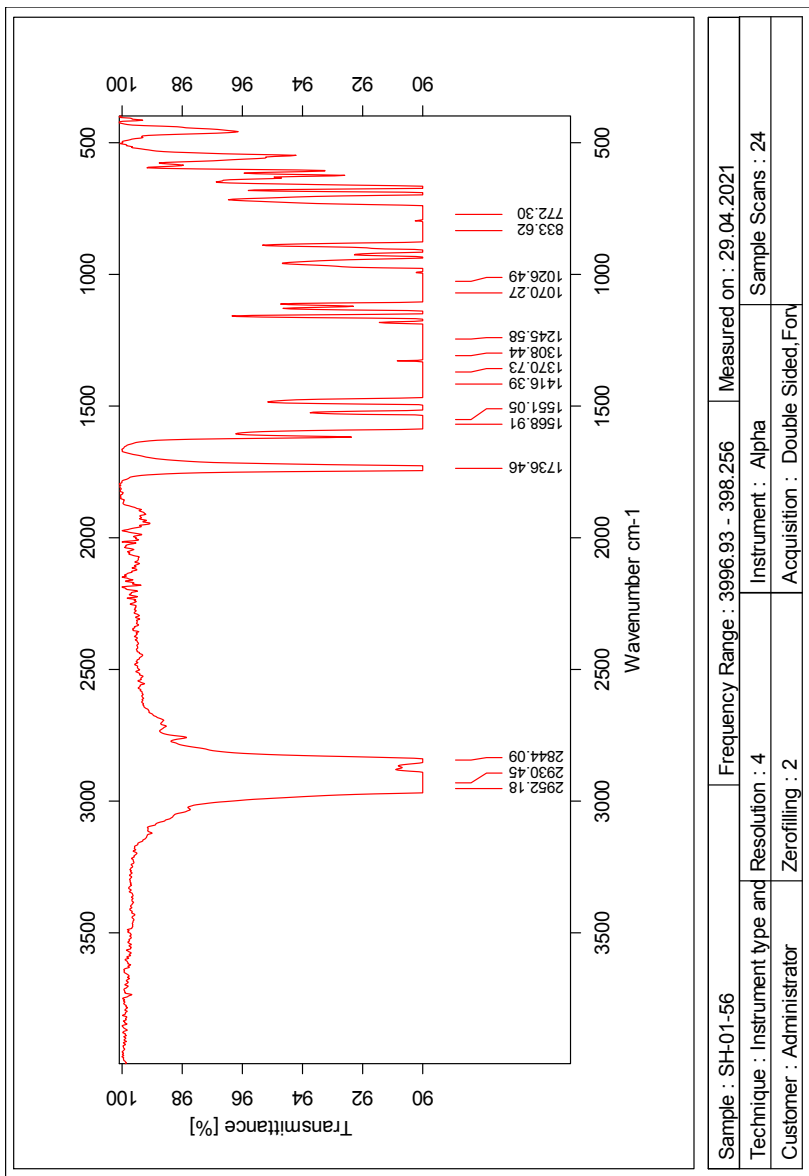
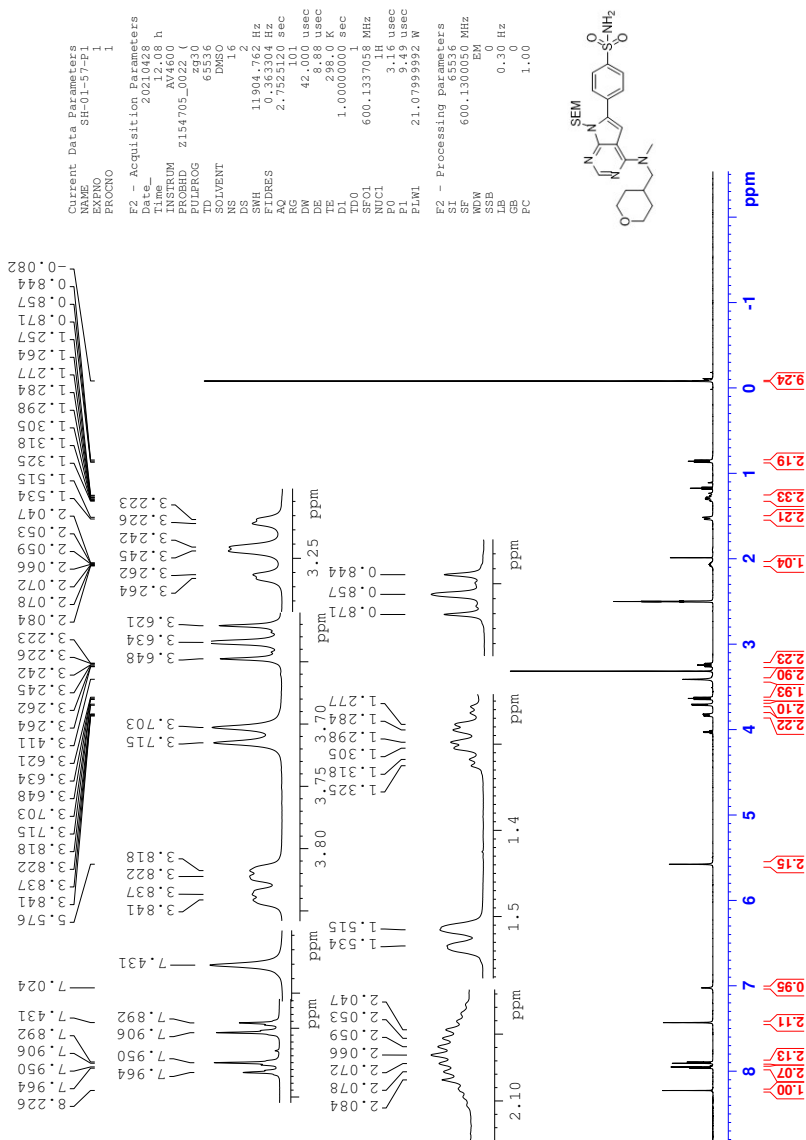
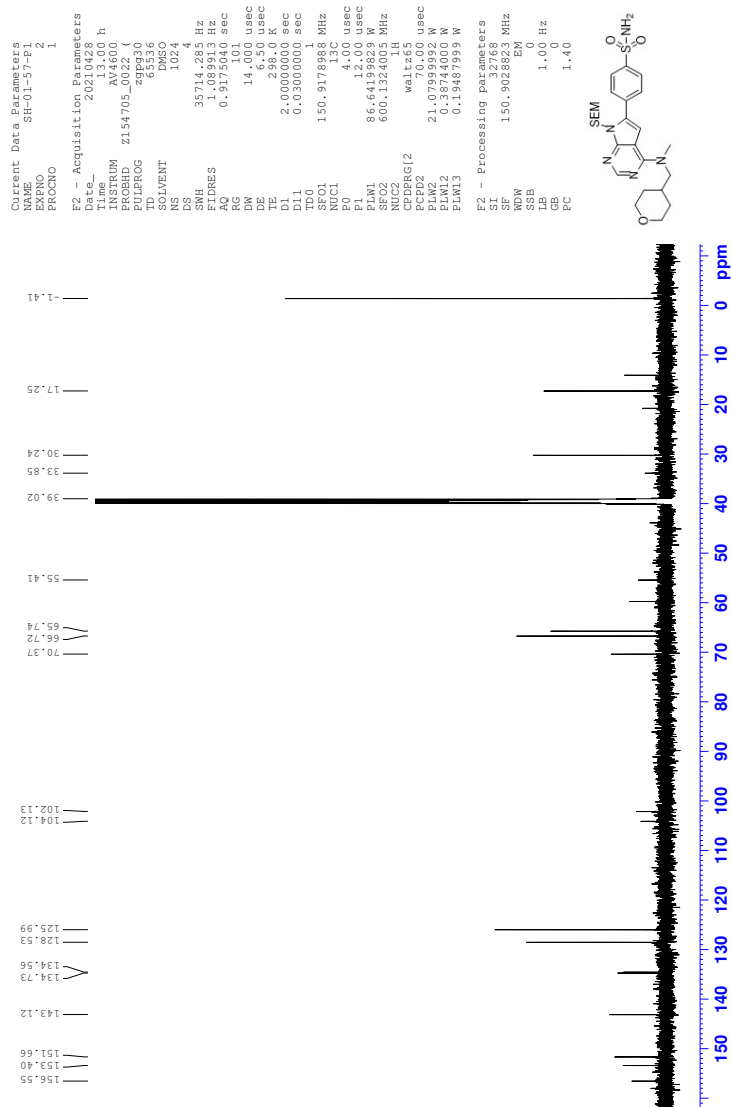


Figure F.8: IR spectrum of compound 7

G Spectroscopic data for Compound 8

Figure G.1: ¹H NMR spectrum of compound 8

Figure G.2: ^{13}C NMR spectrum of compound 8

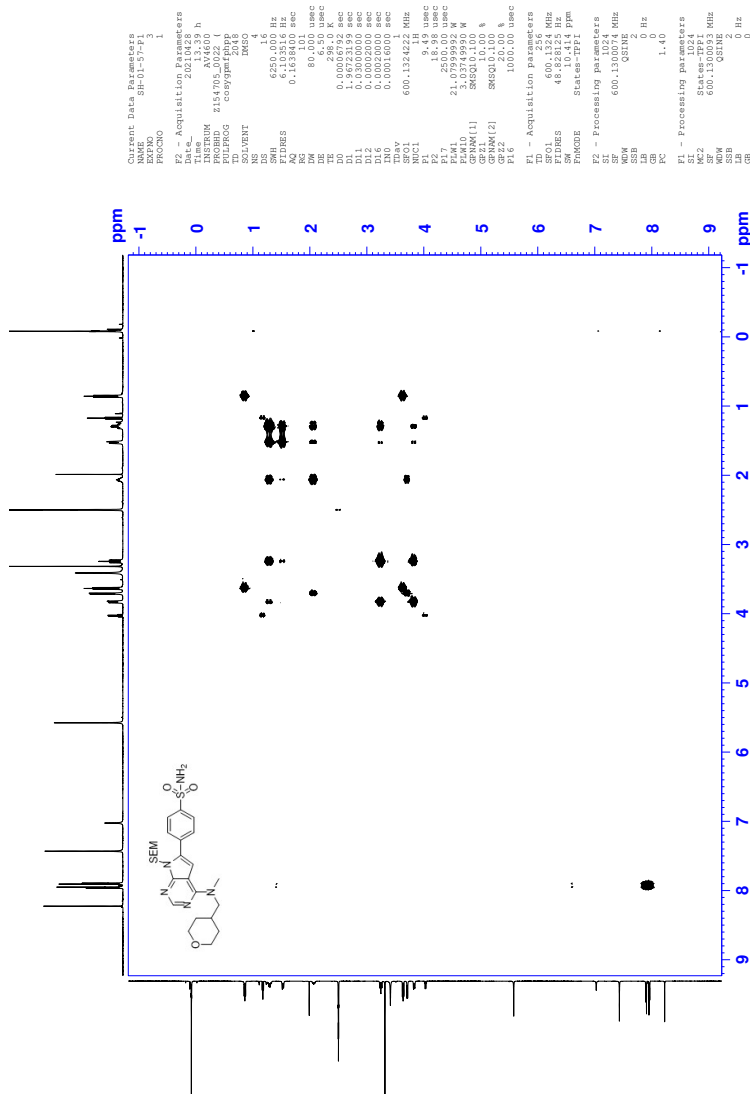


Figure G.3: COSY spectrum of compound 8

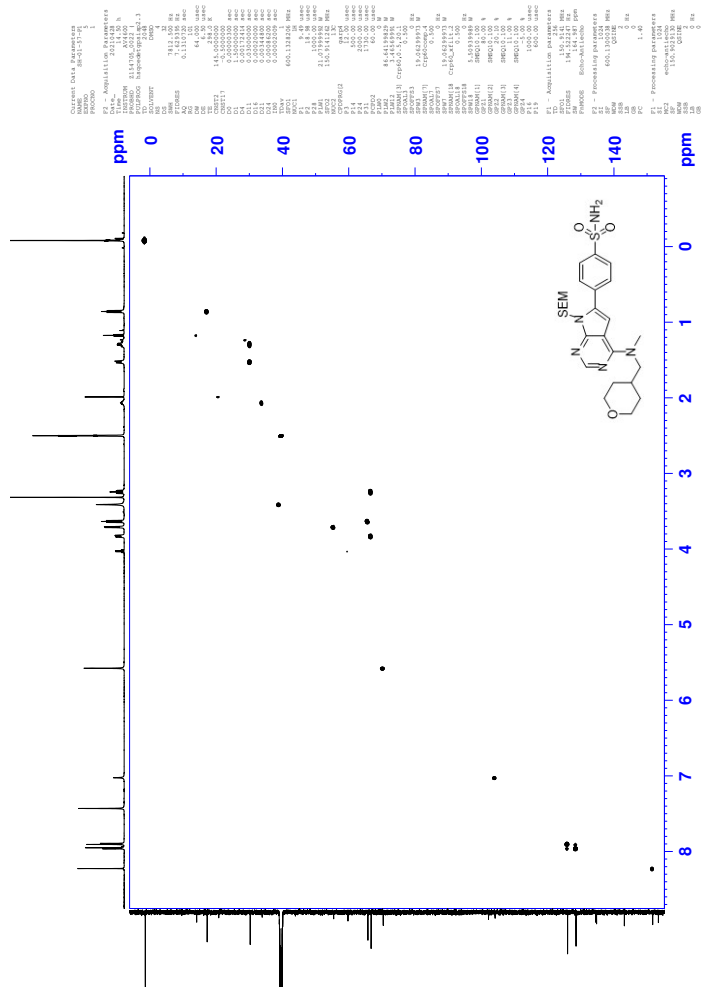
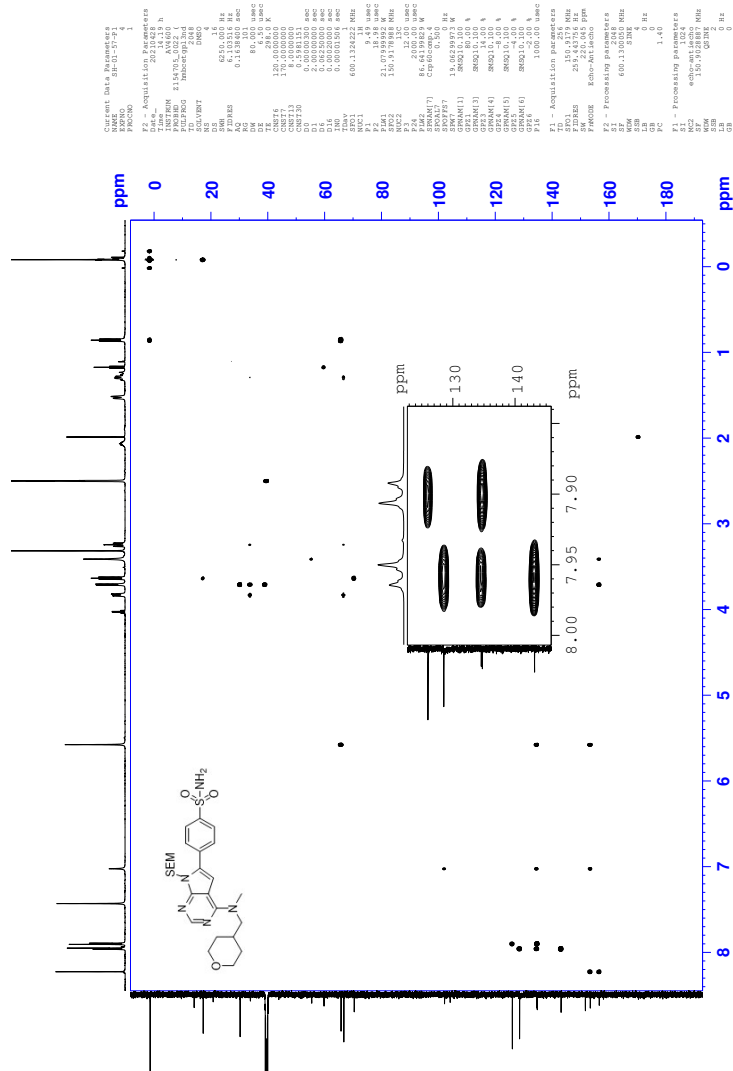


Figure G.4: HSQC spectrum of compound 8



Elemental Composition Report

Page 1

Single Mass Analysis

Tolerance = 2.0 PPM / DBE: min = -10.0, max = 50.0

Element prediction: Off

Number of isotope peaks used for i-FIT = 6

Monoisotopic Mass, Even Electron Ions

3163 formula(e) evaluated with 5 results within limits (all results (up to 1000) for each mass)

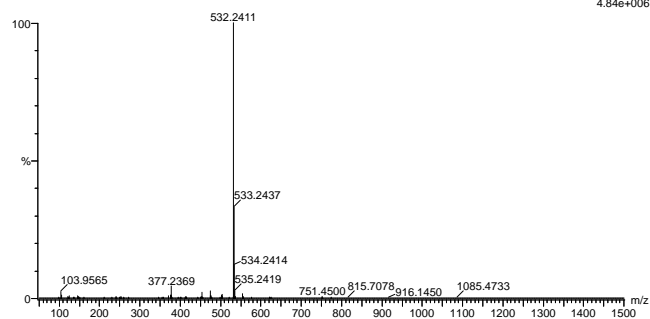
Elements Used:

C: 0-100 H: 0-100 N: 0-5 O: 0-12 Si: 0-2 S: 0-1

2021-301 136 (1.283) AM2 (Ar,35000.0,0.00,0.00); Cm (136:142)

1: TOF MS ES+

4.84e+006



Mass	Calc. Mass	mDa	PPM	DBE	i-FIT	Norm	Conf (%)	Formula
532.2411	532.2414	-0.3	-0.6	10.5	1932.0	0.024	97.65	C25 H38 N5 O4 Si
	532.2400	1.1	2.1	5.5	1935.7	3.766	2.31	C24 H42 N O8 Si
	532.2411	0.0	0.0	10.5	1940.0	7.981	0.03	C24 H38 N5 O5
	532.2420	-0.9	-1.7	19.5	1950.5	18.492	0.00	C33 H34 N3 O2
	532.2407	0.4	0.8	11.5	1956.9	24.967	0.00	C25 H34 N5 O8

Figure G.6: MS spectrum of compound 8

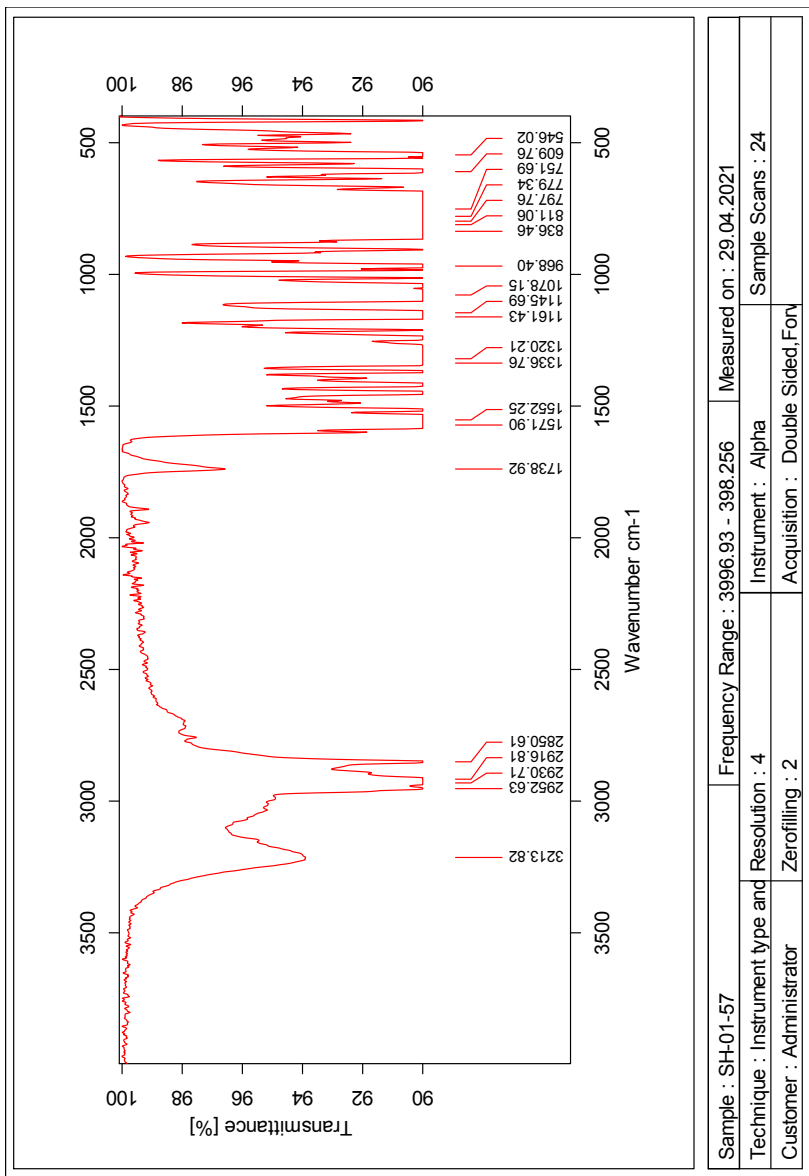
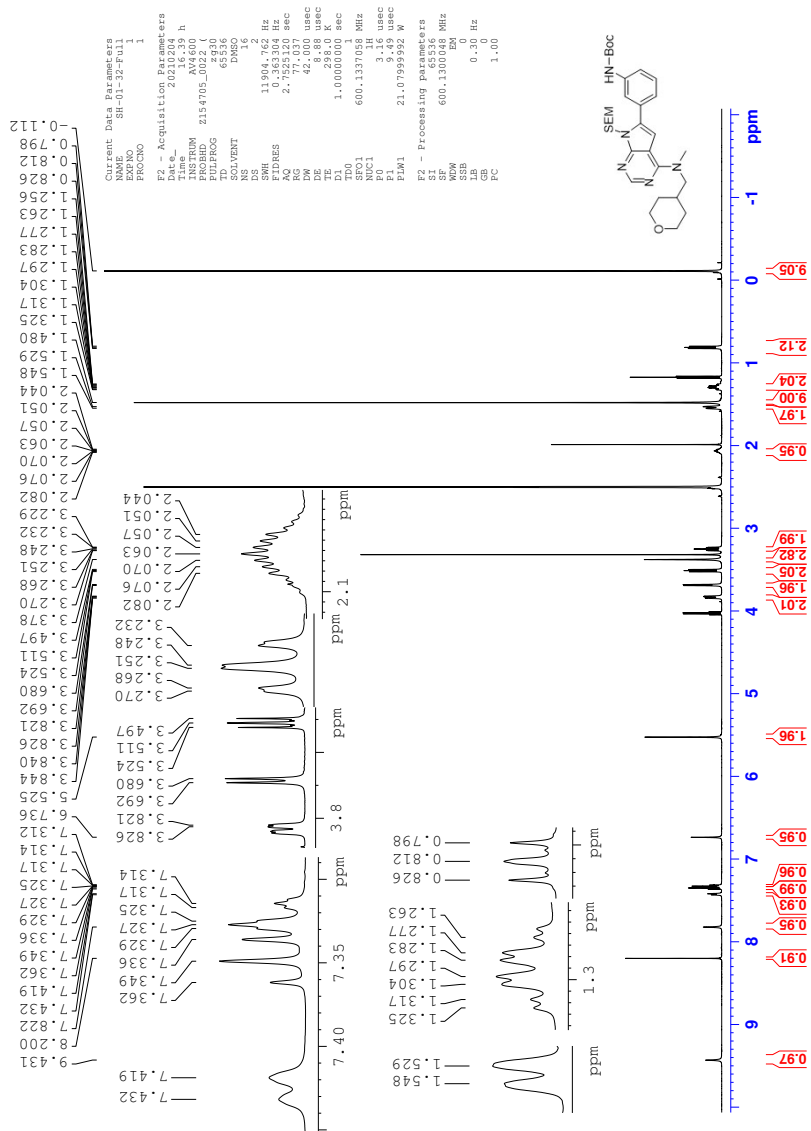


Figure G.7: IR spectrum of compound 8

H Spectroscopic data for Compound 9

Figure H.1: ^1H NMR spectrum of compound 9

```

Current Data Parameters
NAME      SH-01-32-Full1
EXPNO    2
PROCNO   1
F2 - Acquisition Parameters
Date_    20210204
Time     14:56:02 h
INSTRUM  AV4602
PROBHD   z9p830
PULPROG  zgpg30
D1       65536
SOLVENT  DMSO
NS       1024
DS       4
SWH      35714.295 Hz
FIDRES  0.109564 Hz
AQ       0.917540 sec
RG       1.01
DM       14.000 usec
DE       95.50 usec
TE       300.2 K
D11      2.0000000 sec
D12      0.0300000 sec
D13      150.9178981 MHz
NUC1     13C
P0       4.00 usec
P1       86.6112.00 usec
PCPD2    0.0000000 sec
SFO2     800.1324100 MHz
NUC2     1H
CPDPRG2  waltz65
PCPD2    21.079870.00 usec
SFO2     0.38744000 W
PLW12    0.194877999 W
PLW13    0.194877999 W
F2 - Processing parameters
SF       150.9028812 MHz
WDW      EM
SSB      0
GB       0
PC       1.40

```

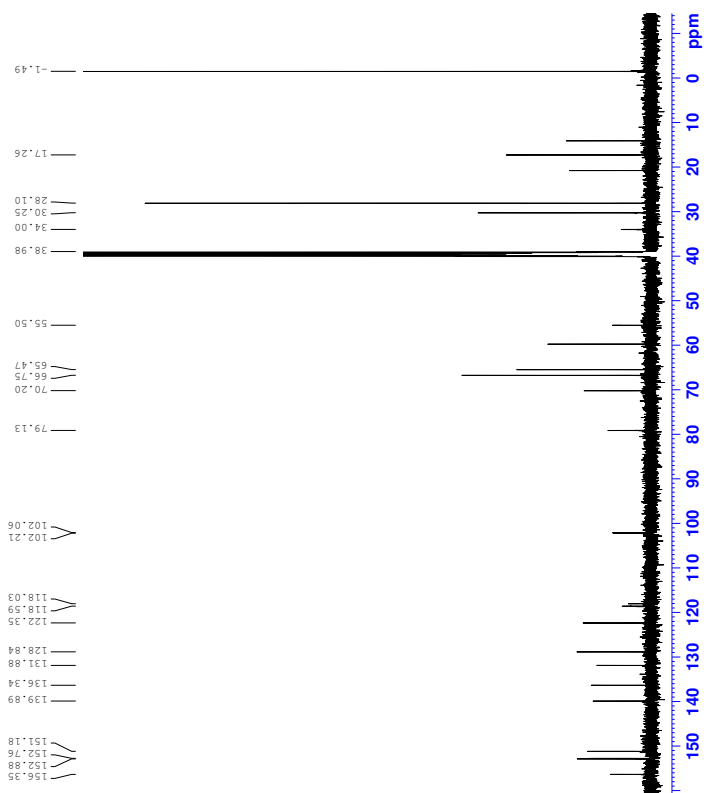
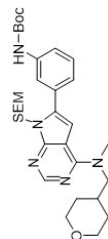


Figure H.2: ^{13}C NMR spectrum of compound 9

Elemental Composition Report

Page 1

Single Mass Analysis

Tolerance = 2.0 PPM / DBE: min = -10.0, max = 50.0

Element prediction: Off

Number of isotope peaks used for i-FIT = 6

Monoisotopic Mass, Even Electron Ions

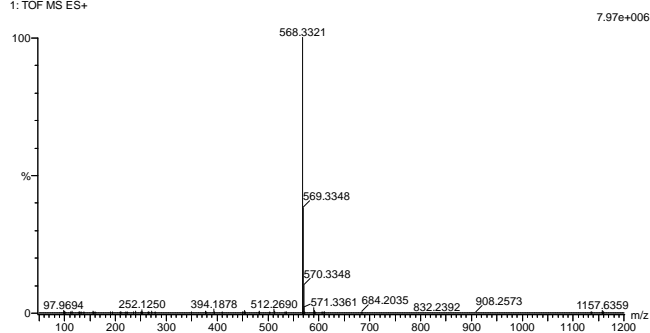
2781 formula(e) evaluated with 3 results within limits (all results (up to 1000) for each mass)

Elements Used:

C: 0-100 H: 0-100 N: 0-9 O: 0-5 Na: 0-1 Si: 0-2

2021-01-04 (0.722) AM2 (Ar:35000.0,0.00,0.00); Cm (63.69)

1: TOF MS ES+



Minimum:

Maximum: 5.0 2.0 -10.0

Mass	Calc. Mass	mDa	PPM	DBE	i-FIT	Norm	Conf (%)	Formula
568.3321	568.3319	0.2	0.4	11.5	1763.8	0.000	100.00	C30 H46 N5 O4
								Si
								C24 H51 N5 O5 Na
								Si2
								C39 H42 N3 O

Figure H.6: MS spectrum of compound 9

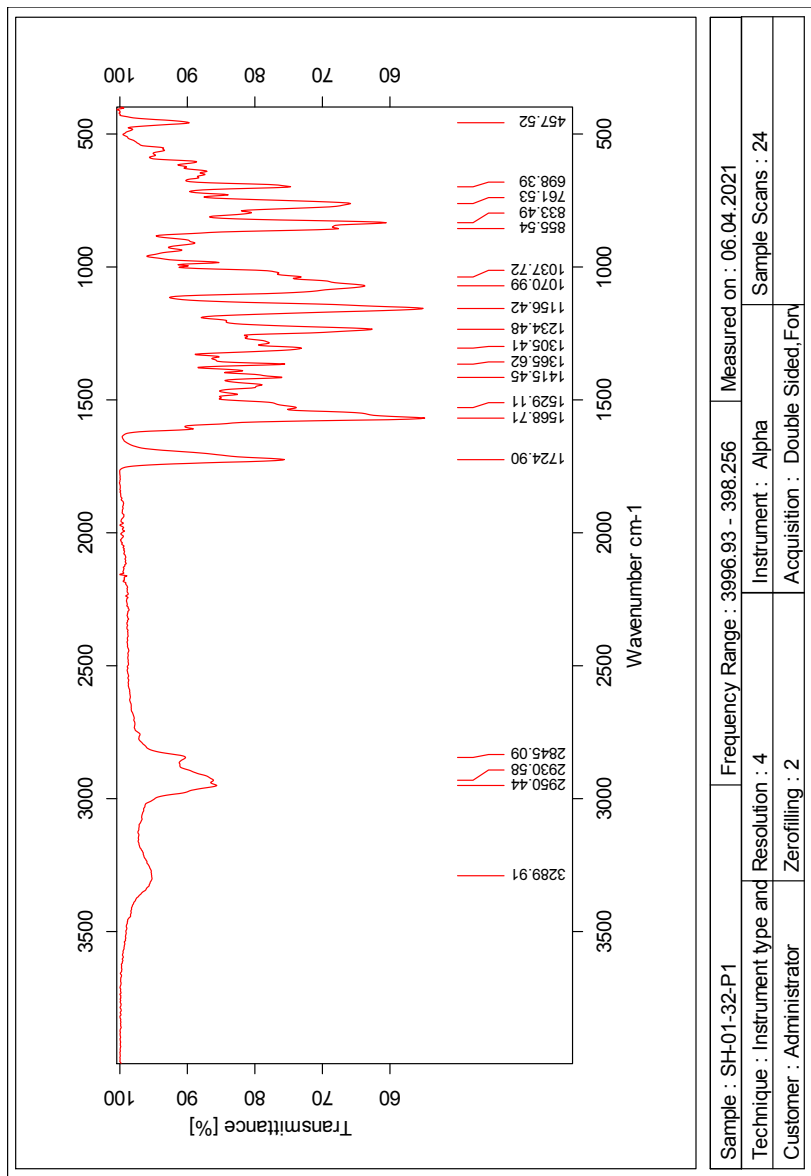


Figure H.7: IR spectrum of compound **9**

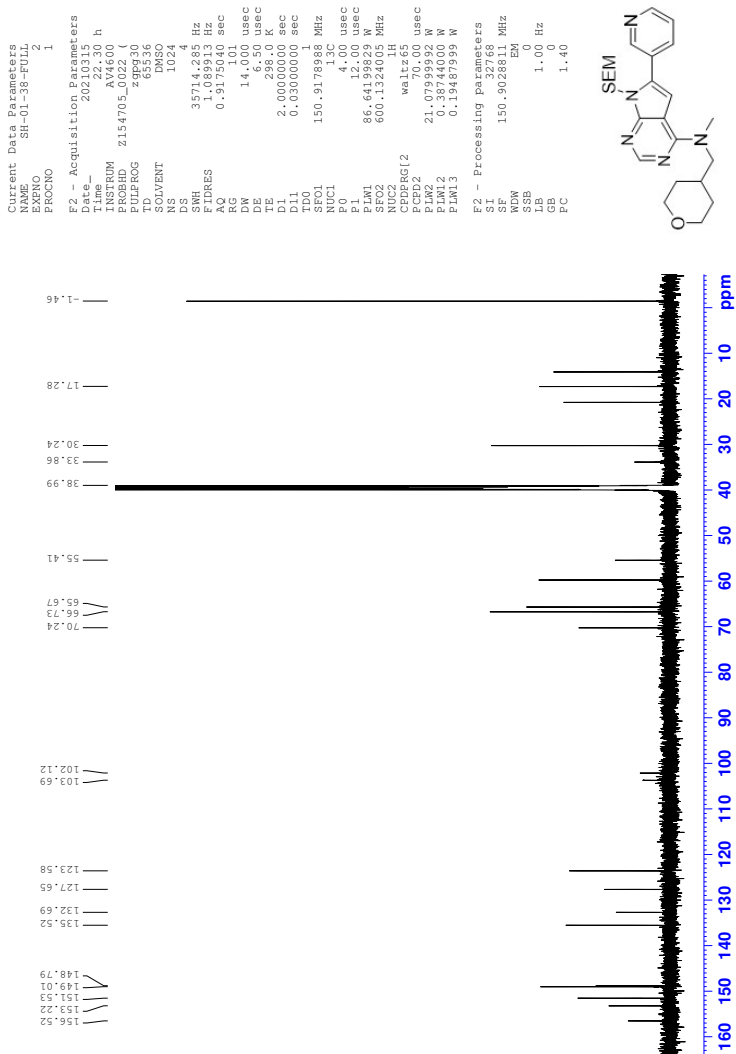


Figure I.2: ^{13}C NMR spectrum of compound 10

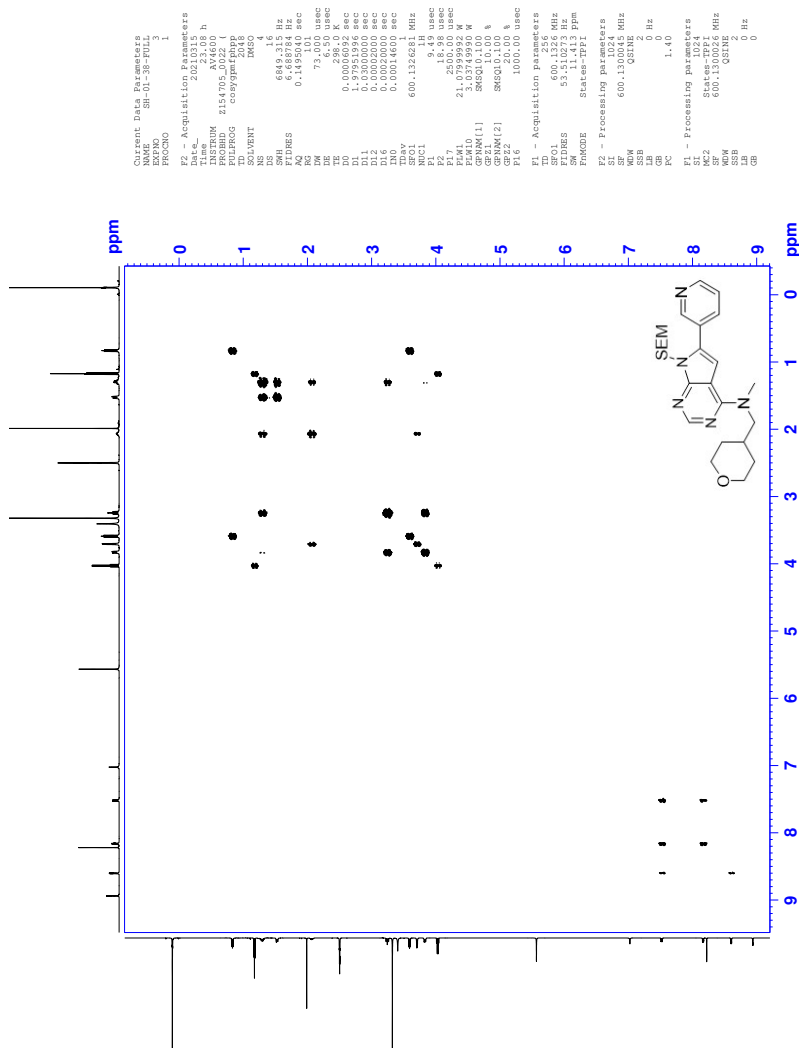


Figure I.3: COSY spectrum of compound 10

Elemental Composition Report

Page 1

Single Mass Analysis

Tolerance = 2.0 PPM / DBE: min = -10.0, max = 50.0

Element prediction: Off

Number of isotope peaks used for i-FIT = 6

Monoisotopic Mass, Even Electron Ions

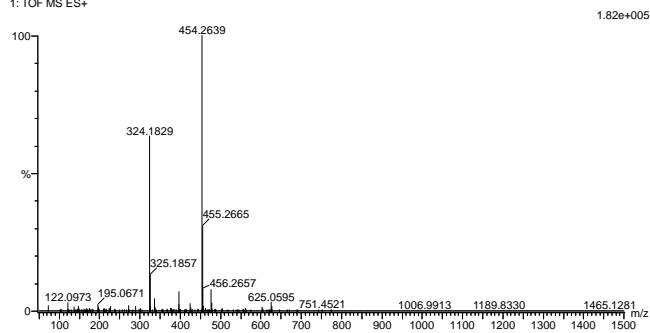
1396 formula(e) evaluated with 1 results within limits (all results (up to 1000) for each mass)

Elements Used:

C: 0-100 H: 0-100 N: 0-8 O: 0-12 Si: 0-1

2021_125_116 (1.093) AM2 (Ar:35000.0,0.00,0.00); Cm (114:116)

1: TOF MS ES+



Minimum:

Maximum: 5.0 2.0 -10.0 50.0

Mass	Calc. Mass	mDa	PPM	DBE	i-FIT	Norm	Conf (%)	Formula
454.2639	454.2638	0.1	0.2	10.5	1298.4	n/a	n/a	C24 H36 N5 O2 Si

Figure I.6: MS spectrum of compound 10

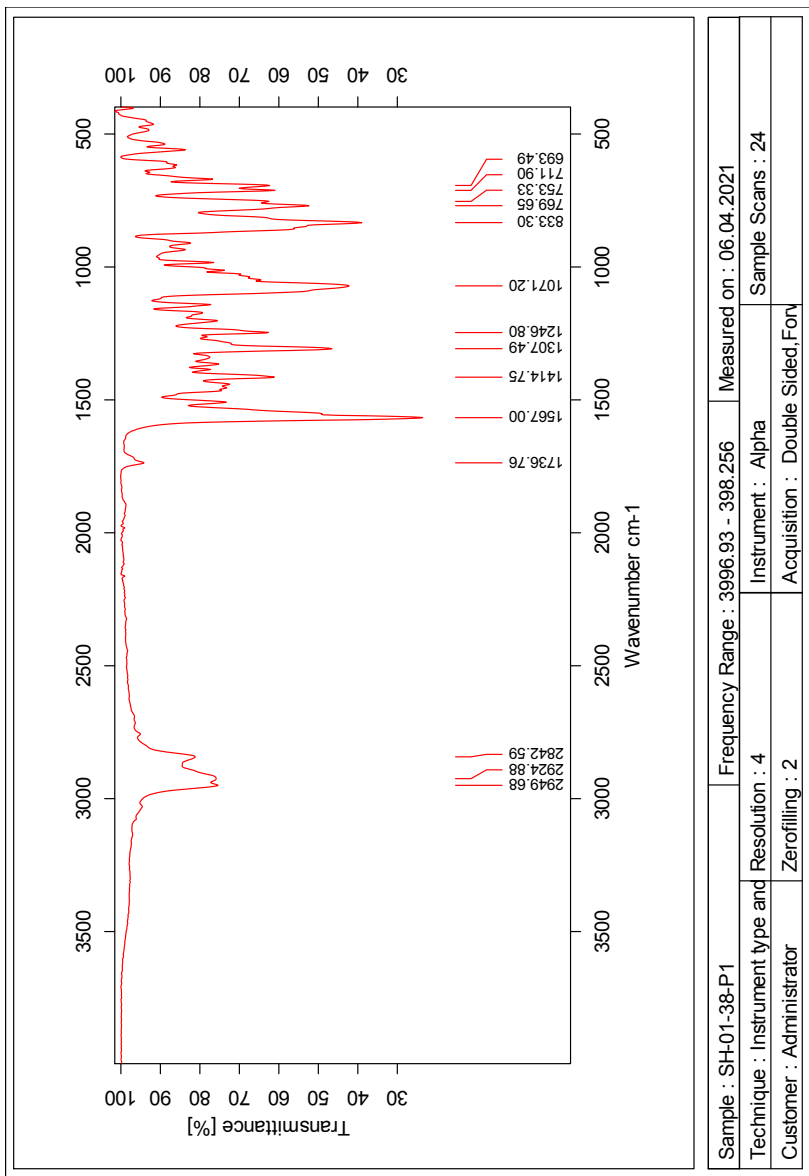


Figure I.7: IR spectrum of compound 10

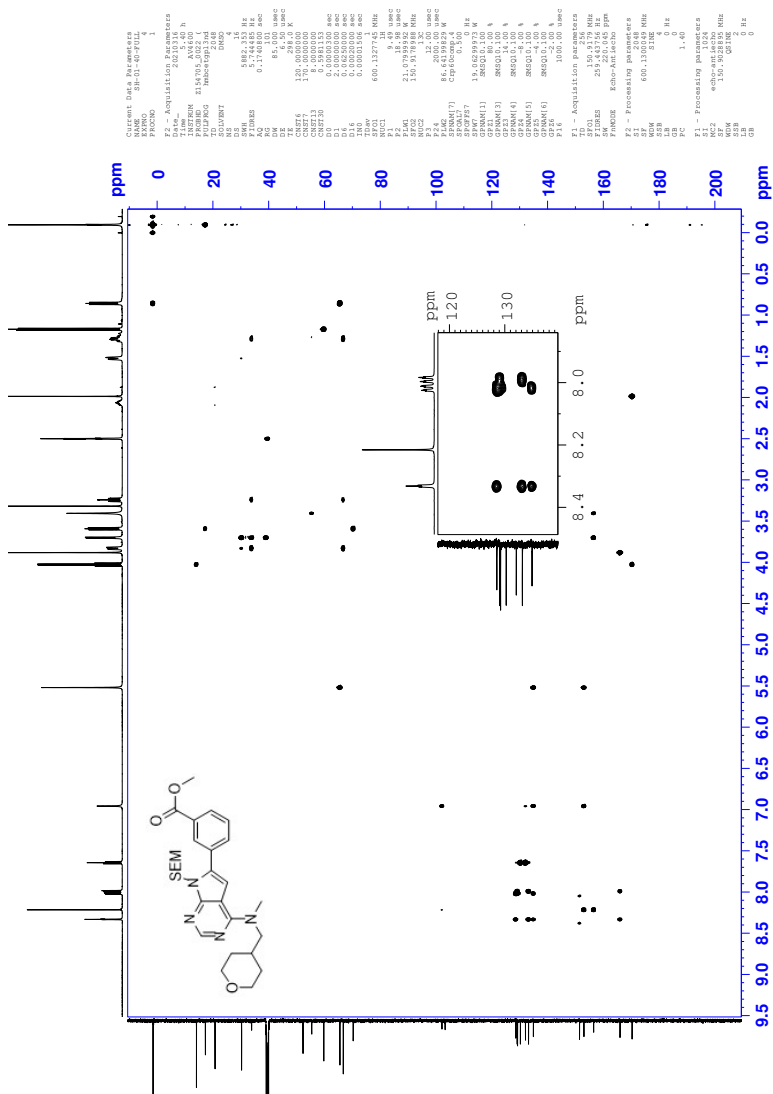


Figure J.5: HMBC spectrum of compound 11

Elemental Composition Report

Page 1

Single Mass Analysis

Tolerance = 2.0 PPM / DBE: min = -10.0, max = 50.0

Element prediction: Off

Number of isotope peaks used for i-FIT = 6

Monoisotopic Mass, Even Electron Ions

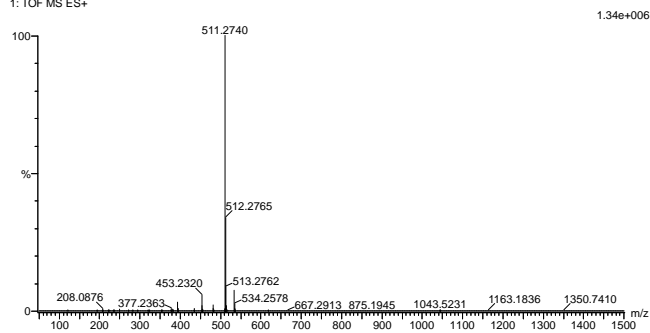
1582 formula(e) evaluated with 2 results within limits (all results (up to 1000) for each mass)

Elements Used:

C: 0-100 H: 0-100 N: 0-8 O: 0-12 Si: 0-1

2021_127_102 (0.963) AM2 (Ar:35000.0,0.00,0.00); Cm (102:105)

1: TOF MS ES+



Minimum:

Maximum: 5.0 2.0 -10.0

50.0

Mass	Calc. Mass	mDa	PPM	DBE	i-FIT	Norm	Conf (%)	Formula
511.2740	511.2741	-0.1	-0.2	11.5	1627.7	0.000	100.00	C27 H39 N4 O4
	511.2749	-0.9	-1.8	20.5	1648.1	20.392	0.00	Si C36 H35 N2 O

Figure J.6: MS spectrum of compound 11

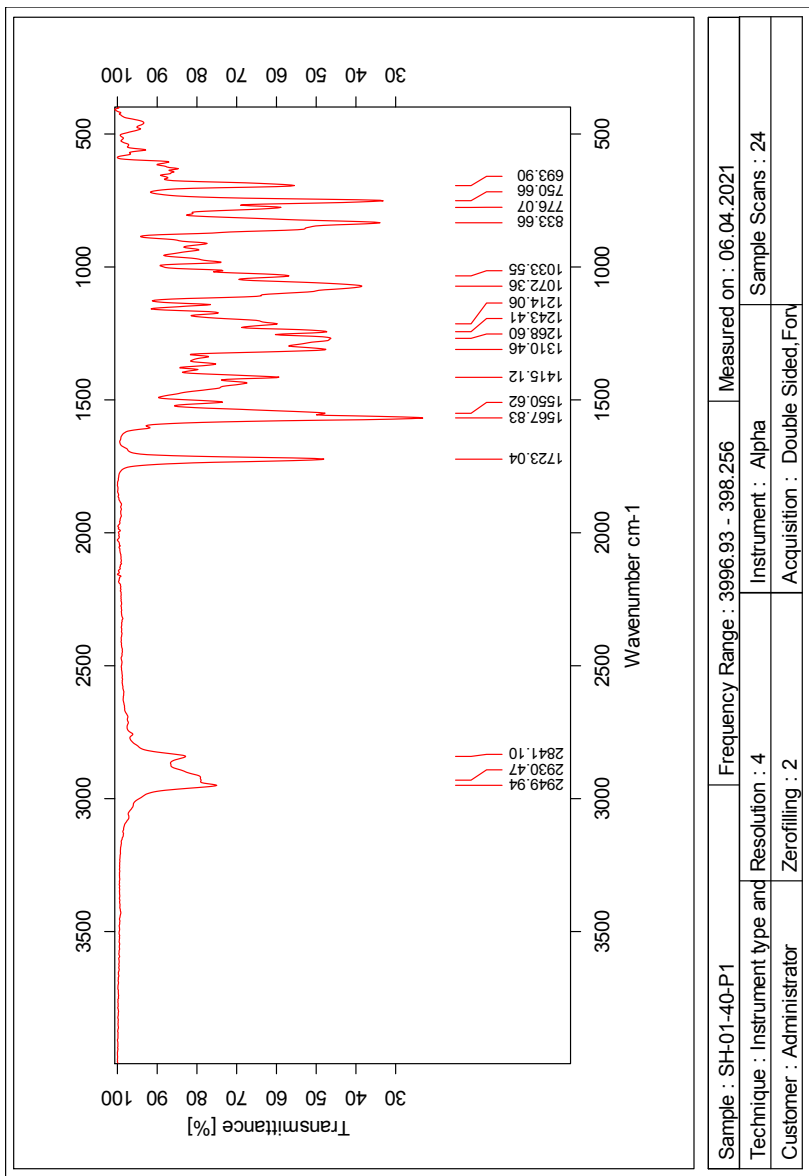
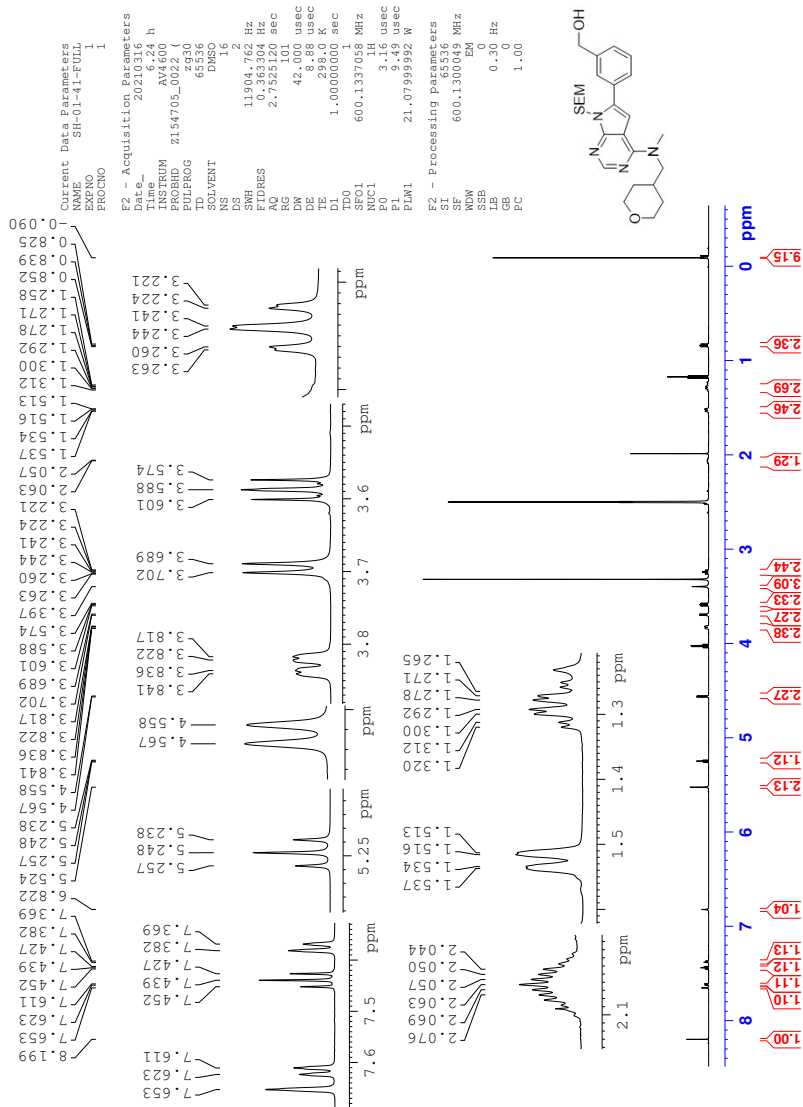


Figure J.7: IR spectrum of compound 11

K Spectroscopic data for Compound 12

Figure K.1: ^1H NMR spectrum of compound 12

```

Current Data Parameters
Name      SH-01-F1-FU12
EXPNO    1
PROCNO   1
F2 - Acquisition Parameters
Date_    20210316
Time     7.16 h
INSTRUM  AV4600
PULPROG  zgpg30
NUC1      13
TD        65536
SOLVENT  DMSO
NS        1024
DS        4
SWH       35714.285 Hz
FIDRES    1.08913 Hz
AQ         0.9175040 sec
RG         14.000 usec
DE         6.50 usec
TE         298.0 K
D1         2.0000000 sec
d11        0.0300000 sec
TD0        1
SFO1      150.9178988 MHz
NUC1      13C
NUC2      13C
P1         12.00 usec
PL1        86.64199629 W
SFO2      600.1324005 MHz
NUC2      1H
PCPDG12   waltz16
PLW2      21.07999992 W
PLW1      0.38744000 W
PLW3      0.19367999 W
F2 - Processing parameters
SI         32768
SF         150.9028912 MHz
WDW        EM
SSB        0
LB         1.00 Hz
GB         0
FC         1.40

```

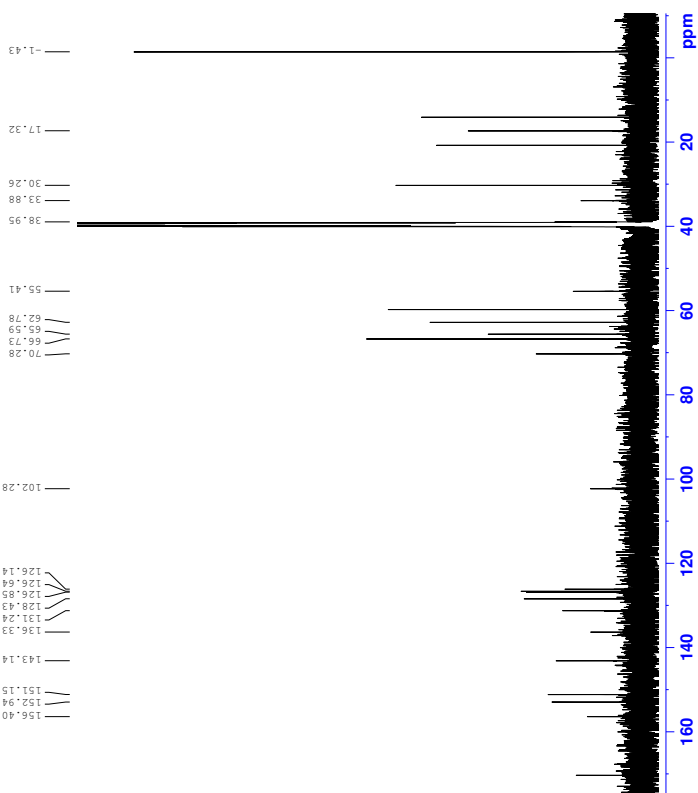


Figure K.2: ^{13}C NMR spectrum of compound 12

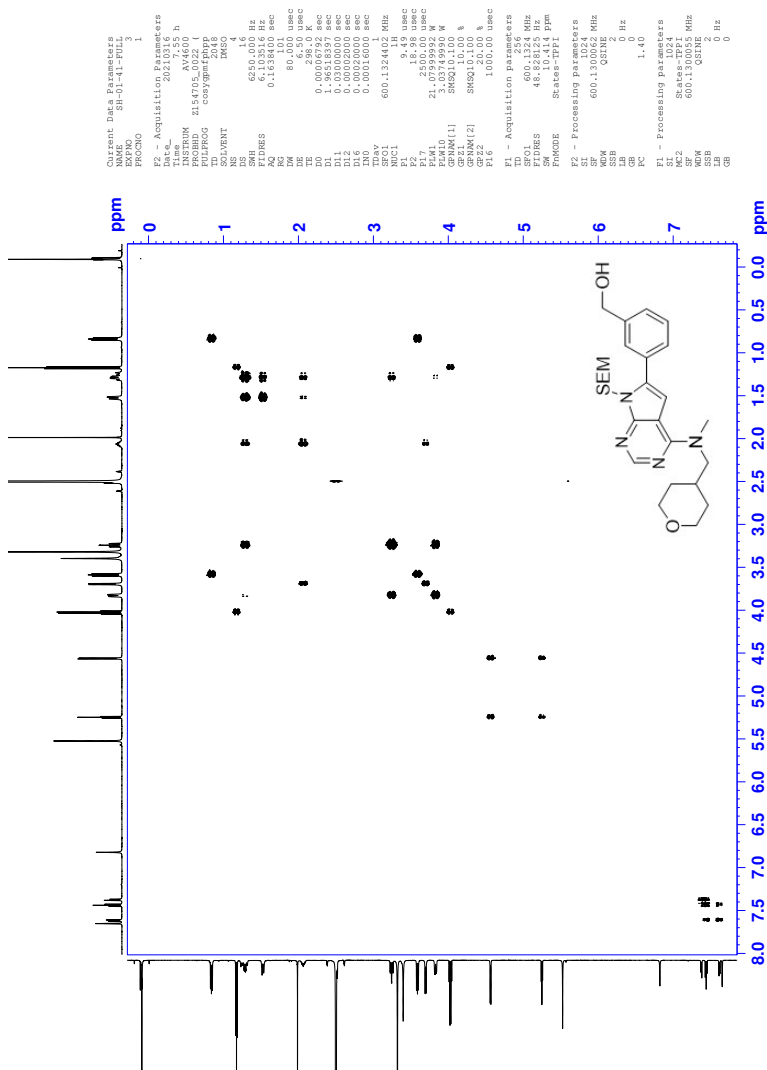


Figure K.3: COSY spectrum of compound 12

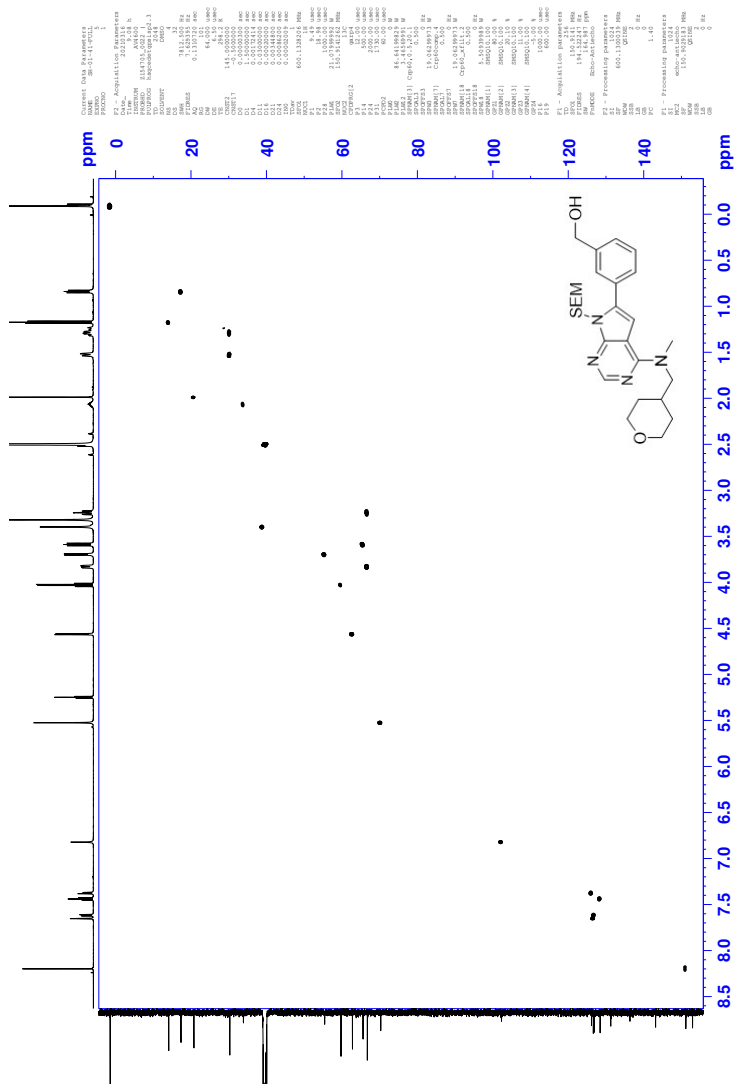


Figure K.4: HSQC spectrum of compound 12

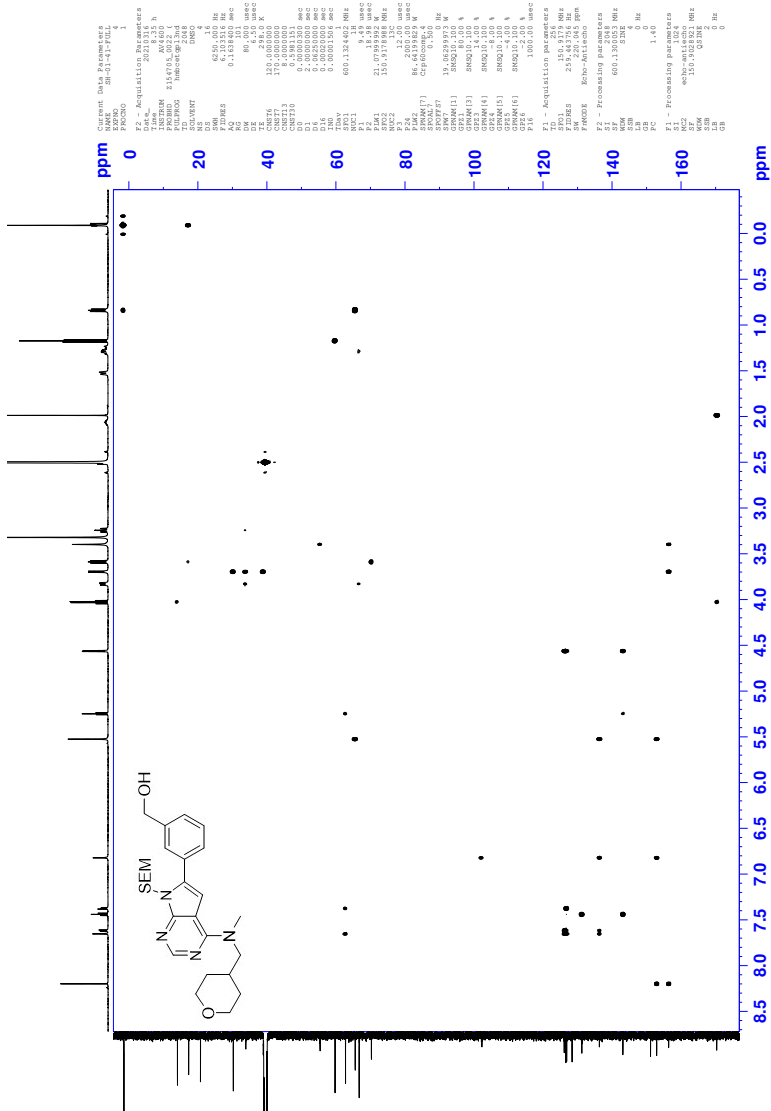


Figure K.5: HMBC spectrum of compound 12

Elemental Composition Report

Page 1

Single Mass Analysis

Tolerance = 2.0 PPM / DBE: min = -10.0, max = 50.0

Element prediction: Off

Number of isotope peaks used for i-FIT = 6

Monoisotopic Mass, Even Electron Ions

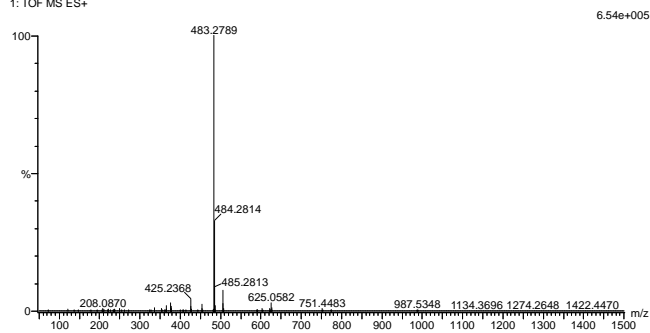
1504 formula(e) evaluated with 1 results within limits (all results (up to 1000) for each mass)

Elements Used:

C: 0-100 H: 0-100 N: 0-8 O: 0-12 Si: 0-1

2021_128_112 (1.058) AM2 (Ar:35000.0,0.00,0.00); Cm (111:113)

1: TOF MS ES+



Minimum:

Maximum: 5.0 2.0 -10.0

50.0

Mass	Calc. Mass	mDa	PPM	DBE	i-FIT	Norm	Conf (%)	Formula
------	------------	-----	-----	-----	-------	------	----------	---------

483.2789	483.2791	-0.2	-0.4	10.5	1450.6	n/a	n/a	C26 H39 N4 O3 Si
----------	----------	------	------	------	--------	-----	-----	---------------------

Figure K.6: MS spectrum of compound 12

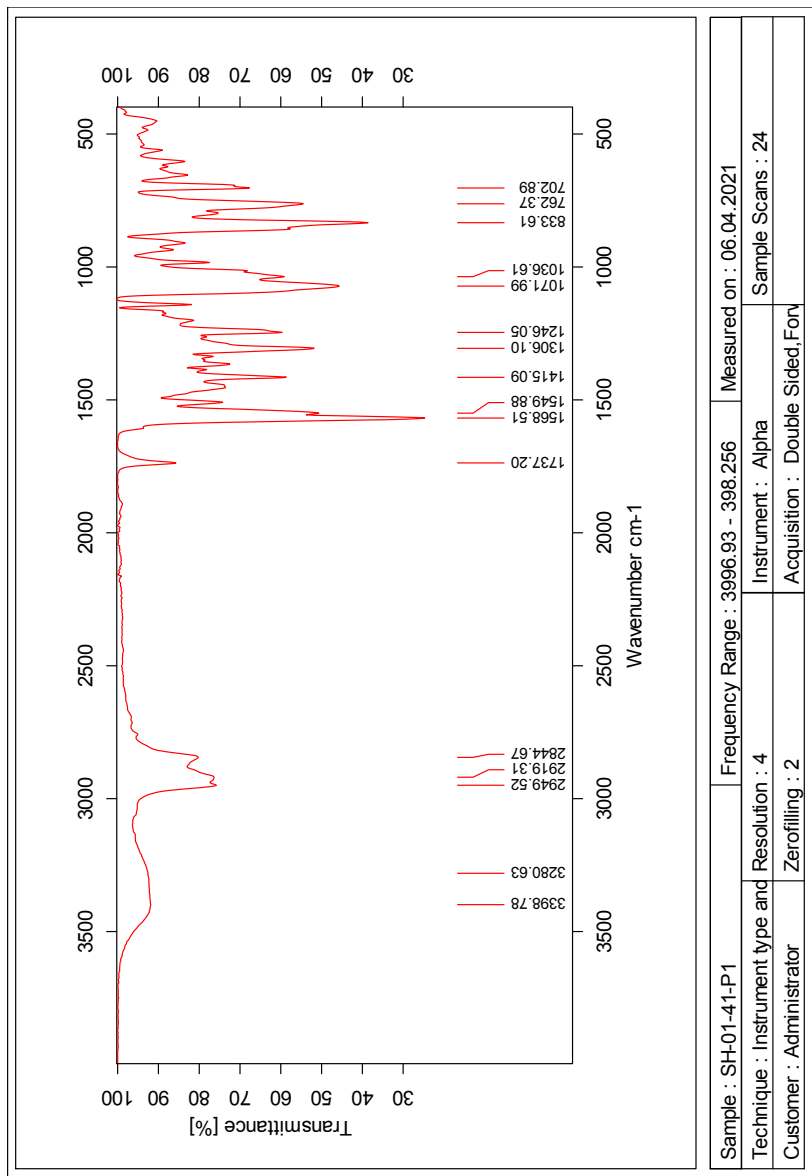


Figure K.7: IR spectrum of compound 12

L Spectroscopic data for Compound 13

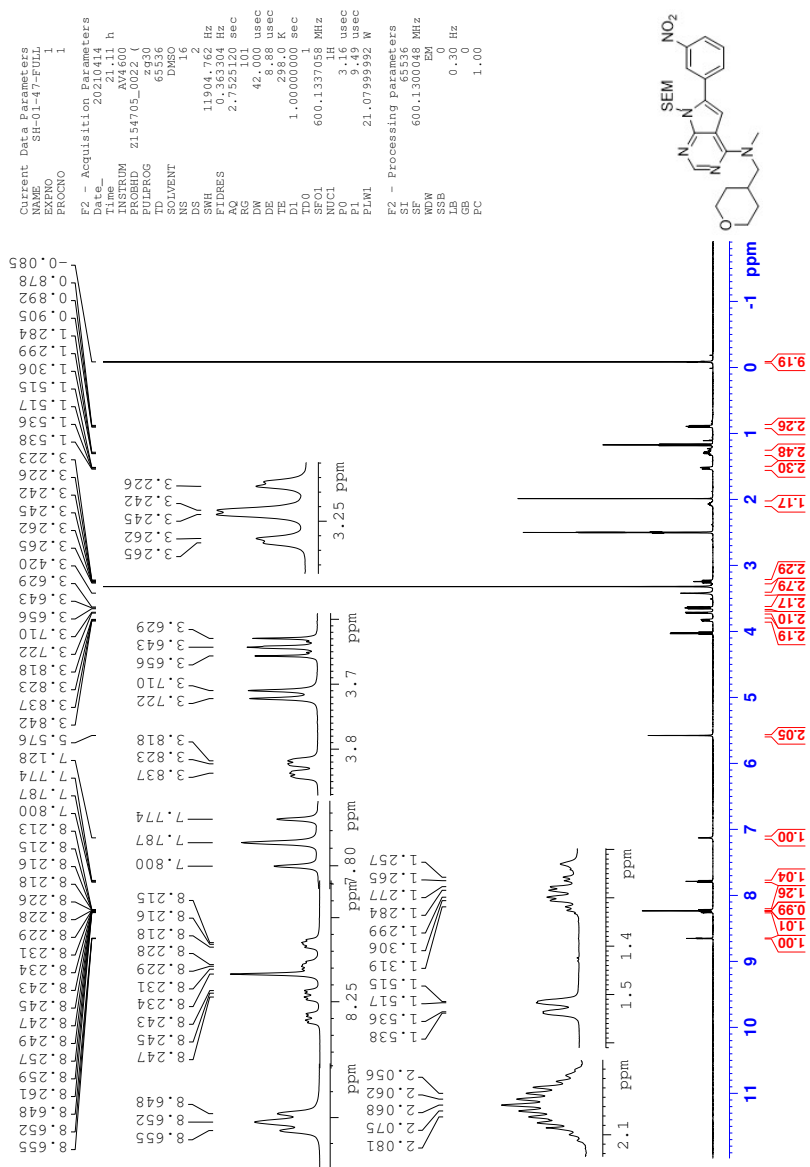
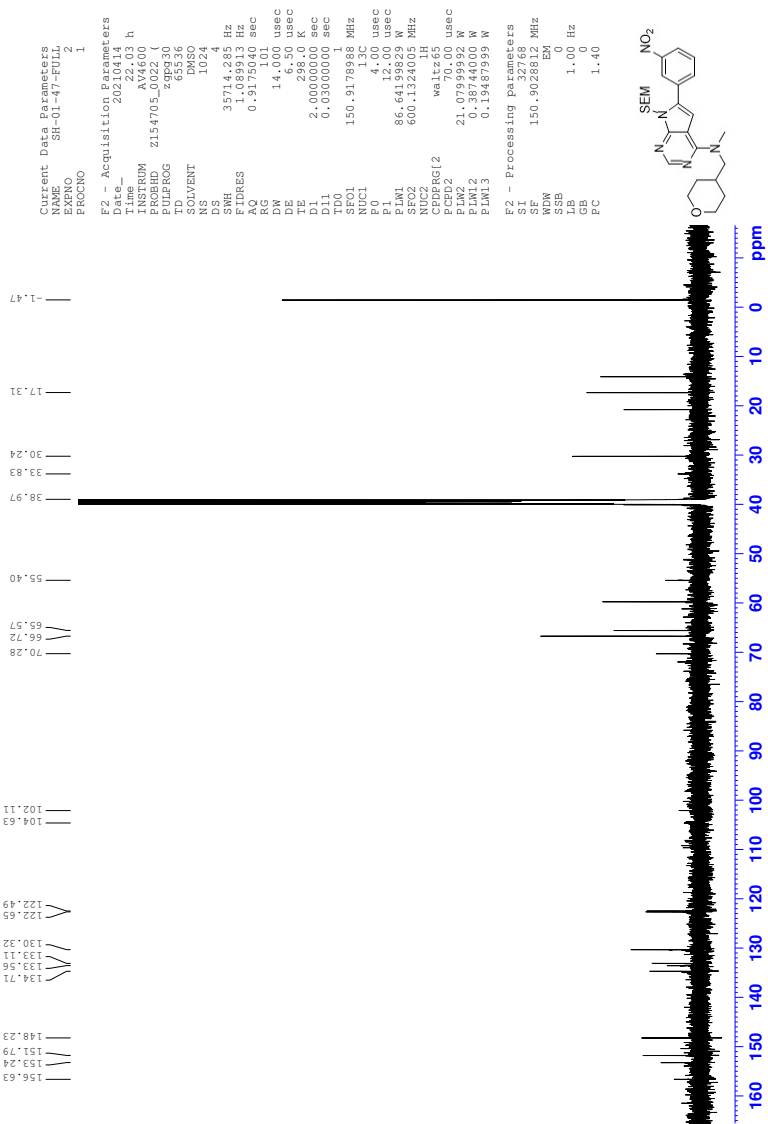


Figure L.1: ^1H NMR spectrum of compound 13

Figure L.2: ^{13}C NMR spectrum of compound 13

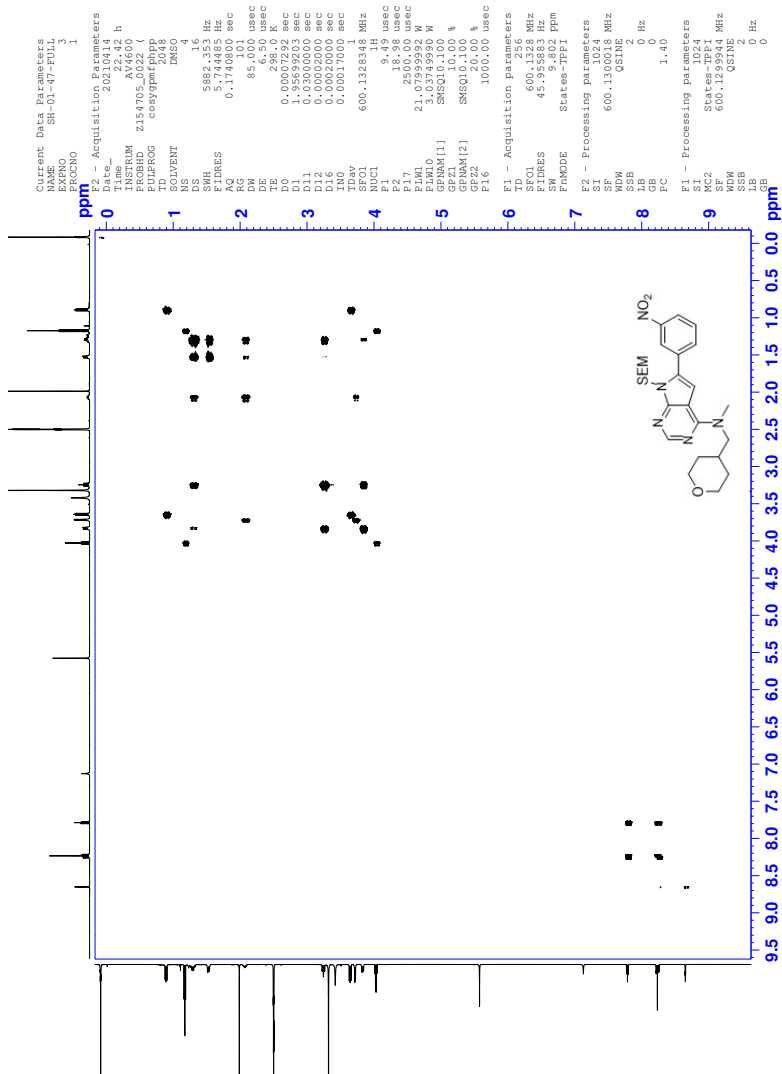


Figure L.3: COSY spectrum of compound 13

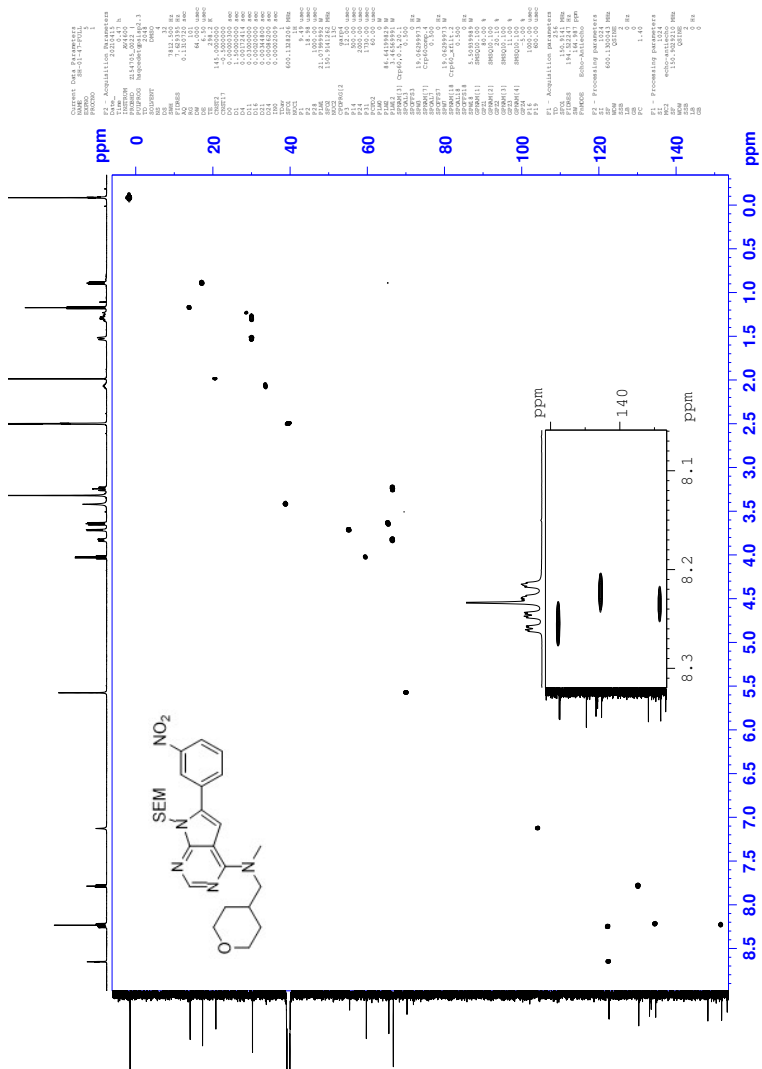
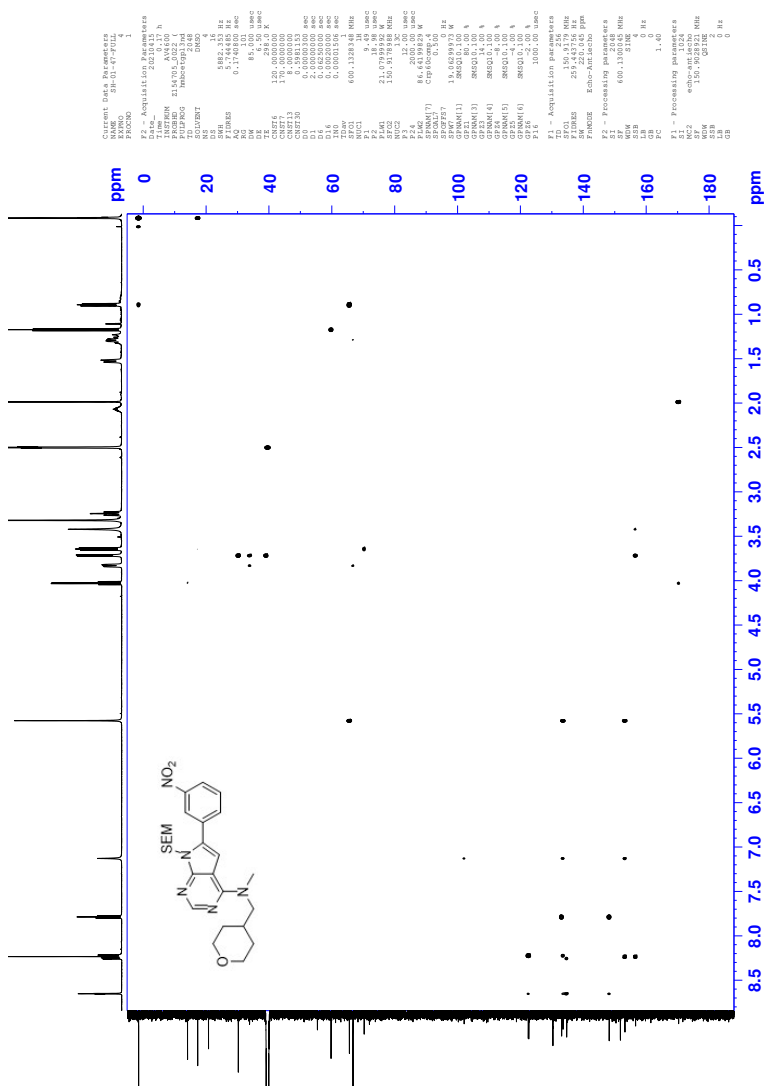


Figure L.4: HSQC spectrum of compound 13



Elemental Composition Report

Page 1

Single Mass Analysis

Tolerance = 2.0 PPM / DBE: min = -10.0, max = 50.0

Element prediction: Off

Number of isotope peaks used for i-FIT = 6

Monoisotopic Mass, Even Electron Ions

1858 formula(e) evaluated with 2 results within limits (all results (up to 1000) for each mass)

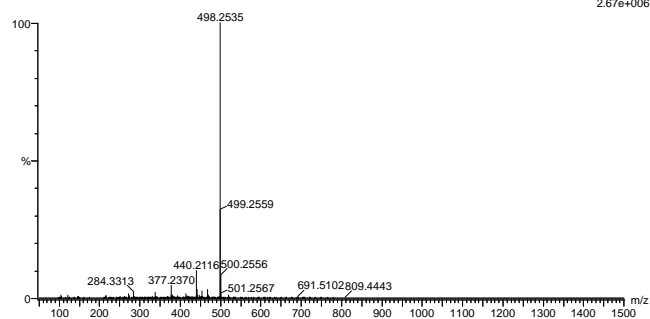
Elements Used:

C: 0-100 H: 0-100 N: 0-12 O: 0-10 Si: 0-1

2021, 237, 117 (1.109) AM2 (Ar:35000.0,0.00,0.00); Cm (107:118)

1: TOF MS ES+

2.67e+006



Minimum: 5.0 2.0 -10.0

Maximum: 50.0

Mass	Calc. Mass	mDa	PPM	DBE	i-FIT	Norm	Conf (%)	Formula
498.2535	498.2537	-0.2	-0.4	11.5	2064.5	0.000	100.00	C25 H36 N5 O4
	498.2537	-0.2	-0.4	8.5	2084.3	19.835	0.00	Si C18 H32 N11 O6

Figure L.6: MS spectrum of compound 13

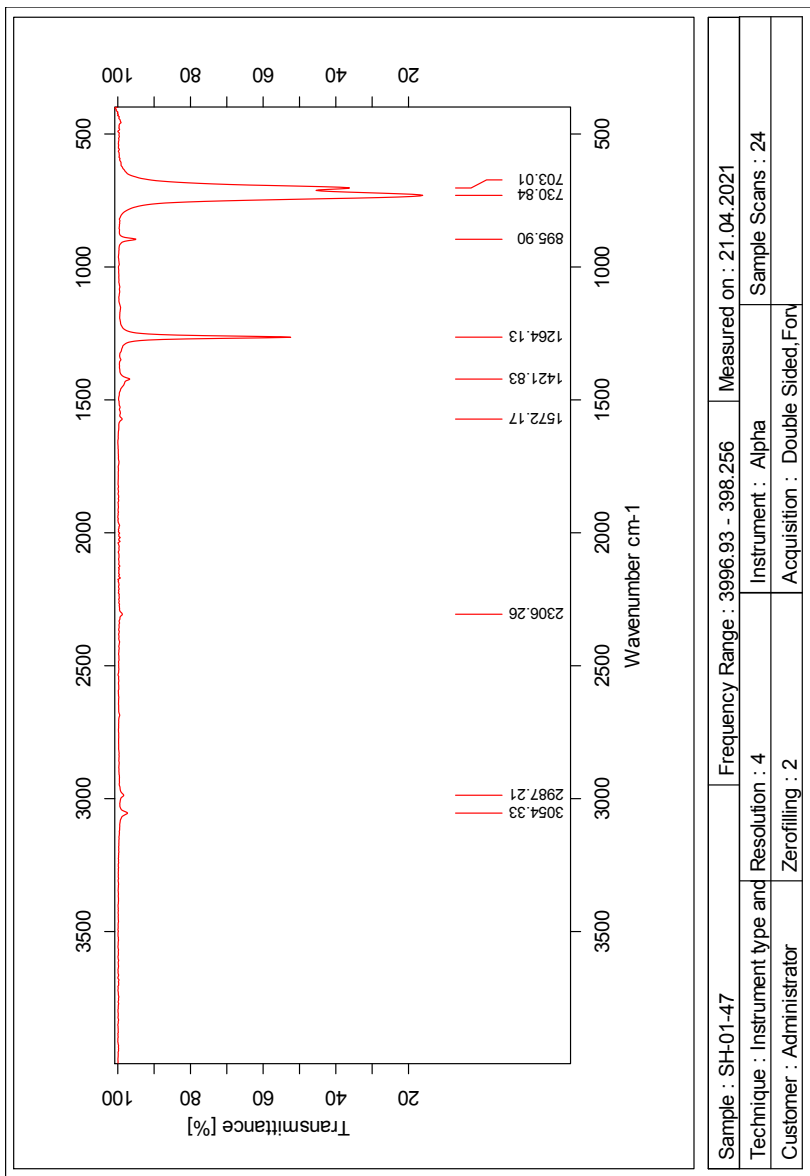


Figure L.7: IR spectrum of compound 13

Current Data Parameters
 NAME SH-01-17-FULL
 EXPNO 2
 PROCNO 1
 F2 - Acquisition Parameters
 Date_ 20201029
 Time 16.19 h
 RunDate 16.00
 PROBNM Z154705-0025
 PULPROG zgpg30
 TD 65536
 SOLVENT DMSO
 DS 2044
 SNH 35714.285 Hz
 FIDRES 1.089913 Hz
 RG 3100
 AC 100
 DW 14.000 usec
 DE 6.50 usec
 TE 300.2 K
 D1 2.000000 sec
 D11 0.0300000 sec
 TD0 1
 SFO1 150.9178988 MHz
 SFO2 150.9178988 MHz
 P0 4.00 usec
 P1 4.00 usec
 PL1 12.00 usec
 PLM1 86.64199829 N
 SFO3 600.1324005 MHz
 NUC2 13C
 NUC1 1H
 CPDPRG12 waltz65
 PCPD2 70.00 usec
 PLM2 21.07999992 N
 PLM3 1.50 usec
 PLM13 0.19487999 N
 F2 - Processing Parameters
 SF 150.9028642 MHz
 SFO 150.9028642 MHz
 EM 0
 WDW EM
 SSB 0
 GB 1.00 Hz
 PC 1.40

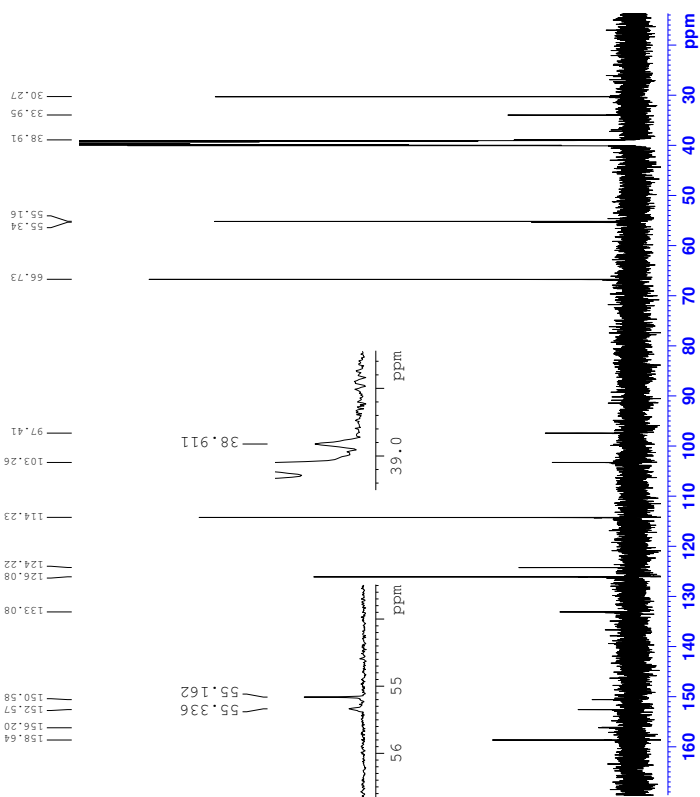
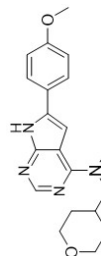


Figure M.2: ¹³C NMR spectrum of compound 14

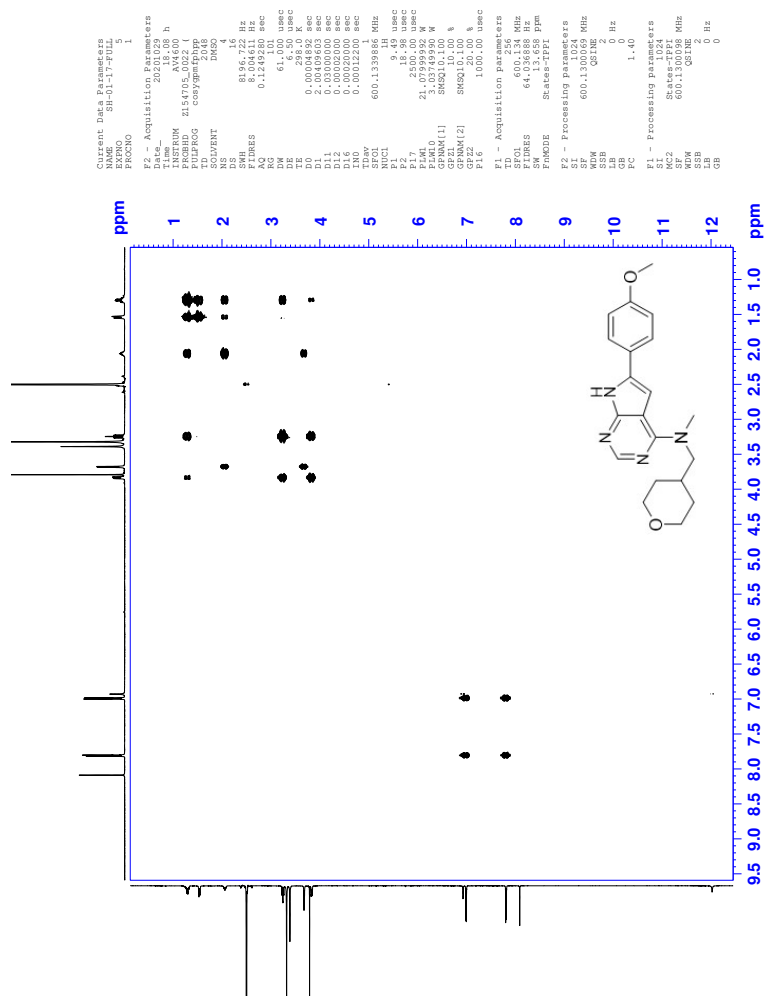


Figure M.3: COSY spectrum of compound (14)

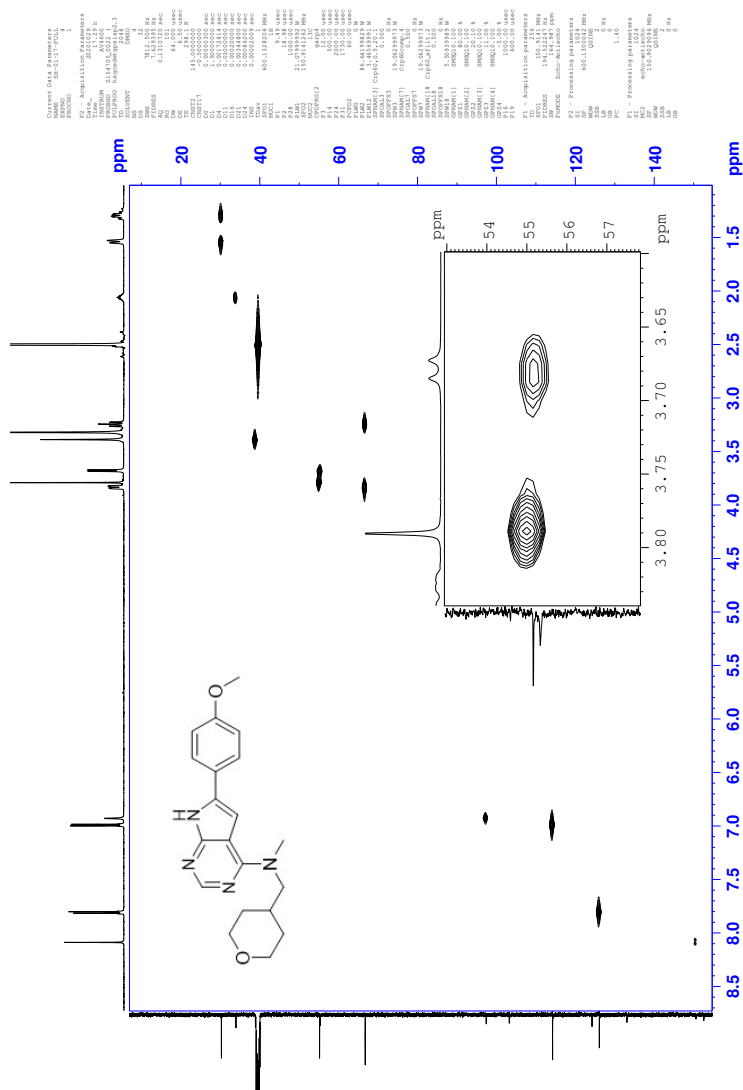


Figure M.4: HSQC spectrum of compound 14

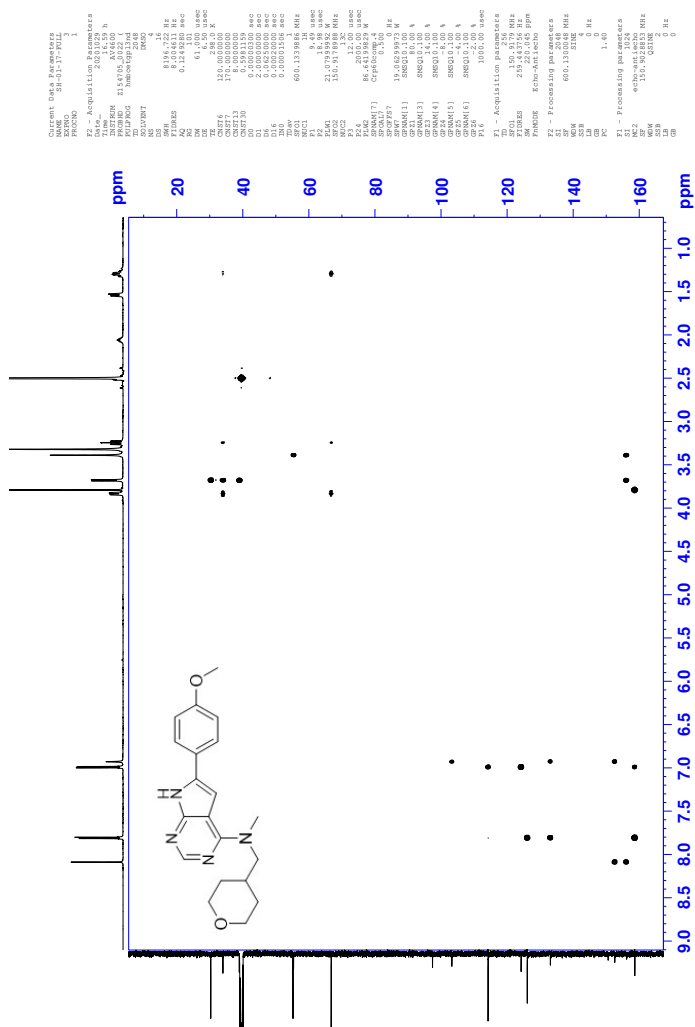


Figure M.5: HMBC spectrum of compound 14

Elemental Composition Report

Page 1

Single Mass Analysis

Tolerance = 2.0 PPM / DBE: min = -50.0, max = 100.0

Element prediction: Off

Number of isotope peaks used for i-FIT = 6

Monoisotopic Mass, Even Electron Ions

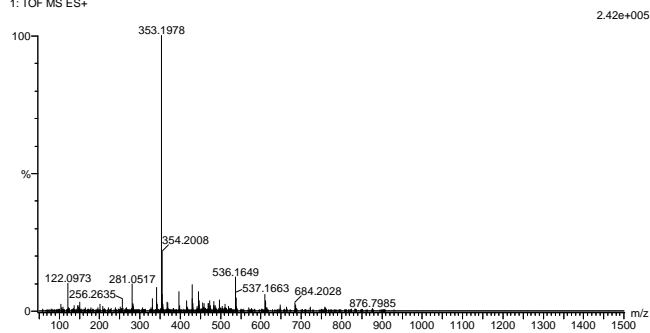
4124 formula(e) evaluated with 4 results within limits (all results (up to 1000) for each mass)

Elements Used:

C: 0-100 H: 0-100 N: 0-8 O: 0-8 Na: 0-1 Si: 0-2

2020_379.54 (0.517) AM2 (Ar:35000.0,0.00,0.00); Cm (49:54)

1: TOF MS ES+



Minimum: -50.0

Maximum: 5.0 2.0 100.0

Mass	Calc. Mass	mDa	PPM	DBE	i-FIT	Norm	Conf (%)	Formula
353.1978	353.1978	0.0	0.0	10.5	1816.1	0.000	100.00	C20 H25 N4 O2
	353.1976	0.2	0.6	-6.5	1841.7	25.664	0.00	C5 H34 N6 O6 Na
	353.1971	0.7	2.0	-2.5	1835.1	19.010	0.00	Si2
	353.1985	-0.7	-2.0	2.5	1834.4	18.370	0.00	C13 H34 O7 Na
								Si
								C14 H30 N4 O3 Na
								Si

Figure M.6: MS spectrum of compound 14

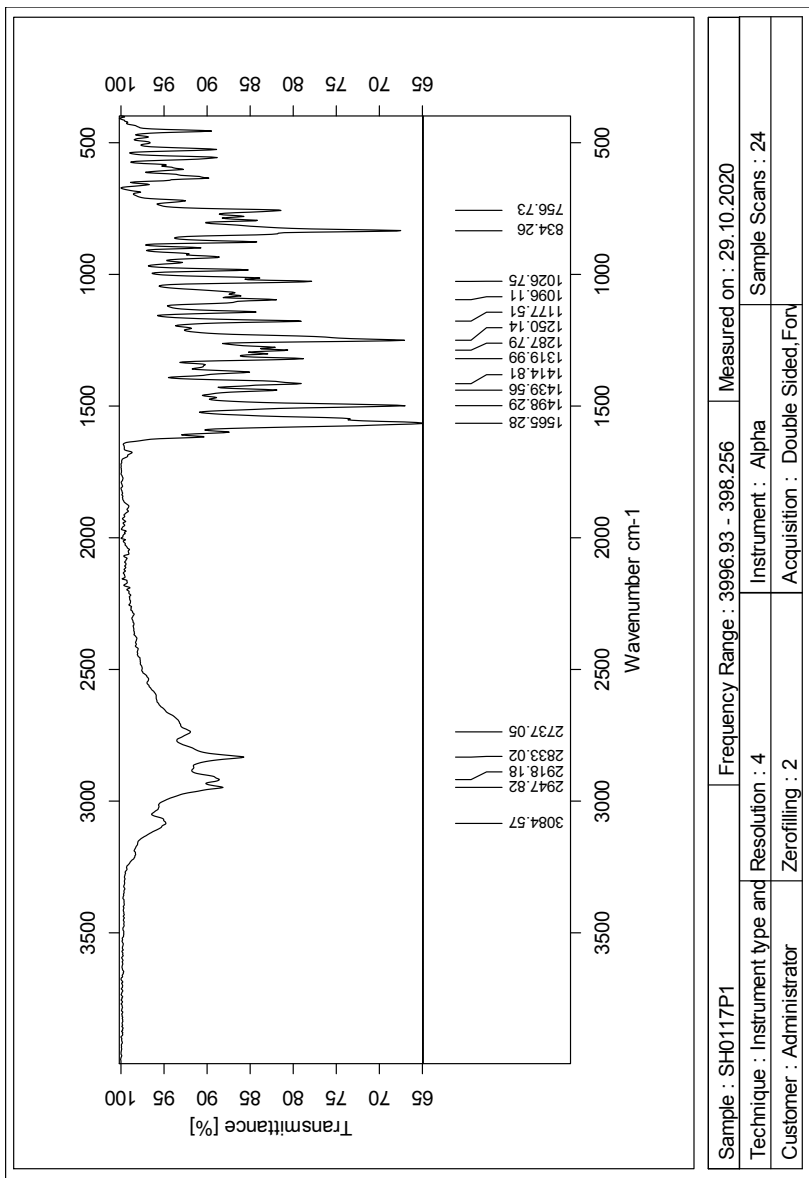
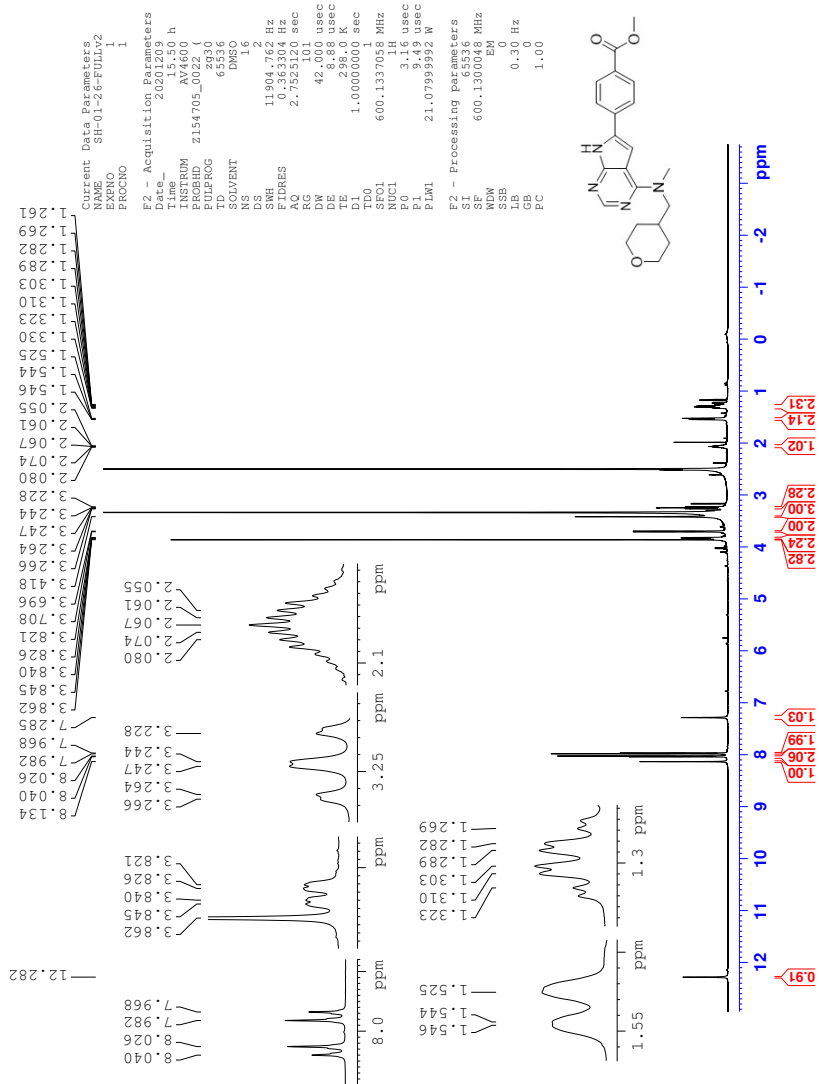
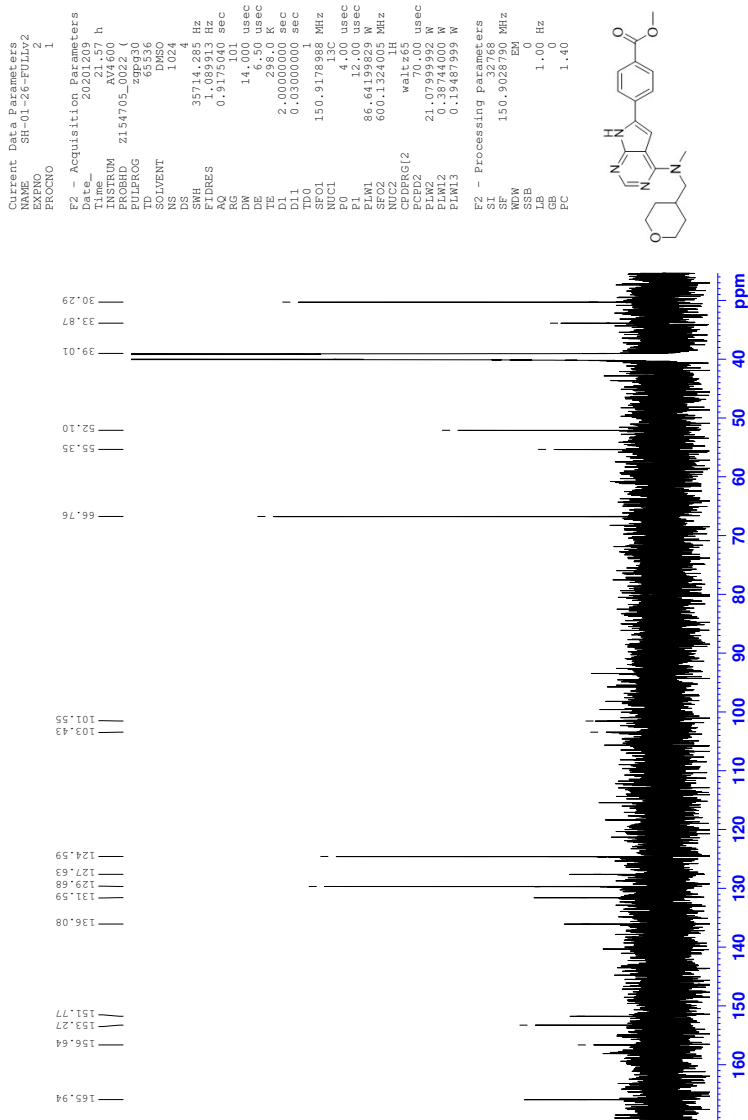


Figure M.7: IR spectrum of compound 14

N Spectroscopic data for Compound 15

Figure N.1: ^1H NMR spectrum of compound 15

Figure N.2: ^{13}C NMR spectrum of compound 15

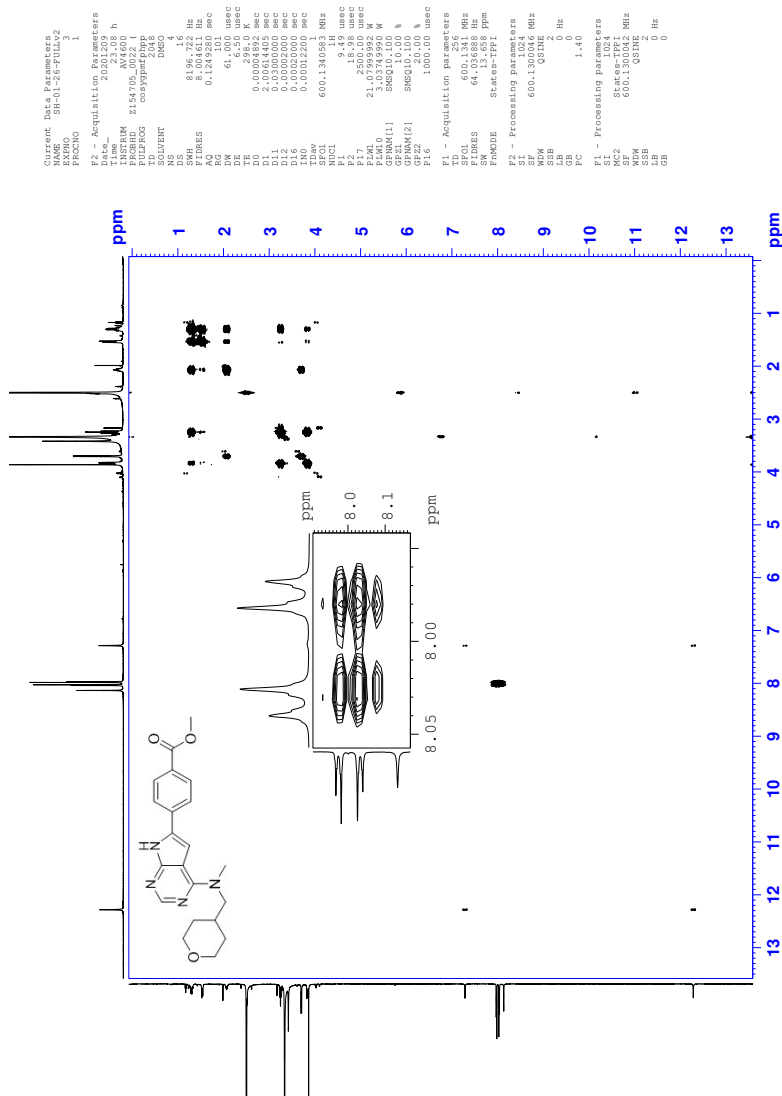


Figure N.3: COSY spectrum of compound 15

Elemental Composition Report

Page 1

Single Mass Analysis

Tolerance = 2.0 PPM / DBE: min = -10.0, max = 50.0

Element prediction: Off

Number of isotope peaks used for i-FIT = 3

Monoisotopic Mass, Even Electron Ions

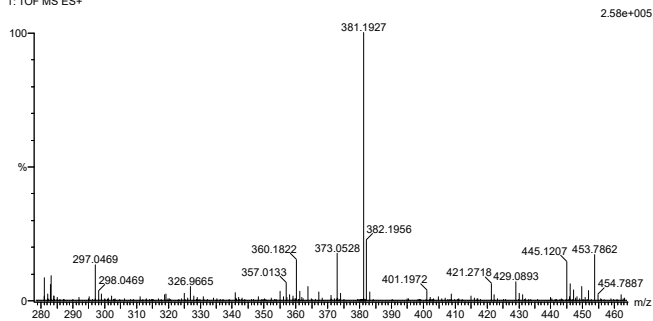
582 formula(e) evaluated with 2 results within limits (up to 50 closest results for each mass)

Elements Used:

C: 0-500 H: 0-500 N: 0-5 O: 0-20

2020_457 56 (0.631) AM2 (Ar,35000.0,0.00,0.00); ABS; Cm (56:58)

1: TOF MS ES+



Minimum: -10.0
Maximum: 5.0 2.0 50.0

Mass	Calc. Mass	mDa	PPM	DBE	i-FIT	Norm	Conf (%)	Formula
381.1927	381.1927	0.0	0.0	11.5	657.2	0.000	100.00	C21 H25 N4 O3
	381.1932	-0.5	-1.3	-6.5	667.9	10.734	0.00	C8 H33 N2 O14

Figure N.6: MS spectrum of compound 15

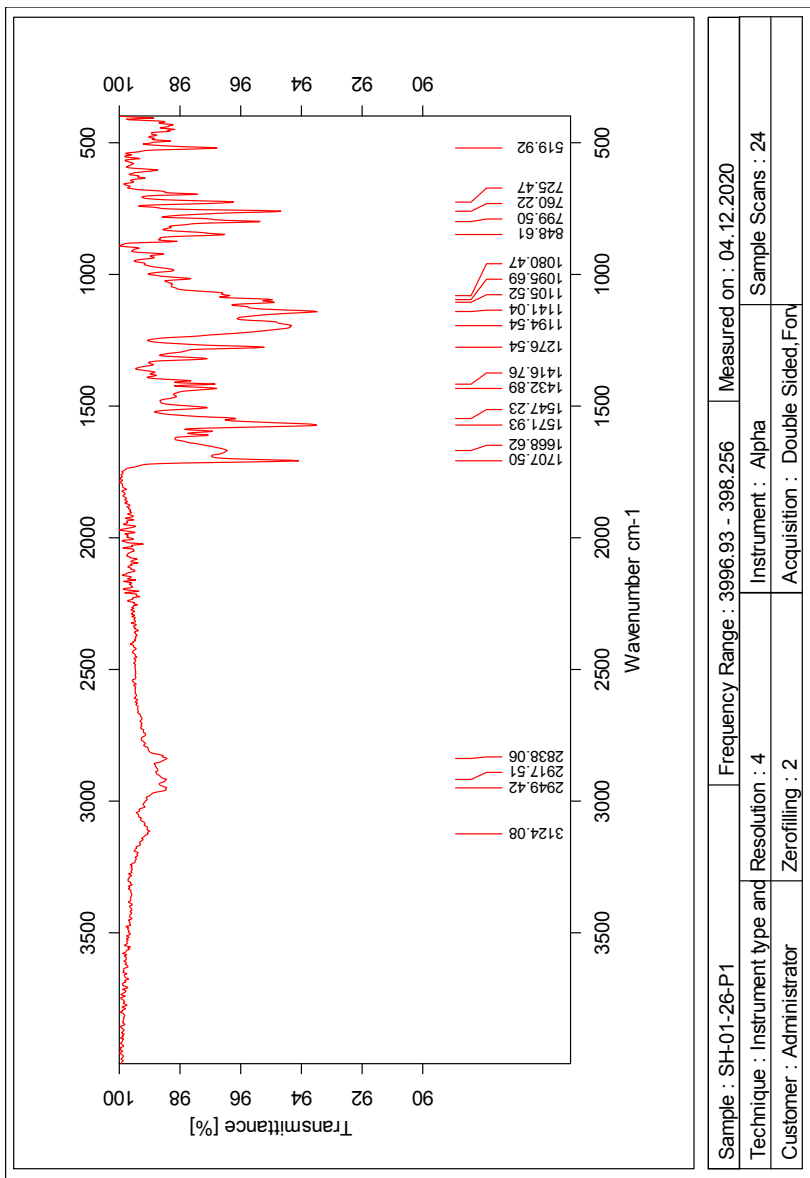
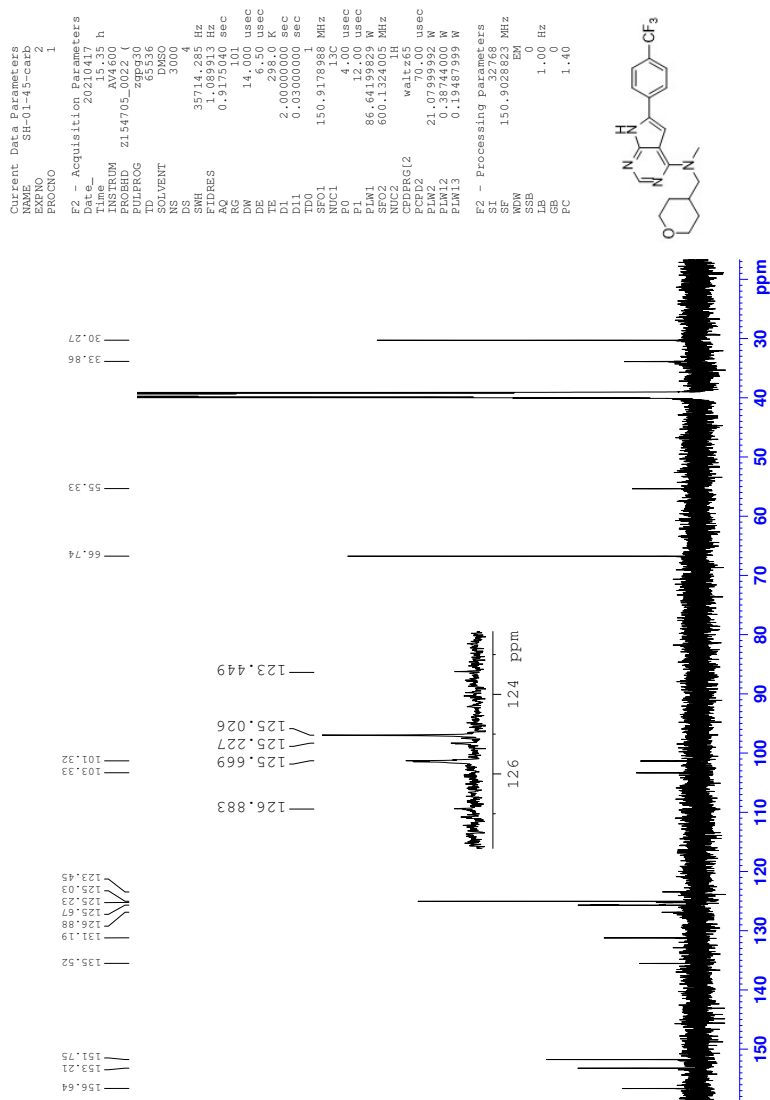


Figure N.7: IR spectrum of compound 15

Figure O.2: ^{13}C NMR spectrum of compound 16

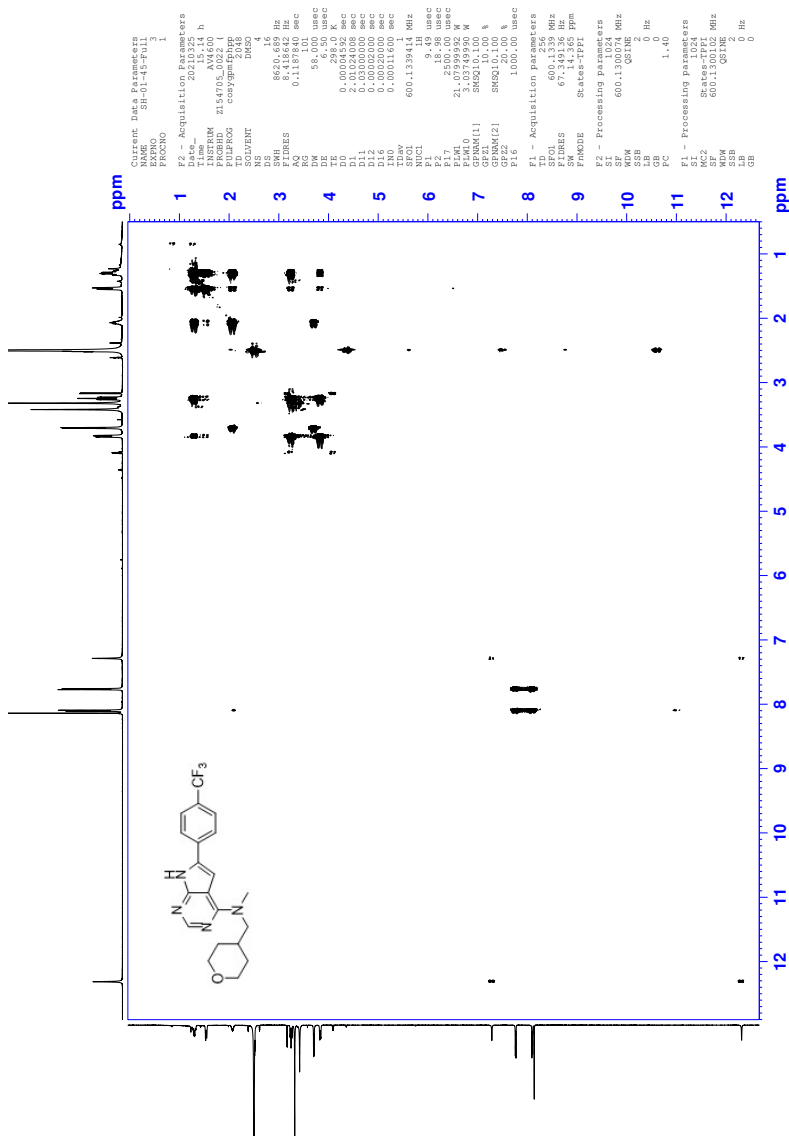


Figure O.3: COSY spectrum of compound 16

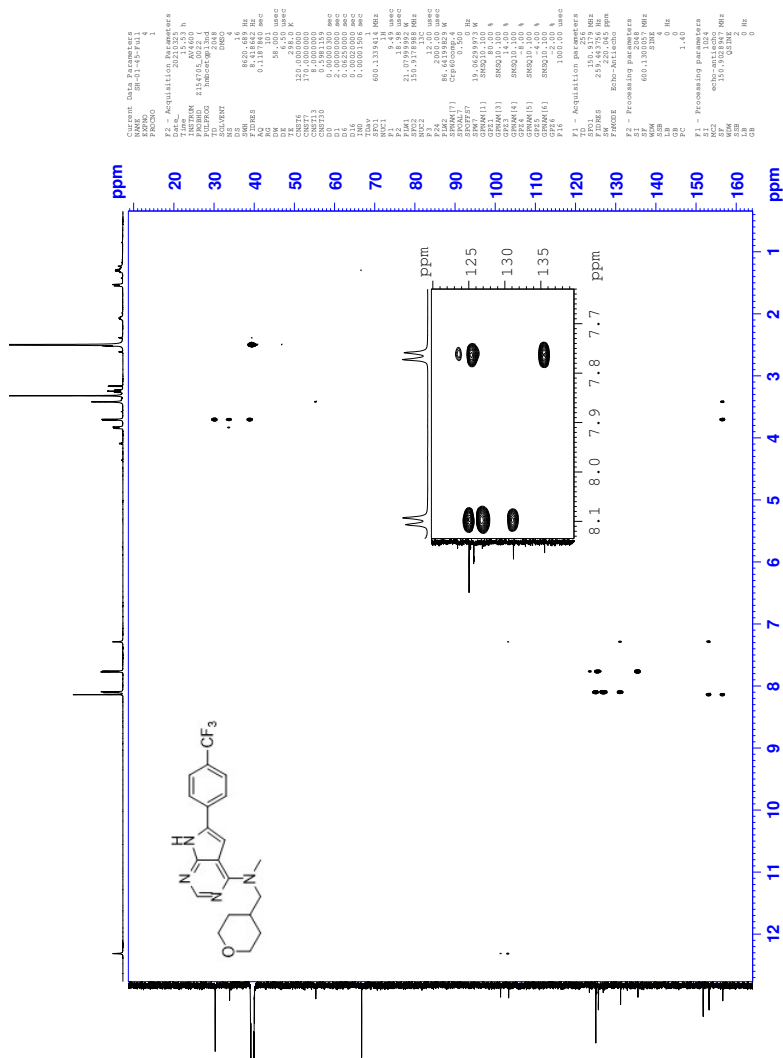


Figure O.5: HMBC spectrum of compound 16

Elemental Composition Report

Page 1

Single Mass Analysis

Tolerance = 2.0 PPM / DBE: min = -10.0, max = 50.0

Element prediction: Off

Number of isotope peaks used for i-FIT = 6

Monoisotopic Mass, Even Electron Ions

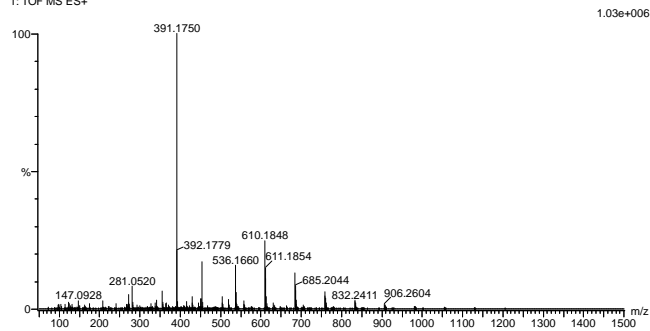
1603 formula(e) evaluated with 3 results within limits (all results (up to 1000) for each mass)

Elements Used:

C: 0-100 H: 0-100 N: 0-6 O: 0-10 F: 0-3

2021_185_69 (0.657) AM2 (Ar,35000.0,0.00,0.00); Cm (66.73)

1: TOF MS ES+



Minimum:

Maximum: 5.0 2.0 -10.0

Mass	Calc. Mass	mDa	PPM	DBE	i-FIT	Norm	Conf (%)	Formula
391.1750	391.1746	0.4	1.0	10.5	2254.8	0.012	98.78	C20 H22 N4 O F3
	391.1757	-0.7	-1.8	8.5	2259.7	4.901	0.74	C21 H27 O7
	391.1753	-0.3	-0.8	1.5	2260.2	5.338	0.48	C11 H25 N6 O7 F2

Figure O.6: MS spectrum of compound 16

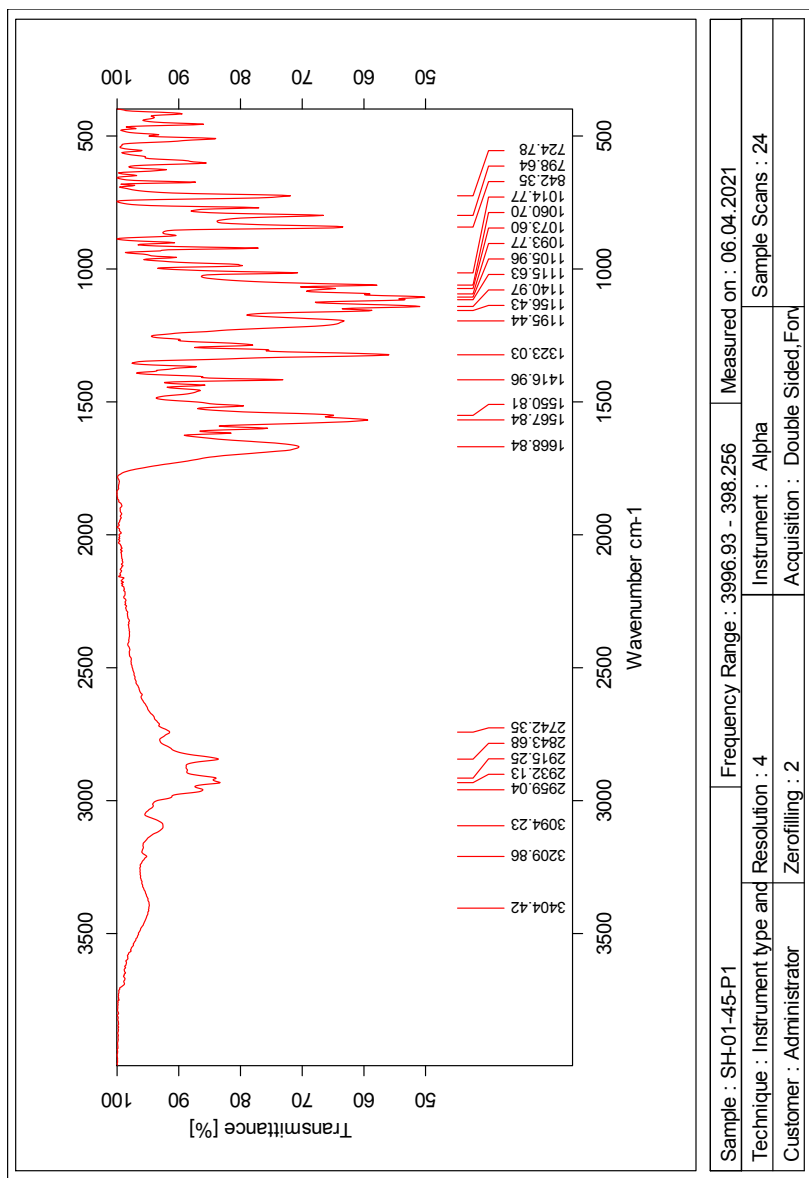


Figure O.7: IR spectrum of compound 16

P Spectroscopic data for Compound 17

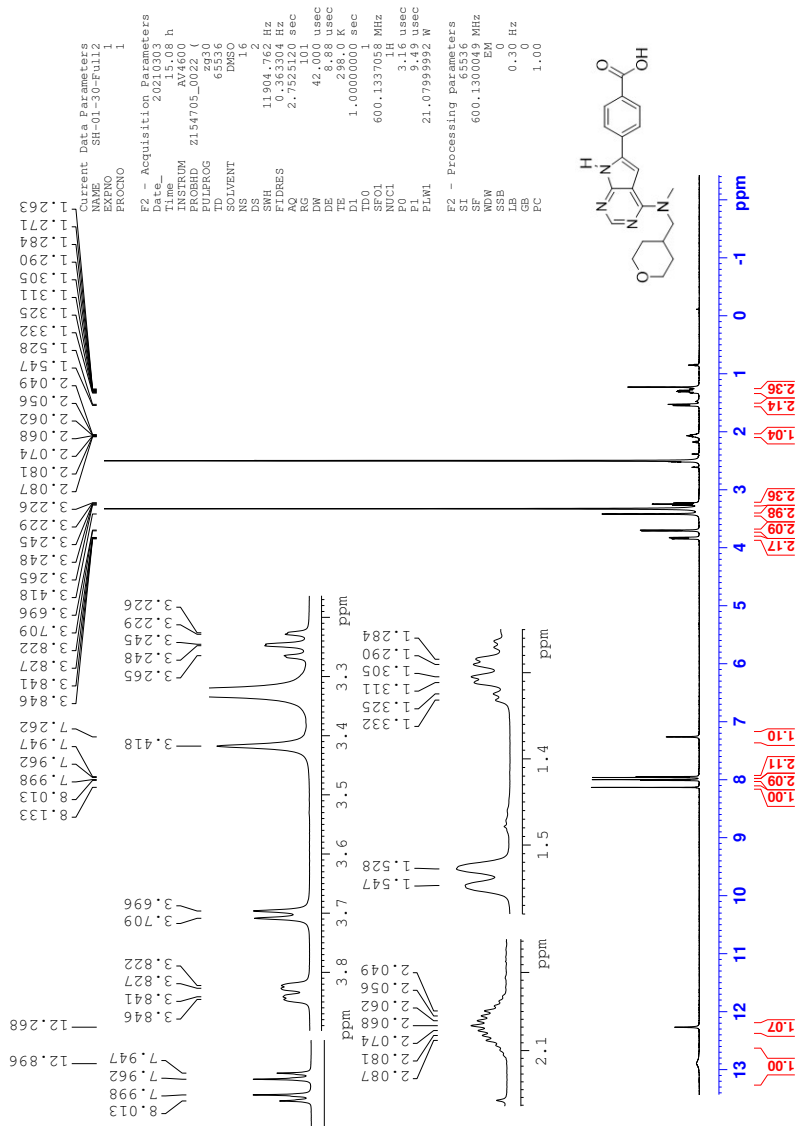
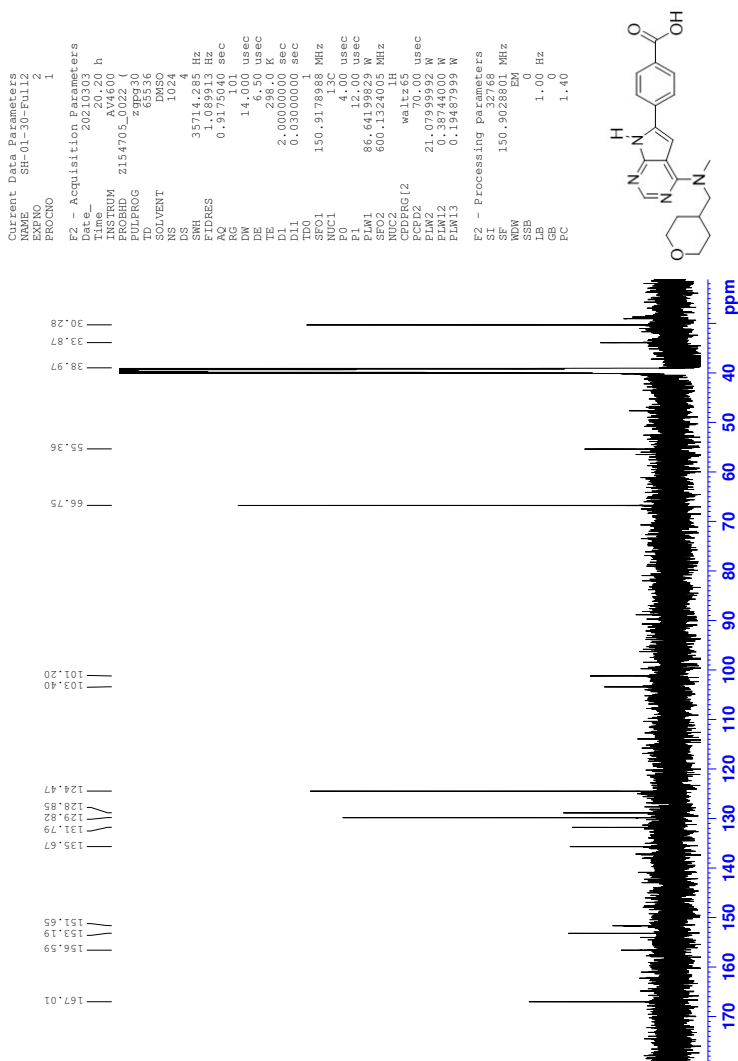


Figure P.1: ^1H NMR spectrum of compound 17

Figure P.2: ^{13}C NMR spectrum of compound 17

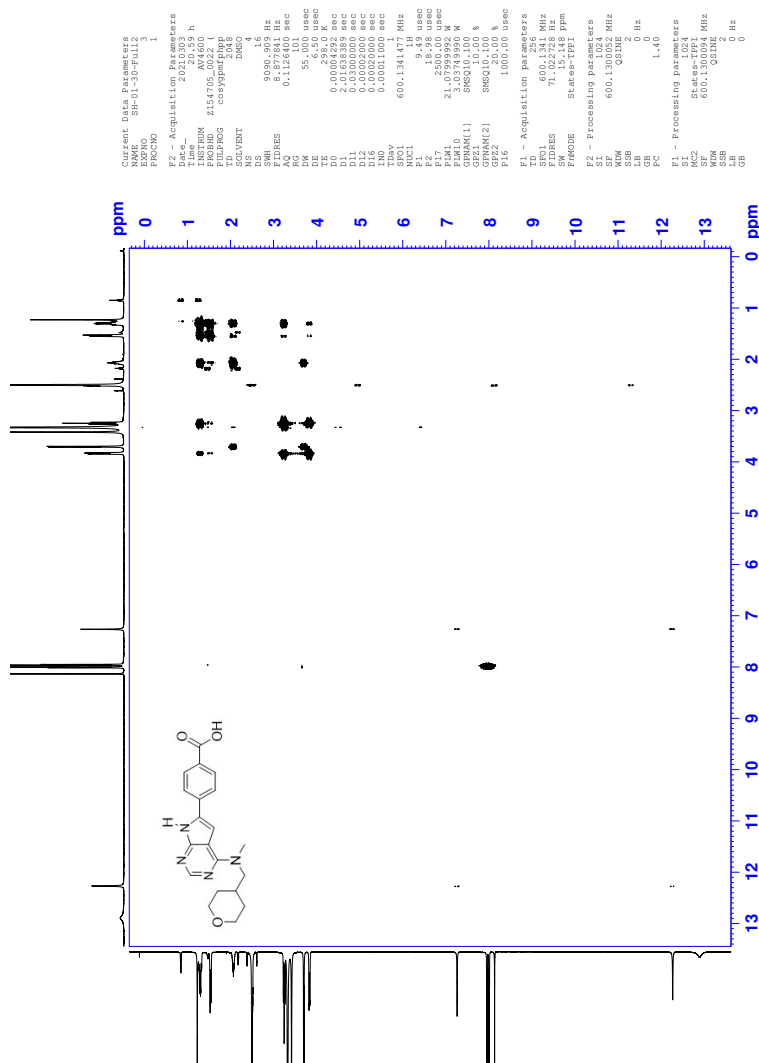


Figure P.3: COSY spectrum of compound 17

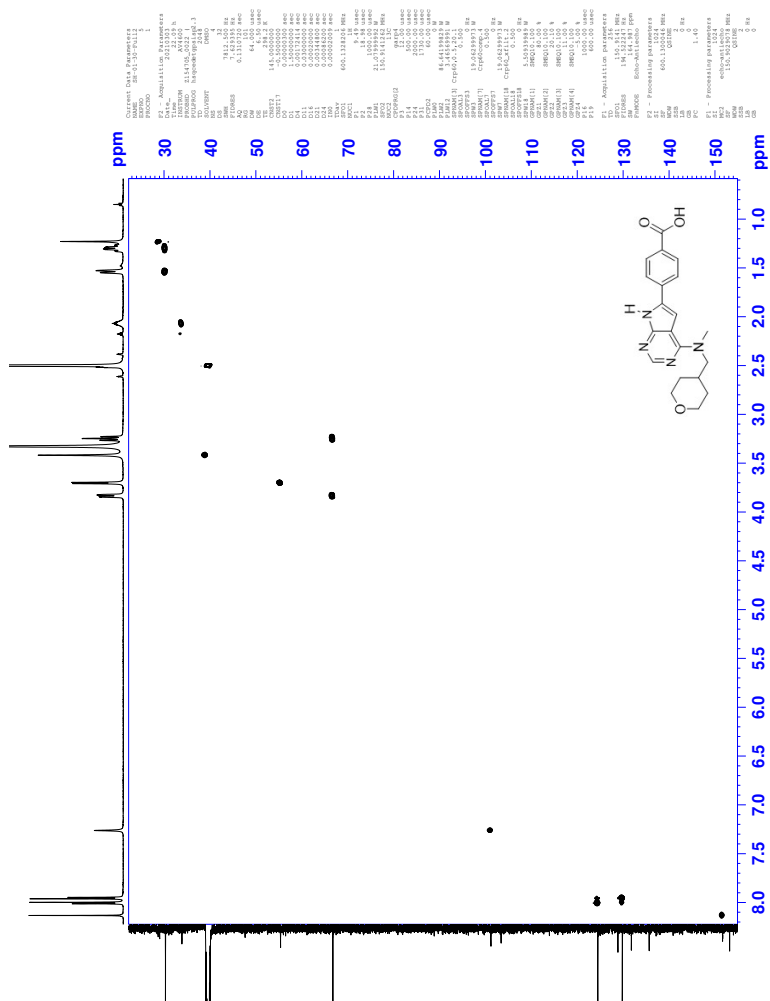


Figure P.4: HSQC spectrum of compound 17

Elemental Composition Report

Page 1

Single Mass Analysis

Tolerance = 2.0 PPM / DBE: min = -10.0, max = 50.0

Element prediction: Off

Number of isotope peaks used for i-FIT = 6

Monoisotopic Mass, Even Electron Ions

664 formula(e) evaluated with 1 results within limits (all results (up to 1000) for each mass)

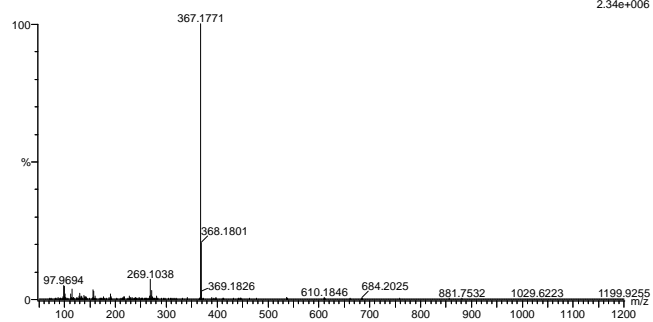
Elements Used:

C: 0-100 H: 0-100 N: 0-9 O: 0-5 Na: 0-1

2021-90-61 (0.690) AM2 (Ar:35000.0,0.00,0.00); Cm (61.69)

1: TOF MS ES+

2.34e+006



Minimum: -10.0

Maximum: 50.0

Mass	Calc. Mass	mDa	PPM	DBE	i-FIT	Norm	Conf (%)	Formula
367.1771	367.1770	0.1	0.3	11.5	2218.6	n/a	n/a	C20 H23 N4 O3

Figure P.6: MS spectrum of compound 17

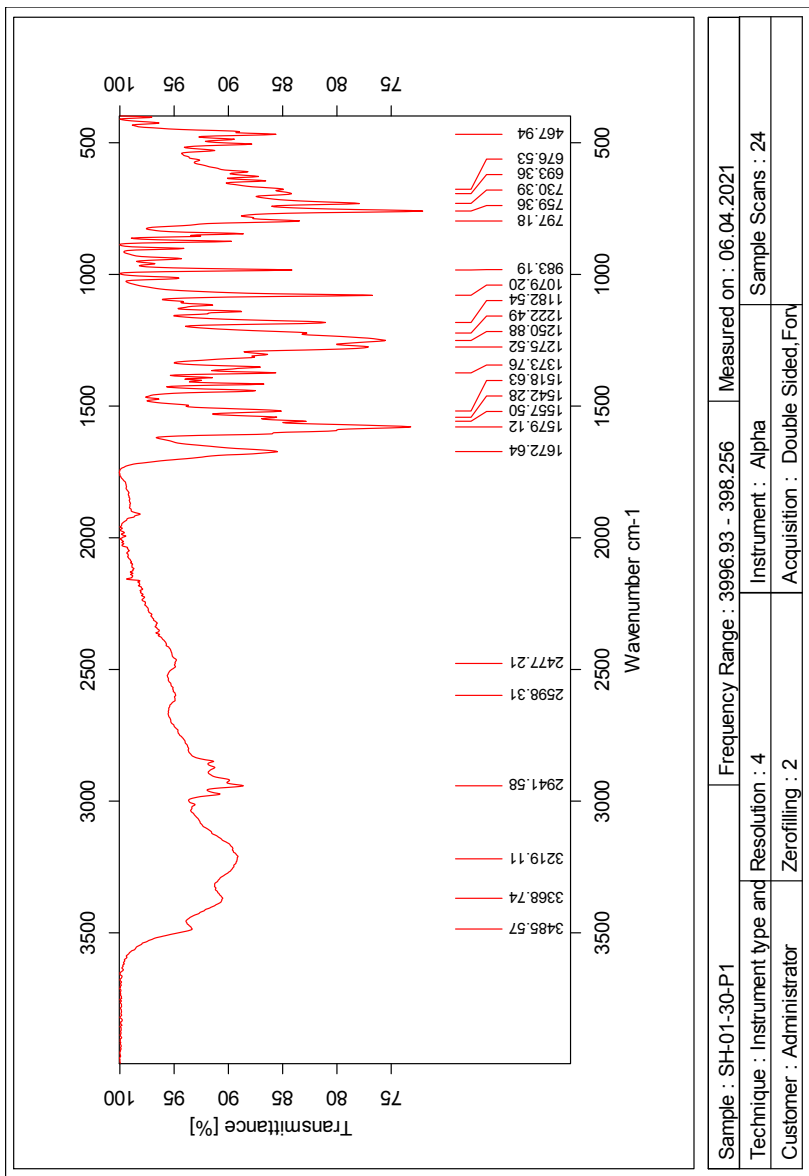


Figure P.7: IR spectrum of compound 17

Q Spectroscopic data for Compound 18

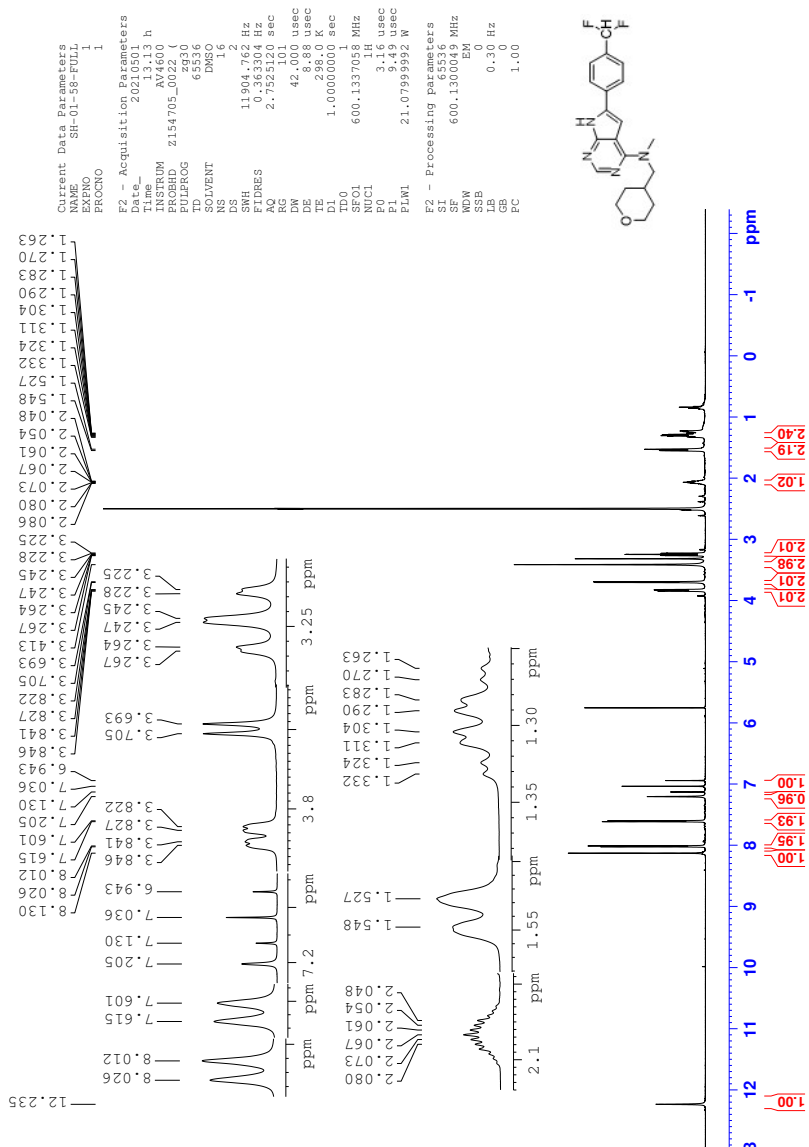
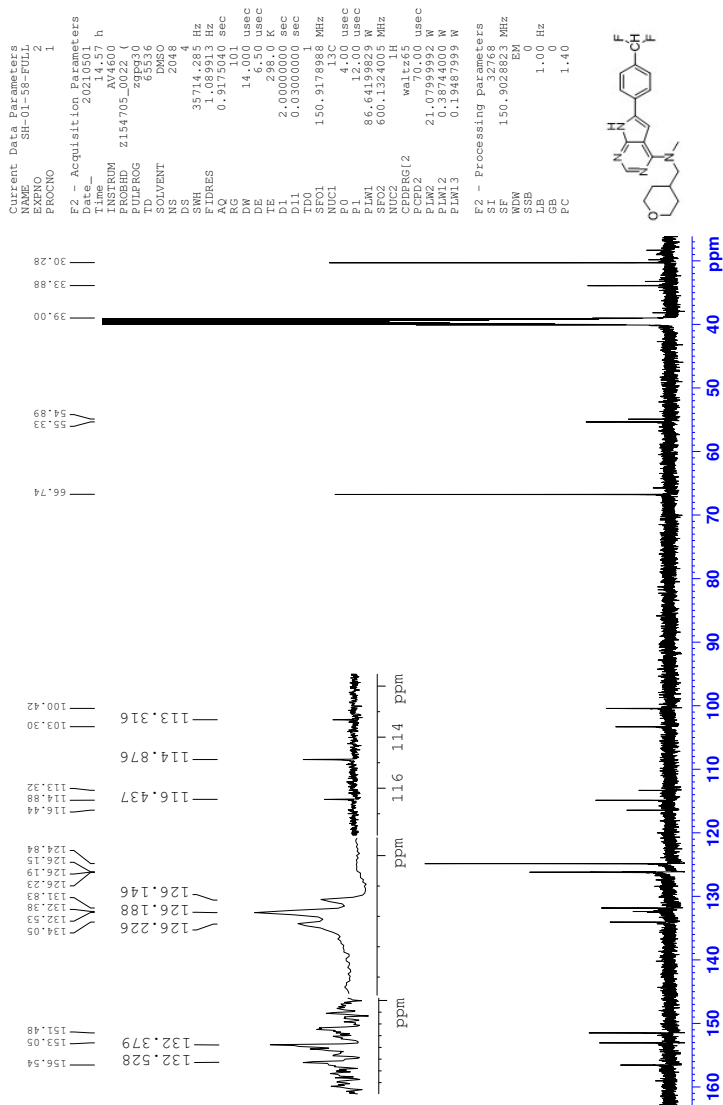


Figure Q.1: ¹H NMR spectrum of compound 18

Figure Q.2: ^{13}C NMR spectrum of compound 18

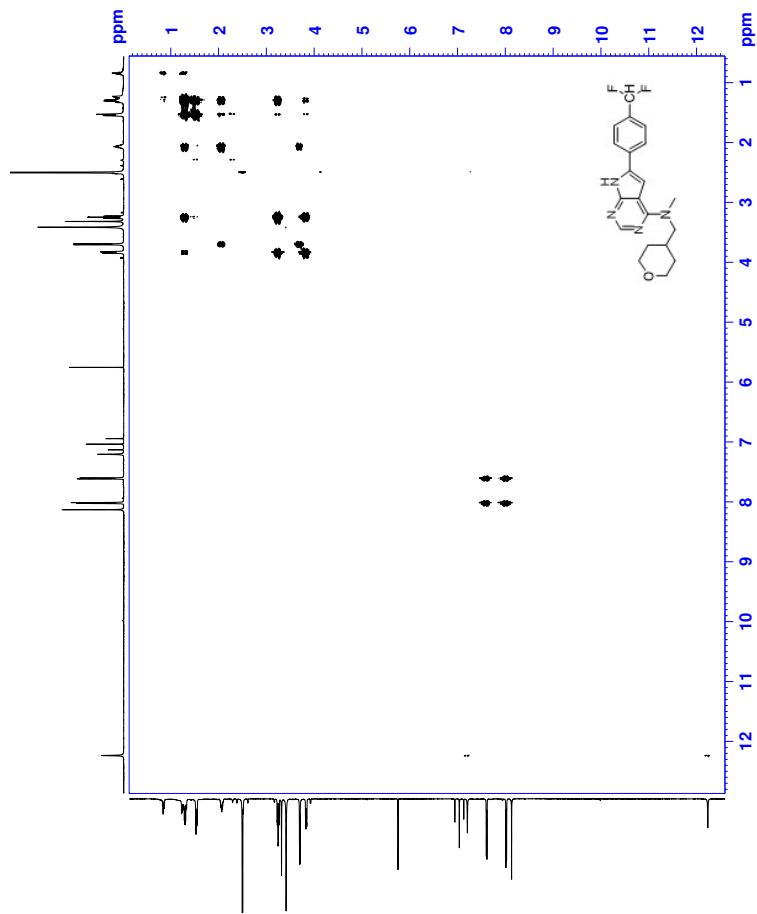


Figure Q.3: COSY spectrum of compound 18

Elemental Composition Report

Page 1

Single Mass Analysis

Tolerance = 2.0 PPM / DBE: min = -1.5, max = 50.0

Element prediction: Off

Number of isotope peaks used for i-FIT = 3

Monoisotopic Mass, Even Electron Ions

1950 formula(e) evaluated with 4 results within limits (up to 50 closest results for each mass)

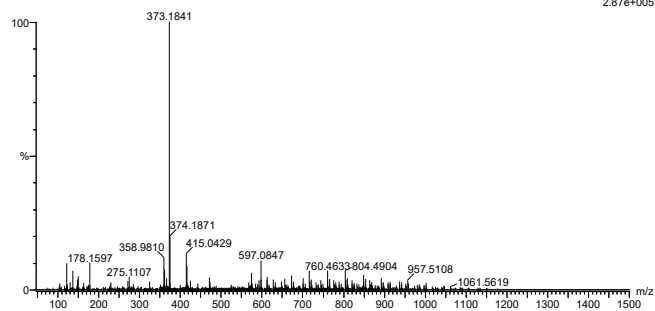
Elements Used:

C: 0-500 H: 0-1000 N: 0-7 O: 0-10 Na: 0-1 F: 0-2

2021_307_170 (1.598)AM2 (Ar.35000.0,0.00,0.00)

1: TOF MS ES+

2.87e+005



Mass	Calc. Mass	mDa	PPM	DBE	i-FIT	Norm	Conf (%)	Formula
373.1841	373.1840	0.1	0.3	10.5	836.3	0.432	64.91	C20 H23 N4 O F2
	373.1838	0.3	0.8	1.5	837.2	1.336	26.29	C16 H30 O8 Na
	373.1836	0.5	1.3	5.5	838.4	2.470	8.46	C14 H25 N6 O6
	373.1847	-0.6	-1.6	1.5	841.6	5.689	0.34	C11 H26 N6 O7 F

Figure Q.6: MS spectrum of compound 18

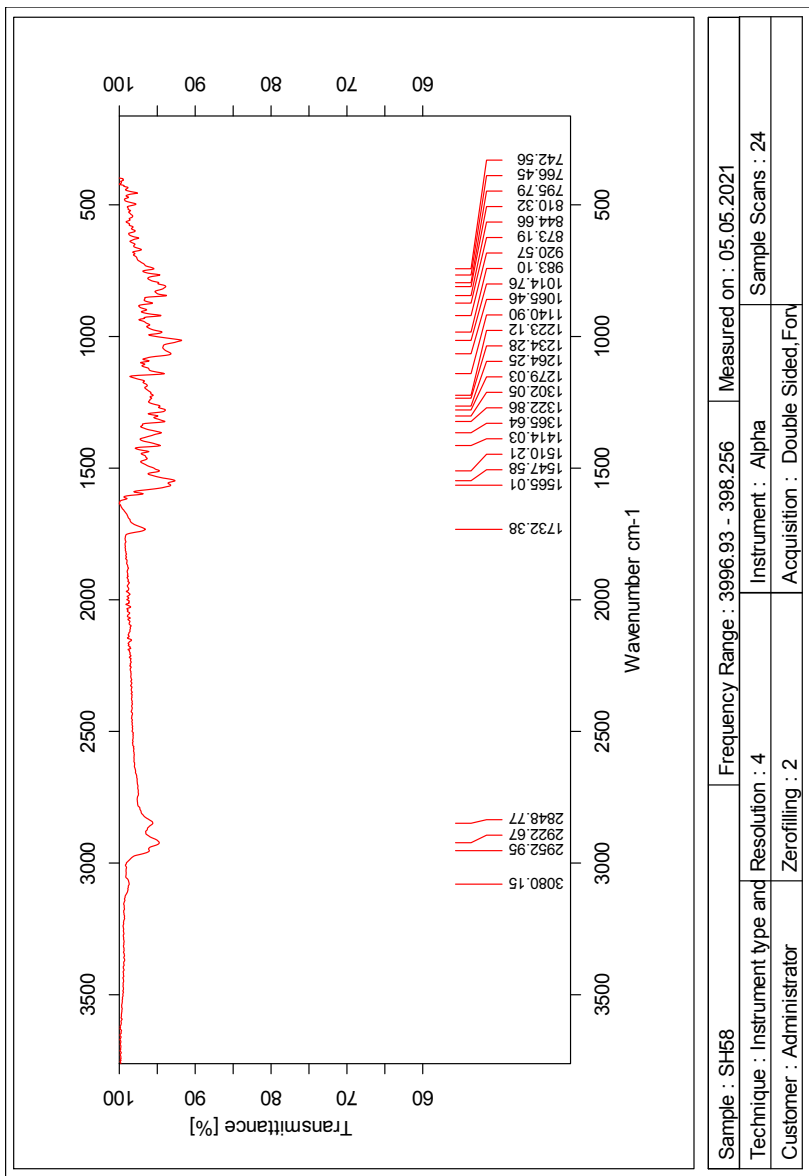
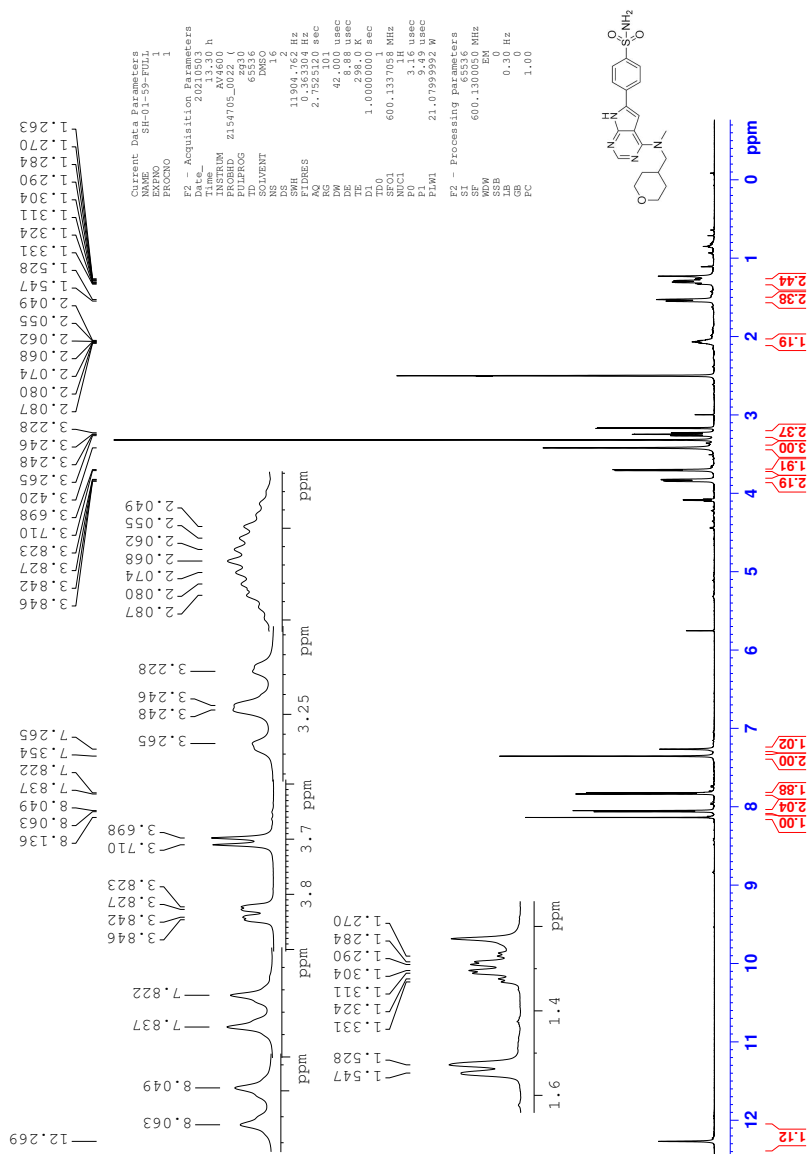


Figure Q.7: IR spectrum of compound 18

R Spectroscopic data for Compound 19

Figure R.1: ^1H NMR spectrum of compound 19

Current Data Parameters
NAME SH-01-59-FULL
PROCNO 1
E2 - Acquisition Parameters
Date_ 20210503
INSTRUM AV4600 h
PROBHD Z154705_0022 (zgr930
PULPROG zgpg30
SOLVENT DMSO
NS 2000
DS 4
SS 37714.28 Hz
SFO1 150.9178988 MHz
SFO2 13C
F0 4.00 usec
F1 86.6413500 usec
SFO1 150.9178988 MHz
SFO2 600.1324005 MHz
NUC1 1H
CPDPRG2 waltz65
PL12 21.07799992 usec
PL13 0.19487999 W
PL14 0.38744000 W
PL15 0.19487999 W
E2 - Processing Parameters
SI 32768
SF 150.9028812 MHz
WDW EM
SSB 0
GB 0
PC 1.40

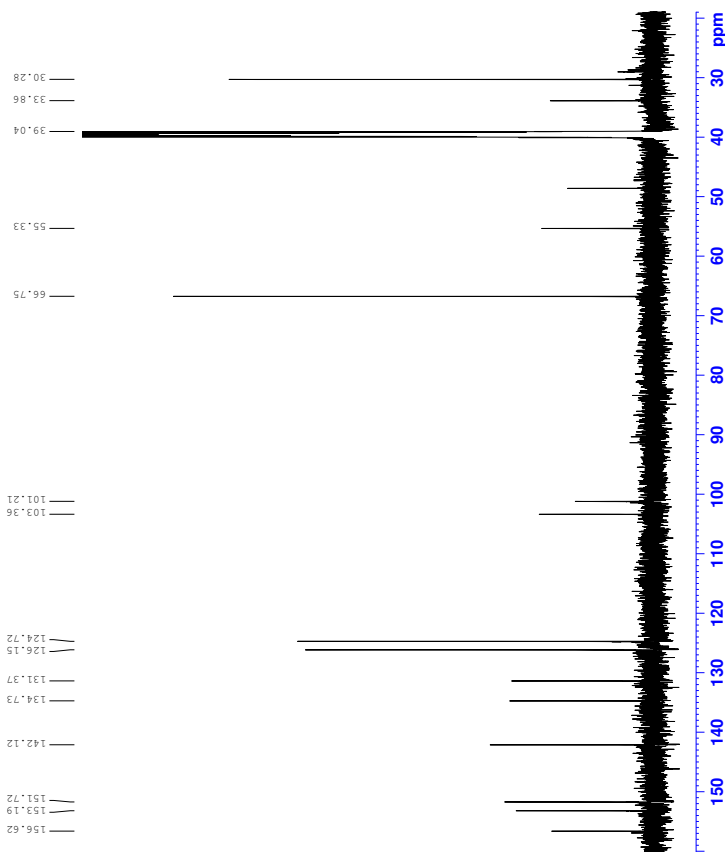
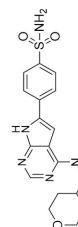


Figure R.2: ^{13}C NMR spectrum of compound 19

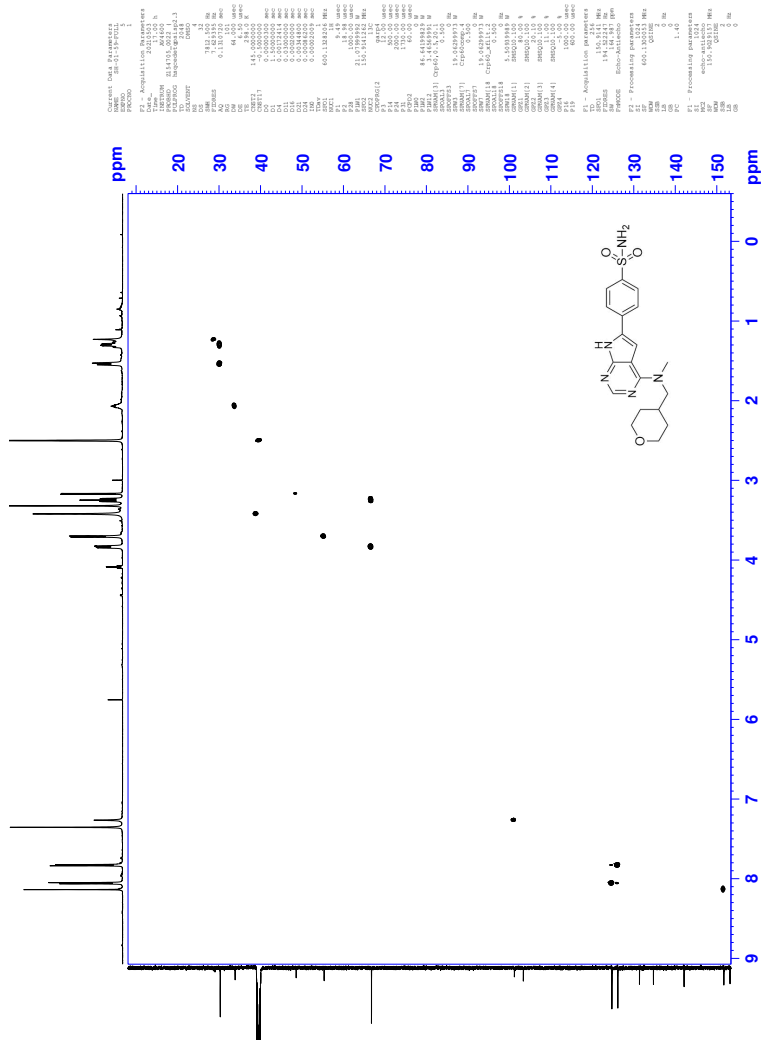


Figure R.4: HSQC spectrum of compound 19

Elemental Composition Report

Page 1

Single Mass Analysis

Tolerance = 2.0 PPM / DBE: min = -1.5, max = 50.0

Element prediction: Off

Number of isotope peaks used for i-FIT = 3

Monoisotopic Mass, Even Electron Ions

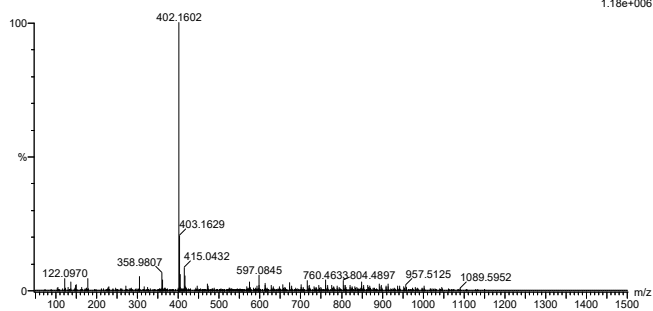
2647 formula(e) evaluated with 5 results within limits (up to 50 closest results for each mass)

Elements Used:

C: 0-500 H: 0-1000 N: 0-7 O: 0-10 Na: 0-1 S: 0-3

2021_308 173 (1.624) AM2 (Ar,35000.0,0.00,0.00); Cm (173:174)

1: TOF MS ES+



Minimum: -1.5
Maximum: 5.0 2.0 50.0

Mass	Calc. Mass	mDa	PPM	DBE	i-FIT	Norm	Conf (%)	Formula
402.1602	402.1600	0.2	0.5	10.5	977.6	0.001	99.93	C19 H24 N5 O3 S
	402.1610	-0.8	-2.0	2.5	985.0	7.384	0.06	C14 H29 N5 O3 Na S2
	402.1601	0.1	0.2	3.5	988.3	10.763	0.00	C13 H25 N5 O8 Na
	402.1595	0.7	1.7	4.5	988.4	10.860	0.00	C19 H32 N O2 S3
	402.1606	-0.4	-1.0	19.5	990.8	13.191	0.00	C27 H20 N3 O

Figure R.6: MS spectrum of compound 19

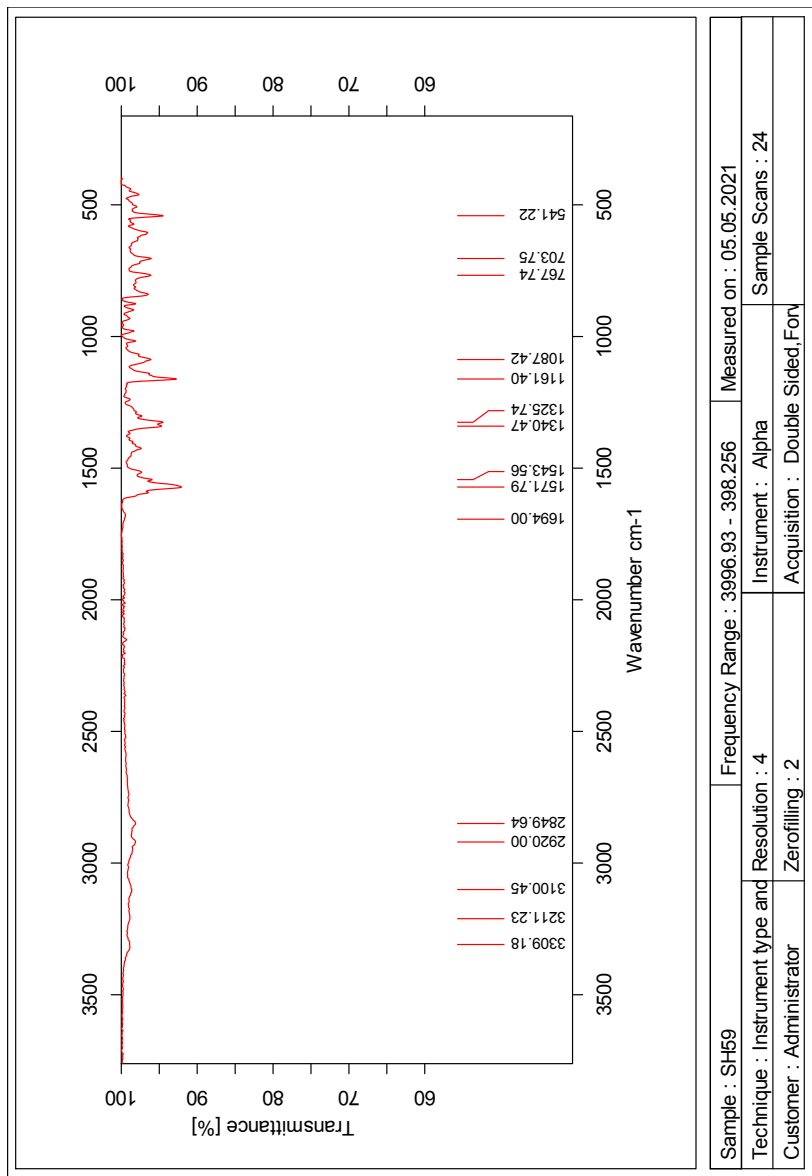
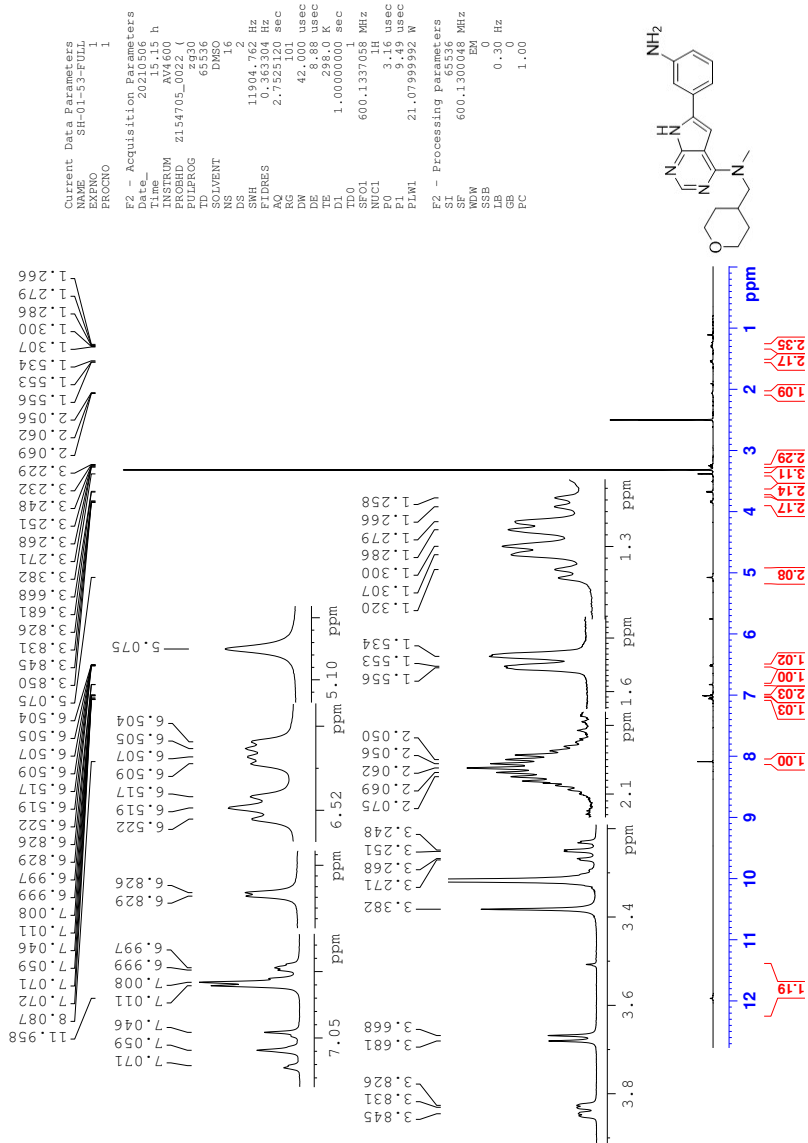
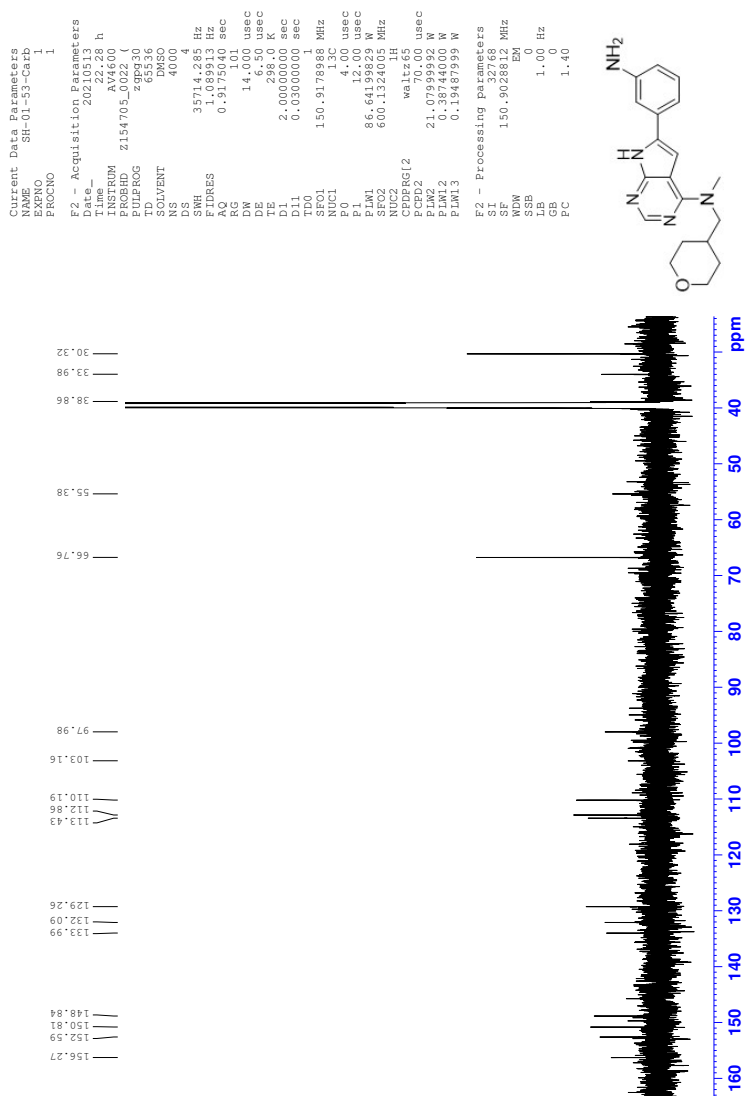


Figure R.7: IR spectrum of compound 19

S Spectroscopic data for Compound 20

Figure S.1: ^1H NMR spectrum of compound 20

Figure S.2: ^{13}C NMR spectrum of compound 20

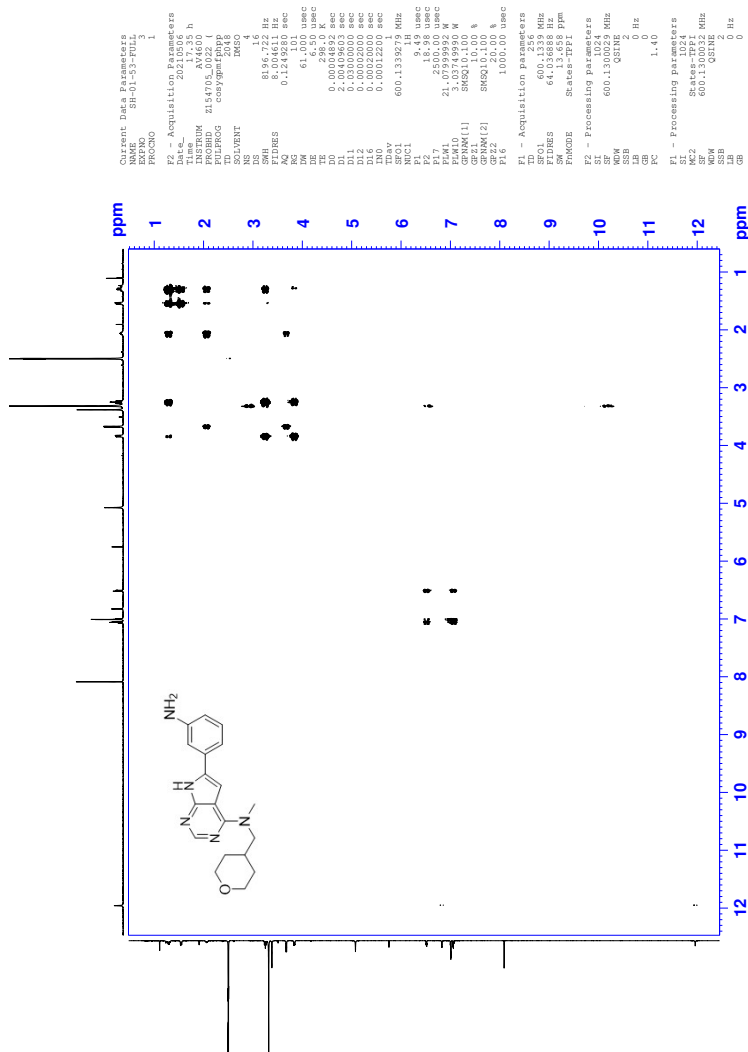


Figure S.3: COSY spectrum of compound 20

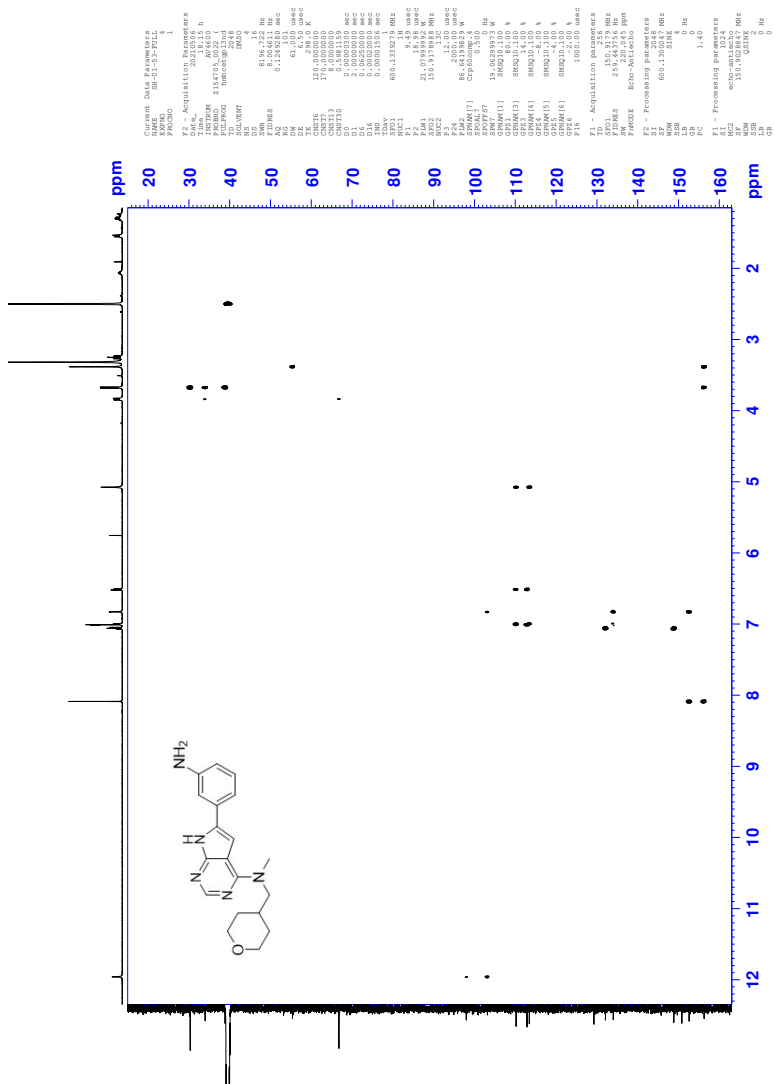


Figure S.5: HMBC spectrum of compound 20

Elemental Composition Report

Page 1

Single Mass Analysis

Tolerance = 2.1 PPM / DBE: min = -10.0, max = 50.0

Element prediction: Off

Number of isotope peaks used for i-FIT = 6

Monoisotopic Mass, Even Electron Ions

574 formula(e) evaluated with 1 results within limits (all results (up to 1000) for each mass)

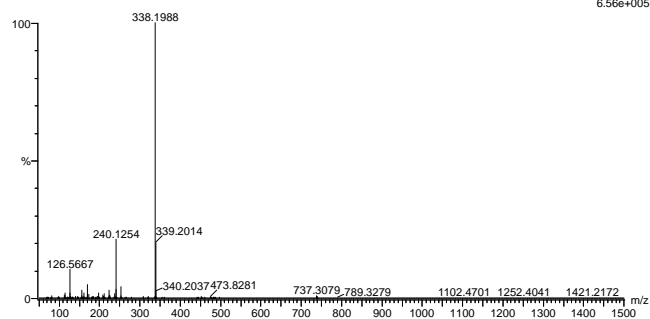
Elements Used:

C: 0-100 H: 0-100 N: 0-6 O: 0-7 Na: 0-1

SVG: 20210304_SH37 186 (3.437) AM2 (Ar:35000.0,0.00,0.00)

1: TOF MS ES+

6.56e+005



Minimum: -10.0

Maximum: 50.0

Mass	Calc. Mass	mDa	PPM	DBE	i-FIT	Norm	Conf (%)	Formula
338.1988	338.1981	0.7	2.1	10.5	1803.7	n/a	n/a	C19 H24 N5 O

Figure S.6: MS spectrum of compound 20

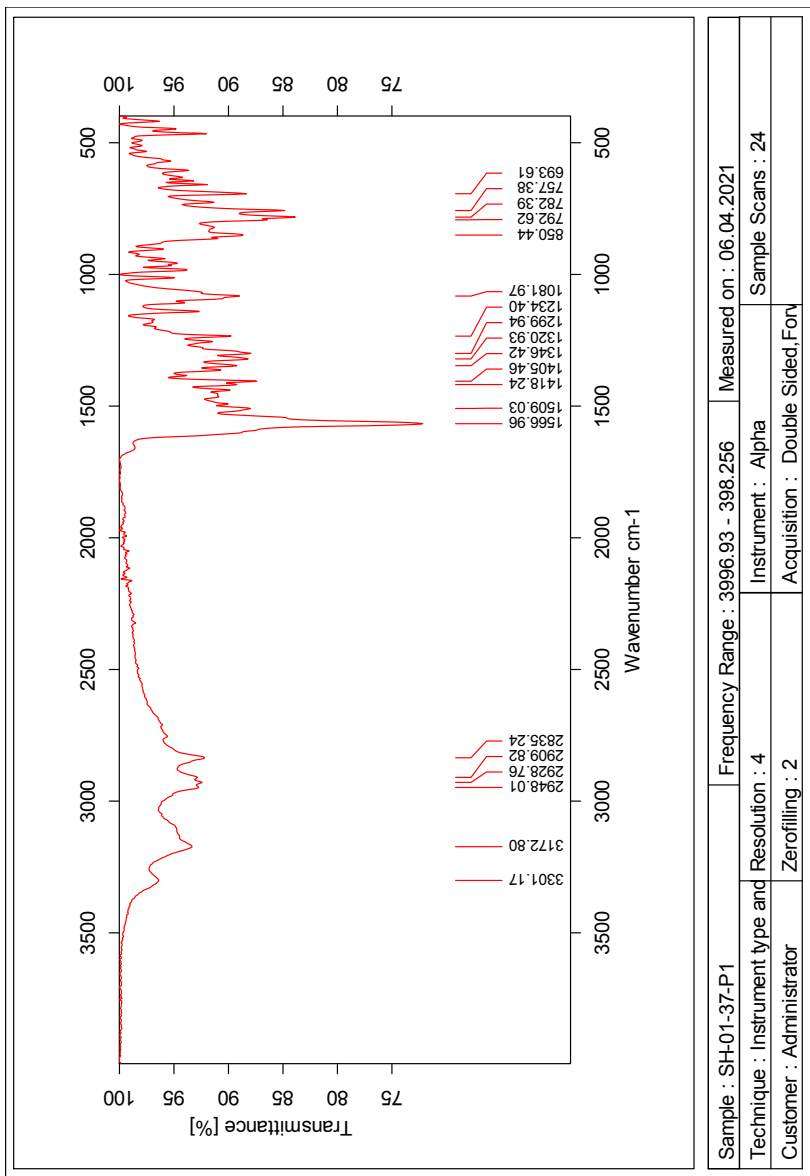
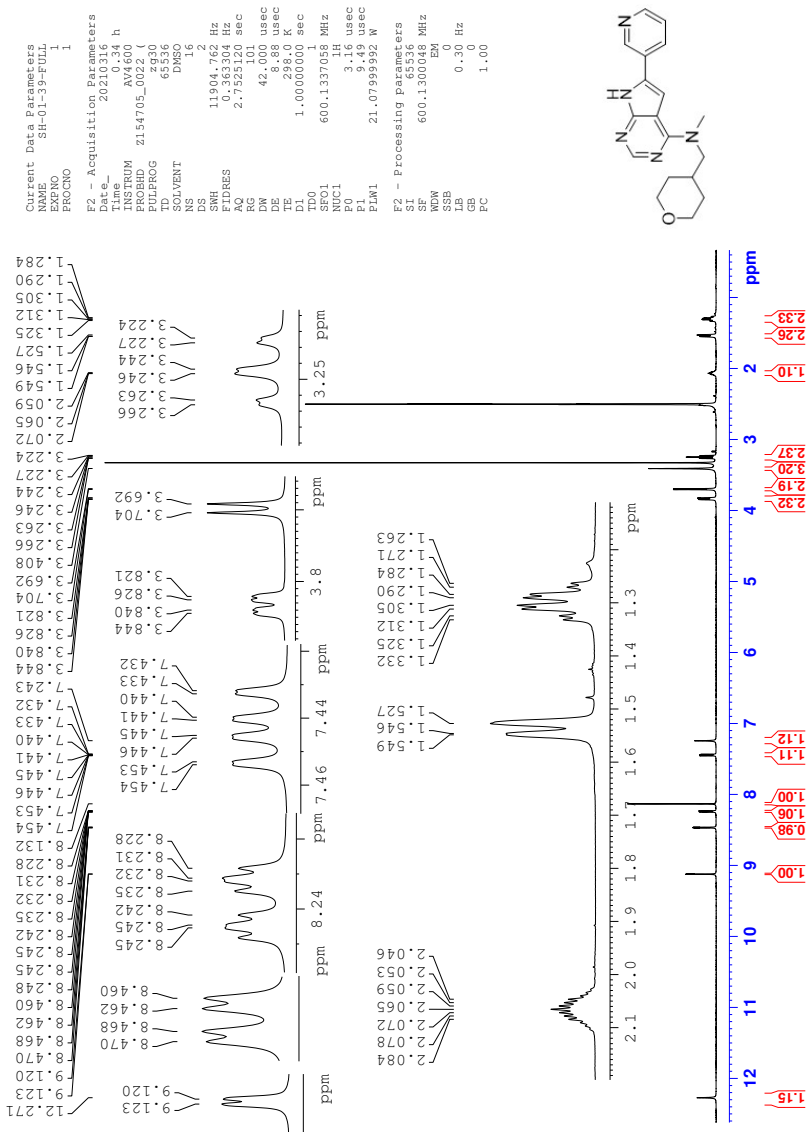
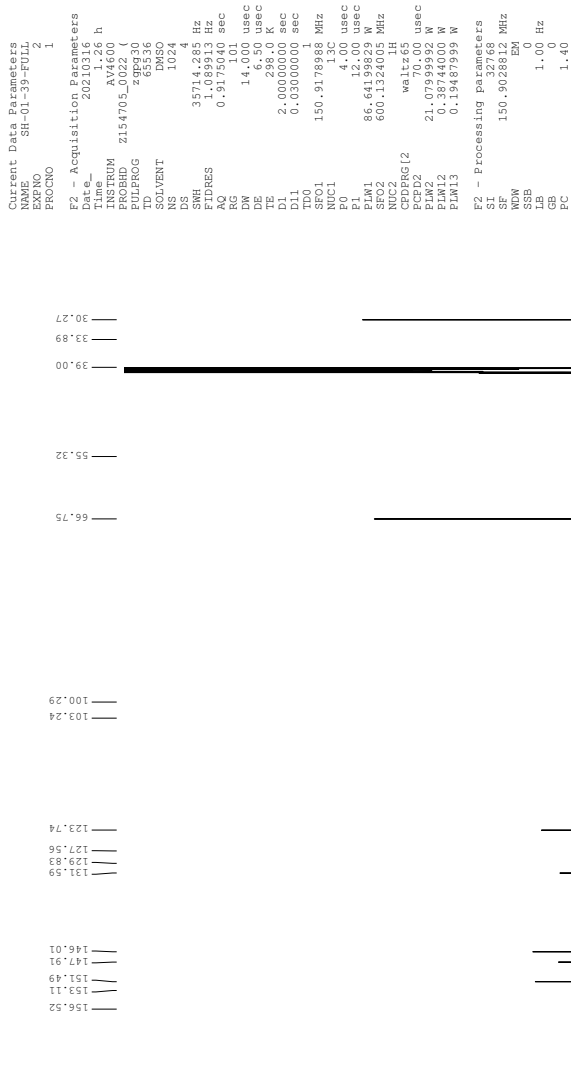


Figure S.7: IR spectrum of compound 20

T Spectroscopic data for Compound 21

Figure T.1: ^1H NMR spectrum of compound 21

Figure T.2: ^{13}C NMR spectrum of compound 21

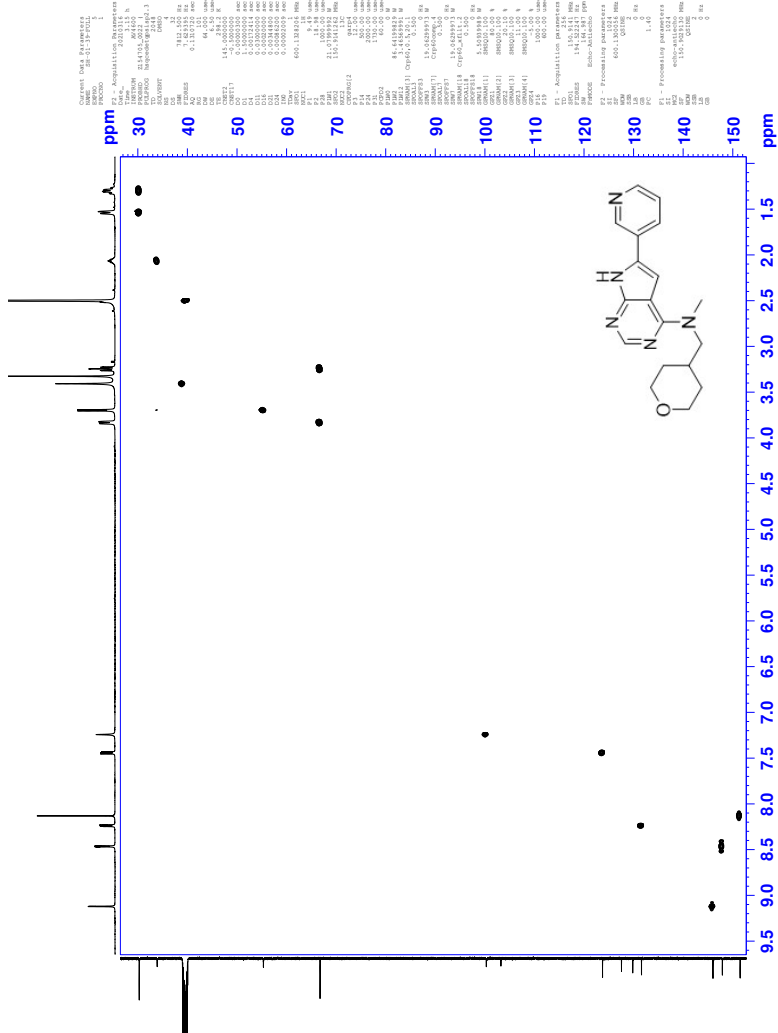


Figure T.4: HSQC spectrum of compound 21

Elemental Composition Report

Page 1

Single Mass Analysis

Tolerance = 2.0 PPM / DBE: min = -10.0, max = 50.0

Element prediction: Off

Number of isotope peaks used for i-FIT = 6

Monoisotopic Mass, Even Electron Ions

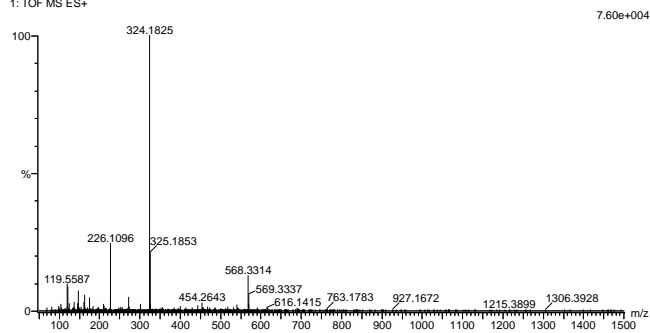
1023 formula(e) evaluated with 2 results within limits (all results (up to 1000) for each mass)

Elements Used:

C: 0-100 H: 0-100 N: 0-8 O: 0-12 Si: 0-1

2021_126_99 (0.936) AM2 (Ar,35000.0,0.00,0.00); Cm (99:104)

1: TOF MS ES+



Minimum:

Maximum: 5.0 2.0 -10.0

50.0

Mass	Calc. Mass	mDa	PPM	DBE	i-FIT	Norm	Conf (%)	Formula
324.1825	324.1824	0.1	0.3	10.5	1188.8	0.000	100.00	C18 H22 N5 O
	324.1829	-0.4	-1.2	-7.5	1201.8	13.025	0.00	C5 H30 N3 O12

Figure T.6: MS spectrum of compound 21

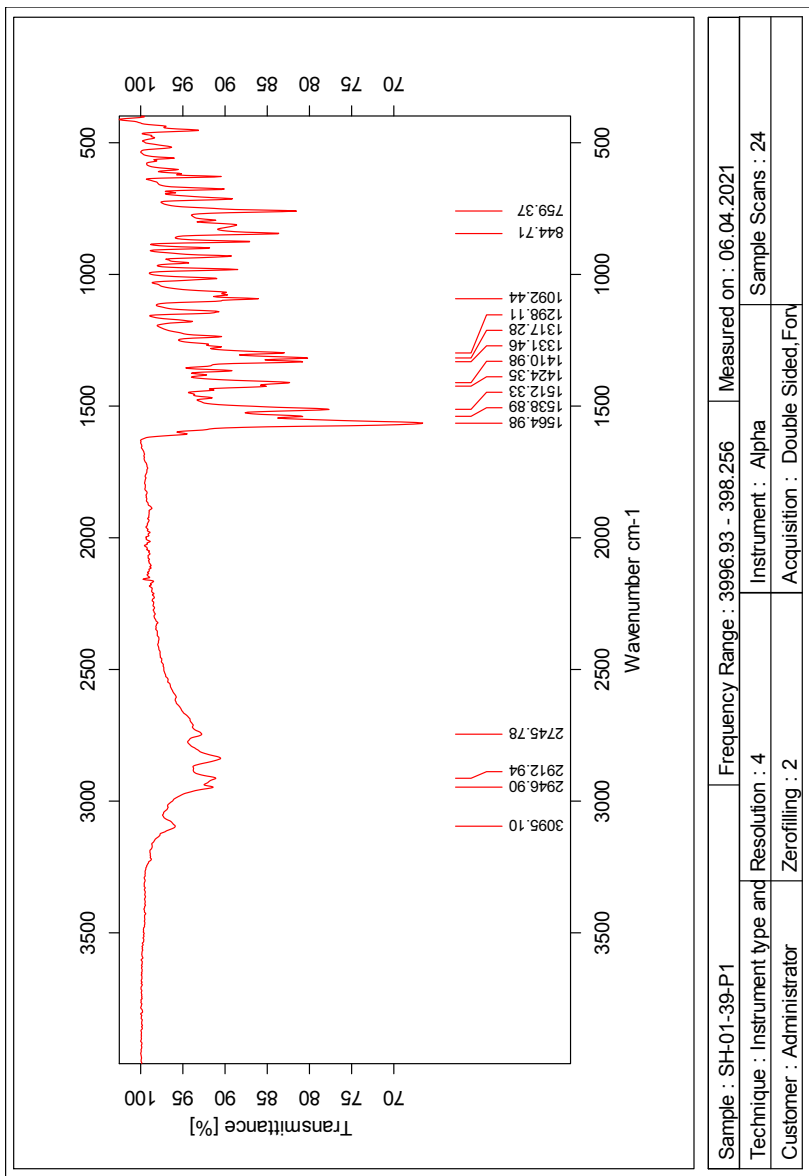
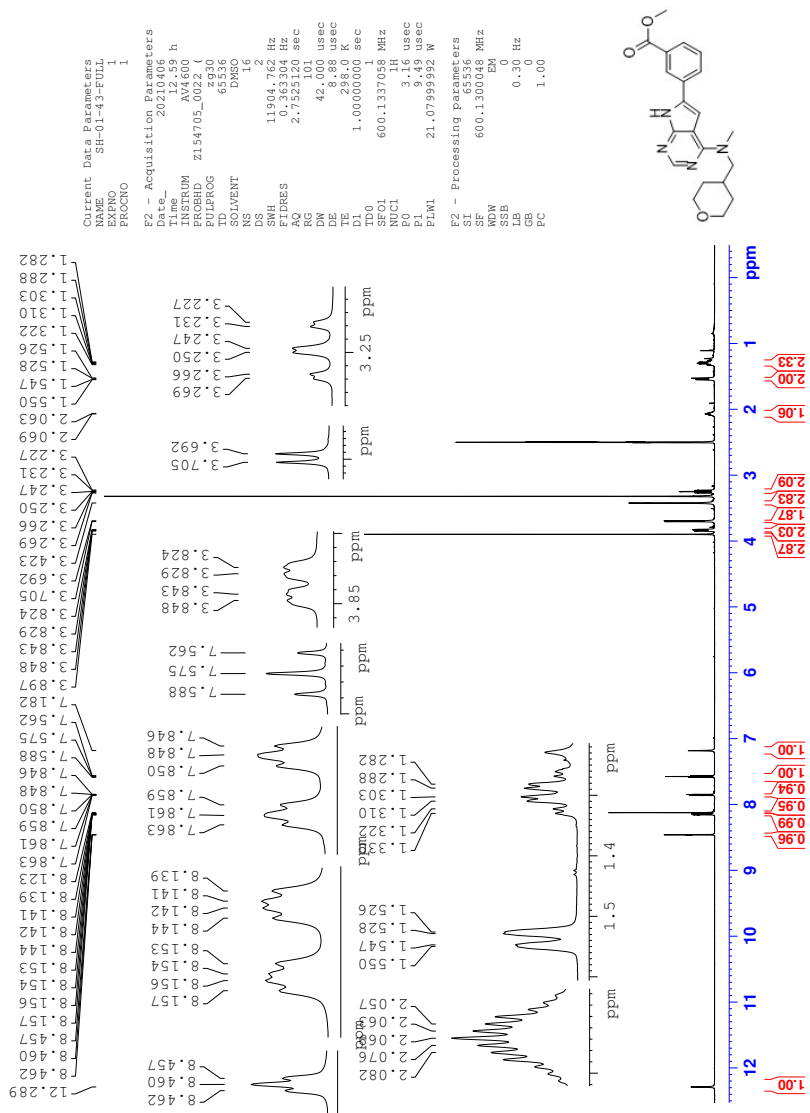
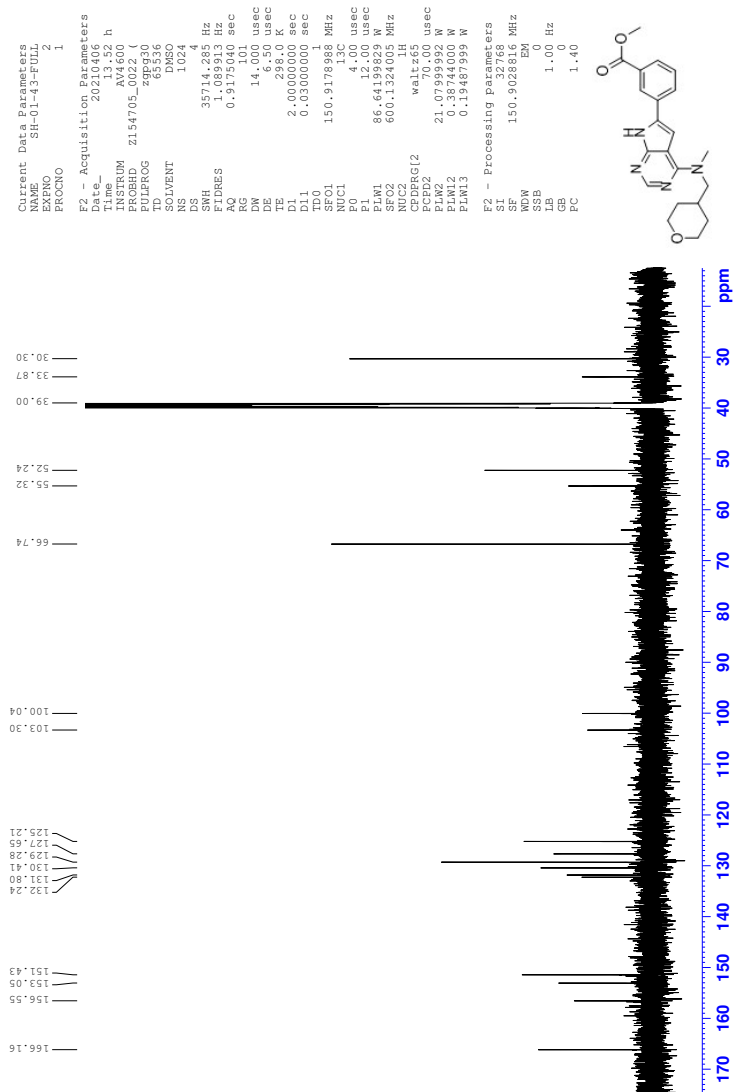


Figure T.7: IR spectrum of compound 21

U Spectroscopic data for Compound 22

Figure U.1: ^1H NMR spectrum of compound 22

Figure U.2: ^{13}C NMR spectrum of compound 22

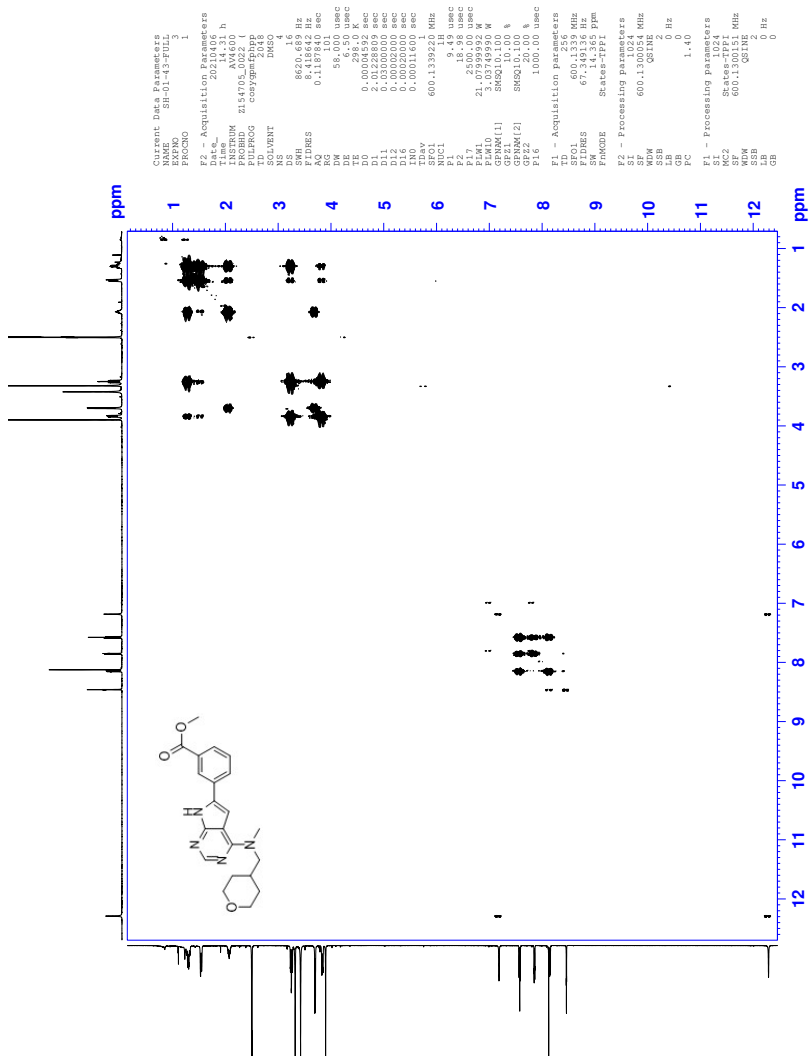


Figure U.3: COSY spectrum of compound 22

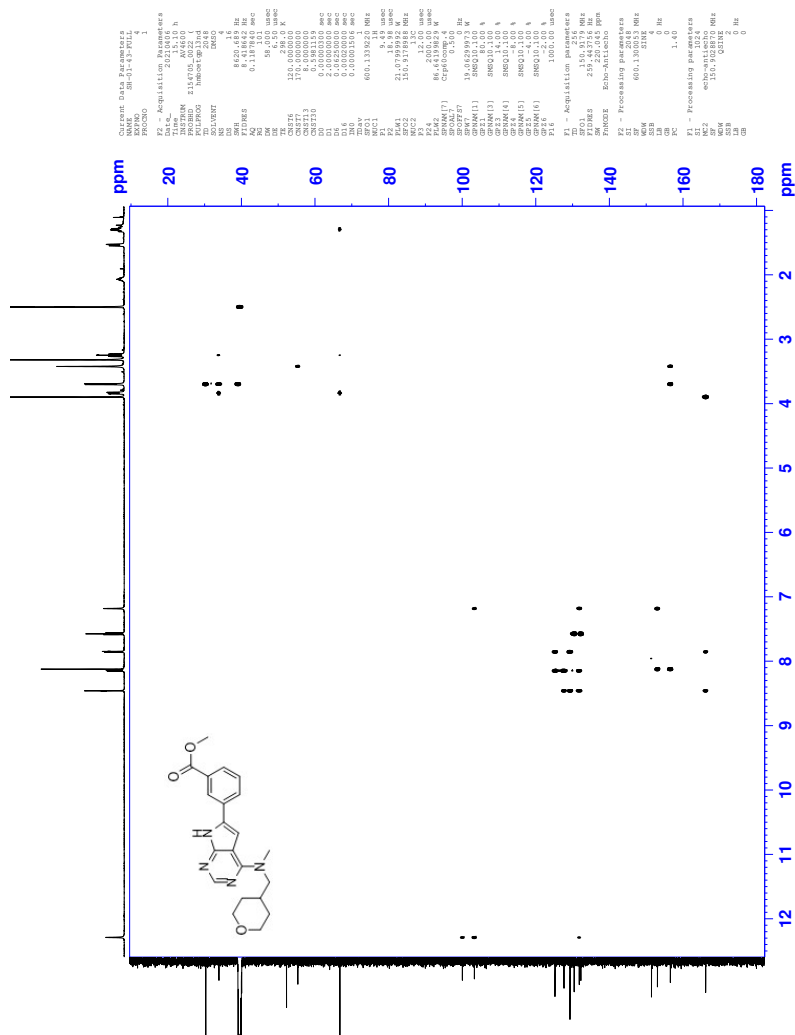


Figure U.5: HMBC spectrum of compound 22

Elemental Composition Report

Page 1

Single Mass Analysis

Tolerance = 2.0 PPM / DBE: min = -10.0, max = 50.0

Element prediction: Off

Number of isotope peaks used for i-FIT = 6

Monoisotopic Mass, Even Electron Ions

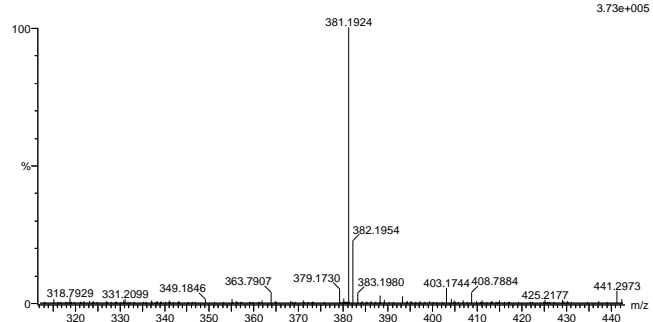
507 formula(e) evaluated with 1 results within limits (all results (up to 1000) for each mass)

Elements Used:

C: 0-100 H: 0-100 N: 0-4 O: 0-8 Na: 0-1

2021-160 47 (0.536) AM2 (Ar,35000.0,0.00,0.00); Cm (47:52)

1: TOF MS ES+



Minimum:

Maximum: 5.0 2.0 -10.0

50.0

Mass	Calc. Mass	mDa	PPM	DBE	i-FIT	Norm	Conf (%)	Formula
381.1924	381.1927	-0.3	-0.8	11.5	1735.6	n/a	n/a	C21 H25 N4 O3

Figure U.6: MS spectrum of compound 22

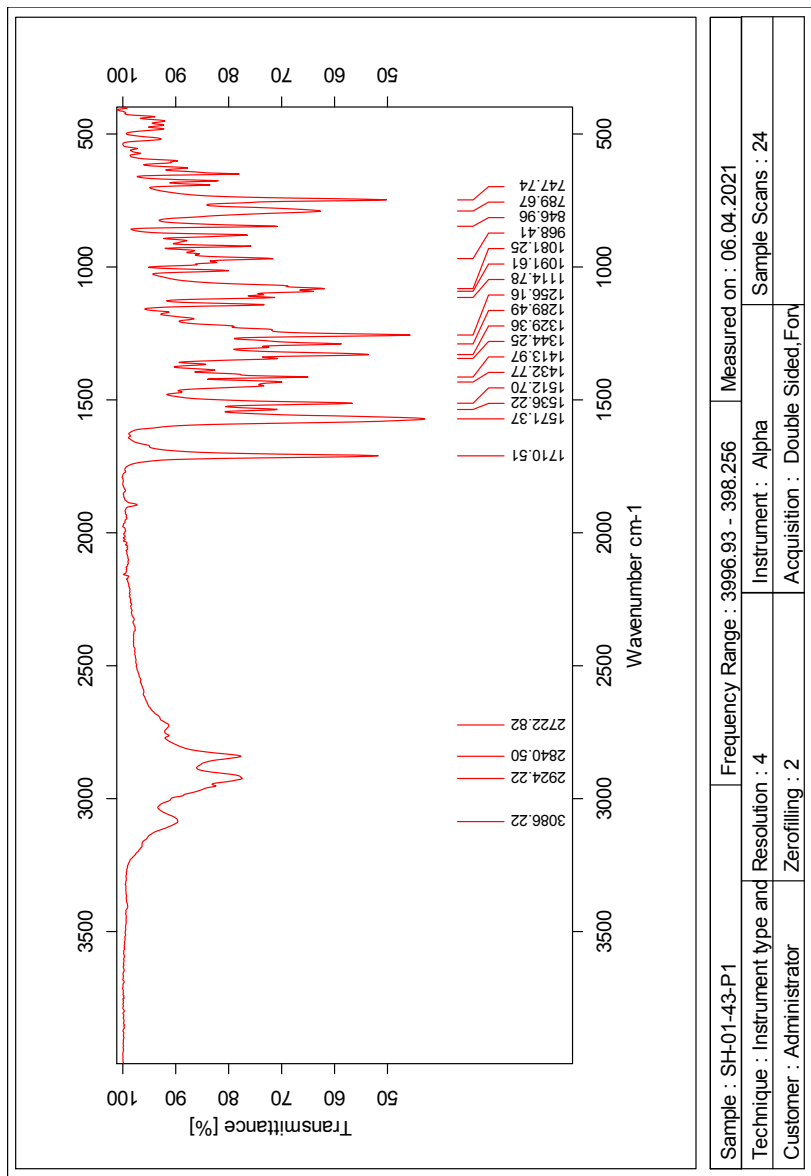


Figure U.7: IR spectrum of compound 22

V Spectroscopic data for Compound 23

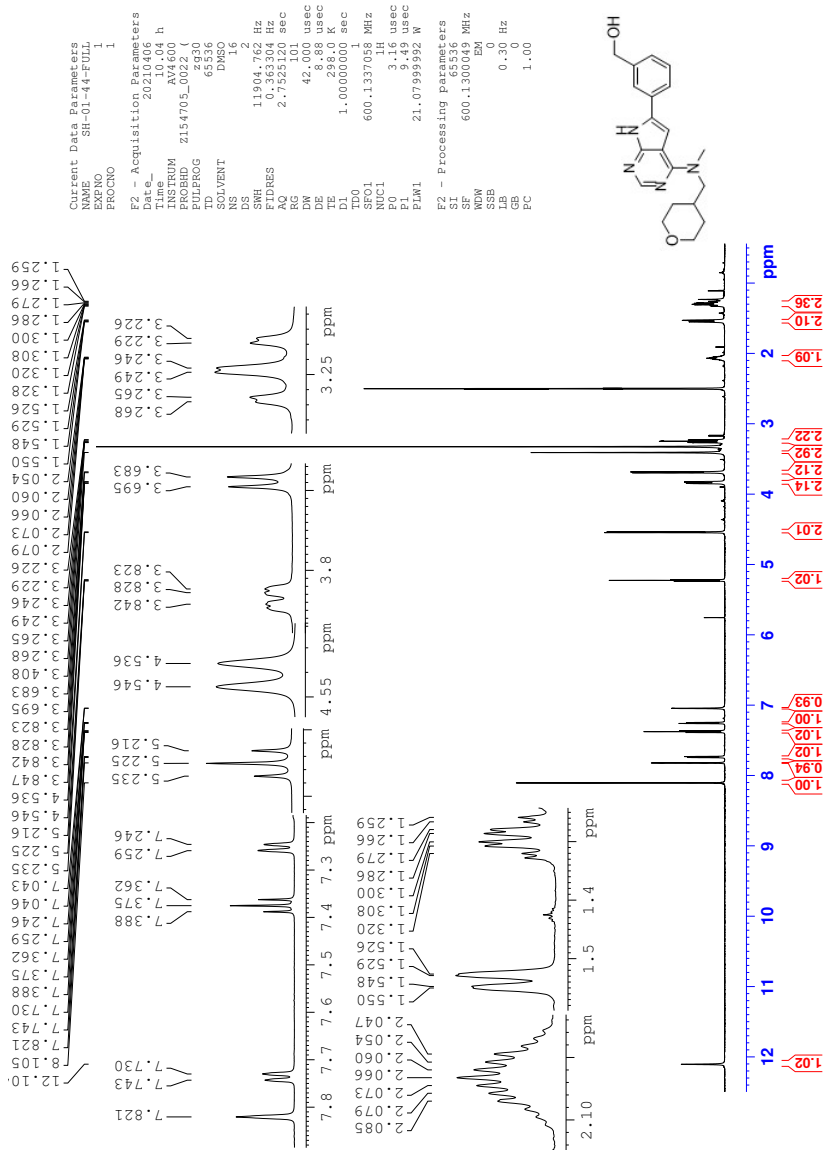
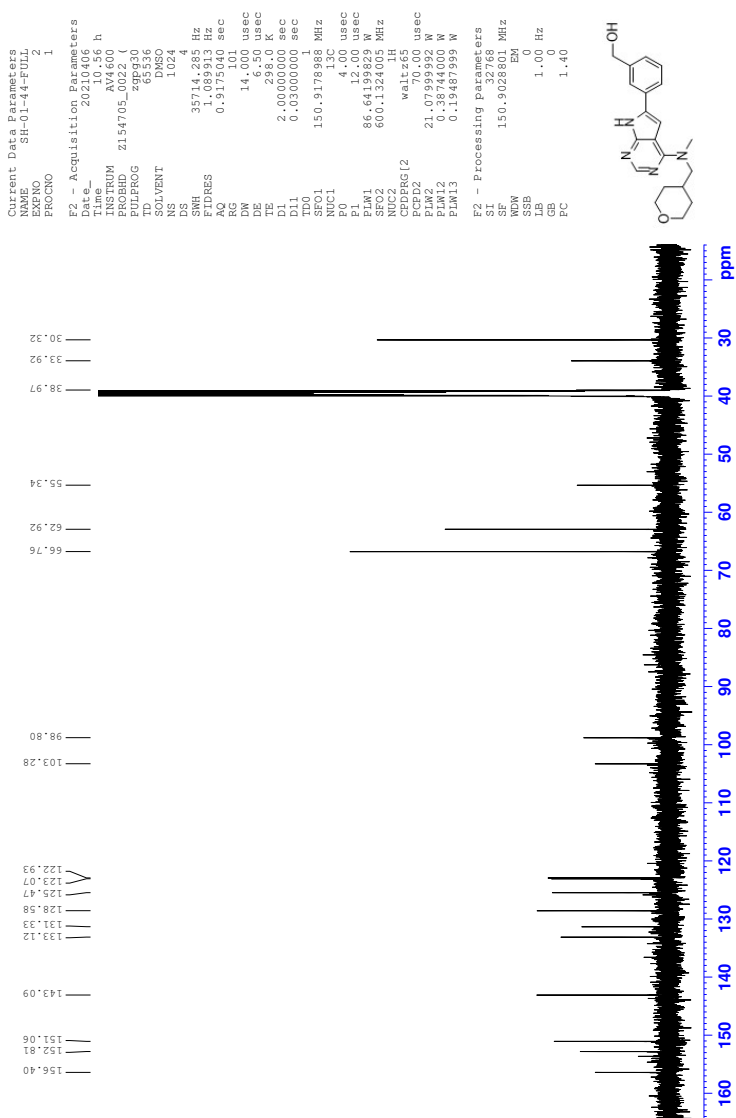


Figure V.1: ^1H NMR spectrum of compound 23

Figure V.2: ^{13}C NMR spectrum of compound 23

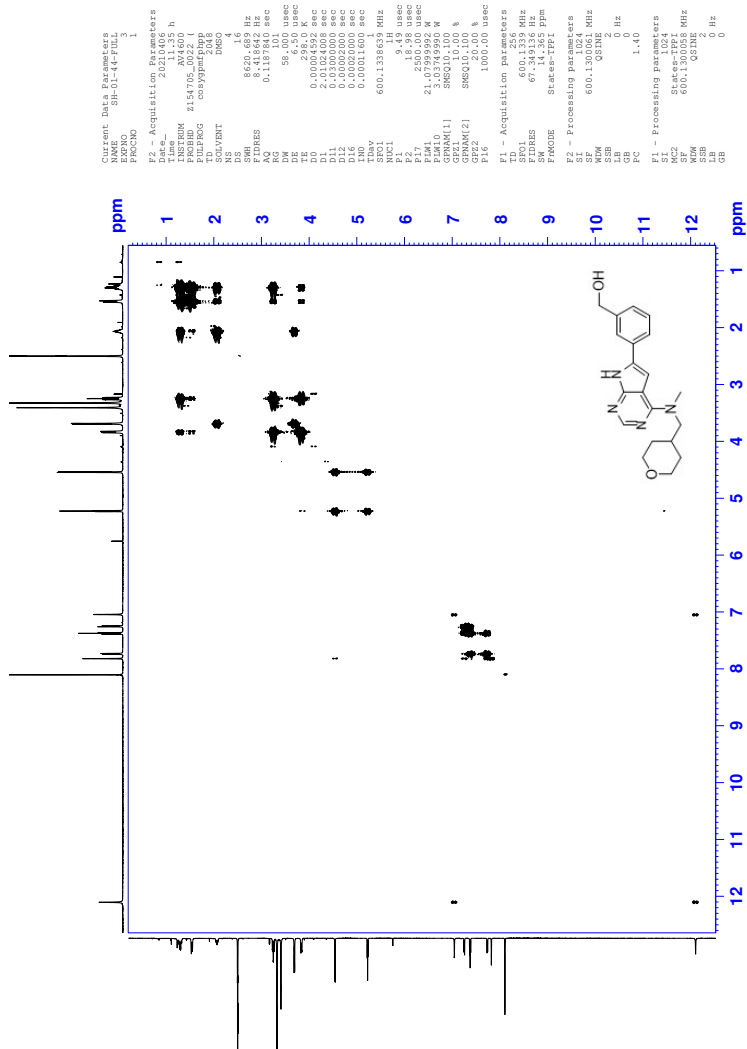


Figure V.3: COSY spectrum of compound 23

Elemental Composition Report

Page 1

Single Mass Analysis

Tolerance = 2.0 PPM / DBE: min = -10.0, max = 50.0

Element prediction: Off

Number of isotope peaks used for i-FIT = 6

Monoisotopic Mass, Even Electron Ions

477 formula(e) evaluated with 1 results within limits (all results (up to 1000) for each mass)

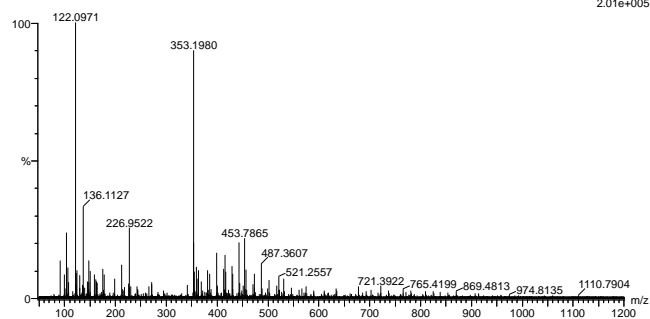
Elements Used:

C: 0-100 H: 0-100 N: 0-4 O: 0-8 Na: 0-1

2021-161 147 (1.632) AM2 (Ar,35000.0,0.00,0.00); Cm (143;147)

1: TOF MS ES+

2.01e+005

Minimum: -10.0
Maximum: 50.0

Mass	Calc. Mass	mDa	PPM	DBE	i-FIT	Norm	Conf (%)	Formula
353.1980	353.1978	0.2	0.6	10.5	2142.3	n/a	n/a	C20 H25 N4 O2

Figure V.6: MS spectrum of compound 23

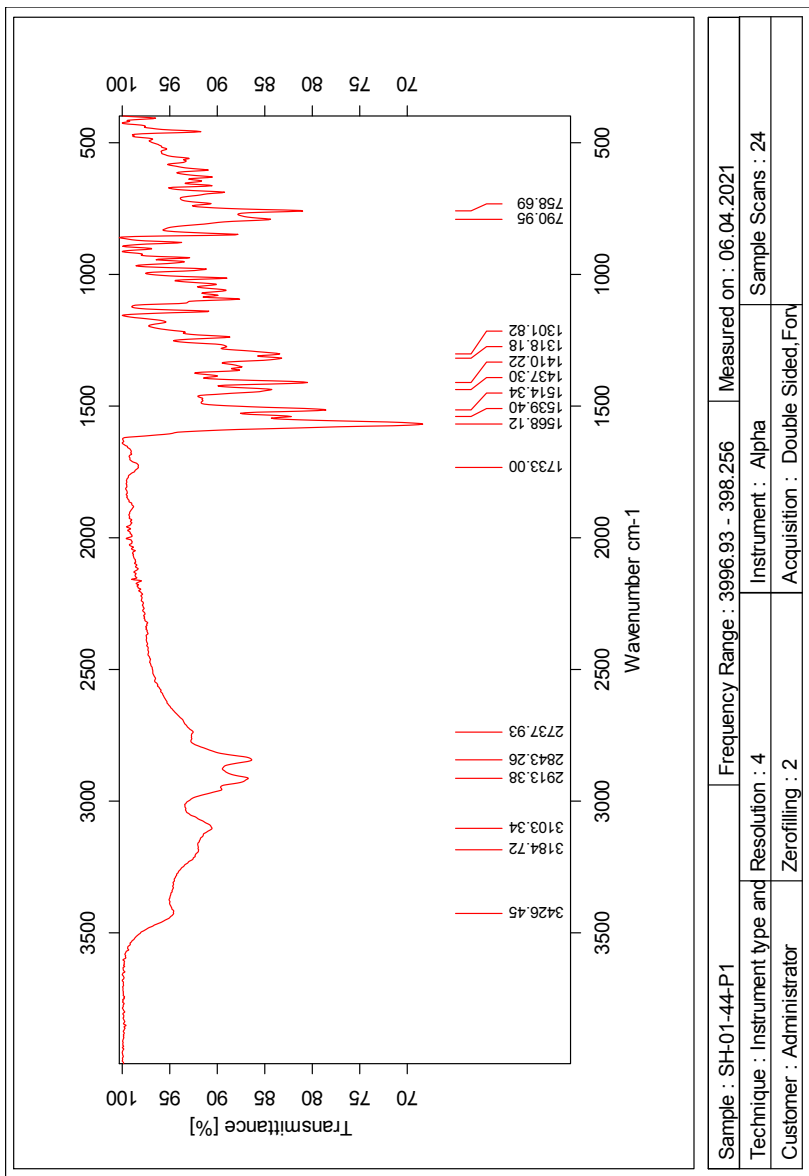


Figure V.7: IR spectrum of compound 23

W Spectroscopic data for Compound 24

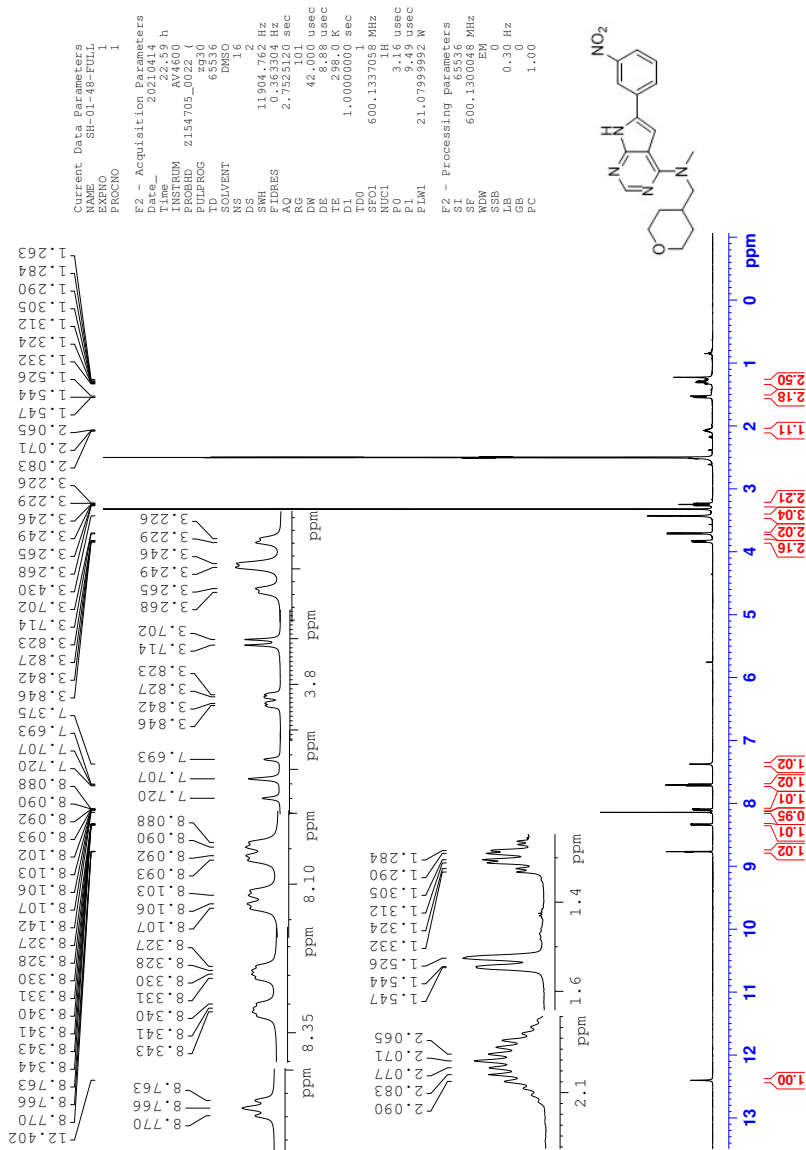


Figure W.1: ^1H NMR spectrum of compound 24

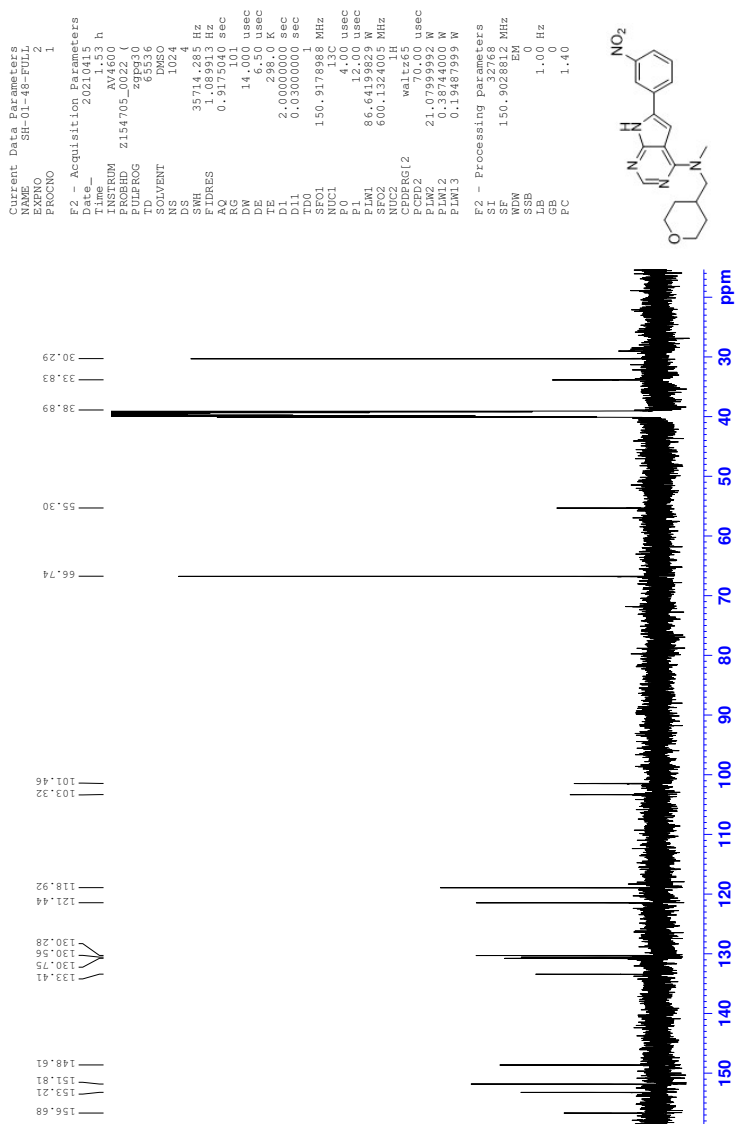


Figure W.2: ^{13}C NMR spectrum of compound 24

Elemental Composition Report

Page 1

Single Mass Analysis

Tolerance = 2.0 PPM / DBE: min = -10.0, max = 50.0

Element prediction: Off

Number of isotope peaks used for i-FIT = 6

Monoisotopic Mass, Even Electron Ions

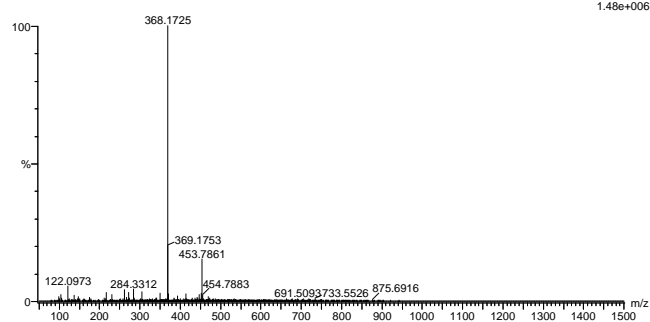
1413 formula(e) evaluated with 2 results within limits (all results (up to 1000) for each mass)

Elements Used:

C: 0-100 H: 0-100 N: 0-12 O: 0-10 Si: 0-1

2021.238 143 (1.345) AM2 (Ar:35000.0,0.00,0.00); Cm (143:151)

1: TOF MS ES+



Minimum: 5.0 2.0 -10.0

Maximum: 50.0

Mass	Calc. Mass	mDa	PPM	DBE	i-FIT	Norm	Conf (%)	Formula
368.1725	368.1723	0.2	0.5	11.5	2306.5	0.000	99.99	C19 H22 N5 O3
	368.1727	-0.2	-0.5	7.5	2315.8	9.258	0.01	C11 H22 N11 O2 Si

Figure W.6: MS spectrum of compound 24

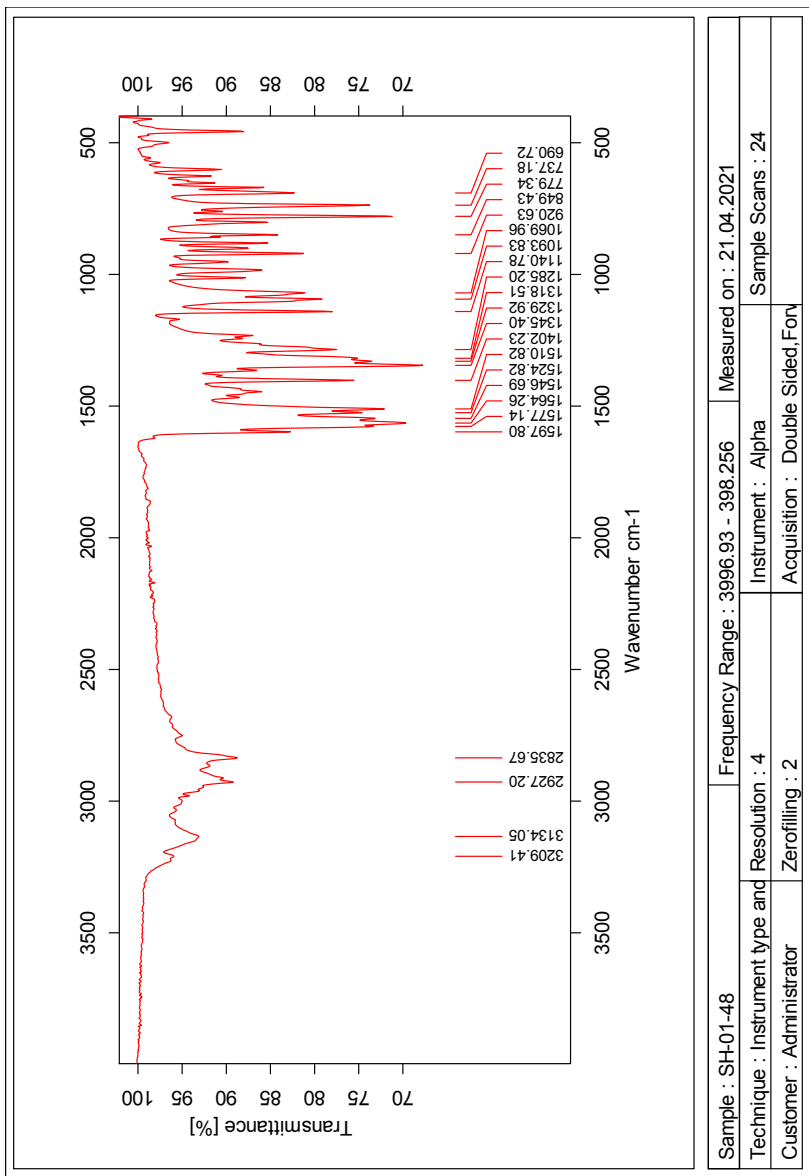
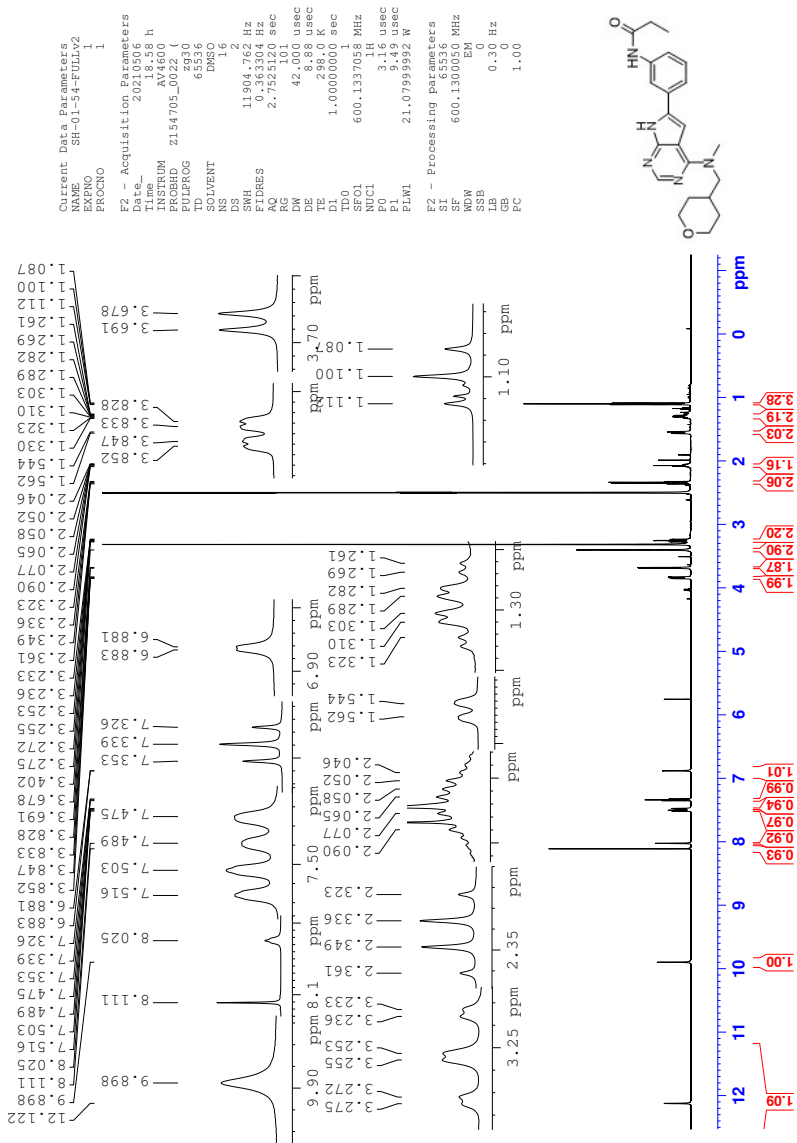
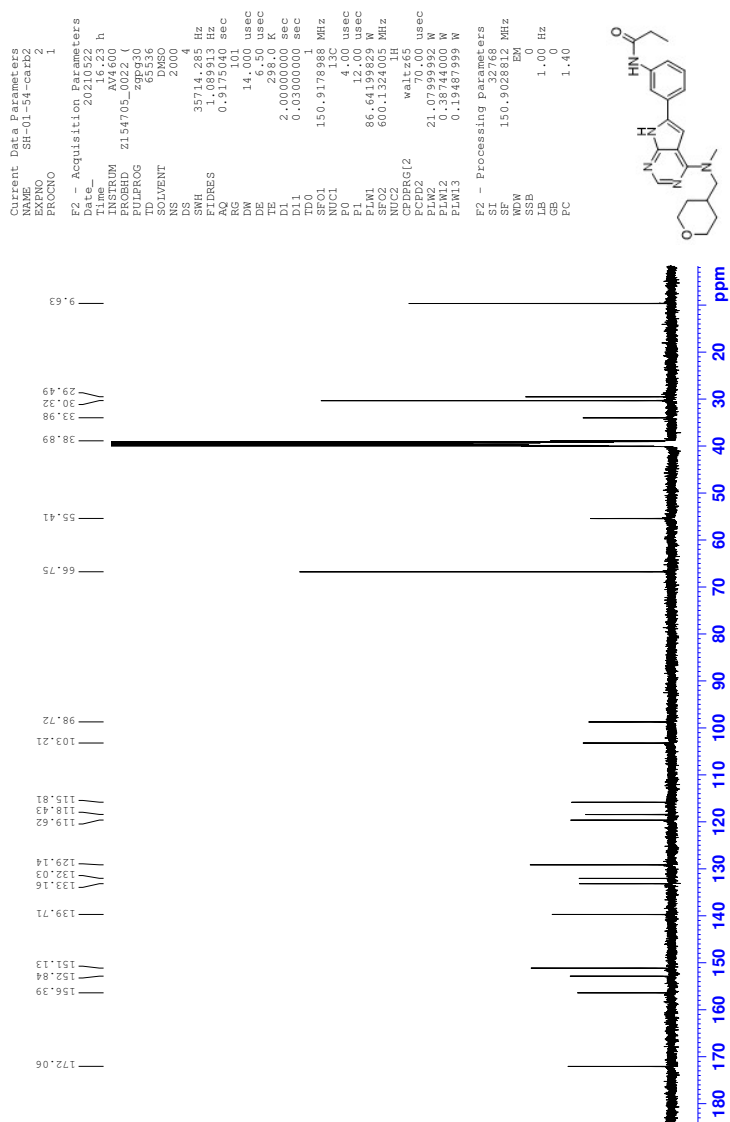


Figure W.7: IR spectrum of compound 24

X Spectroscopic data for Compound 25

Figure X.1: ^1H NMR spectrum of compound 25

Figure X.2: ^{13}C NMR spectrum of compound 25

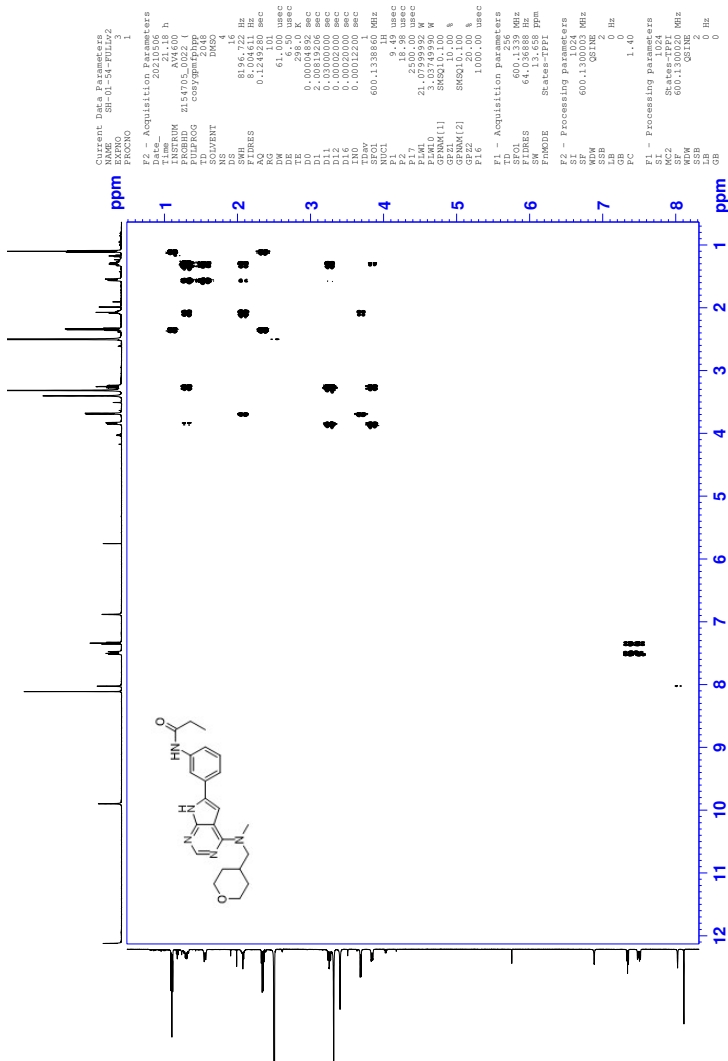


Figure X.3: COSY spectrum of compound 25

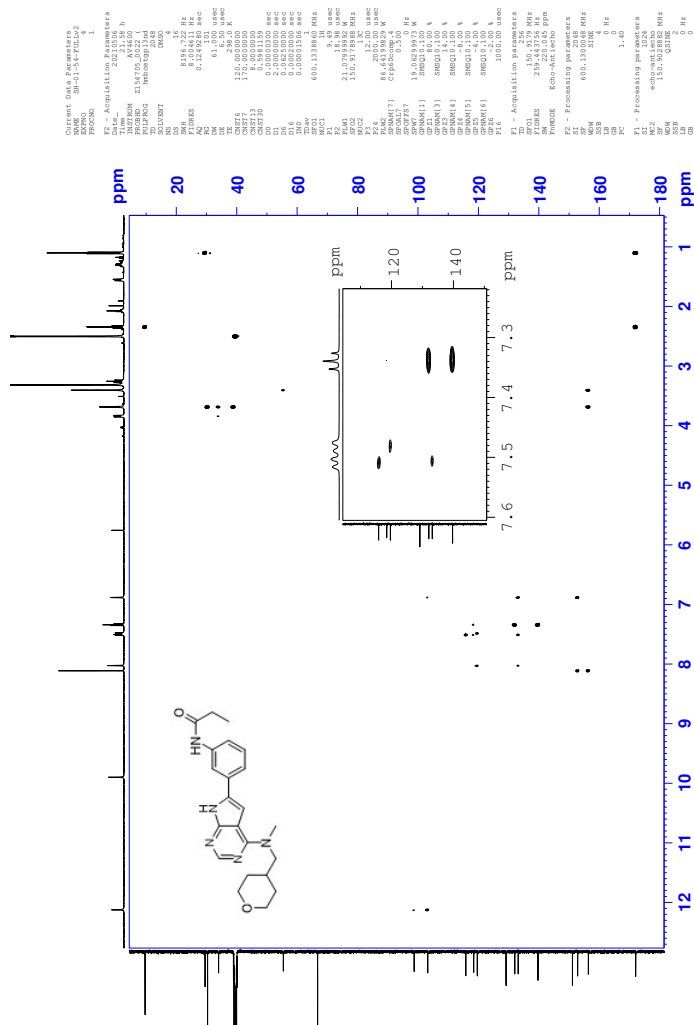


Figure X.5: HMBC spectrum of compound 25

Elemental Composition Report

Page 1

Single Mass Analysis

Tolerance = 2.0 PPM / DBE: min = -10.0, max = 50.0

Element prediction: Off

Number of isotope peaks used for i-FIT = 6

Monoisotopic Mass, Even Electron Ions

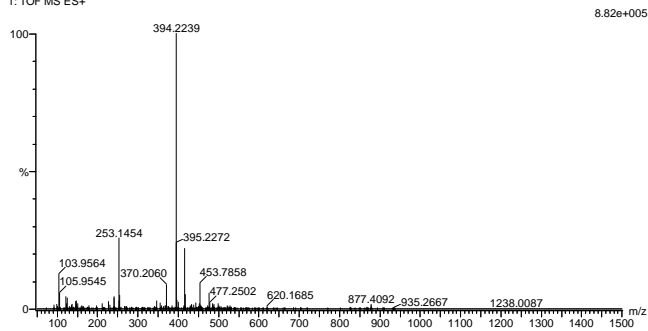
3719 formula(e) evaluated with 3 results within limits (all results (up to 1000) for each mass)

Elements Used:

C: 0-100 H: 0-100 N: 0-10 O: 0-12 Si: 0-2 I: 0-2

2021-299 167 (1.571) AM2 (Ar.35000.0,0.00,0.00); Cm (163:167)

1: TOF MS ES+



Minimum: -10.0

Maximum: 5.0 2.0 50.0

Mass	Calc. Mass	mDa	PPM	DBE	i-FIT	Norm	Conf (%)	Formula
394.2239	394.2243	-0.4	-1.0	11.5	2059.4	0.000	99.99	C22 H28 N5 O2
	394.2234	0.5	1.3	5.5	2074.1	14.712	0.00	C20 H36 N O3
	394.2234	0.5	1.3	2.5	2069.0	9.648	0.01	S12 C13 H32 N7 O5 Si

Figure X.6: MS spectrum of compound 25

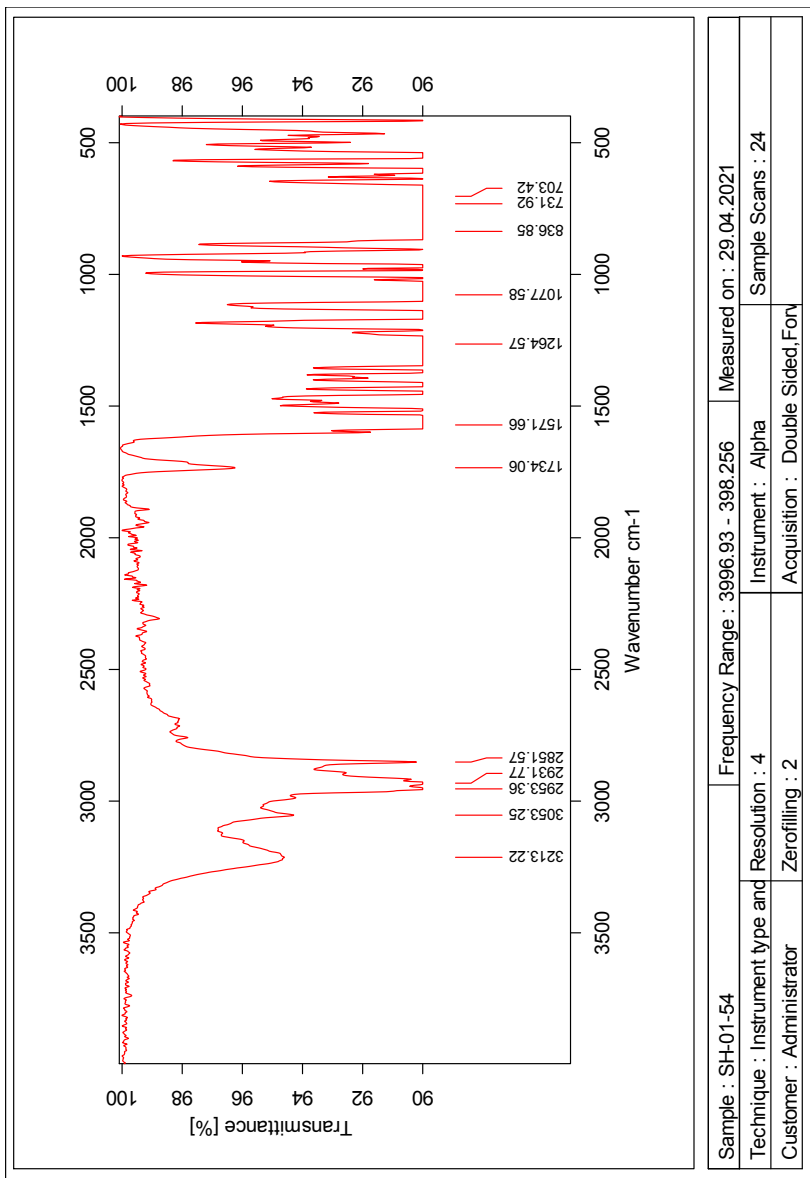


Figure X.7: IR spectrum of compound **25**

